UNIVERSITÀ DEGLI STUDI DI MILANO

PhD course in Biochemical Sciences, XXXI cycle

Department of Medical Biotechnology and Translational Medicine

Synthesis and biological evaluation of new neuraminidase inhibitors derived from sialic acid as potential antiviral agents

Paolo LA ROCCA
Matr.: R11334

Supervisor: Prof. Pietro ALLEVI

Coordinator: Prof. Sandro SONNINO

A.Y. 2017/2018

Index

ABSTRACT

The development of new, potent and selective bacterial, viral and human sialidase (neuraminidase) inhibitors is an important issue to be pursued in order to achieve both useful therapeutical and biochemical tools. In fact, these hydrolytic enzymes can represent a good target since they play key roles in some physio-pathological processes by regulating the levels of sialic acid (such as the *N*-acetyl neuraminic acid; Neu5Ac) presents in glycoconjugates. In addition, in the design of inhibitors against a specific member of this class of enzymes is critical to take into account that these proteins share some common features such as the tridimensional structure of their catalytic domain, but, on the other hand, they show a very low sequence identity. Indeed, the only conserved residues are some active site amino acids essential for the catalytic mechanism.

This thesis work was focused on the synthesis of hemagglutinin-neuraminidase (HN) inhibitors against the Newcastle virus (NDV), a member of the *Paramyxoviridae* family and strictly related to human parainfluenza viruses (hPIVs). NDV is a single-stranded RNA virus which could affect most species of both domestic and wild birds, causing significant and substantial economic losses in the poultry industry. To date, vaccination is the preferential instrument to border the infection, but when this procedure is not applicable, an efficient antiviral therapy could be the only useful way to control NDV outbreaks. At this purpose, the HN glycoproteins of paramyxoviruses represent an excellent target to be hit because they have some key roles in viral lifecycle: a) allowing viral attachment to the target cell; b) promoting the fusion process and, finally c) ensuring the release of the neo-synthesized virions.

Over the past years, while some 2,3-unsaturated Neu5Ac derivatives (DANA derivatives) have been marketed as inhibitors against influenza virus neuraminidases (belonging to *Orthomyxoviridae* family), no compounds reach the clinical phase for paramyxoviruses treatment. In particular, few molecules have been developed for NDV-HN, and the *N*-trifluoroacetyl derivative of DANA (FANA) was still the best inhibitor until my thesis work. So, the necessity to find new, potent and possibly selective inhibitors against paramyxoviruses-HNs remain a key issue.

At this purpose, the successful strategy, resulted fundamental to develop new NDV-HN inhibitors, was based on a multidisciplinary approach that combined the use of a) the chemical synthetic procedures, b) the computational docking studies and c) some biochemical activity assays. More in detail, the attention was directed to the study of two classes of inhibitors:

- Some C5 or C4/C5 modified 2,3-unsaturated DANA derivatives, as *reversible* inhibitors.

- Some scarcely investigated C2 modified 3,4-unsaturated Neu5Ac analogues, as *irreversible* ones.

We finally reached satisfying results, regarding both classes of inhibitors:

a) The understanding of the influence of the C5 *N*-perfluorinated substituents on the inhibitory activity of some 2,3-unsaturated DANA analogues, as potent and reversible NDV-HN inhibitors.
b) The discovery of a new C5 *N*-perfluorinated inhibitor against NDV-HN as potent as FANA (the best NDV-HN inhibitor previously published) but more selective for NDV-HN towards human NEU3.
c) The significant achievements of five new, potent and selective C4 and C5 modified 2,3-unsaturated DANA derivatives. All these compounds, combining the C4 azido or C4 *p*-toluensolfonamido group with the C5 *N*-perfluorinated chains, showed IC_{50} values in the nanomolar range; thus, they are up to 15-fold more potent than FANA.
d) The set-up of more efficient synthetic procedures to achieve the 3,4-unsaturated Neu5Ac derivatives in high yields and β-anomeric stereoselectivity.
e) The set-up of a smart and rapid method to unequivocally attribute the C2 configuration of the 3,4-unsaturated Neu5Ac inhibitors, *via* a 1,7-lactonization reaction.
f) The mechanism elucidation of an unreported and unexpected chemical scrambling between the C4 and the C5 position of Neu5Ac derivatives (through a previously uncharacterized reaction intermediate).

In addition, the rigid and induced fit docking simulation results permitted me to speculate on the interactions of the synthesized inhibitors with some active site amino acids, such as Lys236, a well know key residue involved in NDV-NH catalytic site activation mechanism and in fusion promotion activity. The comprehension of ligand/receptor interactions could lead to the development of molecules able to block, not only the neuraminidase activity of NDV-HN or other paramyxoviruses-HN, but also other viral functions mediated by these enzymes.

Some of the obtained results allowed the publication of two scientific articles:

- Rota, P., La Rocca, P., Piccoli, M., Montefiori, M., Cirillo, F., Olsen, L., Orioli, M., Allevi, P., and Anastasia, L. (2018) Potent Inhibitors against Newcastle Disease Virus Hemagglutinin-Neuraminidase, *ChemMedChem 13*, 236-240.
- Rota, P., Papini, N., La Rocca, P., Montefiori, M., Cirillo, F., Piccoli, M., Scurati, R., Olsen, L., Allevi, P., and Anastasia, L. (2017) Synthesis and chemical characterization of several perfluorinated sialic acid glycals and evaluation of their in vitro antiviral activity against Newcastle disease virus, *MedChemComm 8*, 1505-1513.

1.INTRODUCTION

This introduction aims to provide some information, referring to the current state of the art, useful for the understanding of my PhD thesis project directed to study the hemagglutinin-neuraminidase of Newcastle disease virus (NDV-HN) role in the virulent processes and to develop some new and potent NDV-HN inhibitors.

Initially, a brief description of sialic acids family (Sias), having *N*-acetylneuraminic acid (Neu5Ac) as the most representative member, is given. In particular, the structures, the functions and the metabolism of these acidic 9-carbon backbone carbohydrates, have been clarified in order to introduce the natural substrates of the enzymes object of our interest: the sialidases/neuraminidases (N). Then, a brief overview about these enzymes, able to catalyze the hydrolysis of terminal sialic acids present in glycoconjugates, their classification and their catalytic mechanism, are presented.

In addition, considering the important role played by sialidases in viral lifecylce, cleaving sialic acid residues and permitting to the newly formed virions to leave the target cell (enhancing the infection process), they represent the ideal pharmacological target to block viral infection. Thus, al lot of sialidase inhibitors have been synthesized and, to date, the main compounds derive from Neu5Ac. In particular, during these last years, a great interest has been directed to the 2,3-unsaturated Neu5Ac derivatives, with a well assessed inhibitory activity against viruses and bacteria sialidases[1-5]. On the other hands, few reports are dedicated to the investigation of the chemistry and the therapeutically applicability of the 3,4-unsaturated analogues[6, 7].

Finally, starting from the description of bacterial, viral and mammalian sialidases, a particular focus it has been directed to hemagglutinin-neuraminidase of Newcastle disease virus, a viral envelope tetrameric glycoprotein, with crucial roles in different phases of viral lifecycle, in order to better understand the characteristic of its peculiar and flexible active site. Furthermore, a comparison between the characteristics of the NDV-HN active site and the parainfluenza virus hemagglutinin-neuraminidase (hPIVs-HN) one is herein proposed, showing how the high degree of similarity makes possible to transpose the obtained results on hPIVs-HN.

1.1 The sialic acids: an extended family

As previously anticipated, the chemical diversity of sialic acids (Sias) family contribute to the huge variety of glycan structures on cell surfaces and the peculiar "makeup" of different cell types. This heterogenicity of compounds derived, principally, from the presence of modifications of the three "core" Sia molecules: *N*-acetylneuraminic acid (Neu5Ac), *N*-glycolylneuraminic acid (Neu5Gc) and ketodeoxynonulosonic or 3-deoxy-non-ulosonic acid (KDN)[8] (Figure 1.1).

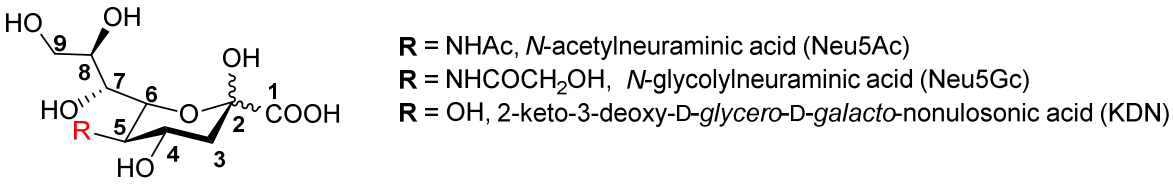

Figure 1.1 *Sialic acids family: the three main derivatives*

These modifications include the substitutions on the hydroxyl groups at C4, C7, C8, and C9 with *O*-acetyl, *O*-methyl, *O*-sulfate, or *O*-lactyl functions. This variety of modifications can determine their recognition and their biological functions.

1.1.1 *N*-acetylneuraminic acid structure

The most common member of this family, in human, is *N*-acetylneuraminic acid (Neu5Ac), a negatively charged sugar forming a pyranosidic ring in solution *via* intramolecular hemiketal condensation. It is classically named 5-acetamido-3,5-dideoxy-D-*glycero*-D-*galacto*-2-nonulosonic acid and the carbon atoms of the molecule are numbered consecutively giving 1 to carboxylic carbon and 2 to the anomeric carbon, as shown in Figure 1.1.

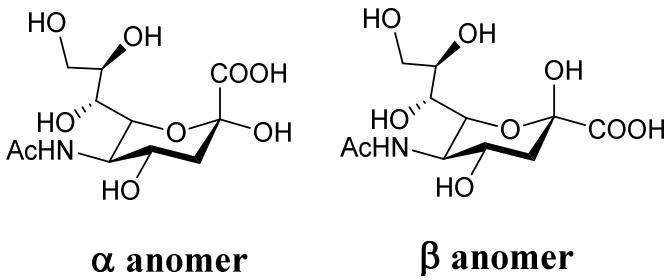

Figure 1.2 *N*-acetylneuraminic acid: α and β anomers.

This sugar, in solution, exists as equilibrium of α/β anomer mixture (Figure 1.2). Usually, Neu5Ac molecules are present in the most stable β anomer configuration form (90%). On the contrary, when this sugar is bound to glycans it is in its α configuration, with the exception for the complex CMP-Neu5Ac (the activated form of Neu5Ac)[8, 9].

1.1.2 Metabolism in mammalians and bacteria

The sialic acids metabolism follows a specific anabolic pathway from the synthesis (a) to the transport inside the cell compartments, the glycan attachment and the transfer on the cell membrane (b). On the other hand, the catabolic way provides the Sias removal from glycans, operated by sialidases (c), followed by their recycling or degradation (d)[8, 9]. In detail:

(a) *Synthesis of Neu5Ac.*

- The first step to obtain Neu5Ac is common to all species and it consists in the transformation of UDP-*N*-acetylglucosamine (UDP-GlcNAc) into *N*-acetyl-D-mannosamine (ManNAc) performed by the enzyme UDP-GlcNAc-2-epimerase, called also ManNAc kinase (Figure 1.3).
- Then, **in mammalians** ManNAc is phosphorylated by the same enzyme to ManNAc-6-phosphate, which is condensed with phosphoenolpyruvate (PEP), by Neu5Ac-9-P synthase, to obtain Neu5Ac-9-phosphate. Finally, dephosphorylation by a specific phosphatase gives Neu5Ac released in the cytoplasmic compartment (Figure 1.3). In contrast, **in bacteria**, the Neu5Ac biosynthesis involves directly the condensation of ManNAc with phosphoenolpyruvate catalyzed by Neu5Ac synthase[8, 9].

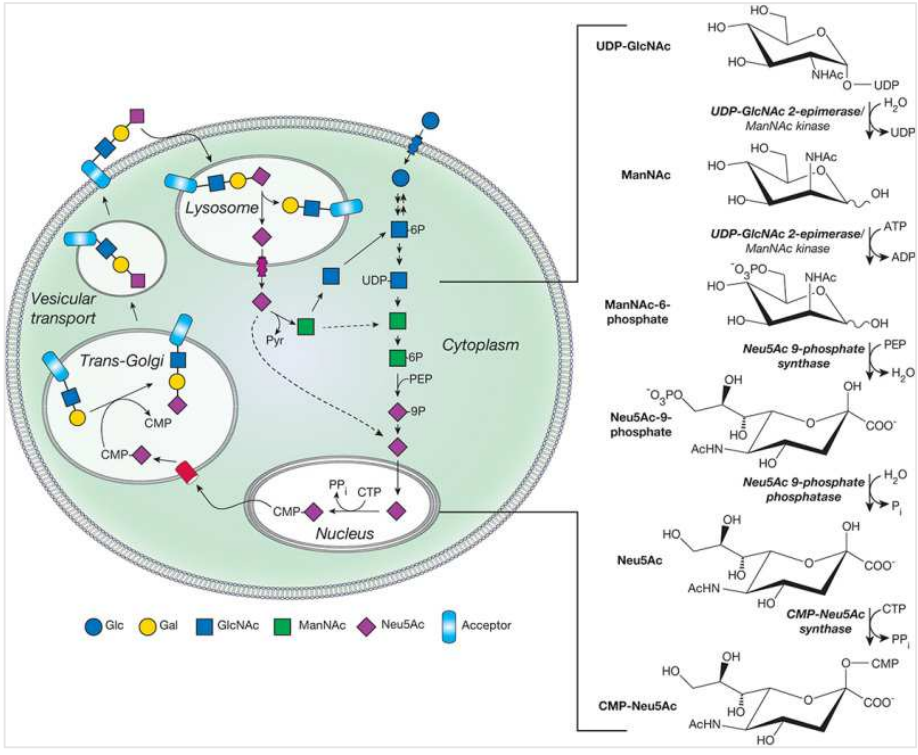

Figure 1.3 *Crucial phases of sialic acids biosynthesis in mammalians (Varki et al., 2015).*

(b) The transport inside the cell compartments, the glycan attachment, the transfer on the cell membrane.

- **In mammalians,** Neu5Ac reaches the nucleus where the activated form of sialic acid, CMP-sialic acid, is generated by CMP-Neu5Ac synthetase using cytosine triphosphate (CTP) as donor (Figure 1.3). The synthesized CMP-Neu5Ac is delivered into the Golgi compartments where sialyl residues were transferred to newly synthesized glycoconjugates by a family of linkage-specific sialyl-transferases (STs). On the contrary, **in bacteria**, CMP-Neu5Ac is synthesized in the cytoplasm and directly used in the assembly of cell-surface glycans[8-10].

(c,d) The Neu5Ac removal operated by sialidases and the final recycling/degradation process

- During sialic acid catabolism an important role is assigned to sialidases, specific enzymes involved in sialic acid removal from membrane glycoconjugates[8, 9].

  In mammalians, specific sialidases, having different functions, are localized in different cellular compartments: the lysosomal NEU1, the cytosolic NEU2, the plasma membrane NEU3 and the mitochondrial/lysosomal/intracellular membranes NEU4[11]. Cleaved Neu5Ac is released into the lysosome of a mammalian cell and then, it is delivered back to the cytoplasm by a specific exporter called Sialin, to be reused. On the other hands, if Neu5Ac is not immediately recycled it is degraded by cytoplasmic Neu5Ac-specific pyruvate lyases, that cleave the molecule into *N*-acetyl-mannosamine and pyruvate[8].

  Interestingly, **bacteria** catabolism involves sialidase too, although the occurrence is limited to a handful of species. The main roles of these enzymes in bacteria are: a) the removal of Sias from higher-order gangliosides present in mucous surfaces, b) the unmasking of toxin receptors and c) the biofilm formation. The canonical degradation pathway involves five enzymes able to transform free Neu5Ac into *N*-acetylglucosamine-6-P (GlcNAc-6-P), *via N*-acetylmannosamine (ManNAc) and phosphoenolpyruvate (PEP) intermediates. Finally, the GlcNAc-6-P is converted into fructose-6-P (Fru-6-P), which is a substrate in the glycolytic pathway[12-14]. However, some different variations have been reported and, consequently, this discussion cannot be generalized to all procariotes[14].

1.1.3 *N*-acetylneuraminic acid functions

The different functions exerted by Sias present in membrane glycoconjugates (Figure 1.4) are:

- modulation of transmembrane signaling processes (e.g. cellular cross-talking);

- regulation of cell growth and differentiation (e.g. involvement in tumor progression);
- binding and transport of different types of ions and drugs;
- stabilization of the conformation of proteins protecting them from proteases or glycosidases attack with the subsequent extension of the cell lifetime;
- modulation of the viscosity of mucins, sialoglycoproteins present in the mucous secretion of the respiratory and gastrointestinal tracts;
- masking action of antigenic sites and receptors;
- ligand for the binding of a variety of viral, bacterial and animal lectin-like proteins (hemagglutinin) and sialidases[8, 9].

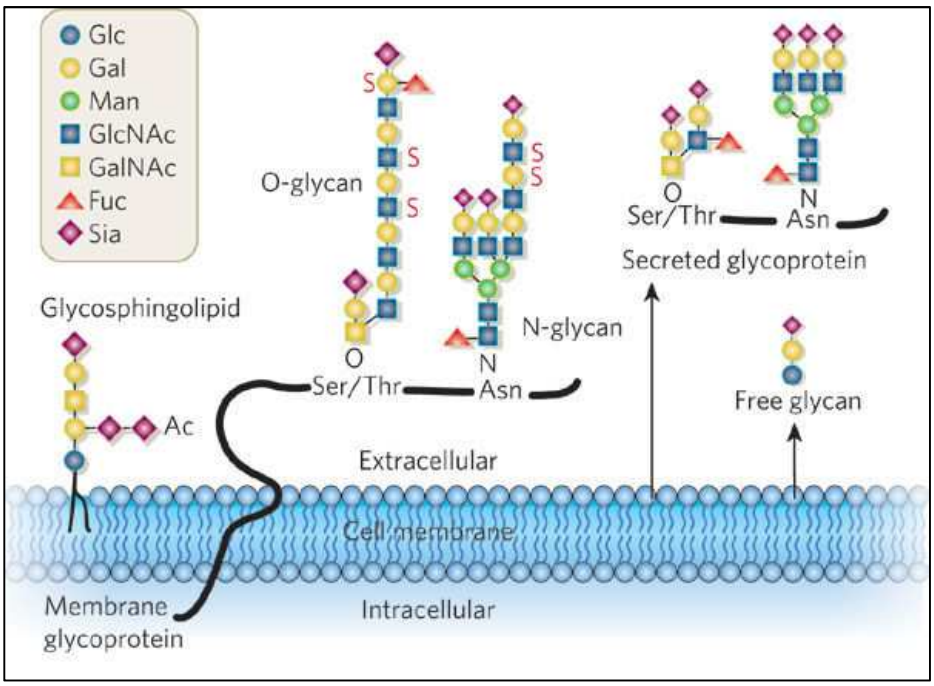

Figure 1.4 *Membrane glycoconjugates: glycosphingolipids, O-glycan, N-glycan, secreted glycoprotein and free glycans (Xiong et al., 2017).*

1.2 Sialidases superfamily: general and common characteristics

Sialidases belong to a family of proteins called glycoside hydrolase, a group of enzymes that hydrolyze the glycosidic bond between carbohydrates or between a sugar and a non-carbohydrate moiety. In particular, sialidases can hydrolyze the α2-3, α2-6 and α2-8 glycosidic bonds present at the terminal sialic acid residues of oligosaccharides, glycoproteins, glycolipids and other natural or synthetic substrates. They could be classified, according to Carbohydrate Active Enzymes database (CAZy), in different families: GH33 (includes bacterial and eukaryotic enzymes), GH34 (includes influenza viruses enzymes), GH83 (includes other viral sialidases) and, finally, GH58 (includes bacteriophage

endosialidases)[15]. Nowadays the term "sialidase" is preferred over the older term "neuraminidase", currently used only for viral enzymes (for historical reasons)[9].

1.2.1 Sequence and structure

Considering the primary structure, the comparison among different bacterial neuraminidase catalytic domains gives a general medium/low sequence identity (≈30%)[16]. In addition, a very low identity has been demonstrated, also, within viral neuraminidase (and hemagglutinin-neuraminidase) group by different sequence alignments. Thus, as we can observe in literature, only the catalytic site amino acids resulted conserved passing from bacterial to viral neuraminidases (Table 1.1)[17].

SIALIDASE FROM:	ACTIVE SITE RESIDUES							
Influenza Virus	Arg118	Asp151	Arg224	Glu276	Arg292	Arg371	Tyr406	Glu425
C. sordelli	Arg55	Asp80	Arg115	Glu253	Arg270	Arg330	Tyr365	Glu380
C. perfringens	Arg37	Asp62	Arg97	Glu235	Arg252	Arg312	Tyr347	Glu362
S. thyphimurium	Arg37	Asp62	Arg97	Glu236	Arg251	Arg309	Tyr342	Glu364

Table 1.1 *The conserved active site amino acids of some bacterial and influenza virus sialidases (Colman et al., 1993).*

Furthermore, considering mammalian sialidases, for example NEU2 (the only crystallized human one), it is well known that they share, with bacterial and viral neuraminidases, the same active site amino acids, their architecture and the spatial disposition. These highly conserved residues are: a) the arginine triad that binds the carboxylate group of the ligand, b) a tyrosine/glutamate nucleophile pair and c) an aspartate that acts as the acid/base catalyst[15]. This strengthens the hypothesis of a common ancestor of sialidases despite the low sequence identity[18]. The resolved 3D structures of the catalytic domain of viral sialidases, bacterial and the human NEU2, until now obtained, show a typical common beta-propeller fold structure, consisting of six four-stranded, antiparallel beta-sheets arranged as blades of a propeller around a pseudo-six-fold axis (Figure 1.5) [14, 15]. They also show the presence of a T/FYRI/VP motif (a conserved *N*-terminal motif containing one arginine of the arginine triad) and a variable number of Asp-box motifs on the beta-propeller structure. The Asp-boxes have always the same position and might be involved in the secretion process[16]. In conclusion, despite the large divergence in primary structure, all sialidases share some structural features and a well conserved positioning of the active site amino acids (essential for their catalytic activity).

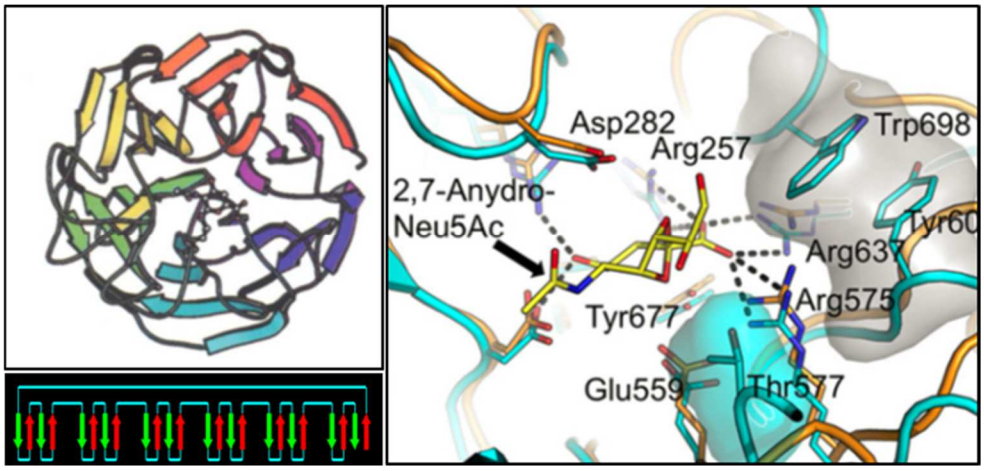

Figure 1.5 *On the left: up) a 3D representation of the beta-propeller structure; down) the common beta-propeller fold structure, consisting of six four-stranded, antiparallel beta-sheets. On the right: an example of catalytic site of a bacterial sialidase crystallized with the molecule 2,7-anhydro-Neu5Ac.*

1.2.2 Proposed catalytic mechanisms

The catalytic mechanism of sialidases could be based on a retention or an inversion of anomeric configuration. This thesis will focus on the retention one, typical of sialidases belonging to GH33, GH34 and GH83 families. This particular mechanism has been, firstly, proposed and studied for **β-glycosidases**, providing for two different theories:

A. Koshland, in 1953, proposed a catalytic mechanism where one carboxylic group acts as an acid catalyst, protonating the oxygen involved in glycosidic bond, thus promoting the glycosidic linkage cleavage and a second carboxylic group that operates as nucleophile, generating at the anomeric position a covalent glycosyl-enzyme intermediate. At this point the deglycosilated portion diffuses away from the active site, being replaced by a molecule of water and the reverse process take place: the carboxylated side-chain group deprotonates the water molecule, that attacks the anomeric center displacing the newly formed covalent glycosyl-ester bond. Both the steps involved transition-states having a substantial oxocarbenium-ion character[19-21] (Figure 1.6, A).

B. Phillips, in 1967, proposed a variant of the previously described mechanism, which involves a long-lived oxocarbenium-ion intermediate rather than the formation of a covalent glycosyl-enzyme one[22] (Figure 1.6, B).

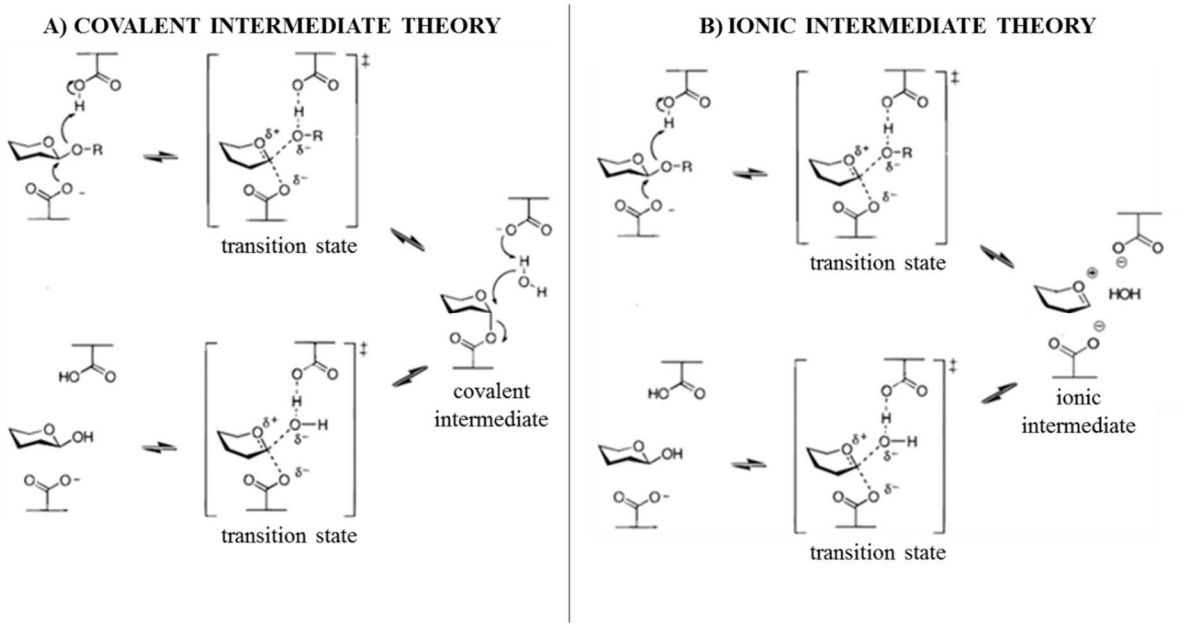

Figure 1.6 *β-glycosidase catalytic mechanism of retention of configuration, in according to Koshland model (left, A) or Phillips model (Right, B).*

Now, focusing specifically on sialidases, one of the firstly proposed catalytic mechanism was published by Chong, Von Izstein and coworkers, which sustained the presence of an ionic intermediate (Figure 1.6B). In fact, they studied viral sialidases catalytic process using some isotope effects and NMR methods, confirming the formation of an electrostatic environment in enzyme active site, which is favorable to the charged reaction intermediate[23-25]. According to these data, some literature reports implicitly assume that the glycal sialidase inhibitor 5-acetamido-2,6-anhydro-3,5-dideoxy-D-glycero-D-galacto-non-2-enoic acid (DANA) is a good mimic of the oxocarbenium transition state[25, 26]. More recent theories are favorable to a mechanism based on a covalent intermediate (Figure 1.6A), in fact, despite the absence of a glutamate (or an aspartate) correctly positioned to perform the nucleophilic attack, as in other glycosidases, it has been demonstrated that a tyrosine could support this role. Phenolic group of this amino acid presents a poor nucleophilic tendency but anyhow, its central role in the catalytic mechanism, leading to the formation of a covalent sialosyl-enzyme intermediate, has been demonstrated in bacteria and viruses (Figure 1.7)[14, 25, 27-29]. In addition, the same mechanism has been, independently, proposed for hNEU2[11]. In conclusion, some divergencies about the catalytic mechanism explanation are evident: "has the enzyme-bound intermediate covalent or ionic nature?", this question has not a unique response nowadays. Certainly, the existence of a long-lived oxocarbenium ion has never been empirically demonstrated, on the contrary, a lot of mutagenesis experiments and difluoro-sialic acids studies confirmed the presence of the putative covalent-bound intermediate (Figure 1.6 and 1.7)[25]. These data

permitted to reformulate, more precisely, the general catalytic mechanism for sialidases (Figure 1.7) and resulted extremely useful to identify new generation "mechanism-based" sialidase inhibitors (see paragraph 1.3.3).

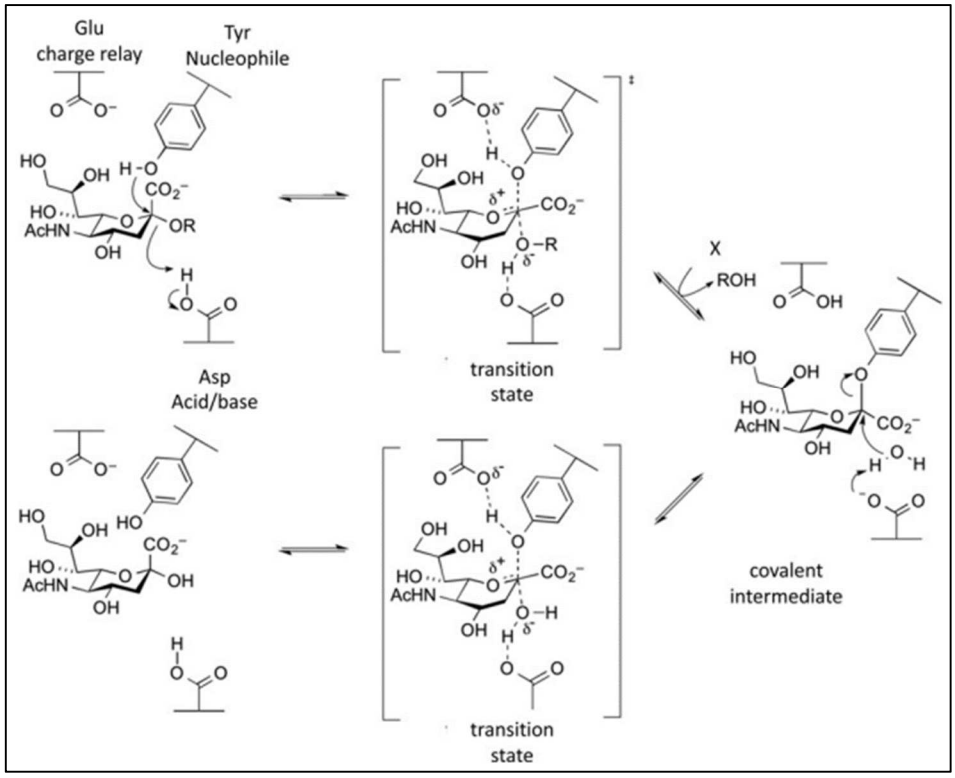

Figure 1.7 *Catalytic mechanism of sialidases with the formation of a covalent intermediate. The substrate binds to the active site in a $^2C_5$ chair conformation, then, after a conformational change, the active site tyrosine acts as a nucleophile reacting with the anomeric carbon of the substrate in a $B_{2,5}$-like boat conformation (not shown). So, a covalently bound sialosyl-enzyme intermediate (in a $^2C_5$ chair conformation) is formed. Finally, hydrolysis of this intermediate via a $B_{2,5}$ boat conformation specie (not shown) formation and a subsequent conformational change is followed by the diffusion of the product out of the active site (From Chan and Bennet, 2012).*

1.3 A brief introduction to sialidase inhibitors

To better understand the different types of sialidase inhibitors it is worth mentioning the difference between reversible and irreversible inhibition.

- **Reversible inhibitors**: these types of inhibitors bind reversibly to the enzyme with only weak interactions, so the inhibitor-enzyme complex could easily dissociate. They are defined *competitive inhibitors*, if the formation of the complex can be biased to favor the binding of the substrate, simply increasing its concentration. Instead, they are defined as *uncompetitive inhibitors* if the binding of the substrate to the active site create an allosteric site where the inhibitor could bind, blocking the enzyme activity. And finally, they are defined *non-competitive inhibitors* if they interact with a pre-existing allosteric site causing some structural rearrangements in the protein, resulting in a reduction of binding affinity of the substrate in the active site.
- **Irreversible inhibitors**: they bind tightly to the active site by a covalent or strong non-covalent binding, or they irreversibly modify a functional group that is essential for the enzymatic activity.

1.3.1 The 2,3-unsaturated inhibitors

DANA (5-acetamido-2,6-anhydro-3,5-dideoxy-D-*glycero*-D-*galacto*-non-2-enoic acid, Table 1.2) was the first 2,3-unsaturated sialidase inhibitor discovered and its activity was deeply investigated by Meindl and coworker[30, 31]. They demonstrated its reversible and competitive inhibition at micromolar level against viral, bacterial and mammalian sialidases (Table 1.2)[30, 32, 33]. In fact, this high inhibitory activity could be explained by its 2,3-unsaturated structure mimicking the transition state proposed in the catalytic mechanism (Figure 1.7). Furthermore, this compound has used as reference molecule in a lot of sialidase inhibition studies. The group of Meindl[30] also described the high inhibitory activity of trifluoroacetyl derivative of DANA, the FANA (Table 1.2) on bacterial and viral sialidases. Unfortunately, both these inhibitors are scarcely selective, showing micromolar inhibitory activity against viral and bacterial enzymes, but also towards human silaidases.[30, 32]

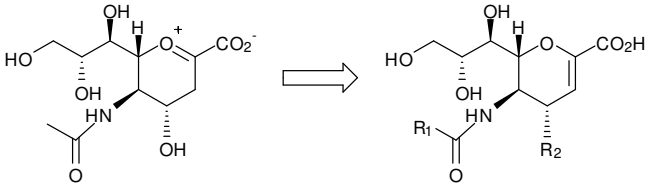

Transition state

DANA $R_1 = Me; R_2 = OH$
FANA $R_1 = CF_3, R_2 = OH$
Zanamivir $R_1 = Me; R_2 = NH(C=NH)NH_2$

	Vibrio cholerae	Newcastle disease virus	Influenza A virus	Influenza B virus	hNeu3
DANA	30 μM	13 μM	20-30 μM	90 μM	7.7 μM
FANA	2.5 μM	1.9 μM	5 μM	21 μM	-
Zanamivir	52 μM	-	~$1x10^{-3}$ μM*	≈$4x10^{-3}$ μM*	4.0 μM

Table 1.2 *IC_{50} values relative to the neuraminidase inhibition assay performed with DANA, FANA and Zanamivir on different sialidases published in various literature works.*[30, 34, 35].
**these IC_{50} values are taken from the literature*[35] *but they could variate considering the different Influenza A and B virus strains.*

Starting from these evidences, in the last years, a large number of DANA derivatives, as new potent sialidases inhibitors, have been studied. Von Izstein research group, very active in this field, developed Zanamivir (Table 1.2), which possess a very high inhibitory activity against influenza virus neuraminidases. In 1999, following the success in clinical trials, Zanamivir was approved by the US Food and Drug Administration (FDA) as the first neuraminidase inhibitor targeting influenza virus, with the trade name of Relenza®.[1] Successively, a lot of differently substituted DANA derivatives have been developed as possible sialidases inhibitors, directed towards influenza and parainfluenza viruses[1-5, 36], pathogenic bacteria[33, 37-39] and human sialidases[34, 40, 41] (Figure 1.8).

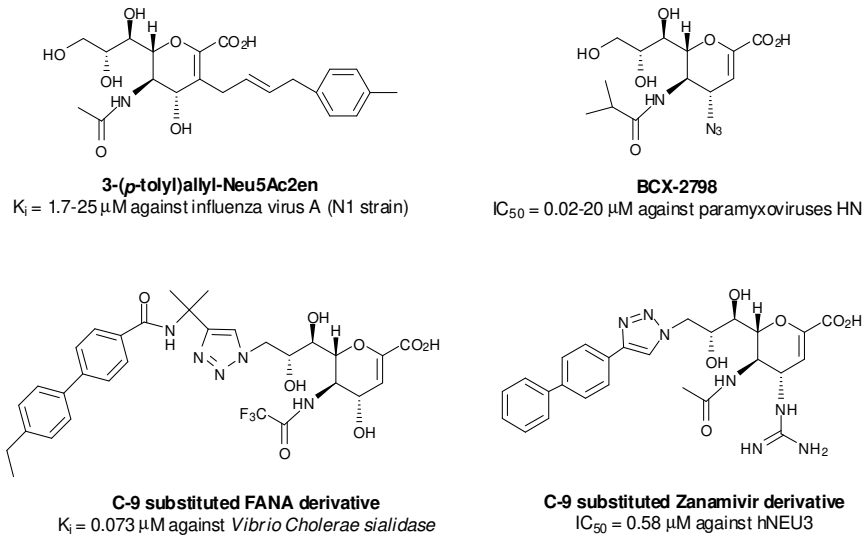

Figure 1.8 *Representation of some of the most active inhibitors of viral, bacterial and human sialidases*[2, 34, 36, 38]

1.3.2 The 3,4-unsaturated inhibitors

Another class of sialidase inhibitors belongs to the family of 3,4-unsaturated sialic acid derivatives (Figure 1.9). Despite the presence of an unsaturation, they do not mimic the transition state. This double bond, as postulated by Maudrin and coworkers in 1994, could be useful to generate some putative irreversible inhibitors[42].

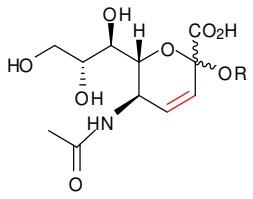

Figure 1.9 *3,4-unsaturated derivatives.*

They hypothesized that a 3,4-unsaturated derivative could be recognized as substrate analog by the enzyme and consequently hydrolyzed in an open-chain molecule, able to generate a conjugated unsaturated α-keto-acid (Figure 1.10). Indeed, this structure presents an electrophilic carbon susceptible to a Michael-type addition that could occur with a nucleophile group (Asp, Glu or Tyr) present in enzyme active site, forming an irreversible covalent bond. Unfortunately, they finally experimentally demonstrated[42] that these molecules, against influenza virus neuraminidases, are reversible competitive inhibitors (K_i = 7mM), instead irreversible ones. Probably, because influenza virus neuraminidase does not possess a nucleophile residue in the close proximity of the double bond or the inhibitor is unable to form a covalent bond by a Michael-type reaction.

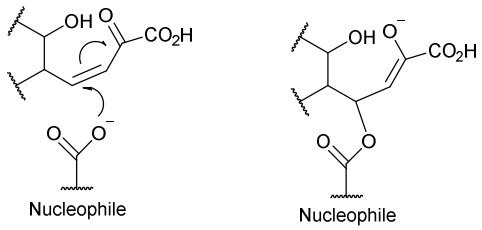

Figure 1.10 *Hypothetical Michael-type addition on a putative α-keto-acid in the enzyme active site.*

Similar results have been achieved by Ikeda and coworkers, who studied some 3,4-unsaturated derivatives and their competitive nature, determining IC_{50} values by a neuraminidase inhibitory activity assay performed towards human parainfluenza virus 1 (IC_{50} = 2.9-94 mM)[6, 7]. On the other hand, these results do not exclude the possibility that, in other sialidases with a slightly different active site, a covalent binding could be formed.

1.3.3 Other inhibitors

Focusing on viral neuraminidase inhibitor world, other compounds, having a structure derived from DANA, have been developed against influenza virus neuraminidases, such as BANA113 with an aromatic scaffold, Oseltamivir having a cyclohexene scaffold and Peramivir containing a five-membered ring scaffold (Figure 1.11)[1, 43-45]. Unfortunately, extensive use of Zanamivir and Oseltamivir led to the development and diffusion of inhibitor-resistant viral strains[46].

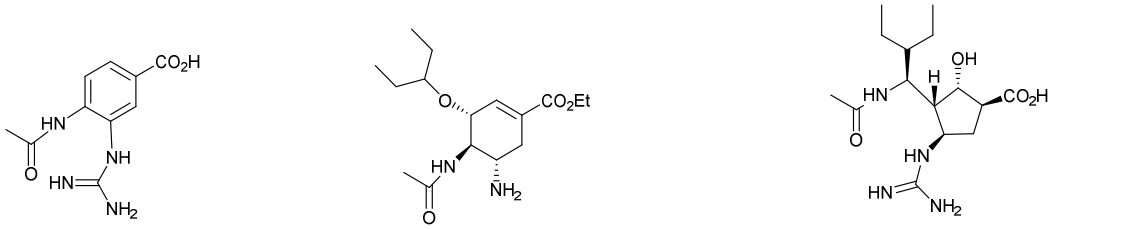

BANA113
IC_{50} = 27 μM against influenza virus A
IC_{50} = 2.6 μM against influenza virus B

Oseltamivir
$IC_{50} = 1.34*10^{-3}$ μM against influenza virus A/H1N1
$IC_{50} = 1.30\ 10^{-2}$ μM against influenza virus B

Peramivir
$IC_{50} = 1.10*10^{-3}$ μM against influenza virus A
$IC_{50} = 2.00\ 10^{-4}$ μM against influenza virus B

Figure 1.11 *Other neuraminidase inhibitors mimicking the scaffold of DANA and directed towards influenza A or B virus neuraminidases: BANA113, Oseltamivir and Peramivir (and their IC_{50} values)[1].*

In addition, some new generation inhibitors have been recently developed and classified as mechanism-based inactivators. An example of this class of compounds are the 2,3-difluoro-sialic acids derivatives (Figure 1.12), that mimic the structure of the substrate. The presence of a fluorine atom at C3, adjacent to the anomeric position, serves (due to its high electronegativity) to destabilize the formation of a positive charge at the anomeric carbon.

This situation slows down the rate of glycosylation and de-glycosylation and reduces the lifetime of the putative oxocarbenium transition state. On the other hand, the presence of a second fluorine atom (as good releasing group) at C2 accelerate the phase of glycosylation favoring the accumulation of the covalent intermediate. Thus, these mechanism-based inactivators are chemically inert and require specific activation by the catalytic machinery of the enzyme[27, 47]. A lot of molecules based on the 2,3-difluoro backbone have been proposed as viral neuraminidases and hemagglutinin-neuraminidase inhibitors[3, 29, 48] (Figure 1.12). Interestingly, some of the mechanism-based inhibitors have been demonstrated to act, also, as irreversible, suicide inhibitors for sialidases[49].

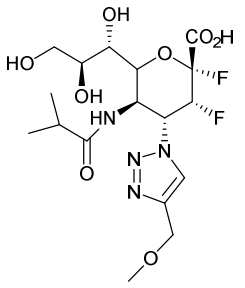

2,3-difluorosialic acid derivative
IC_{50} = 6.75 μM against hPIV-3 HN

Figure 1.12 *A 2,3-difluorosialic acid derivative tested against paramyxoviruses.*

Finally, to complete this general overview, it is important to cite the high number of natural extracts and naturally derived molecules that have been, recently, demonstrated to act as neuraminidase inhibitors[50, 51].

1.4 Viral neuraminidases (viral sialidases)

Viral neuraminidases represent a very interesting and attractive therapeutic target due to their involvement, as key enzymes, in the viral lifecycle. Two important groups of viruses will be considered in this thesis:

- Orthomyxoviruses group, which contains human and animal influenza type A viruses and human type B and type C ones.
- Paramyxoviruses group, which comprises Newcastle disease virus, mump and parainfluenza type 1-4 viruses[52].

Viral neuraminidases have some typical structural characteristics common to all sialidases but, unlike bacterial and mammalian ones, they maintain some peculiar features such as a flexible active site presenting, in most cases, large cavities adjacent to C4 and C5 positions. In general, they are involved in the phase of viral progeny release but some viruses belonging to paramyxoviruses group possess enzymes which maintain both the neuraminidase and the hemagglutinin activities (hemagglutinin-neuraminidase, HN)[53]. These HNs are, also, involved in the phase of viral attachment to the target cell. In the next paragraphs, the two above cited groups will be deeply described, considering influenza A virus as an example of orthomyxoviruses and, on the other hand, Newcastle disease virus (NDV) and human parainfluenza viruses (hPIVs) as examples of paramyxoviruses. Finally, particular emphasis is given to the description of the double function of NDV and hPIV hemagglutinin-neuraminidases (NDV-HN and hPIVs-HN, respectively), its biological significance and its implication in enzyme inhibitors development.

1.4.1 Influenza viruses

1.4.1.1 The virus, some of its key proteins and the neuraminidase active site

As above anticipated, influenza viruses belong to the orthomyxoviruses group (*Orthomyxoviridae* family), which is classified into three serologically distinct types: A, B and C (influenza C virus does not seem to cause significant disease in humans).

Influenza A virus, the most clinically relevant and widely studied, presents three key protein on its envelope (Figure 1.13), essential for its lifecycle:

- An *M2 ion-channel protein*: it is a pH-activated proton channel that mediates acidification of the internal region of viral particles entrapped in endosomes. For this reason, it results important in endocytosis and in virion assembly and budding;
- The *lectin-like hemagglutinin protein (H):* it is a protein formed by three identical subunits and anchored to a viral envelope. This glycoprotein seems to play two substantial roles: a) ensure an initial point of contact for the virus to target the cell-surface glycoconjugates and b) to trigger the virus internalization process through the fusion of the viral envelope with the host cell membrane. To date, there are 18 hemagglutinin protein subtypes, classified by their antigenic properties, named from H1 to H18[54] (Latest data from: *Center for Disease control and Prevention U.S. Department of Health & Human Services*).

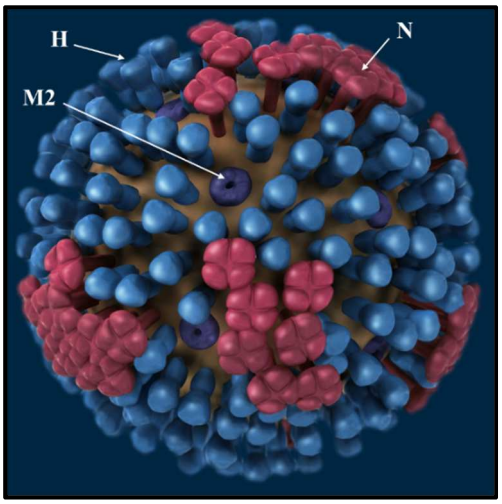

Figure 1.13 *Influenza virus with its envelope glycoprotein: M2 ion channel, hemagglutinin and neuraminidase. (From http://ricochet science. com).*

- Finally, the *neuraminidase (N)* it is an enzyme formed by four identical disulfide-linked subunits attached to the viral membrane. Each subunit is constituted by four distinct domains: the crystallized and well characterized "head" (or catalytic) domain[1, 55, 56], a "stem" domain (connecting the head to the transmembrane one), the transmembrane domain and, finally, the cytoplasmic one. The significant role of this protein is to assist in the movement of virus particles through the upper respiratory tract as well as in the release of newly formed virion progeny from infected cells[57]. There are 11 distinct subtypes of neuraminidase proteins, named N1 to N11. In according to phylogenetic analysis and structure, the subtypes are divided into three distinct groups: group 1 comprises N1, N4, N5, N8, group 2 N2, N3, N6, N7, N9, and group 3 includes influenza A-like N10 and N11[58] (Latest data from: *Center for Disease control and Prevention U.S. Department of Health & Human Services*).This classification, together with the hemagglutinin one, result useful to name the different influenza A virus strains (H1N1, H1N3, etc).

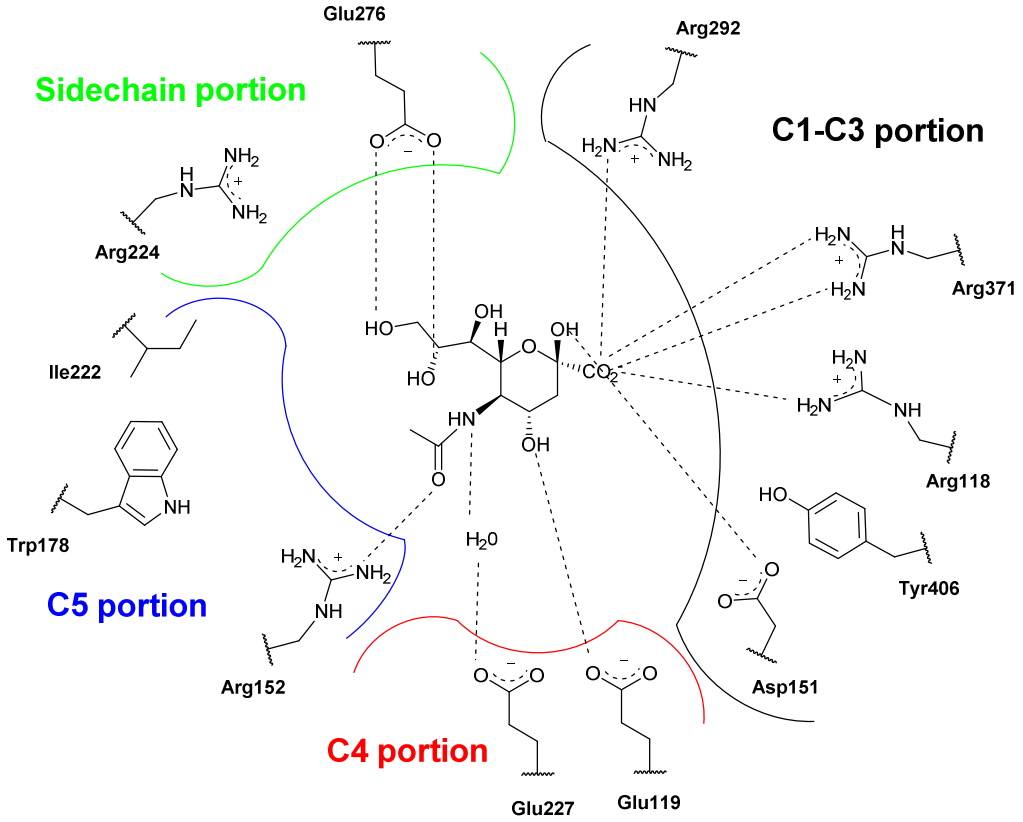

Figure 1.14 *Influenza virus neuraminidase active site represented with Neu5Ac and their interactions. (Adapted from Von Itzstein, 2007)*

In general, influenza virus neuraminidase (N) "head" domain is characterized by the typical beta-propeller fold structure and the active site presents the common characteristic residues[1, 57], previously described (paragraph 1.2.1). More specifically, in the catalytic site (Figure 1.14):

- **C1-C3 portion**: constituted by the arginine triad (Arg118, Arg292, and Arg371), the Asp151 considered important in the catalytic mechanism and the Tyr406, orienting its hydroxyl group very close to the C1-C2 bond of the substrate.
- **C4 portion**: presents an interesting peculiarity, in fact it is constituted by cavity with two negatively charged amino acids: Glu119, interacting with the C4 substituent and Glu227, interacting *via* a water molecule to NH at C5. Thanks to this basic information, some computational docking screenings have been applied to develop a large number of inhibitors, supported by the presence of well define crystal structures.[1]
- **C5 portion:** forms a pocket, able to accommodate the sialic acetyl moiety and characterized by the presence of Ile222, Trp178 and Arg152 (which makes an interaction with the acetyl oxygen).
- **Sidechain portion**: characterized by the Arg224 and Glu276, involved in H-bonding with the sidechain hydroxyls.

1.4.1.2 Zanamivir: an example of the strategy to develop new inhibitors

Antiviral drugs, like Zanamivir, Oseltamivir and Peramivir (Figure 1.15) have been synthesized after the understanding of the neuraminidase mechanism of action. The development of Zanamivir, the first sialidase-targeting anti-influenza drug commercialized with a K_i in low nanomolar range against influenza virus neuraminidases, is a perfect example of strategy involving a modern computational approach. Indeed, Von Itzstein and coworkers used computational tools (docking and molecular dynamic simulations) to evaluate the insertion of new functionalities on DANA backbone, determining the energetically favored interactions between the different substituent groups and the amino acids inside the catalytic pocket[1, 59, 60]. Considering the presence of a negatively charged region at the C4, they decided to test the insertion of an amino group at C4 position. This substituent resulted in a better inhibition than the normal hydroxyl moiety, due to its capacity to give a salt bridge with Glu119. Successively, after deeper analysis they demonstrated that enzyme active site C4 cavity was large and it could accommodate also bulkier substituents than amino one. Consequently, they assumed that the guanidino group, with its double aminic function, could well interact with both the two conserved glutamate residues. This hypothesis has been, successively, confirmed by experimental data[1].

1.4.1.3 150 cavity, a second sialic acid binding site and new generation inhibitors

Recent interesting studies, regarding the discovery of new peculiarities of influenza virus neuraminidase protein, permitted the rational development of new generation inhibitors. Specifically, in the last years a 150-cavity (a region adjacent to C3 position in enzyme active site) and a second sialic acid binding site have been discovered. The presence of the 150-cavity was confirmed only in group 1 neuraminidases. Thus, the development of a new C3 modified inhibitor (3-(p-tolyl)allyl-Neu5Ac2en, Figure 1.15) has been accomplished in the last years[34]. This molecule, with K_i values in low micromolar range (1.7-25 μM against N1 strains) and highly selective for group 1 neuraminidase, showed a inhibitory activity towards neuraminidases with oseltamivir acquired resistence[36, 61].

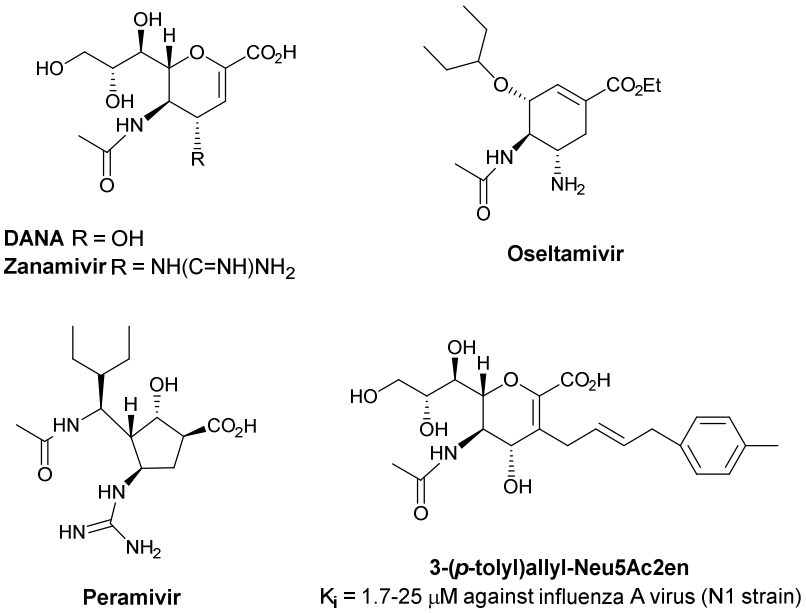

Figure 1.15 *Representation of DANA, Zanamivir, Oseltamivir, Peramivir and the recently discovered C-3 substituted DANA derivative (3-(p-tolyl)allyl-Neu5Ac2en) targeting the 150 cavity (Rudrawar et al., 2010).*

More recently, a couple of new potent and selective influenza virus neuraminidase inhibitors, based, for example, on the classical Oseltamivir backbone and active in low nanomolar range, have been also developed. Some of them (guanidino and triazole Oseltamivir derivatives, Figure 1.16) showed *Ki* values ranging from 0.46 to 430 nM. A reduced susceptibility to Oseltamivir resistance mutations was also observed in the guanidino derivative. Instead, the triazole ones seemed to be able to interact, additionally, with residues in the 150-cavity[46, 62].

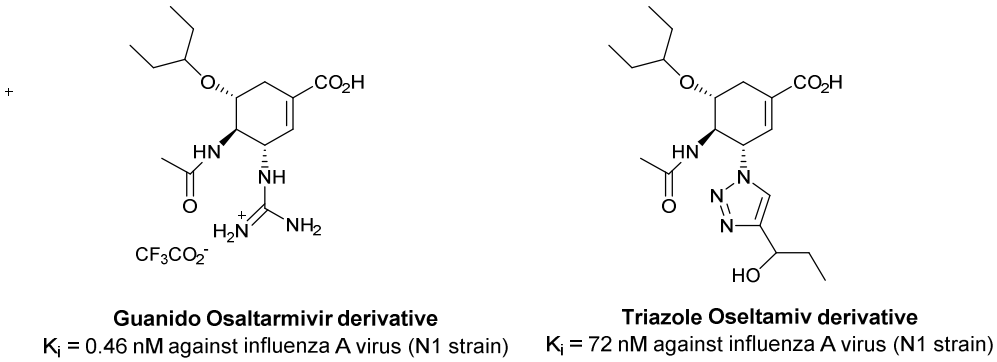

Figure 1.16 *Representation of two example of new generation influenza virus neuraminidase inhibitors. A guanidino derivative and a triazole one (which is able to target the 150 cavity).*

Finally, the discovery of a second binding site for sialic acid in viral neuraminidases resulted crucial. It seems to be composed by residues extremely conserved in avian strains but no in human and swine ones[63, 64]. The role of this Site II seems to be the enhancement of the catalytic efficiency[64] of neuraminidase activity and for this reason it could be considered an additional target for a future new generation drugs development.

1.4.2 Newcastle disease virus (NDV)

1.4.2.1 The virus, its lifecycle and the key proteins

Newcastle disease (ND) is one of the highly pathogenic viral diseases affecting avian species. It was first reported in Indonesia (1926) and in the Newcastle upon Tyne in England (1927), then it diffused in different parts of the world. In particular, lately reported outbreaks, confirmed the high persistence of this disease[65] (Latest data from *United States Department of Agriculture*). This pathology could affect most species of domestic birds (chickens, turkeys, ducks, geese, pigeons, quails, pheasants, guinea fowls and ostriches) and many species of both caged and wild fowls (Figure 1.17). ND is caused by Newcastle disease virus (NDV, called also APMV-1), the most studied among the twelve different serotypes of avian paramyxoviruses (APMVs) and belonging to the *Paramyxoviridae* family under genus *Avulavirus* (Avian *Rubulavirus*). NDV strains could be classified as lentogenic (low virulence), mesogenic (moderate virulence) and velogenic (high virulence). Velogenic ones could be viscerotropic or neurotropic and they may result in 100% mortality in poultry[66, 67]. These reasons account for the strong impact of this pathology and the subsequent large economic losses on the poultry industry. Nowadays, commercial vaccines are available for the prevention of this infection but in some cases, if the vaccination procedure is not applicable, an efficient antiviral therapy could be the only useful way to fight and control the contagion.

Figure 1.17 *A chicken affected by NDV infection: acute respiratory diseases, tremors, paralysis, depression and diarrhea are the principal symptoms, that could cause the 100% of mortality in chickens. In humans, NDV could cause only conjunctivitis, fever, headache and mild*

This virus, as the other Paramyxoviruses, is a pleomorphic enveloped virus around 200–300 nm of diameter, with a genome composed by a non-segmented, negative sense, single-stranded RNA (Figure 1.18). The RNA molecule is coated by the *nucleocapsid protein NP*, which has the role to cover and protect the genome by the action of nucleases. Another essential viral protein is the *large RNA polymerase protein L* which synthesizes the viral mRNA and assists in genomic RNA replication. It also performs the 5'capping methylation and poly A polymerase activity on the newly transcripted mRNAs. Finally, a *phosphoprotein P* functions as a homo-oligomer with a crucial role in viral replication and transcription.

In fact, L and P protein associate together and form the viral polymerase complex (*L-P complex*). Then, the helical nucleoprotein complex, formed by RNA coated by *NP protein* acts as a template which is recognized by the *L-P complex* to form an active viral polymerase complex permitting the transcription/replication to start.

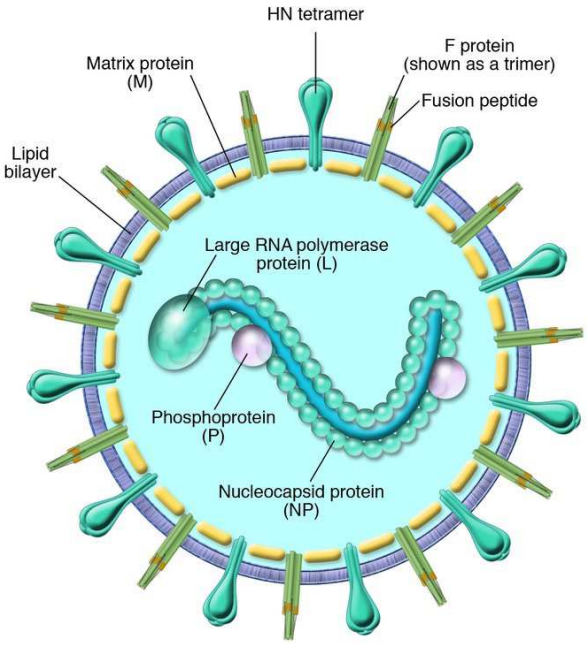

Figure 1.18 *Representation of a Paramyxovirus and its essential proteins: NP, L, P, M, F and HN (from Moscona, 2005).*

Then, a hydrophobic peptide located between the nucleocapsid and the viral envelope called *matrix protein M*, performs different functions: a) it controls the viral RNA synthesis; b) it interacts with actin; c) it helps in assembling virion on the host cell membrane; d) it might be responsible for maintaining the spherical shape of the nucleocapsid and e) it helps in the virus budding process by interacting with the host cell plasma membrane. The viral envelope, composed by a lipid bilayer, is dressed with the *fusion protein F* which mediates the fusion with the host cell membrane. It is synthesized as an inactive precursor F_0 which is cleaved by a cellular protease into two subunits, F_1 and F_2. Further, these subunits are processed in the trans Golgi network, inside the mammalian cell, forming the disulfide-linked F_1–F_2 *active protein*. The active form of the protein causes the viral envelope/host cell fusion, permitting the viral particles to penetrate inside the cell. It can also lead to cell-cell fusion with the formation of syncitya (multinucleate cells), enhancing virus spread[66, 67].

The *hemagglutinin-neuraminidase protein HN* is a glycoprotein present on viral envelope, as a tetramer, and it is involved in different crucial phases of the viral lifecyle[66-68]. About that, the paramyxoviruses lifecycle can be divided into 4 different phases[69] (Figure 1.19):

- *Binding*. It consists in the attachment of the virus, mediated by the HN protein, to sialic acid residues present on the receptors of the target cell.
- *Fusion*. The fusion of the viral envelope with the target cell is mediated by the active form of the F protein. The entire fusion process is triggered and enhanced by HN protein.

- *Uncoating and genome replication*. After the entrance of the viral genome inside the cell, its replication, mediated by *L-P complex* interacting with *helical nucleoprotein complex*, could be accomplished.
- *Budding and release*. The newly synthesized virion particles are ready to leave the infected cells. In this step, the sialidase activity of the HN protein is used to hydrolyze and release the sialic acid residues bound to host cell glycans, allowing the virus to leave the cell.

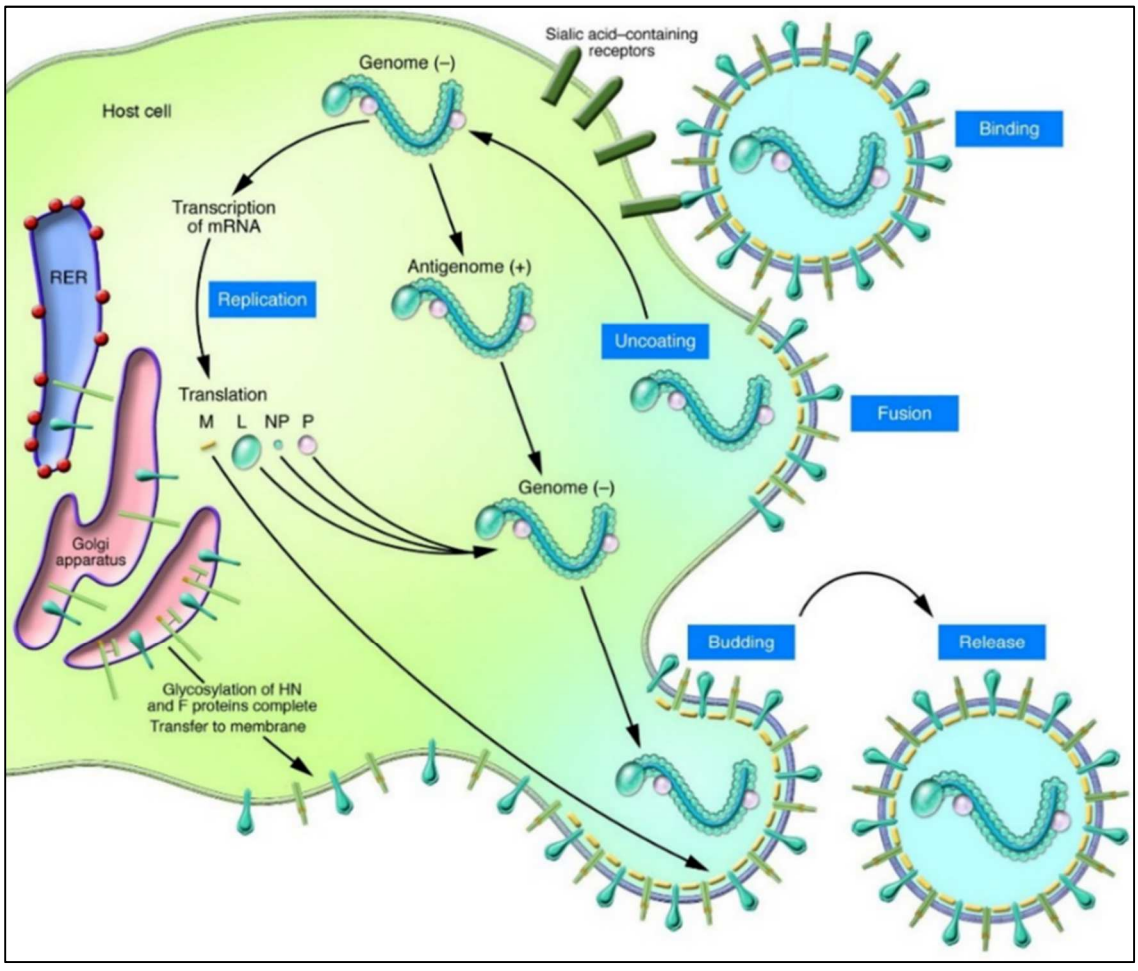

Figure 1.19 *Schematic representation of paramyxoviruses lifecycle phases: 1) binding, 2) fusion, 3) uncoating and genome replication, 4) budding and release (from Moscona, 2005).*

1.4.2.2 NDV-HN structure, catalytic site (Site I) and role of the second sialic acid binding site (Site II)

As above described, a key protein in NDV life cycle is the hemagglutinin-neuraminidase (NDV-HN, figure 1.20) and for this reason, it could be a very interesting pharmacological target for the development of new antiviral strategies. Most evidence confirmed that HN is present on *Paramyxoviridae* surface as covalently linked dimers, usually disulfide-linked *via* Cys123[53, 70-73], associated to form a tetramer. Anyhow, the absence of this linkage does not interfere with the formation of non-covalently linked dimers and tetramers, permitting to conclude that this disulfide bond is only responsible for the enhancement of the structure stability[53, 72]. The entire structure is composed, as influenza virus neuraminidase, by four different domains: "head" (catalytic) domain, a "stalk" domain, a transmembrane domain and a cytoplasmic domain. The complete head globular region of this protein has been crystallized by Crennell and coworkers[53] in various conditions, obtaining dimers in three different crystal forms:

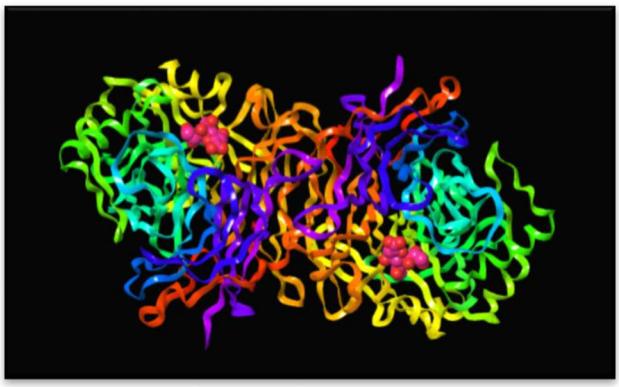

Figure 1.20 *Representation of NDV-HN with DANA (pink) co-crystallized in its active site (Adapted from Crennell 2000, PDB:1e8v).*

- An orthorhombic crystal form (resolved at 2.5 Å), obtained at pH 4.6, as ligand-free structure (PDB: 1e8t);
- A hexagonal crystal form (resolved at 2.8 Å), obtained at pH 6.5 by co-crystallization with Neu5Ac, observing the final presence of DANA bound in the active site (Figure 1.22) (PDB: 1e8v);
- An orthorhombic crystal form (resolved at 2.0 Å) achieved at pH 4.6 by co-crystallization with 2,3-sialyllactose, affording the β-anomer of Neu5Ac linked in the active site (Figure 1.23) (PDB: 1e8u).

By comparing the two orthorhombic crystal forms with the hexagonal one, it was observed that the overall structure of the single monomer is very similar, showing the six-bladed β-propeller fold typical of all neuraminidases. All these structures contain HN in its dimeric form, but the association of monomers is dramatically different among the two orthorhombic structure and the hexagonal one. By studying the hexagonal crystal form, it can be extrapolated a clear picture of the catalytic site[53] (Figure 1.21, 1.22):

- **C1-C3 portion**: there is the typical arginine triad (Arg174, Arg416 and Arg498) which well interact with the carboxylic group and Arg174 it is stabilized by Glu547, then a Tyr526 orienting its hydroxyl group very close to the C1-C2 bond interacting with Glu401. In addition Asp198 (equivalent to Asp 151 of influenza virus) is considered important in the catalytic mechanism but, in this case, it is positioned on a flexible and disordered loop pointing out from the active site;
- **C4 portion**: as demonstrated by some published studies, C4 pocket is a very large hydrophobic cavity in which the hydroxyl group of DANA does not give any interaction. Some of the amino acids surrounding this cavity are conserved across all HNs (Ile192, the methylene side groups of Arg174 and Asp198), while others are not conserved (Ile175), maintaining anyway the hydrophobic character of this region. The cavity is also lined with some polar and basic side chains (Asn190 and Lys236). This peculiar binding pocket seems to be a specific of paramyxoviruses family.[53, 74]

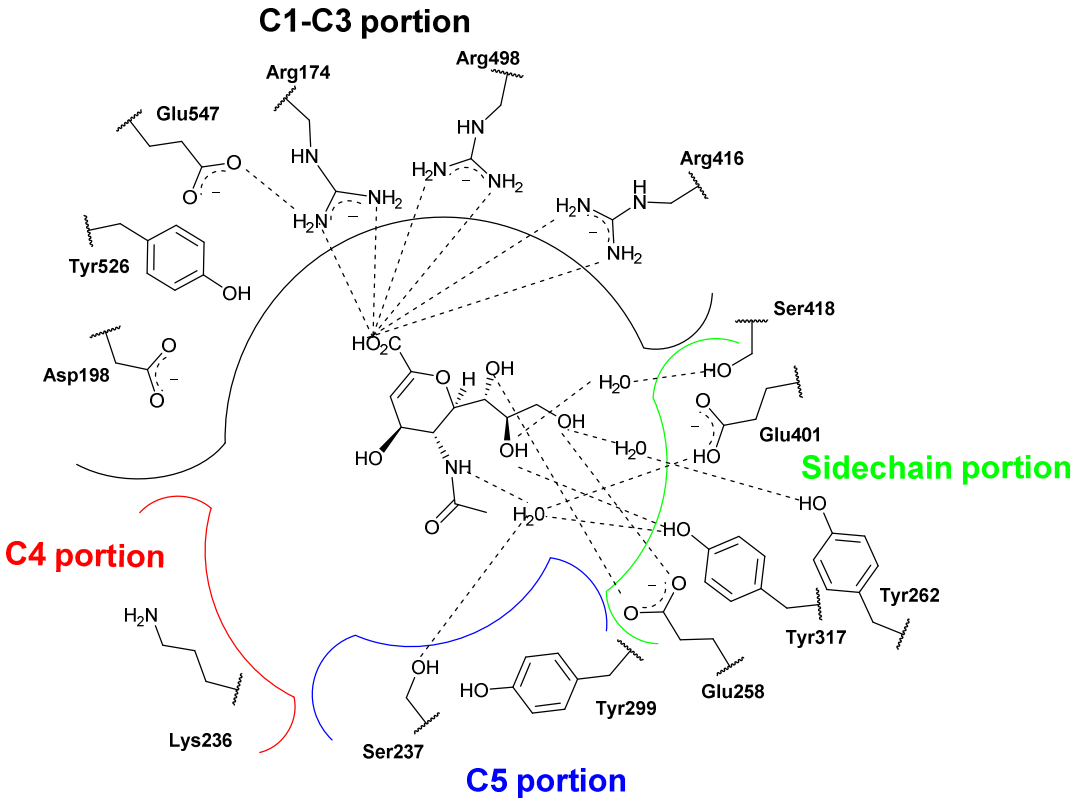

Figure 1.21 *NDV-HN active site represented with DANA and their interactions. (Adapted from Crennell, 2000).*

- **C5 portion**: It can accommodate the acetyl moiety, in fact the methyl group gives a hydrophobic interaction with Tyr299 while N5 interacts *via* a water molecule with

Ser237, Tyr317 and Glu401. A peculiarity of this region, in NDV-HN, is that it could, theoretically, accommodate also bulky groups than the acetyl one (Figure 1.22).

- **Sidechain portion**: The glycerol chain is accommodated in a region with a highly conserved sequence in virus strains (Glu258, Tyr317, Tyr262 and Ser418). A peculiarity of HNs is that all the three hydroxyl groups seem to be fundamentally involved in the interaction within active site[53].

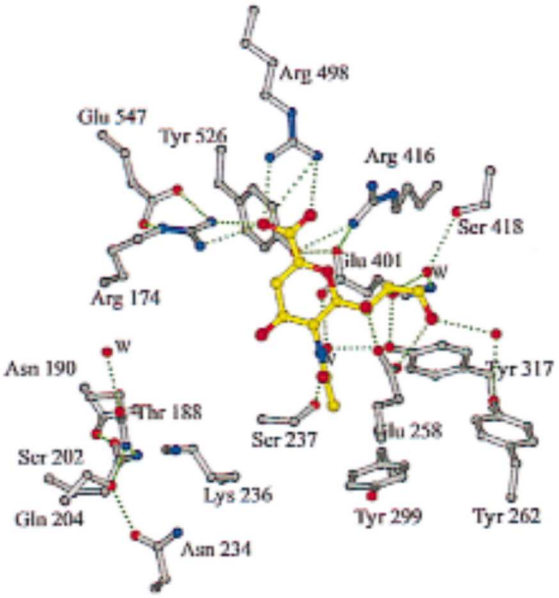

Figure 1.22 3D *representation of NDV-HN active site crystallized with DANA and their interactions (From Crennel 2000).*

Proceeding by comparing the two orthorhombic crystal forms with the hexagonal one, we could find substantial differences, leading to postulate that the NDV-HN active site is very flexible and it could exist in two different states: a catalytic (switched on) state and a sialic acid binding (switched off) state (Figure 1.23).

The hexagonal crystal form, previously described, represents the catalytic or "switched on" form. On the other hands, the orthorhombic one represents the "switched off" or sialic acid binding state, which differs from the first one for an unusual positioning of some key amino acids (Figure 1.23)[53,64]:

- Arg174 is not in its usual position (forming the arginine triad) but it is swung within the large C4 cavity;
- Lys236 moves out of the cavity to enable accommodation of Arg174, maintaining the charge equilibrium. Thus, Lys236 reaches the C5 moiety interacting with the acetyl group.
- Tyr526 moves out from the catalytic position (after Ile175 rotation).

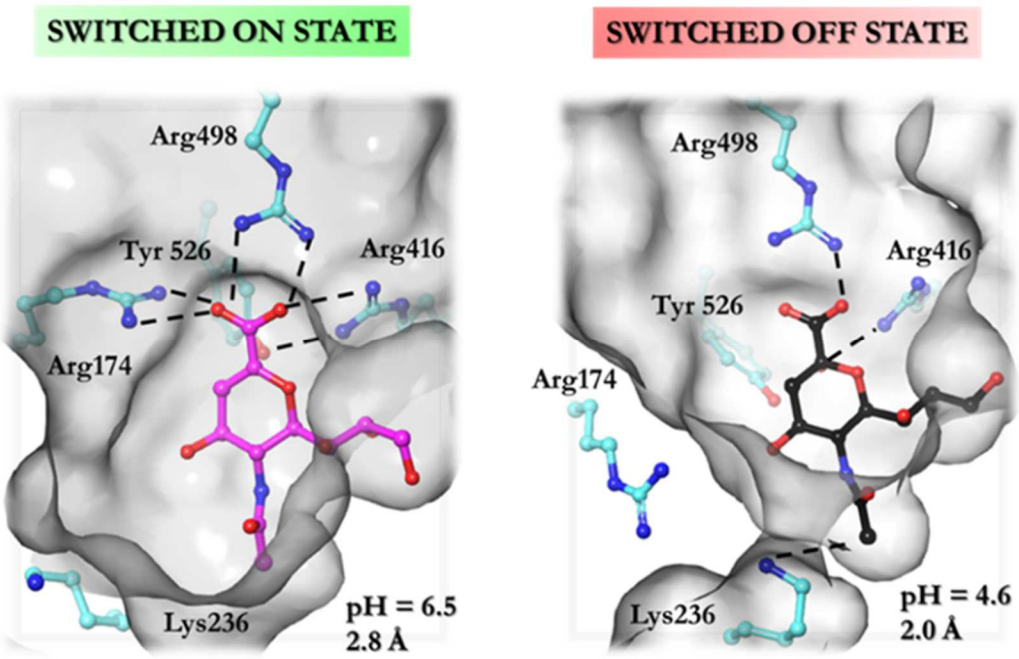

Figure 1.23 R*epresentation of NDV-HN active site in its switched on or catalytic state and in its switched off or "sialic acid binding" state (Adapted from Crennell, 2000).*

These data sustain the double function accomplished by a single enzymatic site having both hemagglutinin (binding) and neuraminidase (catalytic) activities[53]. On the contrary, other works, sustained the presence of two sites having the two distinct functions[71, 75]. In reality, we know that the truth lies somewhere in between, in fact, it has been recently demonstrated that, while the catalytic site possesses both neuraminidase and hemagglutinin activities[53], a second binding site (Site II), located at monomers interface, presents only a very strong hemagglutinin activity[76-80]. This second binding site was detected using a disaccharide thiosialoside (Figure 1.24), that was co-crystallized with NDV-HN (PDB: 1usr, 1usx), revealing DANA in the active site and the disaccharide bound to a symmetrical site at the HN dimer interface[76]. Site II presents some peculiar characteristics:

- Six conserved water molecules;
- Five hydrogen bonds involving the main chain;
- Arg516 seems to be important in the hydrogen bond network;
- The acetamido group is accommodated in a hydrophobic pocket (that seems to be conserved in all paramyxoviruses) formed by Gly169, Leu552 and Phe553 of one monomer and Phe156, Val517 and Leu561 from the other one.

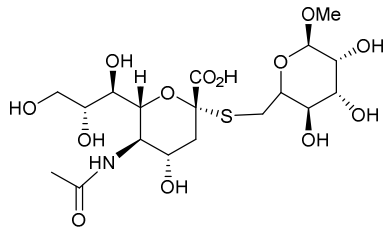

Figure 1.24 *Disaccharidic thiosialoside able to bind Site II.*

Finally, it can be concluded that that NDV-HN binds to sialic acid-containing receptors through two separates sites, one at the catalytic pocket (in its "switched off" state) and the other site around Arg516[80]. In addition, it was, recently, proposed that both the binding sites (Site I and Site II) play an important role, also, in the membrane fusion process.[77] Briefly:

- The binding and the subsequent cleavage of sialic acid receptors, in the catalytic site, cause conformational changes triggering and promoting the fusion by F protein. In other words, if a molecule, for example Zanamivir, well interacts with this site, mimicking the transition state intermediate, could produce these conformational changes. These modifications are reflected, through the dimer interface, to site II activating its binding activity and promoting the fusion process. In fact, it has been well demonstrated that, after the engagement of site II, the F protein is triggered to insert its fusion peptide into the target membrane and, consequently, fusion can ensue (Figure 1.25). This data, also, confirmed the ability of HN to transmit conformational changes from the head to the stalk domain of the protein[77].
- In addition, the activation of the second binding site it is important to maintain a close proximity of the cell membrane and the viral envelope, during the entire fusion process. In fact, a loss of the second binding site, by mutation, cause a less efficient fusion promotion activity, leading to a slower viral growth[76, 80].

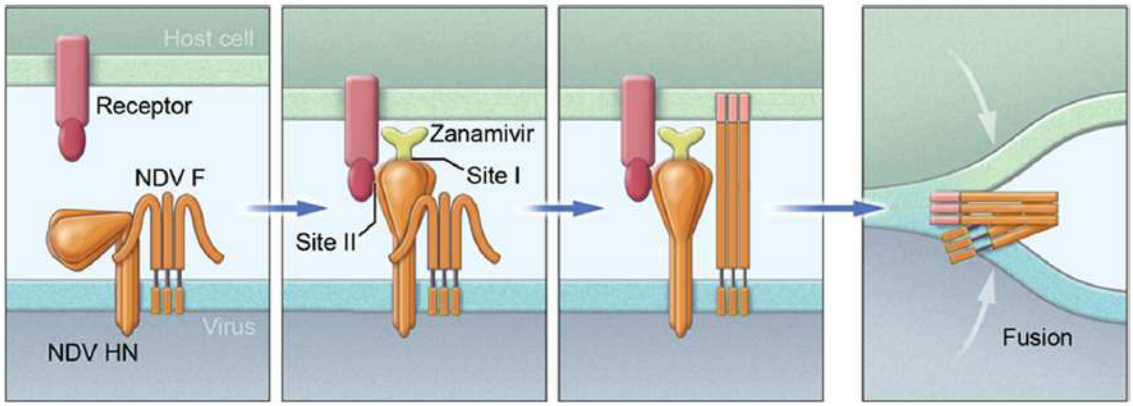

Figure 1.25 *Schematic representation of fusion activation process triggered by HN protein (From Porotto, 2012).*

1.4.2.3 Studies on NDV-HN Site I and Site II inhibition

Some NDV-HN inhibition studies demonstrated that the Site I of this enzyme is sensitive to the three transition state analogs inhibitors: DANA, Zanamivir and BCX-2798 (Figure 1.26). On the other hands, the NDV-HN Site II is not affected by Zanamivir or BCX-2798 and only in a limited extent by DANA[78-80]. Furthermore, the trisaccharide 2,3-sialyllactose (Figure 1.26) is a proven inhibitor of binding, inhibiting both Site I and Site II activity. More specifically, it has been experimentally demonstrated that it is able to directly bind Site I, blocking its activity, and to inhibit indirectly Site II. In fact, after the binding to Site I, it is not capable to induce the conformational changes necessary to activate the secondary site[79].

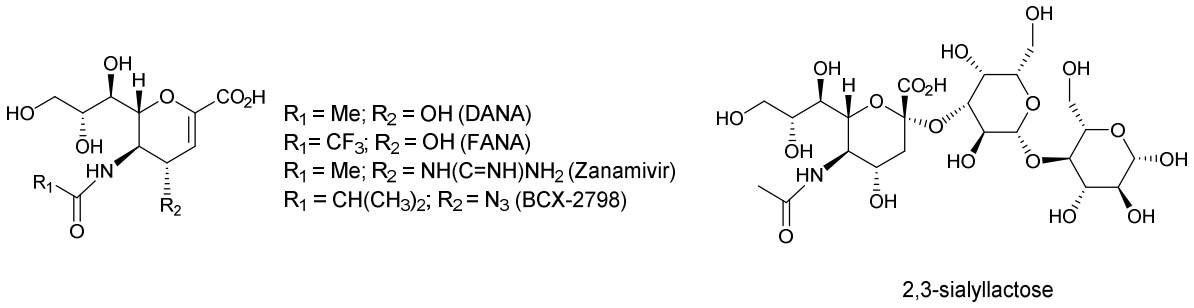

Figure 1.26 *Representation of DANA, FANA, Zanamivir and BCX-2798(left); 2,3-sialyllactose (right).*

Apparently, it seems that the interplay between the two sites is needed for a proper activation of the fusion mechanism and it results essential for the development of new generation inhibitors. In view of the above, it seems necessary to find molecules which are able to block Site I without activating Site II (as 2,3-sialylactose) or molecules which are able to block both sites. At the moment, FANA remains the most active inhibitor of NDV-NH, reported in the literature, showing an IC_{50} of 1.9 μM for neuraminidase activity compared to the value of 13 μM obtained for DANA. Unfortunately, FANA did not affect Site II binding, resulting in no detectable inhibition of hemagglutinin acitivity[30].

1.4.3 Human parainfluenza viruses

1.4.3.1 The virus and its lifecycle

Human paramyxoviruses (hPIVs), as avian paramyxoviruses (APMVs), are pleomorphic enveloped RNA viruses, belonging to the *Paramyxoviridae* family. They are the cause of different respiratory diseases in infants, children, immunocompromised and chronically ill people and elderlies. There are four antigenically distinct types of hPIVs:

- hPIV-1 is the leading cause of croup (acute laryngotracheobronchitis) in children, a respiratory inflammation of the larynx and trachea, associated with infection and breathing difficulties. It is responsible for outbreaks of croup in the autumn;
- hPIV-2 causes croup in children, but doctors detect it much less often than hPIV-1, because it is frequently overshadowed by hPIV-1 or hPIV-3 infections;
- hPIV-3 causes infection generally associated with pneumonia and bronchiolitis, involving swelling from inflammation in the smallest airways in lungs. It, regularly, causes infections in the spring and early summer, but it appears throughout the year.
- hPIV-4 (A or B) is rarer than the other one, in fact only a small number of studies have reported on the isolation or epidemiology of this viral strain. Unlike the others, there are no known seasonal patterns[81].

It is, also, important to underline that the four parainfluenza viruses are divided into two different genera: parainfluenza types 1 and 3 belong to the *Respirovirus* genus, and parainfluenza types 2, 4 (A and B) belong to the *Rubulavirus* genus. In general, hPIVs possess a genome composed by a non-segmented, negative sense, single-stranded RNA and they present the same viral protein asset and envelope composition previously described for NDV (Figure 1.18). They share, also, the same lifecycle organization which is common for all paramyxoviruses[69, 81] (Figure 1.19).

1.4.3.2 hPIVs-HN structure and catalytic/active site (Site I)

Hemagglutinin-neuraminidase of human parainfluenza viruses (hPIVs-HN) is a tetrameric glycoprotein with a crucial role in different phases of the viral lifecycle. Each subunit is composed, as influenza neuraminidase and NDV-HN, by four different domains: globular head (catalytic) domain, a "stalk" domain, a transmembrane domain and a cytoplasmic domain. In particular, HN of hPIV-3, which shares 24% of sequence identity with NDV-HN, is the only crystallized protein among hPIVs[81, 82]. Instead, no crystal structures of hPIV-1 or hPIV-2, but only a homology model of hPIV-1, constructed on the basis of hPIV-3 structure, has been described in literature[4]. Lawrance and coworkers[82], in 2004, obtained the crystal structure of hPIV-3 in its dimeric form (PDB: 1v3d) and they defined the main structural characteristics. These key features, compared with those of NDV-HN are:

- The secondary structure generally well conserved, with variations in some of the loop lengths and in some other little regions;
- Five of the seven cysteine residues present in its structure are conserved in NDV-HN;
- Ca^{2+} ion, also present in NDV-HN, is located in a specific loop;

- One glycosylation site (Asn351) is conserved from hPIV-3-HN to NDV-HN. The protein present two additional glycosylation sites (Asn308 and Asn323), different from those of NDV-HN;
- The general conformation of the two monomers is very similar to that of NDV-HN monomers;
- In contrast to NDV-HN, the dimeric associations into the hexagonal and orthorhombic crystal structures are very similar.

While, from a careful analysis of the hPIV-3 HN catalytic site crystallized with DANA, some peculiar characteristics can be resumed (Figure 1.27):

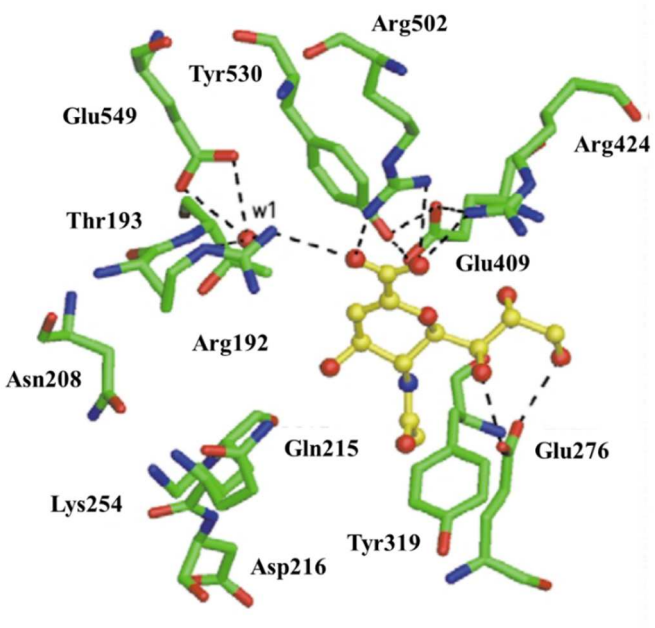

Figure 1.27 hPIV-3 HN active site, crystallized with the inhibitor DANA (From Lawrence, 2004).

- **C1-C3 portion**: there is the arginine triad (Arg192, Arg424, and Arg502) well interacting with the carboxyl group and Tyr530 with its hydroxyl group very close to the C1-C2 bond, interacting with Glu409;
- **C4 portion**: this pocket is a large hydrophobic pocket and the hydroxyl group at C4 of DANA do not give any interaction with the active site residues. It is well known that this region could accommodate large hydrophobic substituents, as demonstrated by a couple of recent studies[3, 5]. In fact, the presence of a large cavity at C4 (216-cavity) which is locked by a loop called "216 loop" (from amino acidic residue 210 to 221), gives some flexibility to the enzyme active site permitting the accommodation also of the molecule with bulky groups[83]. This 216-cavity seems to be a peculiarity of

hPIV-3 HN, even if, at the moment, there are no crystal structures of the other hPIVs-HN.

- **C4/C5 portion**: Lys 254 (corresponding to Lys236 of NDV-HN) is hydrogen bonded with Asn208 and *via* a water molecule with Asp1. It could also interact with some C4 bulky substituents[3].
- **C5 portion**: the C-5 pocket region could accommodate the acetyl moiety: the methyl group gives a hydrophobic interaction with the aromatic ring of Tyr319. This region could also accommodate bulkier substituents, such as the isopropyl group of BCX-2798 (Figure 1.26).
- **Sidechain portion**: The glycerol chain interacts with the conserved Glu276.

Considering the other hPIVs-HN, recent experiments, supported by simulation data on the homology model, demonstrated that hPIV-1 HN active site presents some peculiar differences if compared to that of hPIV-3 HN, reflecting, also, the different inhibitory effect exploited by the tested inhibitors[4].

1.4.3.3 hPIVs-HN second sialic acid binding site (Site II)

Finally, it is important to report a recently discovered feature regarding both hPIV-1 and hPIV-3 HN. It seems that they possess some "hidden second sialic acid binding sites" at the dimer interface revealed performing some mutagenesis experiments. This is an important discovery, because, while it is well known, that NDV-HN contains two distinct receptor binding sites, it has never been clarified if other viruses of the genera *Respiravirus* and *Rubulavirus* presented this peculiarity. In this regard:

- In **hPIV-3** a second sialic acid binding site was not identified through the simple analysis of the crystal structure, but it needed some deep investigations. In fact, some published data, from biochemical and computational studies proposed a second sialic binding site positioned in correspondence of Asn552 at the dimer interface (very close to the Site I)[84, 85]. It resulted sensible, as Site I, to DANA but insensible to Zanamivir and it is involved in fusion promotion activity[84]. The existence of this site was sustained by some crystallographic data obtained performing some difluorosialic acid analogues experiments[86]. On the contrary, in some recent works, Alymova and coworkers[87, 88] belittled the presence of a second binding site close to Asn552, because this residue resulted distant from the location of the conserved hydrophobic pocket typical of NDV-HN Site II and capable to accommodate acetamido group. They alternatively, proposed and demonstrate the presence of a new Site II masked by a

glycosylation at position Asn523 which correspond to the same site in NDV-HN and it is in close proximity of the previously cited hydrophobic pocket, formed by Leu174, Thr186, Val187 and Phe563 (corresponding to Phe156, Thr168, Phe553 and Leu561 of NDV HN). In addition, Arg173, as Arg516 of NDV HN, seems to be important in the interaction with carboxylate group[87, 88]. The unmasking of this site (mutating the corresponding residue) lead to a decreasing in infection multiplicity in cell culture but an increase of infectivity *in* vivo[88]. Anyhow, further investigations on the effect and the nature of these mutations are needed.

- In **hPIV-1** it was, at first, proposed the presence of a putative Site II in correspondence of Asn523 of naturally occurring mutants[89]. Contrarily, mutations in this site seem to not affect the fusion promotion activity and the grow kinetics. More recently, Alymova[87, 90] proposed (as for hPIV-3) the presence of a masked (by a glycosylation) second sialic acid binding site at Asn173 (activated after the interaction of substrate or substrate analogues at Site I). It has been demonstrated that this site is located in correspondence of the analog in NDV-HN: the hydrophobic pocket is composed by Leu176, Leu555, Phe563, and Leu521 (which would correspond to Phe156, Phe553, Leu561, and Val517 of NDV-HN). In addition, the key residue Arg516 in NDV-HN, which interacts with the sialic acid carboxylate group, is conserved in hPIV-1 HN (Arg520)[87].

  The mutated strain at this glycosilation site (N173S) remain sensitive to BCX-2798 (Figure 1.28) for neuraminidase activity but they were more than 10,000-fold less sensitive to the compound in hemagglutinin inhibition tests if compared to wild-type (WT)[87] (Table 1.3).

Virus (hPIV-1)	HA activity (IC_{50} µM)	NA activity (IC_{50} µM)	Growth in cells (EC_{50} µM)
WT	0.11 ± 0.020	0.06 ± 0.03	1.3 ± 0.040
N173S	>1000	0.08 ± 0.03	6.5 ± 0.30

Table 1.3 *HA, NA and growth cell inhibition observed in wt and N173 mutant strains.*

The advent of this theory, indicating that hPIVs could utilize Site II for binding, might change the strategy for new HN inhibitors design. In addition, the recently obtained results on NDV-HN[77], about the engagement of site II in fusion promotion activity, seem to be applicable to all paramyxoviruses[77, 84, 85]. In fact, it has been hypothesized that, also in hPIV-HN, the conformational changes could be efficiently transmitted from the head to the stalk domain of

the protein. Altogether, these findings supported the biological role and the importance of Site II. Nowadays, some naturally evolved mutants, lacking the glycosylation site and consequently showing a second binding site, has been isolated. In fact, in a relatively recent work[88], hPIV-3 mutants exhibiting the loss of the *N*-linked glycan at Asn523 were found in one to three clones (ten clone total) in four human samples, confirming the circulating of viruses presenting the unmasked second binding site in nature. So, their clinical relevance could be prominent, but it is not yet clarified[88].

1.4.3.4 Studies on hPIVs-HN inhibitors

BCX-2798 was one of the firstly reported, potent and specific, hPIVs-HN inhibitors. It was designed starting from the crystal structure of NDV-HN and it resulted in a very potent neuraminidase and hemagglutinin activity inhibitor against all the hPIVs, showing substantial differences in IC_{50} values passing from one strain to another, ranging from 0.020 to 20 μM for neuraminidase inhibitory activity (NI) and from 0.10 to 4.8 μM for hemagglutinin inhibitory activity (HI)[2, 4, 5, 91-93]. Successively, in some recent works, a new family of BCX-2798 derivatives has been synthesized. They were C4 triazole substituted compounds and they have been designed considering the previously described 216 cavity in hPIV-3 (Figure 1.28). These inhibitors show IC_{50} values against hPIV-3 of 2.7 μM (NI) and 1.5 μM (HI)[3, 5, 83]. Finally, a very recent study demonstrates the presence of a previously unexplored pocket adjacent to C3 position of hPIV-3 HN that is occluded after ligand engagement. This discovery could open the possibility to develop new classes of C3 substituted inhibitors[94]. It is not yet known if this feature is common to all paramyxoviruses HNs, such as NDV-HN.

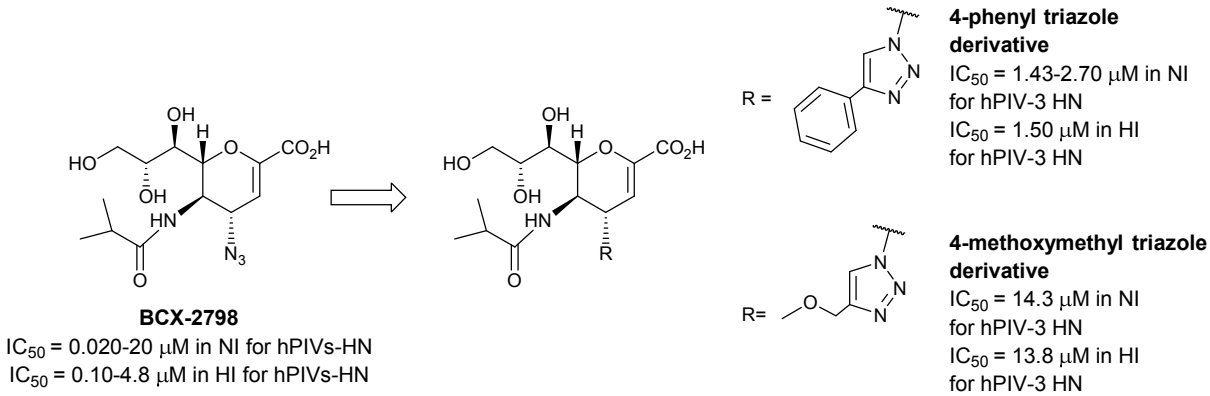

Figure 1.28 *Representation of BCX-2798 and two examples of its C4 substituted triazole derivatives.*

1.5 Mammalian sialidases

Mammalian sialidases are enzymes involved in different crucial biological processes, including the regulation of cell proliferation and differentiation, control of cell adhesion and migration, metabolism of gangliosides and glycoproteins, immune system cells function, receptor remodeling, remyelination processes and tumors. They are encoded by different genes and classified, as anticipated in the first part of this introduction, in lysosomal (NEU1), cytosolic (NEU2), plasma membrane (NEU3) and mitochondrial/lysosomal/intracellular membranes (NEU4) sialidases. All these proteins differ in their subcellular localizations, optimal pH, kinetic properties, responses to external stimuli and substrate specificities. Even if, there seems to be little overlap in function of the individual sialidases, they share a common mechanism of action[11]. In detail:

- NEU1 has a lysosomal/endosomal localization with an involvement in cell-surface molecules recycling;
- NEU2 has a cytosolic localization with a still unknown function. It has been hypothesized an involvement in muscle cell differentiation and tumoral processes. It is the only crystallized human sialidase[11, 18] (PDB: 1snt);
- NEU3 is plasma membrane sialidase that is specific for gangliosides and it is involved in cell signaling, apoptosis and cell-cell contacts;
- NEU4 has a lysosomal, mitochondrial and endoplasmic reticulum localization and it is, probably, involved in different physio-pathological processes, such as differentiation (neuronal differentiation) and cancer cells metastasis[11, 15, 95].

All the structural information has been collected thank to the crystal structure of NEU2. Indeed, structural models of NEU1, NEU3, and NEU4 have been generated by molecular replacement based on the atomic coordinates of the NEU2 crystal structure (homology modeling)[96].

1.5.1 Human NEU3 (hNEU3)

Now, human NEU3 sialidase will be considered, since its extracellular localization, it can be well compared with viral envelope neuraminidases. This protein shows a high level of sequence identity with NEU2 and, together with NEU4 and NEU1, shares the same β-barrel structure (Figure 1.29) as demonstrated by homology modeling[96]. The NEU3 active site (as in other NEUs), presents some interesting characteristics:

- **C4 portion:** Mammalian sialidases present only a small cavity in correspondence of C4 position, formed by invariant residues (Glu43, Arg45, Asp50, Asn88 for NEU3).

This pocket is capable to accommodate only a low range of small substituents (hydroxyl group of DANA or guanidino group of Zanamivir)[34, 53, 96].

- **Sidechain portion:** A very large pocket is present in correspondence of the sidechain (formed by the conserved residues Val222, Val224, Pro247, and His277 for NEU3), so large substituent attached at C7/C9 of DANA backbone could be efficiently accommodated[34, 97].

Concerning its biological function, it is important to underline that this enzyme is able to modify the ganglioside pattern, not only of the cells where it is located, but also of adjacent cells, suggesting a possible involvement in cell-to-cell interactions. Another noteworthy characteristic of this specific plasma membrane enzyme, is the connection to viral contagion: in fact, during virus (for example NDV) infection sialic acid-containing molecules act as receptors, so it may be reasoned that an extensive modification of the cell-surface ganglioside pattern, induced by the overexpression of NEU3, may interfere with the virus-host interaction[11].

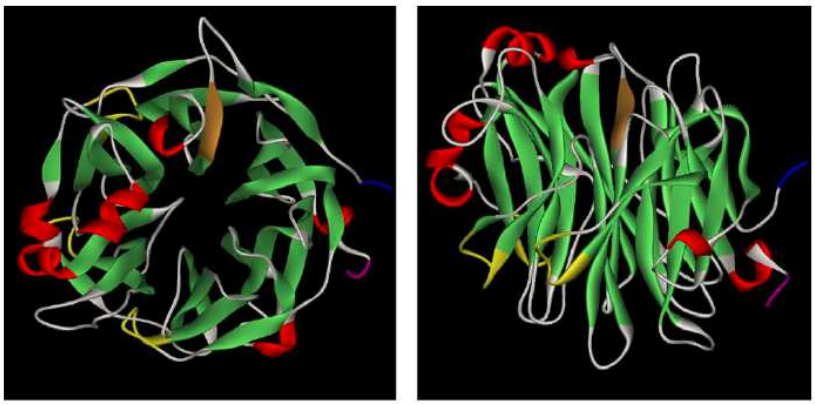

Figure 1.29 *3D structure of hNEU3 obtained from homology modeling (starting from NEU2 structure) (Magesh et al., 2006).*

1.5.2 Specific hNEU3 inhibitors

In the last years, selective inhibitors for NEU3 have been identified in a library of DANA analogues where oxime- and amino-linked aromatic groups replaced the glycerol side chain. One inhibitor resulted in a high inhibitory activity and selectivity against hNEU3, showing an IC_{50} value in micromolar range[34, 98]. Successively, considering that the one of the most active viral inhibitors against hNEU3 is Zanamivir (IC_{50} = 4.00 μM)[34, 41, 97] and the importance of the large C9 cavity, two new potent and selective hNEU3 inhibitors have been, very recently, proposed (Figure 1.30). They showed an IC_{50} value of 0.58 μM and 0.61 μM, respectively[34].

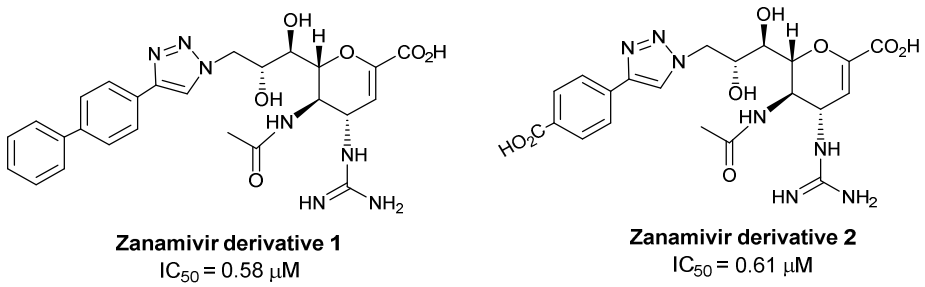

Figure 1.30 *Two C9 substituted Zanamivir derivatives, resulted in potent and selective hNEU3 inhibitors.*

2. AIM OF THE WORK

My PhD work, detailed in the next chapters, is a part of a great, stimulating and ambitious project directed to the development of new and selective Neu5Ac derivatives as inhibitors of sialidases (neuraminidases) and haemagglutinin-neuraminidases of bacteria, viruses, and mammalians. This hard-working aim can be achieved through a multidisciplinary approach which combines the use of a) chemical synthetic procedures b) computational docking studies and c) biochemical activity assays. More in detail, I focused my three years PhD work on the study and development of specific and selective inhibitors directed versus a specific sialidase, the hemagglutinin-neuraminidase of NDV (NDV-HN), not only to obtain more potent antiviral molecules against this specific virus but, also, to collect important information about its highly flexible active site.

At this purpose some specific objectives have been defined:

1. Synthesize and fully physico-chemical characterize some new inhibitors belonging to the two classes of the 2,3-unsaturated and 3,4-unsaturated Neu5Ac derivatives, using also the support of rational design;
2. Set-up a smart biological screening of the synthesized inhibitors based on IC_{50} values calculations, in order to select the most potent compounds;
3. Extend the biological evaluation of the most active molecules;
4. Perform some computational docking simulations to investigate ligand-enzyme interactions.

To achieve these ambitious goals, I have also planned to collaborate with other national and international research groups, such as the molecular modeling group of Prof. L. Olsen at the University of Copenhagen and the Istituto Zooprofilattico Sperimentale delle Venezie direct by Dr C. Terregino.

Overall, the collected data could, finally, help to clarify the role of HN inhibitors in modulating the three main HN functions: a) neuraminidase b) hemagglutinin and c) fusion promotion activities. Furthermore, considering the high similarity of some key amino acids involved in the catalytic process within paramyxoviruses (see Introduction section), the acquired information on NDV-HN could also be useful to better understand the role of hemagglutinin-neuraminidase of human parainfluenza viruses.

3. RESULTS AND DISCUSSION

In this chapter, the results obtained during my 3 years PhD project, finalized to improve the knowledge on sialidase/inhibitor interactions and to develop new and potent inhibitors against NDV-HN, will be presented and discussed. Main attention will be focused on two different classes of compounds: some 2,3-unsaturated DANA analogues and the 3,4-unsaturated derivatives of Neu5Ac. For clarity, the collected data, including synthetic protocols, biological evaluations and computational studies will be divided in three different sections:

- In the first section, an interesting study on the influence of the C5 substituents on the inhibitory activity of the 2,3-unsaturated DANA (Figure 3.1) analogues, as potent and reversible NDV-HN inhibitors, will be described. This goal has been accomplished by a chemical synthesis approach and an in-depth biological investigation, also supported by docking simulation studies, in collaboration with the molecular modeling group of Prof. L. Olsen of the University of Copenhagen.
- In the second section, new C4 and C5 modified 2,3-unsaturated derivatives will be discussed. After the description of preliminary computational screening results, necessary to select the best molecules to be synthesized, the relationship between C4/C5 modifications and biological inhibitory activity will be elucidated.
- In the last section, the attention will be concentrated on the 3,4-unsaturated molecules (Figure 3.1), as both potential irreversible inhibitors of NDV-HN and/or useful intermediates for the synthesis of new 2,3 modified derivatives. Starting from the few literature data regarding their synthesis and biological activity[6, 7, 42], it has been decided to set up more efficient synthetic procedures to achieve these molecules. In addition, some important aspects concerning the attribution of the anomeric configuration of these compounds, their stability in protic solvents and the unexpected formation of an interesting synthetic intermediate, will be clarified. Finally, the biological inhibitory activity against NDV-HN and their selectivity will be illustrated.

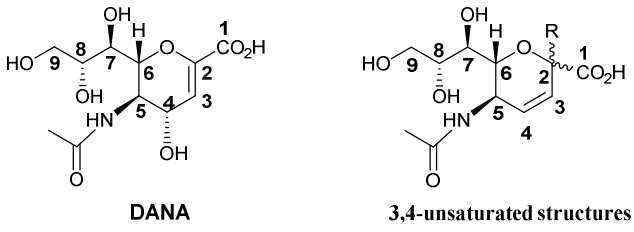

Figure 3.1 *Structures of DANA and 3,4-unsaturated derivatives.*

3.1 The 2,3-unsaturated derivatives: C5 substitutions

The 2,3-unsaturated derivatives of Neu5Ac (based on DANA backbone), as anticipated in the introduction, are deeply studied sialidase inhibitors[1-4, 34]. In particular, I focused my attention on the investigation of the inhibitory activity, on NDV-HN, of some C5 modified Neu5Ac glycals, having both a normal 4α or epimeric 4β configuration. The choice to study these modifications was based on an in-depth literature analysis, in fact, it was noteworthy, before my PhD thesis work, that the most active inhibitor towards NDV-HN was FANA (Figure 3.2), with an IC_{50} value of 1.9 μM[30]. In addition, previously published studies[2] demonstrated that an isopropylic chain at the C5 amido group could well fit inside the corresponding cavity in enzyme active site of NDV-HN and other paramyxoviruses (hPIVs-HN). In fact, the compound BCX-2798 (Figure 1.26), bringing this group at C5, showed a well assessed high inhibitory activity towards all hPIVs-HN (0.002-20 μM)[2, 92]. So, in order to define the more suitable C5 modification, considering the fluorofilic properties of C5 cavity (as showed for FANA), I decided to use fluorinate alkylic chains as substituents. Moreover, fluorine atoms insertion during inhibitor development both mimic the C-H linkage and give unique properties to these molecules[99-101]: they increase the inhibitor stability and bioavailability and they give a sort of "polar-hydrophobicity", permitting the stabilization of hydrophobic forces but also the formation of Van der Waals (VdW) and other weak interactions.
The synthetic protocols used to obtain these C5 perfluorinate inhibitors and their biological screening, will be reported below. Then, the evaluation of the C5 cavity fluorophilic properties achieved by the support of some docking studies, will be illustrated. Finally, some in-depth biological evaluations on selectivity of these inhibitors towards sialidases will be described, together with a cytotoxicity evaluation of the most active (and selective) one.

3.1.1 Chemical synthetic approach

At first, I set up two chemical protocols to achieve all the selected C5 substituted derivatives of DANA **1a**, compounds **1b,c**, **2a-e**, **3a** and **4a-c**). These two different synthetic protocols allowed to achieve, respectively:

- *Protocol A*. 4α and 4β perfluorinated derivatives (**2a-c** and **4a-c**, respectively) were achieved using a protocol involving a *N*-transacylation reaction, a procedure recently, published by our laboratory[102-104]. This reaction permits the achievement of *N*-perfluorinated derivatives with a one-pot rapid and chemoselective way (Scheme 3.1).

- <u>*Protocol B*</u>. Longer 4α perfluorinated derivatives (**2d,e)** and 4α unfluorinated molecules (**1b,c)** were achieved by a normal acylation of the deprotected amine, obtained from a laborious pathway[4] (Scheme 3.2).

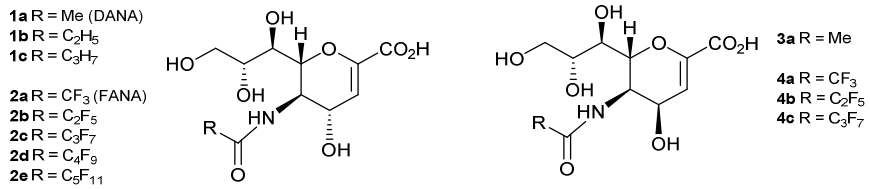

Figure 3.2 C5 *substituted 4α and 4β derivatives synthesized in my thesis work.*

3.1.1.1 Synthesis of the C5 modified 2,3-unsaturated derivatives

In order to synthesize all the inhibitors above cited, I started from a common precursor the glycal **5**[105], already described in the literature. The synthesis of 4α compounds **1a** and **2a-c** was achieved as reported in scheme 3.1. DANA **1a** was obtained after a rapid two-step hydrolysis procedure directly accomplished on intermediate **5**[105], using Zemplén reaction followed by saponification with K_2CO_3 in MeOH/H_20 (10:1, v/v)[106-108]. Perfluorinated compounds **2a-c** were achieved by basic *N*-transacylation performed on precursor **5**[105], using the appropriate perfluorinated anhydride and Et_3N in CH_3CN, through the intermediates **6a-c** and successive two-step hydrolytic procedure. The hydrolysis of **6b,c** was identical to that above described, instead that used to achieve **6a** needed Et_3N in MeOH and H_20 mixture[109], for the presence of a labile trifluoroacetyl amido group (Schema 3.1).

On the other hand, the synthesis of the corresponding 4β epimers **3a** and **4a-c** was achieved *via* intermediate **7**[110] formation achieved from **5**[105] through three synthetic steps: a) oxazoline formation, b) ring opening and c) re-acetylation of the 4β hydroxyls[109-111]. The compound **3a**, with a normal *N*-acyl group was obtained after two-step hydrolytic procedure applied directly on compound **7**[110], while inhibitors **4a-c** were yielded after *N*-transacylation of intermediate **7**[110], followed by selective hydrolysis (Scheme 3.1). All the final compounds were obtained in good total yields (71-87%) after final hydrolysis. They were purified by preparative HPLC and fully characterized using 1D and 2D NMR analysis and MS-spectrometry for the correct structures attribution. The presence of the perfluorinated group in the molecule was confirmed by the well defined coupling constant values between the amidic carbonyl carbon (~159 ppm) and the α-carbon fluorine atoms (37 Hz for **2a** and **4a** and 26 Hz for **2b,c** and **4b,c**).

The two perfluorinated 4α compounds **2d,e** were, otherwise, synthesized starting from the known intermediate **9**[4] obtained, according to literature[4], from the common glycal precursor **5**[105] after few steps (Scheme 3.2). Then, after acylation of **9**[4] with the opportune perfluoroacyl

chlorides in Et_3N using CH_2Cl_2 and successive deprotection, compounds **2d,e** were achieved. Finally, following the same protocol (using unfluorinated acyl chlorides), I accomplished the synthesis of the 4α unfluorinated analogues **1b,c** to compare the inhibitory activity of these compounds to the corresponding fluorinated analogues (**2b,c**). These studies should give me additional information on the role of fluorine in inhibitor-active site interactions.

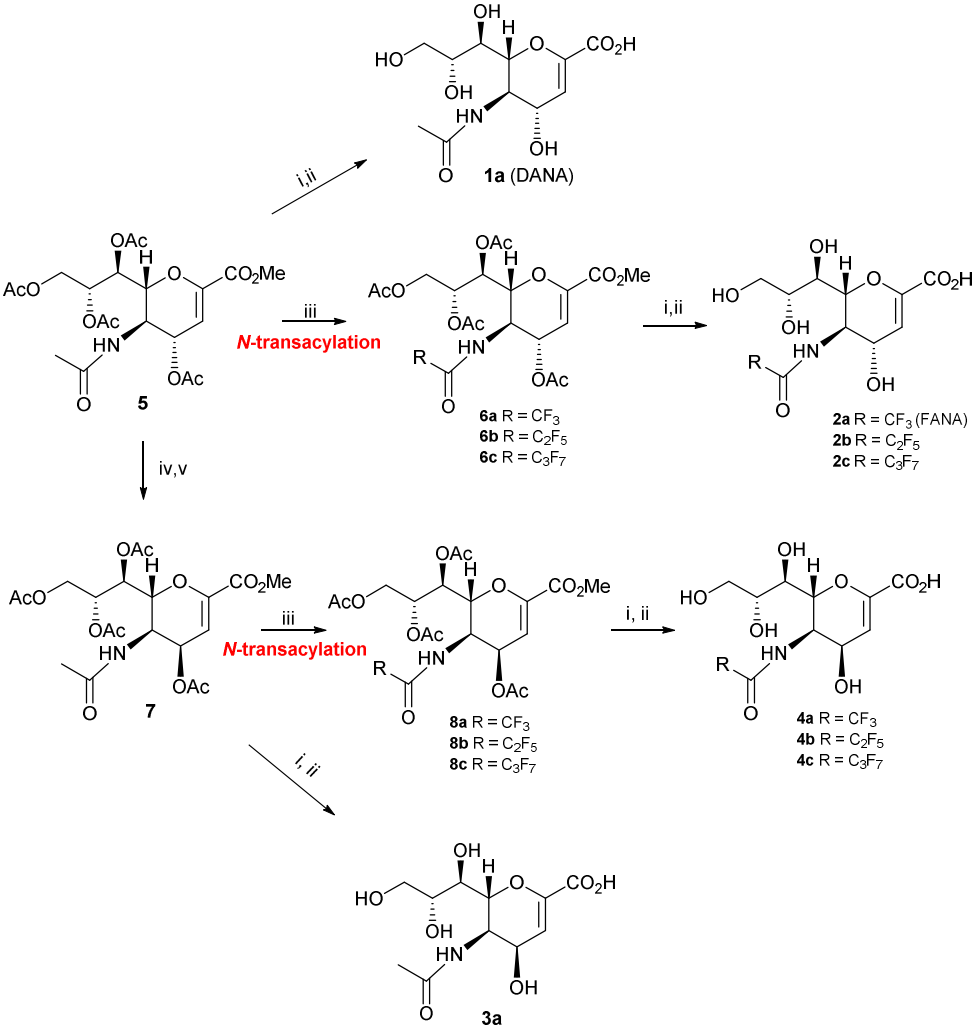

Scheme 3.1 *Synthesis of compounds **1a, 2a-c**, **3a** and **4a-c**. Reaction conditions: i) NaOMe, MeOH, 23°C, 1h, 80%; ii) for **5**, **6b,c** and for **7**, **8b,c**: K_2CO_3, MeOH/$H_2$0 (10:1, v/v), 23°C, 12h, 71-75% and for **6a** and **8a**: Et_3N, MeOH/$H_2$0, 23°C, 12h, 87%; iii) perfluorinated anhydride, Et_3N, CH_3CN, 0°C to 135°C, 5-15 min, 78-82%; iv) BF_3Et_2O, CH_2Cl_2, 80°C, 15 min; v) Ac_2O, Et_3N in $H_2$0 23°C, 12h, 92%.*

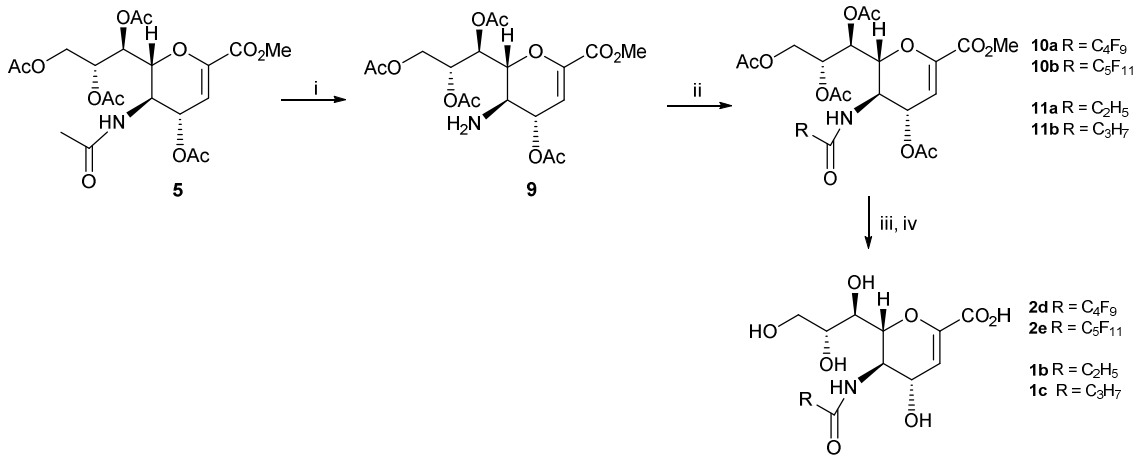

Scheme 3.2 *Synthesis of compounds **2d,e** and **1b,c.** Reaction conditions: i) see Ref. [4]; ii) perfluorinated acyl chloride or normal acyl chlorides: Et_3N, CH_2Cl_2, 0°C to 23°C, 3-5 h, 75-78%; iii) NaOMe, MeOH, 23°C, 1h, 80%; iv) K_2CO_3, MeOH/H_20 (10:1, v/v), 23°C, 6-24h, 71-72%.*

3.1.2 Neuraminidase inhibition assay

After the synthesis and the full physco-chemical characterization of all the obtained molecules **1a-c, 2a-e**, **3a** and **4a-c,** in order to investigate their inhibitory potency towards HNs, I decided to perform a fluorimetric neuraminidase inhibition assay (NI) on NDV-HN.

3.1.2.1 Neuraminidase inhibition assay (NI) on NDV-HN

The NI assay was performed on all the free final compounds **1a-c, 2a-e**, **3a** and **4a-c**, using *in toto* purified active NDV and 4-methylumbelliferyl α-D-*N*-acetylneuraminic acid (4-MU-Neu5Ac) as fluorescent substrate[112]. The obtained results were expressed as IC_{50} values, corresponding to the concentration causing the 50% inhibition of neuraminidase activity, and calculated plotting the percentage of inhibition against the concentration of each compound. The final values were reported in Table 3.1.

At first, I confirmed the DANA **1a** and FANA **2a** IC_{50} values (14.6 μM and 2.42 μM, respectively), which are in agreement with the literature data (13 μM and 1.9 μM, respectively)[30]. Then, I performed the same assay on NDV-HN for all the synthesized compounds (Table 3.1). Analyzing, in detail, the results, I found that perfluorinated compounds belonging to 4α (**2a-c**) and 4β series (**4a-c)** showed a very interesting and peculiar trend concerning their inhibitory potency and it is strictly related to the chain length. In fact, moving from trifluoroacetamido (**2a** and **4a**) to the corresponding pentafluropropionamido derivatives (**2b** and **4b**) the inhibitory potency decreases, passing from IC_{50} values of 2.42 μM and 4.16 μM (for **2a** and **4a**, respectively) to five times higher ones: 11.6 μM and 20.8 μM (for **2b** and **4b,** respectively). Interestingly, the NI activity was, successively, restored passing

from pentafluoroproprionamido (**2b** and **4b**) to heptafluorobutyrramido derivatives (**2c** and **4c**) reaching an inhibitory potency of 3.73 µM and 6.38 µM, respectively, not statistically different to that of their trifluoroacetyl homologues, FANA **2a** and its 4β epimer **4a**.

Compound	IC_{50} (µM)[a]	Compound	IC_{50} (µM)[a]	Compound	IC_{50} (µM)[a]
FANA 2a	2.42 ± 0.29	**4a**	4.16 ± 0.48	**DANA 1a**	14.6 ± 1.2
2b	11.6 ± 1.4	**4b**	20.8 ± 2.9	**1b**	25.7 ± 4.8
2c	3.73 ± 0.11	**4c**	6.38 ± 0.87	**1c**	46.2 ± 3.0
2d	43.0 ± 3.4			**3a**	12.2 ± 1.6
2e	151 ± 20				

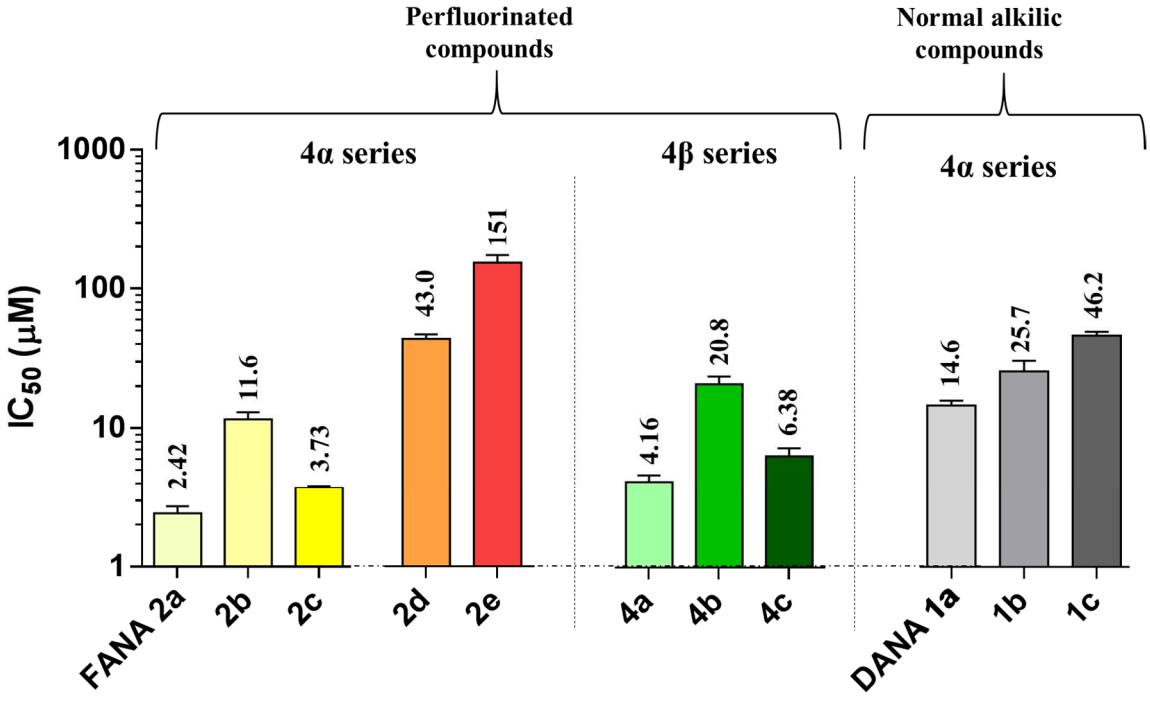

Table 3.1 *NI IC_{50} values of perfluorinated 4α and 4β inhibitors and the 4α unfluorinated ones on NDV-HN.*

[a]Each value represents the mean of three independent experiments carried out in triplicate.

In contrast, this C5 length dependent trend was not observed in the 4α unfluorinated compounds (**1a-c**), which showed a progressive decrease in inhibitory activity passing from DANA **1a** (14.6 µM) to the propionyl derivative **1b** (25.7 µM) and from **1b** to its butirryl homologue **1c** (46.2 µM).

Taken together these results confirmed that the C5 cavity is large and could accommodate bulkier groups than acetyl or trifluoroacetyl ones, but the only presence of a hydrophobic chain is not sufficient to maintain a high inhibition level. In fact, the formation of additional

interactions, ensured by fluorine atoms, is required. These hypotheses were supported and confirmed by some rigid docking studies (see paragraph 3.1.3).

Another important observation regards the similar grade of inhibitory activity showed by 4α and 4β series if compared together (Table 3.1). These results demonstrated that, considering the well documented large dimensions of the C4 cavity in NDV-HN[5, 53], an inversion of hydroxyl geometry cause, only, a limited reduction in inhibitory potency, except for β epimer **3a** (12.2 μM) which maintain an IC_{50} value not statistically different to that of its α analogue DANA **1a** (14.6 μM). In light of this, I could speculate that this slight reduction observed passing from 4α to 4β fluorurated derivatives may be attributed to the C4 hydroxyl group involvement in some steric interactions, that could favor a better positioning of perfluorinated chains (of 4α derivatives) inside the C5 cavity.

Finally, focusing on the results obtained with longer perfluorinated chains derivatives **2d** and **2e**, as depicted in Table 3.1, the molecules showed a dramatic chain length-dependent decrease of inhibitory potency (43 μM and 151 μM, respectively). This suggested the difficulty of the active site to accommodate C5 substituents longer than heptafluorobutyryl amido one.

3.1.3 Docking simulation studies and further biological evaluations

Some rigid docking studies have been performed on compounds **1a** and **2a-c** using NDV-HN crystal structure (PDB: 1e8v), to better elucidate and explain the interesting trend above observed in fluorinated compounds. In fact, rigid docking permits to obtain, rapidly, some suggestions about the ligand/active site interactions maintaining a certain rigidity in active site amino acids[113]. I decided to use this technique because it could give me some useful information about the possible accommodation of the perfluorinated chain in C5 cavity and it could suggest the possible target amino acids. In addition, I decided to accomplish some further biological investigations on compounds **2a-c**, exploring their selectivity. Finally, on the most potent and selective compound, I performed a cytotoxicity test.

3.1.3.1 Rigid docking simulations on C5 substituted derivatives

4α erfluorinated compounds **2a-c**, were subjected to rigid docking simulations and the obtained results were compared with that of DANA **1a**. I started the computational studies performing a validation of the method quality. At this purpose, DANA **1a** was docked in NDV-HN active site (PDB: 1e8v) and the experimental binding mode could be reproduced (RMSD of 0.5 Å). In addition, the overall binding mode and the interactions resulted the same

as these previously reported in the literature for this compound[53]. Then, after the docking of FANA **2a**, the most stable pose was compared to that of DANA **1a** (Figure 3.3), observing that:

- The general binding mode is identical for both compounds, with exception for an additional interaction showed in FANA **2a** docking pose. In fact, trifluoroacetyl group seems to be able to interact with the hydroxyl group of Tyr299, giving some VdW interactions. The presence of these supplementary bond could explain the higher activity of FANA if compared to DANA.
- Both **1a** and **2a** showed the presence of a putative hydrogen bond between hydroxyl function at C4 and the carbonyl group of the amide at C5. The presence of this interaction could be essential for the correct C5 trifluoroacetyl orientation in the C5 cavity.
- **DANA 1a** showed a hydrogen bond between the second hydroxyl of the sidechain (at C-8) and Glu401, on the other hands in **FANA 2a** the same hydroxyl seems to lose this interaction, binding to the pyranosidic ring oxygen**.**

Moreover, I docked the two perfluorinated 4α derivatives **2b,c**, comparing their poses to that of FANA **2a**. It results clear that a modification in the entire inhibitor orientation occurred (Figure 3.3 and 3.4). I observed:

- For compounds **2b,c**, the breaking of the intramolecular hydrogen bond between oxygen at C4 and the carbonyl group at C5 present in FANA **2a**, probably to allow the correct accommodation of the longer fluorinated chains in the large cavity.
- In **FANA 2a** the first hydroxyl group of the sidechain (at C-7) interacts with Glu258 and the second one (at C-8) with the pyranosidic oxygen. Instead, in both compounds **2b** and **2c** the hydroxyl at C7 interacts with Glu401 and that at C8 seems to bind to Glu258, instead of the pyranosidic oxygen.
- The Van der Waals interaction with Tyr299, observed for **FANA 2a** (and essential to maintain its high activity), seems to be loss in both **2b** and **2c**. This event may be responsible of a reduction in inhibitory activity.
- Interestingly, **2c** showed an additional interaction performed by the terminal fluorine atoms of the C5 chain with Lys236. In fact, it seems to be able to reach the adjacent large C4 binding pocket, where this amino acid is located. This issue could explain the inhibitory activity improvement showed by compound **2c** if compared to derivative **2b**.

Taken together, these computational results tentatively explain the peculiar IC_{50} trend previously observed. In addition, these studies could clarify the improvement in inhibitory potency showed by perfluorinated groups when compared to alkylic chains, due to the formation of new key interactions. Finally, it should be stressed that compound **2c**, with its C5 heptafluorobutyrryl chain, is able to reach and interact with the key amino acid Lys236, which is located in the adjacent large C4 cavity. This issue indicates a possible involvement of this inhibitor in active site conformational changes, previously detailed in the "Introduction" chapter.

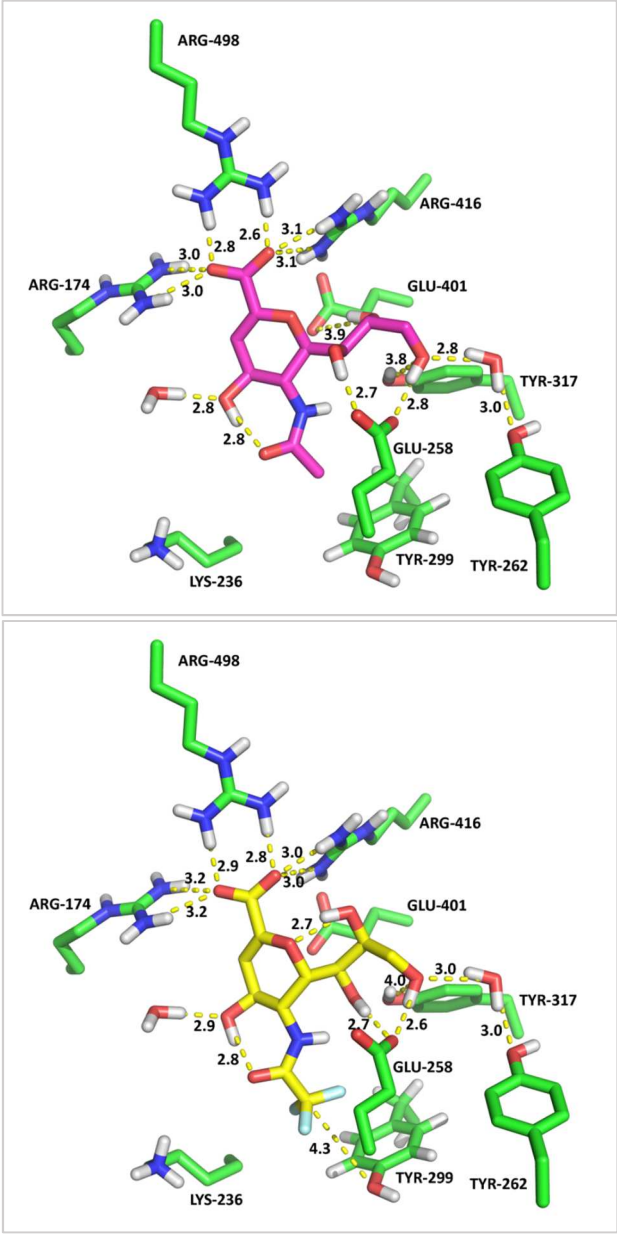

Figure 3.3 *Docking poses of compound **1a**, DANA and **2a**, FANA. The compounds are colored in: magenta (**1a**) and yellow (**2a**). The interactions between the inhibitors and the enzyme are showed as yellow dashed lines, and the distances are measured in Å. Amino acid numeration is kept as in the PDB crystal (1e8v)*

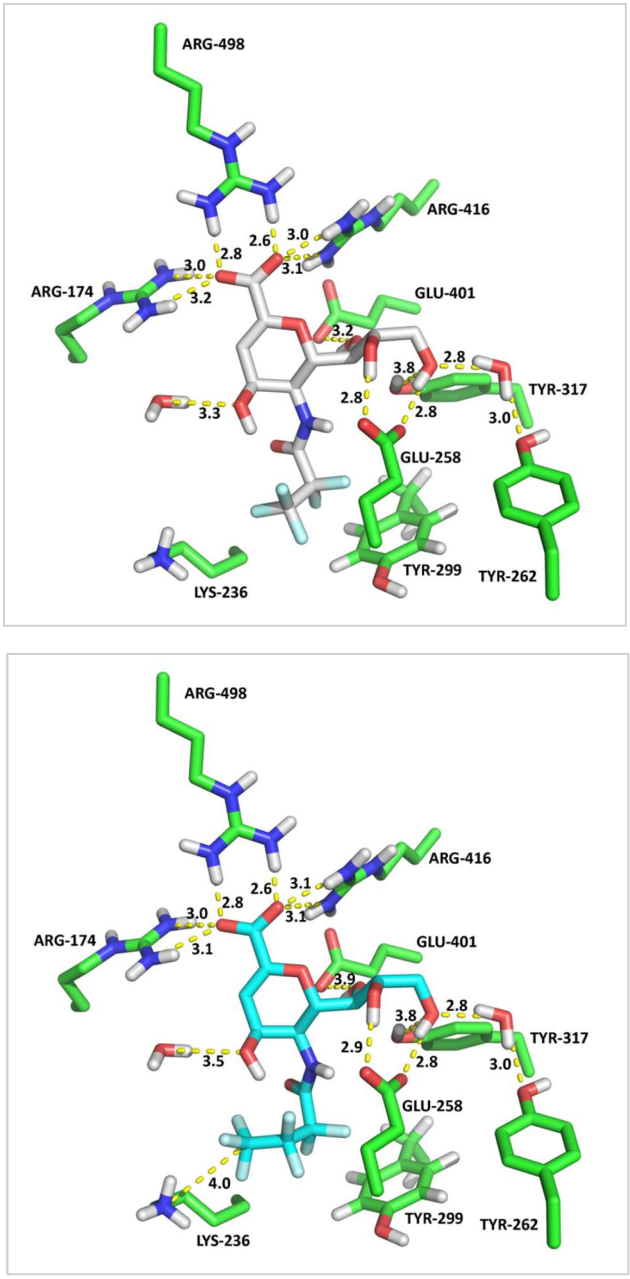

Figure 3.4 *Docking poses of compound **2b** and **2c**. The inhibitors are colored in: light grey (**2b**) and ciano (**2c**). The interactions between the inhibitors and the enzyme are showed as yellow dashed lines, and the distances are measured in Å. Amino acid numeration is kept as in the PDB crystal (1e8v).*

3.1.3.2 Neuraminidase inhibition assay on hNEU3: Preliminary studies on selectivity

I decided to evaluate whether the selected inhibitors **1a** and **2a-c** would affect the human sialidase activity. This is a fundamental issue, in fact the low selectivity of viral inhibitors (DANA, for example) is a great problem due to their ability to interact also with human sialidases, leading to unpredictable side-effects. I focused my attention specifically on the human sialidase NEU3 (hNEU3), firstly, because it could be easily reached by the hydrophilic inhibitors as it is exposed on the outer leaflet on the cell membrane. Secondly, becouse modifications of the ganglioside pattern, mediated by NEU3, may interfere with the virus-host interaction[11]. At this purpose, I performed, in collaboration with the biological unit of our research group, a preliminary test to evaluate neuraminidase activity on hNEU3. The fluorimetric assay provided the use of 4-MU-Neu5Ac as substrate and a protein extract from human embryonic kidney cells 293 (Hek293) overexpressing NEU3. Despite it is well known that the results obtained with this substrate could be different from that achieved using the natural glycolipidic one, I choose 4-MU-Neu5Ac because it allows to compare selectivity on different sialidases.

Compound	IC_{50} (μM) [a]
DANA 1a	3.90 ± 0.90
FANA 2a	3.80 ± 0.70
2b	>1000
2c	>1000

Table 3.2 *IC_{50} values of DANA and the perfluorinated compounds obtained in hNEU3 inhibition assay.*

[a]Each value represents the mean of three different experiments carried out in triplicate.

As shown, DANA has a micromolar activity around 4.00 μM (Table 3.2) similar to literature data on purified NEU3 (around 7.00 μM)[34, 98]. FANA has been tested on hNEU3, for the first time, showing inhibitory potency (3.8 μM) not statistically different from that of DANA. Thus, I can conclude that both DANA **1a** and FANA **2a** have a low selectivity towards hNEU3 and viral HNs. Compound **2b** and **2c** showed no inhibitory activity towards hNEU3, indicating that, the reduced dimension of C5 cavity of human sialidases, permits only the accommodation of small substituents. Taken together, these results permit to select compound **2c** as a good candidate inhibitor, due to the inhibitory potency (not statistically different to that of FANA on NDV-HN), and for its high selectivity.

3.1.3.3 Cytotoxicity test on compound 2c

I decided to perform, on the most promising inhibitor found inhibitor **2c,** an MTT assay using COS7 cells and, in order to investigate the role of fluorine atoms on cytotoxicity, I compared the results with those of DANA **1a**. I tested both DANA **1a** and inhibitor **2c** at two different concentrations (3.73 and 10 μM). As it shown in Figure 3.5, DANA give only a little but not significative cytotoxicity. On the other hand, cells treated with the inhibitor **2c** showed no citotoxicity at 3.73 μM (the IC_{50} of **2c** against NDV-HN) and 10 μM. These results confirmed the absence of cell toxicity in presence of the selective perfluorinated inhibitor **2c**, which could be considered a promising potent HN candidate inhibitor.

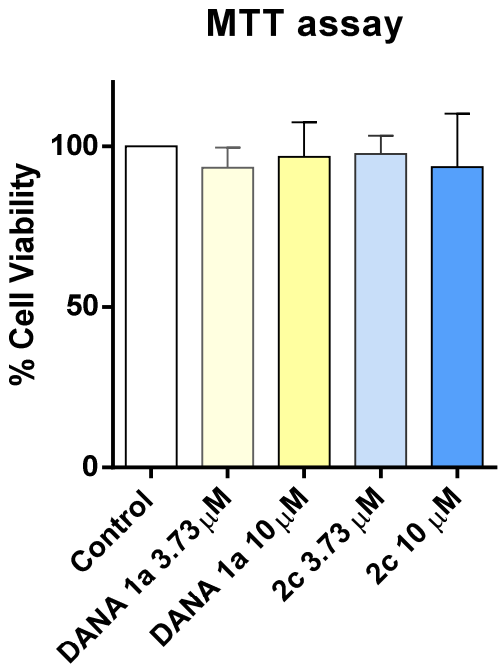

Figure 3.5 *Representation of MTT assay results (each value represents the mean of three different experiments carried out in triplicate).*

3.2 The 2,3-unsaturated derivatives: C4/C5 combined substitutions

In the previous section, I focused my attention on the contribution of the C5 perfluorinated substituents on the inhibitory potency of selective HN inhibitors. I observed that the addition, at the C5 position, of these perfluorinated chains it is important to increase the interactions with some amino acids present in the active site. Then, in order to find new more potent inhibitors, I thought to simultaneously functionalize also the C4 position, keeping in mind that the corresponding C4 cavity in paramyxoviruses is a very large and prevalently hydrophobic pocket.[53] I selected this position considering that some literature works reported the high inhibitory activity of C4 substituted DANA derivatives against hPIVs-HN and they described some key ligand/active interactions[3-5, 29, 114, 115]. However, only one work performed crystallographic studies on NDV-HN using C4 modified DANA analogues[74] and no C4 substituted inhibitors have been tested on this virus.

To find suitable C4 substituents, I set up, in collaboration with a research group of University of Copenhagen, a computational study to screen some different C4 modified derivatives, in order to discover C4 moieties that could well fit inside the corresponding pocket. Then, I synthesized and fully characterized some of the molecules selected by the docking study. Finally, I performed some biological assays to test their neuraminidase and hemagglutinin inhibitory activity towards NDV-HN and I evaluated also their selectivity towards human sialidases.

3.2.1 Docking simulation studies

In the setting-up of a rational design, docking simulation studies could represent a potent tool to screen a variable number of molecules to find substituents that could well fit inside enzyme active site pocket. In this type of studies, the availability of crystal structure of the protein with ligands resulted important. Thus, docking software are able to quickly predict the orientation of the ligand inside enzyme active site in order to quantify the binding, using shape and interactions (Van der Waals, electrostatic and hydrogen bonds). The sum of all these interactions is approximated by a docking score (GScore value), which represents potentiality of binding[116]. In light of this, I choose this smart tool to operate an initial screening on a large number of C4 substituted DANA derivatives.

3.2.1.1 Rigid and Induced-Fit docking simulations

The first purpose was to find the best C4 substituents which would better fit inside the corresponding binding pocket of the catalytic site, in terms of both dimension (bulky) and

polarity (hydrophobic). So, starting from this evidence, I performed a preliminary computational screening using NDV-HN structure crystallized with DANA (PDB:1e8v) in order to dock different C4 substituted compounds into its active site. This study revealed that compound **12a** (Figure 3.6) well satisfy all the requirements. More precisely, compound 12a showed a GScore value (-10.97 of kcal mol^{-1}) higher than DANA **1a** one (-9.33 kcal mol^{-1}), confirming, an increased free energy of binding and, thus, a better accommodation in enzyme active site of p-toluensulfonyl amido compound **12a**, with the formation of some new interactions in C4 pocket (Figure 3.6).

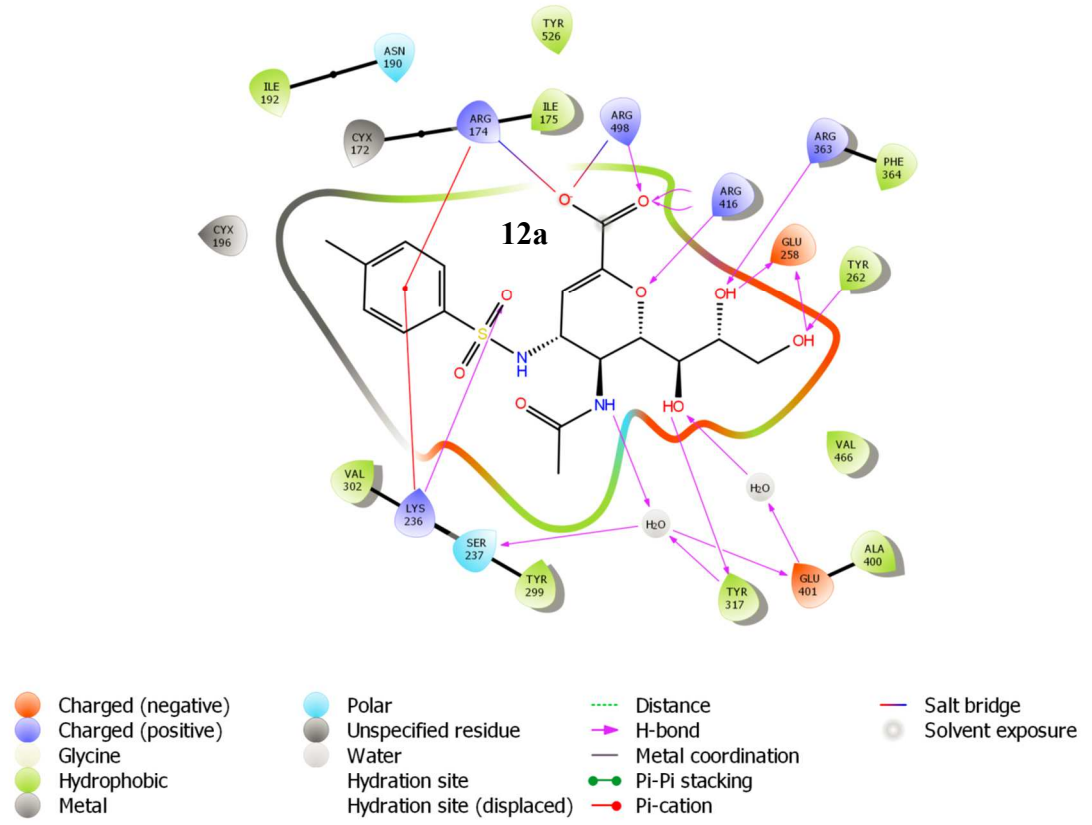

Figure 3.6 *Rigid docking interaction map of ligand **12a**. See the above legend for a complete description of all the elements presented in the scheme.*

After this preliminary analysis, to obtain a more reliable simulation of the possible interactions involved, I set up more detailed docking experiments on compound **12a**. At this purpose, I decided to perform an Induced Fit Docking (IFD) simulation, that, permits the bond flexibility of both the ligand and the amino acids around the active site. In my case this type of analysis allows me to better evaluate the effect of amino acids movement after the insertion of a large substituent at the C4 position. The simulation was performed as described in Material and Method (see paragraph 5.3.3) and the results confirmed those previously described by rigid docking. In fact compound **12a** showed a Gscore value of -11.03 of kcal mol^{-1} higher than that

of DANA **1a**, -10.28 kcal mol^{-1}. Then, I decided to perform a qualitative analysis of the IFD best scored poses (Figure 3.7, 3.8 and 3.9). Thus, the superimposition of DANA to its crystallographic pose, suggested that all the interaction with the active site were maintained, with a RMSD of 0.40 Å. Then, comparing IFD poses of both **12a** and DANA **1a** it seemed that, beyond the classical interaction common in both compounds, some additional ones, involving the C-4 group (Figure 3.8 and 3.9), were established:

- The sulfonyl oxygen of the p-toluensolfonyl amido group at C4 could give a hydrogen bond with Lys236;
- The aromatic ring, perfectly positioned inside the C4 cavity, formed a $\boldsymbol{\pi}$-cation interaction with Lys236 and Arg174, which are probably responsible of the stabilization of this hindering group inside the enzymatic pocket.

These preliminary results led me to postulate that compound **12a** could retain a high inhibitory activity on NDV-HN.

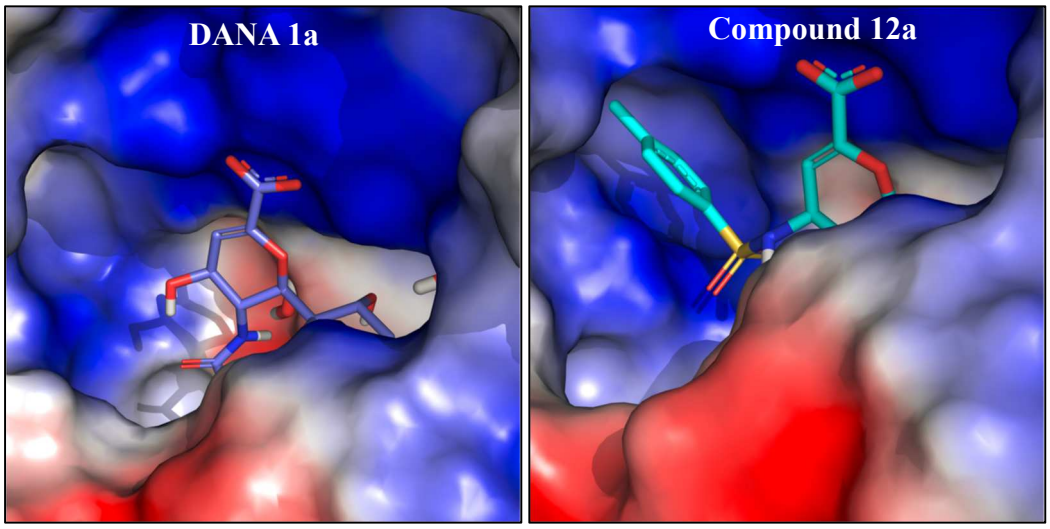

Figure 3.7 *Induced Fit Docking best poses for DANA **1a** (purple) and compound **12a** (cyano). The colours of protein surface reproduce the amino acid electrostatic properties: positively charged amino acids (blue); negatively charged amino acids (red); neutral residues (grey).*

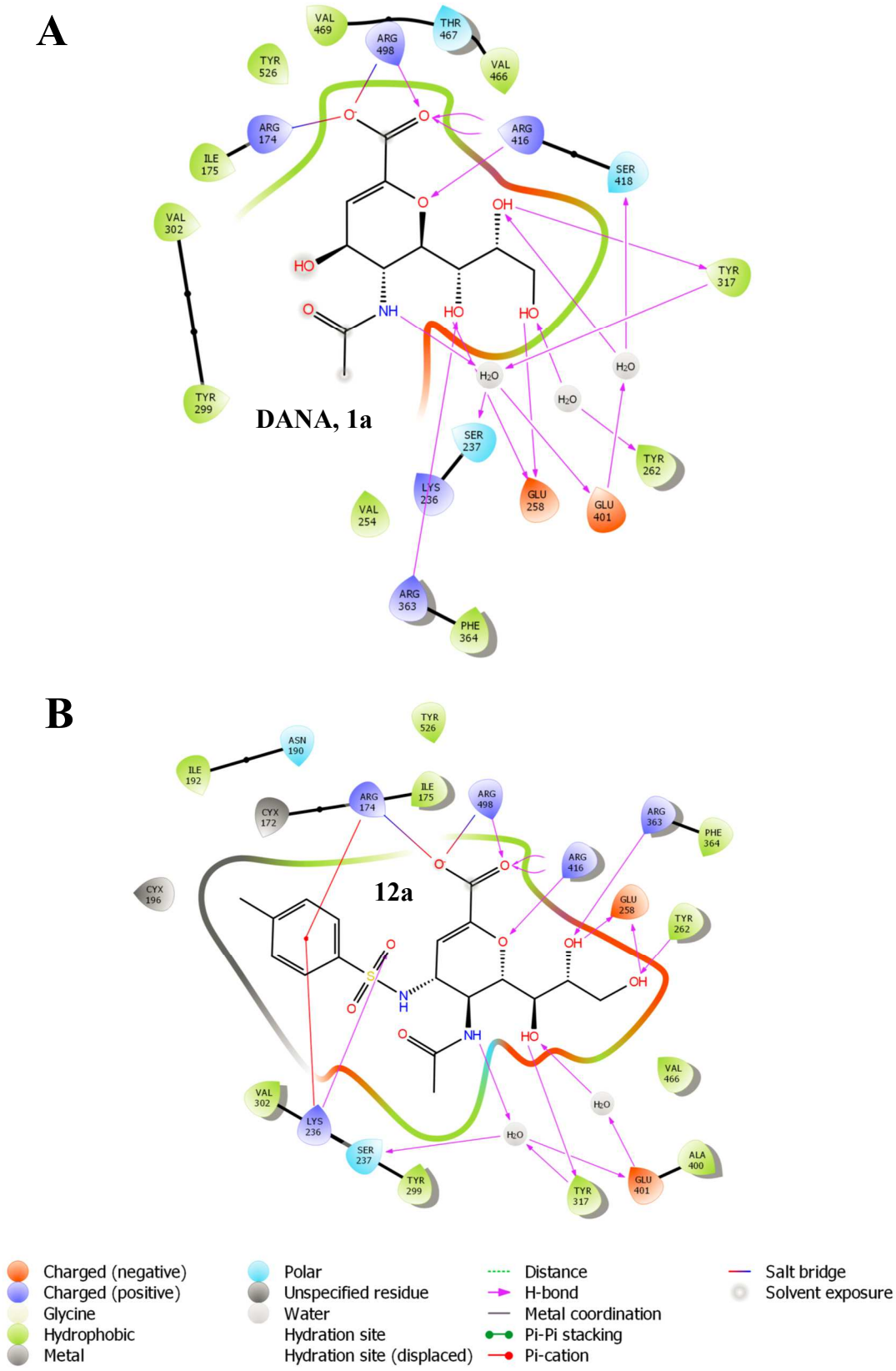

Figure 3.8 *Induced Fit Docking interaction map of DANA* ***1a*** *(up) and compound* ***12a*** *(down). See the above legend for a complete description of all the elements presented in this scheme.*

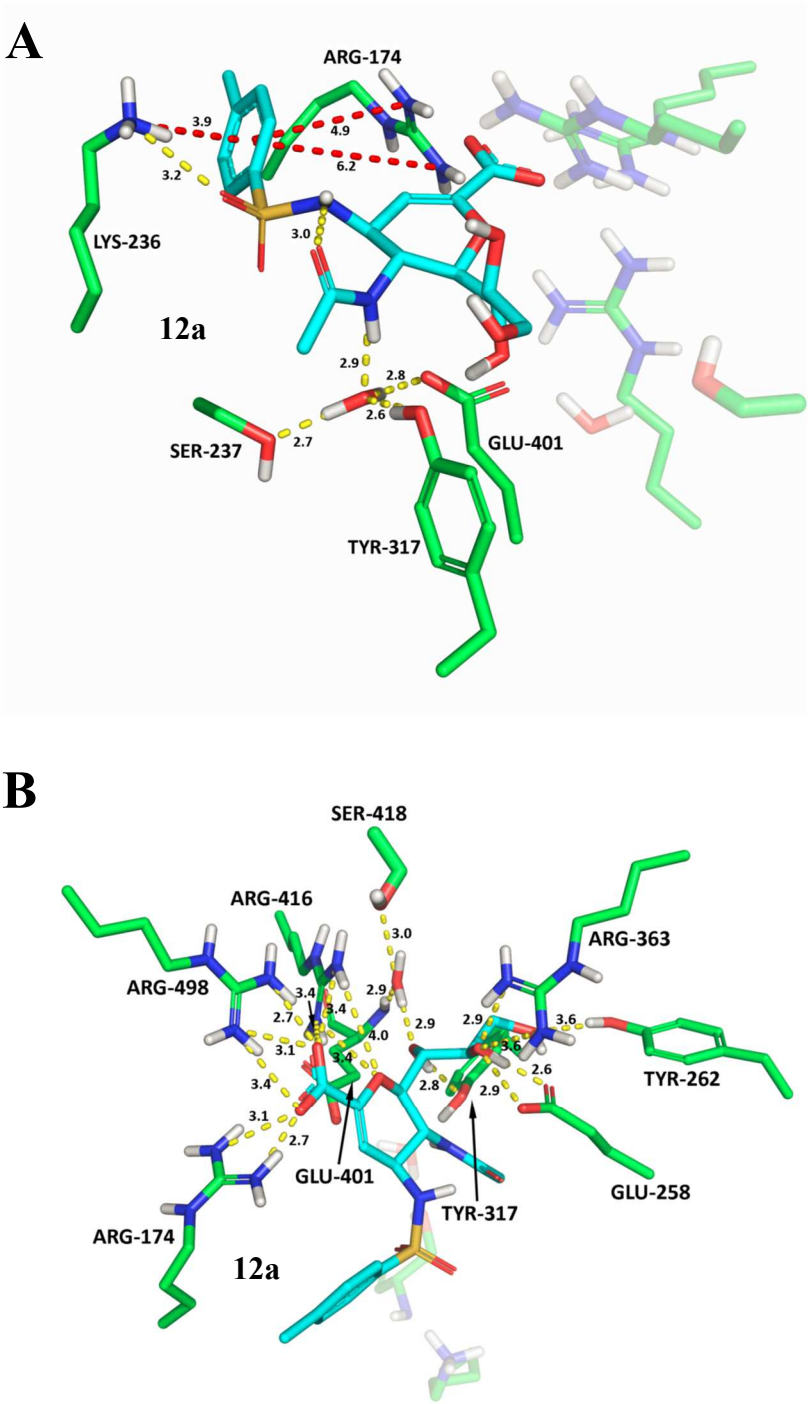

Figure 3.9 *Two different views of the Induced Fit Docking pose of compound* ***12a****. The inhibitor is colored in cyano. The interactions between the inhibitors and the enzyme are showed as yellow dashed lines, and the distances are measured in Å. Amino acid numeration is kept as in the PDB crystal (1e8v).*

3.2.2 Chemical synthetic approach

Prompted by the promising docking results, I proceed with the setting up of a synthetic protocol directed to the *p*-toluensolfonamido derivative **12a** achievement. Noteworthy, to obtain the final molecule the synthesis *via* an azido intermediate (Scheme 3.3) resulted necessary. In addition, azido derivative of DANA, BCX-2798 have been reported to possess a high inhibitory activity against hPIVs-HN[2], probably ensured by new interactions given by the negative charge present at the terminal portion of azido group. Thus, I decided to obtain, also, the free azido derivative **13a**, in order to investigate the inhibitory activity of both these compounds. Successively, I planned a synthetic pathway to achieve C4/C5 modified derivatives combining the just selected modifications with the previously tested C5 perfluorinated chains. At this purpose, for the first time, the direct *N*-transacylation reaction was successfully applied on a molecule containing a very instable azido group, achieving the desired compounds (**12b-d** and **13b-d**, Figure 3.10) in good yields.

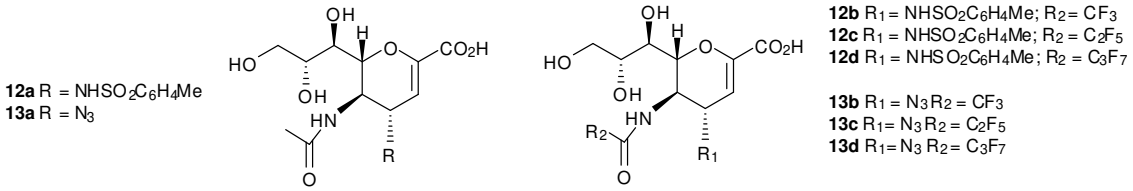

Figure 3.10 *p-Toluensolfonamido and azido derivatives differently substituted at C5 and synthesized in this thesis.*

3.2.2.1 Synthesis of all C4/C5 substituted derivatives

Starting from oxazoline **14**[110] (Scheme 3.3), the protected azido intermediate **15**[4] was obtained, using trimethylsilyl azide (TMS-N_3) in t-BuOH, according to literature[4, 37, 117]. Then, the protected azido derivative was subjected to catalytic reduction using Lindlar catalyst in EtOH under H_2 atmosphere. In this way, compound **17**[117] was obtained after acylation of the free amino intermediate **16**[4] with *p*-toluensulfonylchloride. Finally, compound **15**[4] and **17**[117] were subjected to deacetylation with $NaOCH_3$ in methanol, followed by basic hydrolysis with K_2CO_3 in MeOH/$H_2$0 (10:1, v/v), to give the free acid derivatives **13a** and **12a**, respectively (Scheme 3.3). These compounds were tested for their ability to inhibit NDV-HN neuraminidase activity and resulted very potent nanomolar NDV-HN inhibitors (See paragraph 3.2.3.1).

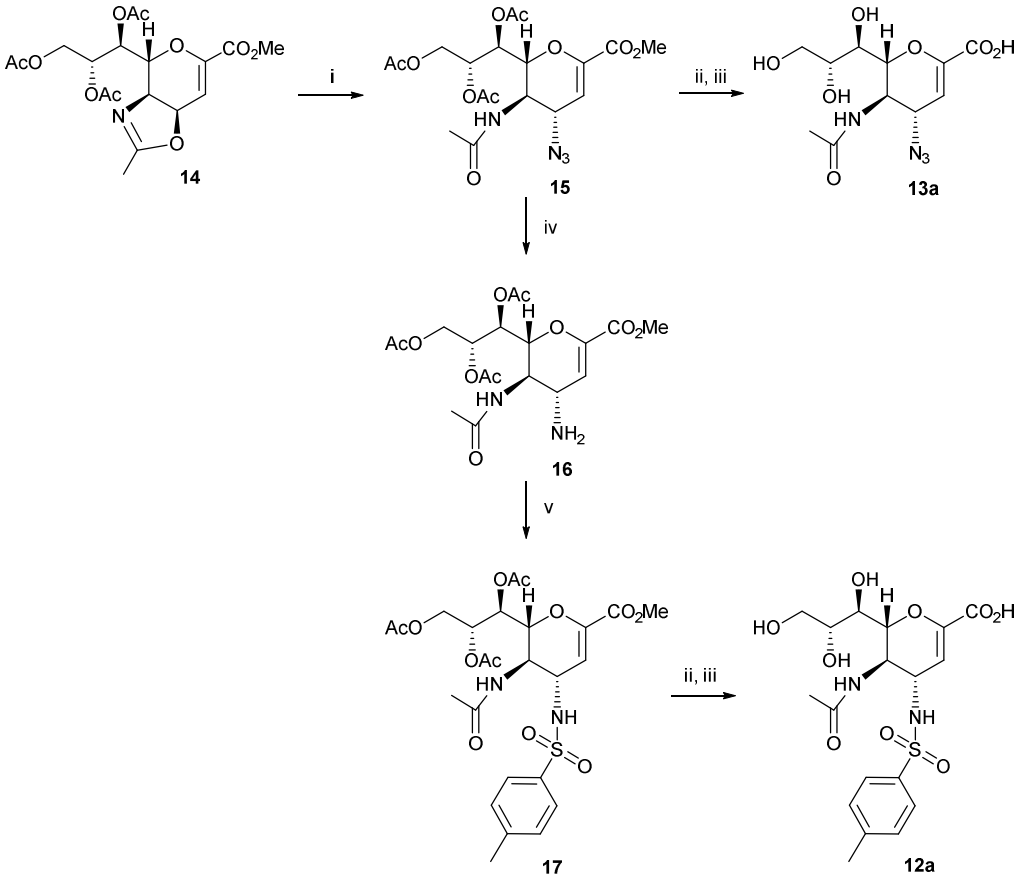

Scheme 3.3 *Synthesis of compounds **12a** and **13a**. Reaction conditions: i) See. [Ref. 4] ii) NaOMe, MeOH, 23°C, 1h, 80%; ii) K_2CO_3, MeOH/H_20 (10:1, v/v), 23°C, 12h, 72-77%; iv) H_2, Lindlar catalyst, EtOH, 23°C, overnight, 70%; v) p-toluensulfonyl chloride, Et_3N, CH_2Cl_2, 0°C to 23°C, 4h.*

Successively, I set up a protocol (Figure 3.4) to obtain the *p*-toluensolfonamido and azido derivatives with the perfluorinated chains at C5 previously selected (trifluoroacetyl, pentafluorpropionyl and heptafluorobutyryl chains). Using the common precursor **15**[4], I performed an *N*-transacylation reaction with different perfluorinated anhydrides (trifluoroacetic, pentafluorpropionic and heptafluorobutyric anhydrides) directly on the azido derivative in order to obtain compounds **18b-d.** Then, these three intermediates were subjected to hydrogenation with Lindlar catalyst giving compounds **19b-d,** as reported above, and they were subsequently acylated with *p*-toluensulfonyl chloride, in presence of Et_3N in CH_2Cl_2 to obtain protected inhibitors **20b-d**. The obtained molecules, **18b-d** and **20b-d** were deacetylated performing Zemplén reaction and then selectively hydrolyzed using K_2CO_3 in methanol/water (9:1) for compounds **18c,d** and **20c,d** and Et_3N in acqueous methanol, for compounds **18b** and **20b**. All the protected new free acidic azido (**13b-d**) and *p*-toluesolfonamido (**12b-d**) derivatives were investigated for their inhibitory potency against NDV-HN.

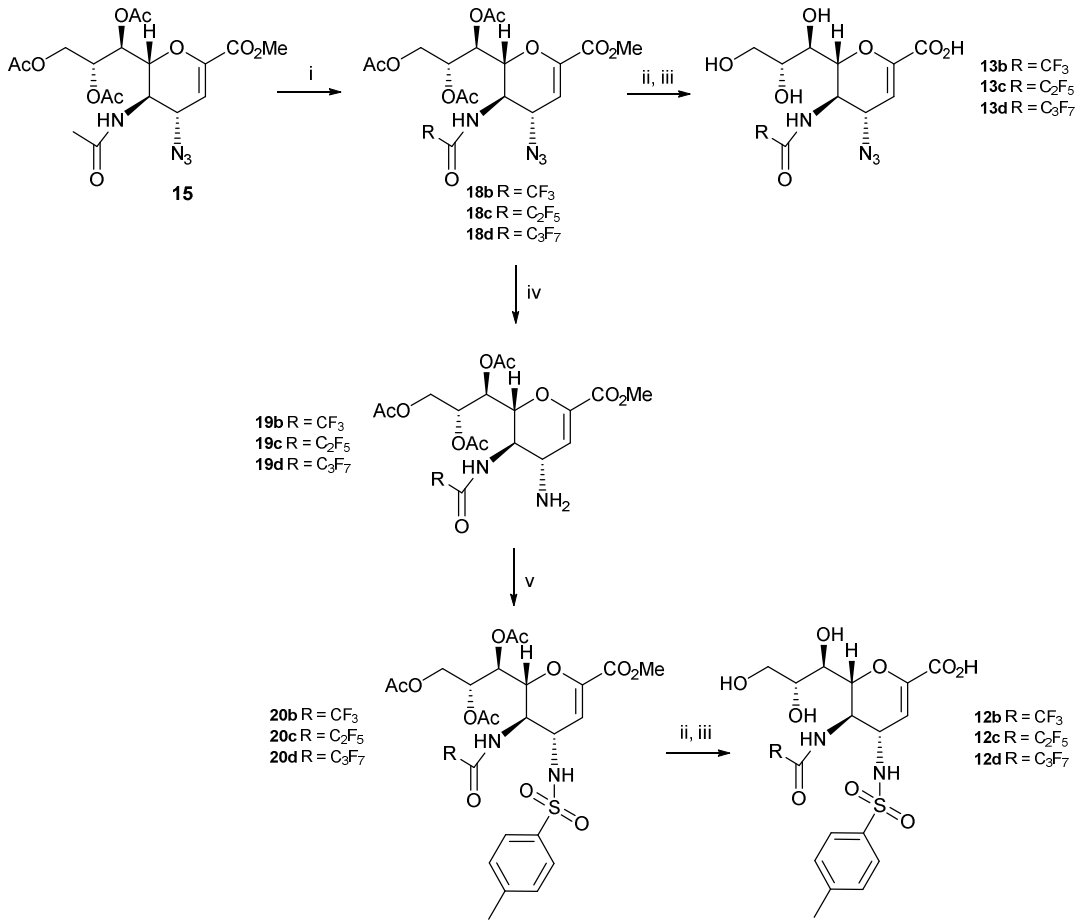

Scheme 3.4 *Synthesis of compounds **12b-d** and **13b-d**. Reaction conditions: i) perfluorinated anhydride, Et_3N, CH_3CN, 0°C to 135°C, 15 minuti, 78-80%; ii) NaOMe, MeOH, 23°C, 1h, 80%; ii) for **12c,d** and **13c,d**: K_2CO_3, $MeOH/H_20$ (10:1, v/v), 23°C, 12h, 68-75% and for **12b** and **13b**: Et_3N, $MeOH/H_2O$ (2:1 v/v), 23°C, 12h, 68-72%; iv) H_2, Lindlar catalyst, EtOH, 23°C, overnight, 68-75%; v) p-toluensulfonyl chloride, Et_3N, CH_2Cl_2, 0°C to 23°C, 2-5h, 75-81%.*

3.2.3 Biological assays

In the next section, I will present the biological investigations in order to evaluate the inhibitory potency and selectivity of the previously synthesized azido and *p*-toluensolfonamido derivatives. A neuraminidase inhibition assay (NI) and a hemagglutinin inhibiton test (HI) were performed on NDV-HN. Then, a NI was accomplished, also, on human NEU3 to obtain some preliminary information about the synthesized inhibitors selectivity.

3.2.3.1 Neuraminidase inhibition assay (NI) on NDV-HN

The NI assay was, firstly, performed on unfluorinated compounds **12a** and **13a**, using *in toto* purified NDV and 4-methylumbelliferyl α-D-*N*-acetylneuraminic acid as fluorescent substrate[112]. The obtained results were expressed as IC_{50} values, corresponding to the concentration causing the 50% inhibition of neuraminidase activity. The final values were reported in Table 3.3. As depicted in the graph, both **12a** and **13a** showed a nanomolar activity against NDV-HN, with IC_{50} values of 0.178 μM and 0.543 μM, respectively. Surprsingly, azido compound **13a** and the *p*-toluensolfonamido derivative **12a** were 5 times and 14 times respectively, more active than FANA (2.42 μM). These results unequivocabilly confirm the large size of the C4 cavity and its ability to perfectly accommodate a bulky hydrophobic substituent (as *p*-toluensolfonamido one) as predicted by docking simulation studies. On the other hand, compound **13a**, due to the negative charge at the terminal portion of azido group, could probably interact with some basic active site amino acid, such as Lys236, giving additional interactions that justify the higher IC_{50} value if it was compared to DANA or FANA.

Using the same assay, I evaluate the inhibitory activity against NDV-HN of all the C5 perfluorinated derivatives **12b-d** and **13b-d**. The IC_{50} values obtained, reported in Table 3.3, were divided into two different series: *p-toluensolfonamido series* and *azido series*.

An accurate analysis of IC_{50} values in *p-toluensolfonamido series* revealed that the trifluoroacetyl derivative **12b** posseses a high nanomolar activity against NDV-HN (0.191 μM), not statistically different from that of its unfluorinated analogue **12a** (0.178 μM). This result suggested that, fluorine atoms of trifluroacetyl group are not able to enhance the inhibitory potency of the molecule in presence of a bulky C4 substituent, as *p*-toluensolfonamido one. Then, considering longer perfluorinated chains, I observed a dramatically decrease in inhibitory activity. Pentafluoropropionyl derivative **12c** and its heptafluorobutyryl homologue **12d** showed IC_{50} values of 62.0 μM and 186 μM, respectively,

indicating that the large *p*-toluensolfonamido group is able to interfere with the accomodation of longer perfluorinated chains.

On the other hand, analyzing *azido series*, it was observed that trifluroacetamido compound **13b** possess a IC_{50} value of 0.166 μM, which is 3 times lower if compared to that of its unfluorinated analogue **13a** (0.543 μM). This indicate that, the presence of a realtively small substituent such as azido group, lead to an increase in inhibitory potency after the addition of a trifluoroacetyl group at C5 (as observed for the previusly described 4α-OH derivatives of DANA, see paragraph 3.1.2.1). Then, considering the interestingly nanomolar IC_{50} value of 0.166 μM showed by compound **13b** and that of its pentafluoropropionamido homolog **13c** (7.43 μM), a reduction in inhhibitory potency is evident. This decrease was followed by an improvement in activity passing from compound **13c** to its heptafluorobutyryl homolog **13d**, which showed a IC_{50} value of 0.213 μM, not statistically different, from that of trifluoroacetyl derivative **13b** (0.166 μM). Analysing the azido series IC_{50} trend, it is noteworthy that despite it is similar to that previuolsy reported for the corresponding C4 hydroxy analogues (see paragraph 3.1.2.1), the overall activities measured showed lower IC_{50} values, confirming the capacity of the azido group to be well accommodated in enzymatic pocket even in presence of C5 perfluorinated chains of different length.

Compound	IC50 (μM)[a]
12a	0.178 ± 0.013
12b	0.191 ± 0.007
12c	62.0 ± 10.6
12d	186 ± 27.5

Compound	IC_{50} (μM)[a]
13a	0.543 ± 0.022
13b	0.166 ± 0.061
13c	7.43 ± 0.29
13d	0.213 ± 0.035

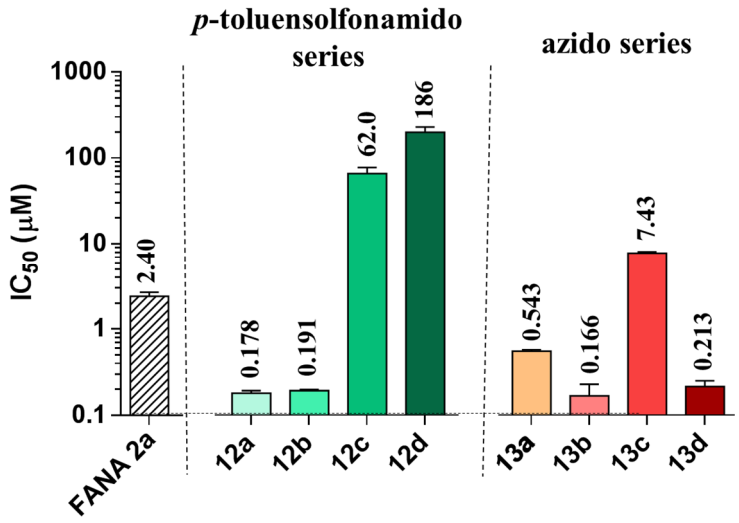

Table 3.3 *NI IC_{50} values of p-toluensolfonamido and azido derivatives on NDV-HN.*

[a]Each value represents the mean of three independent experiments carried out in triplicate

Taken together, these results regarding both the *azido* and *p-toluensolfonamido series* permit me to speculate about the inhibitor/active site interactions, hypothesizing that the strong binding of the *p*-toluensulfonamido group to the C4 pocket region of NDV-HN could induce

a remodeling of the region adjacent to C5 (C5 binding cavity), decreasing its ability to accommodate longer (than trifluoroacetamido one) perfluorinated chains. On the other hand, the azido group give some important interactions, but it is not sufficient to affect the accommodation of C5 chains.

In addition, taking into account all the collected data from both biological investigations on C5/C4 substituted derivatives and the docking simulations, I hypothesized that Lys236 could be the key amino acidic residue targeted by our inhibitors. In fact, as suggested by Induced Fit docking results, when *p*-toluensulfonamido derivative well accommodate in the corresponding pocket, the sulfonyl group and the aromatic ring could give two distinct type of interactions with Lys236. On the other hand, when a small C4 substituent is present, also C5 heptafluorobutyryl perfluorinated chains could reach and interacts with this amino acid (as shown for 4α hydroxy derivatives, see paragraph 3.1.3.1).

Thus, as known Lys236 together with Arg174 are two key amino acids involved in the NDV-HN active site activation and both residue are implicated in a series of conformational changes, interesting the head domain, which should activate the fusion promotion activity of this protein[76, 118]. These findings led me to hypothesize that, all the synthesized inhibitors, could be implicated not only in inhibition of the neuraminidase activity but also they could have an important role in modulating viral fusion promotion activity exploited by HNs. At this purpose future investigations will be necessary.

3.2.3.2 Hemagglutinin inhibition assay (HI) on NDV-HN: Preliminary results

I decided to investigate, also, the possible role of the most active molecules (**12a,b** and **13b,d**) in inhibiting the hemagglutinin activity of NDV-HN. At this purpose, a collaboration with "Istituto Zooprofilattico Sperimentale delle Venezie" was necessary. I set up a protocol to perform a hemagglutinin inhibition assay (HI), using chicken red blood cells (cRBC) and NDV (LaSota), on DANA **1a**, FANA **2a** and compounds **12a,b** and **13b,d**. I reported the qualitative results of some preliminary assay in the table below (Table 3.4). All the tested compounds did not inhibit hemagglutination of RBCs even at the maximum screening threshold of 300 μM. These results suggested that the synthesized molecules, potent and selective neuraminidase activity inhibitors which well bind and inhibit Site I of NDV-HN, are unable to reach Site II and block its hemagglutinin activity.

Compound	IC_{50} (μM)[a]
DANA 1a	>300
FANA 2a	>300
12a	>300
12b	>300
13b	>300
13d	>300

Table 3.4 *HI assay performed on p-toluensolfonamido and azido derivatives on HN of inactivated strain of NDV.*

[a]Each concentration for each inhibitor is tested in duplicate and the experiment repeated three times.

3.2.3.3 Neuraminidase inhibition assay (NI) on hNEU3: Preliminary studies on selectivity

Finally, I evaluate the inhibitory potency of FANA **2a** and all the azido and *p*-toluensolfonamido derivatives (**12a-d** and **13a-d**) on the human membrane sialidase NEU3 (hNEU3) performing, the same test previously reported for hydroxyl derivatives (see paragraph 3.1.3.2).

As shown in Table 3.5, unlike FANA (the most effective NDV-HN inhibitor used as a reference in literature), all the tested compounds lack of inhibitory activity against hNEU3 even at the maximum threshold of 1mM, with the exception of azido derivatives **13a** and **13b**, which showed a micromolar inhibitory activity against the human protein (IC_{50} value of 78.0 μM and 128.0 μM, respectively), which are, otherwise, 100- and 700-fold higher than those of the same compounds tested toward NDV-HN. All these values are in agreement with the notion that mammalian sialidases possess a small C4 binding pocket and, consequently, bullky groups at C4 and/or at C5, are not well tolerated.

Compound	IC_{50} (μM)[a]
12a	>1000
12b	>1000
12c	>1000
12d	>1000

Compound	IC_{50} (μM)[a]
13a	78.0 ± 22
13b	128 ± 35
13c	>1000
13d	>1000

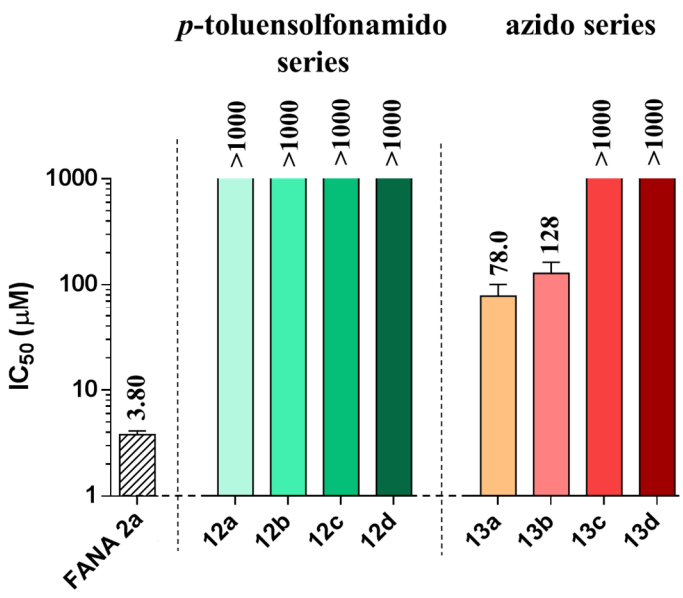

Table 3.5 *NI assay performed on p-toluensolfonamido and azido derivatives on hNEU3.*

[a]*Each concentration for each inhibitor is tested in duplicate and the experiment repeated three times, obtaining identical results.*

3.3 The 3,4-unsaturated derivatives

As above anticipated, in this section a study of a relatively poorly investigated class of molecules, some Neu5Ac derivatives presenting an unsaturation at the C3/C4 position[6, 7, 42], will be presented. In particular, the set-up of more efficient synthetic procedures to achieve these 3,4-unsaturated derivatives **21a,b** and **22a-f** (Figure 3.11) will be reported. In addition, a study of some important aspects concerning their anomeric configuration, their stability in protic solvents and the unexpected formation of an interesting synthetic intermediate, will be performed. Finally, the biological inhibitory activity evaluation on NDV-HN and the selectivity towards human NEU3 will be accomplished.

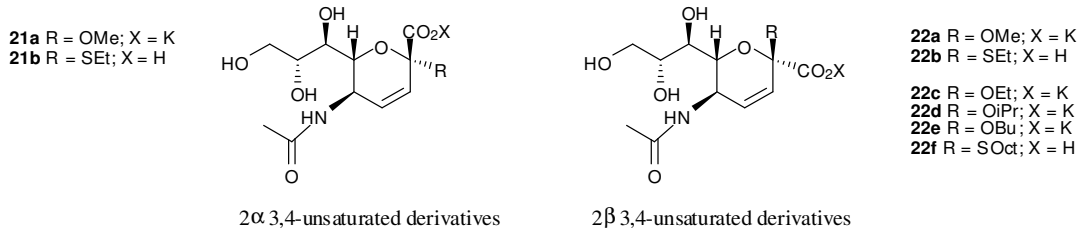

Figure 3.11 *The 2α and 2β 3,4-unsaturated derivatives of Neu5Ac synthesized during my PhD thesis (SOct=SOctyl).*

3.3.1 Chemical synthetic approach

The synthesis of the 3,4-unsaturated sialic acid derivatives was firstly accomplished by Maudrin[42], through a laborious multistep synthetic pathway and, only recently, these molecules have been achieved using a rapid method, proposed by Ikeda and coworkers, *via* a Ferrier glycosylation reaction[6, 7]. This interesting rearrangement involves a nucleophile substitution reaction combined with an allylic shift, occurring in glycals (2,3-unsaturated glycosides). This reaction could be performed in presence of various acid catalysts, such as Lewis acids ($AlCl_3$, $FeCl_3$, BF_3Et_2O, etc.) or other activating agents (activated acidic clays and resins)[119].

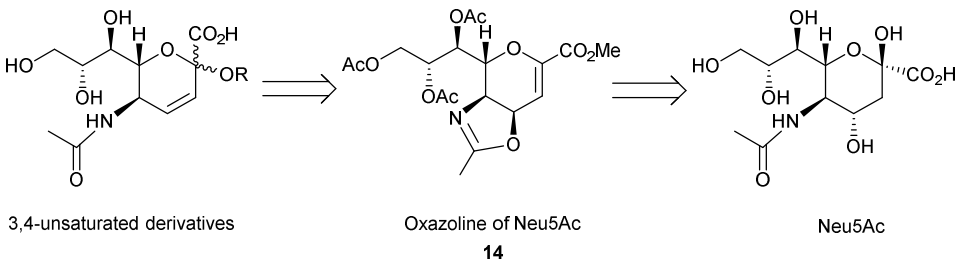

Scheme 3.5 *3,4-unsaturated Neu5Ac derivatives: general retrosynthesis scheme.*

For the synthesis of this class of compounds, in high β stereoselectivity, Ikeda *et al.*[6, 7] proposed as best synthetic conditions, in their Ferrier reaction, a mixture of the acid $Bi(OTf)_3$

and the clay Montmorillonite K-10 in CH_3CN. Despite, the high yields and β stereoselectivity obtained using methanol or ethanol as nucleophiles, the same reaction conditions applied to long- or branched-chain alcohols or thiols, caused a drastic reduction in yields. Unfortunately, they obtained, after hydrolysis, a random mixture of α and β anomers of the free molecules, thus, losing also in anomeric (C2) stereoselectivity.

Starting from the literature results, I planned a retrosynthetic protocol (Scheme 3.5) to obtain 3,4-unsaturated derivatives, *via* a Ferrier reaction and subsequent deprotection (preserving a high stereoselectivity), starting from oxazoline of Neu5Ac **14**[110], which was achieved, in three steps, from Neu5Ac,

I decided to preferentially synthesize the β-anomers on the basis of some preliminary docking studies performed on NDV-HN using as model compounds 2*O*-methyl and 2*S*-ethyl derivatives. The obtained results suggested that, when the β-anomers of these derivatives enter inside the active site, their β substituents at C2 seemed to be orientated toward the large C4 binding pocket in which they could be accommodated (Figure 3.12).

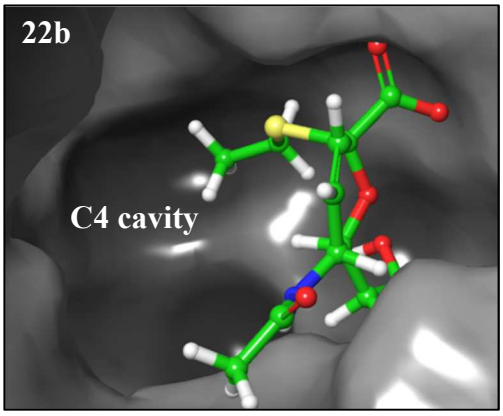

Figure 3.12 *Rigid docking pose of compound* ***22b****, 2βS-ethyl 3,4-unsaturated derivative of NeuAc (green).*

3.3.1.1 Setting up of optimal Ferrier reaction conditions using MeOH as a nucleophile

I started with the synthesis of the oxazoline derivative **14**[110] from Neu5Ac, in three steps, according to literature. Initially, I decided to perform the Ferrier reaction using the same conditions reported by Ikeda *et al.*[6, 7] to obtain the desired, 3,4-unsaturated molecules **23a** and **24a**, as a cromatographically unseparable mixture (Table 3.6). Briefly, oxazoline **14**[110] was solubilized in anhydrous CH_3CN (0.2M) and then methanol was added. Subsequently, a mixture of $Bi(OTf)_3$ and Montmorillonite K-10 (Montmorillonite 40% w/w loading of 20% w/w of $Bi(OTf)_3$) was added, as an acid catalyst, and the reaction was stirred at 23°C, to obtain the protected molecules **23a** and **24a**. The results have been reported in Table 3.6. Unfortunately, the reaction, in my hands, did not work well as described by Ikeda, in fact, I

obtained lower yields (70% versus 95% obtained by Ikeda) and stereoselectivity (α/β ratio of 13/87 versus 9/91 obtained by Ikeda) (Entry 1). These sub-optimal yields could be attributed to the formation of an unstable intermediate, detectable in TLC, but not isolable neither in TLC or flash chromatography, able to evolve in the more stable 4β-OH derivative of Neu5Ac, **25**[37].

Successively, I decided to investigate, the effect of temperature on this reaction, observing a general improvement in reaction times (Entry 2 and 3). An approximately doubling of the temperature (from 23°C to 50°C) led to a variation in the anomeric ratio (α/β ratio of 22/78), keeping the yields almost unchanged (Entry 2). Noteworthy, a further increase in temperature, close to the boiling point of the CH_3CN (80°C), caused a marked reduction in C2 stereoselectivity (α/β ratio of 45/55) (Entry 3).

In addition, conducting the reaction at 80°C, I observed, in the final purified products mixture, the presence of a further by-product. This compound could correspond to the 4β-OMe derivative of DANA **26**, in fact it showed NMR signals according to the structure of the C5-trifluoro 4β-OMe derivative of DANA[111] (that could form in acidic environment at high temperature), except for the signals at C5 (data not shown in this thesis).

So, considering these preliminary results, I decided to evaluate the individual contribution of these two catalysts, at different temperatures. In particular, the use of $Bi(OTf)_3$ led to a high reduction in reaction times, already at 23°C, but with a significative reduction in yields (40%) (Entry 4). Otherwise, increasing the temperature, from 23°C to 50°C, I registered an improvement in yield (from 40% to 60%, Entry 5) which, then decreases (40%) at 80°C (Entry 7). Noteworthy, the 4-OMe by-product has been detected also using these conditions (10-25% at 50°C and 55% at 80°C, of the overall yields), suggesting that the real yields of the desired compounds **23a+24a** were lower than those reported. In addition, the previously revealed temperature-dependent decreasing in stereoselectivity has been also registered (α/β ratio of 43/57 at 50°C, Entry 6).

Then, checking the effects of the exclusive use of Montmorillonite K-10 as an acid catalyst, at 23°C I observed very long reaction times (Entry 8). Surprisingly, the increase in temperature from 23°C to 80°C, led to a progressive great improvement in both reaction time and yields (2-3h, 85% respectively, Entry 10), not affecting the stereoselectivity (from α/β ratio of 17/83 at 50°C to 18/82 at 80 °C, Entry 9-10).

These collected crude Ferrier mixtures showed clean NMR spectra, without the presence of by-products, only the α/β anomers mixture signals were registered. This data suggested that Montmorillonite used alone, could be an optimal acid catalyst to obtain a clean reaction

without by-products formation. This is probably due to its capacity to absorb water and to catalyze the reaction steps in high regio- and stereo-selective way. In fact, montmorillonite is a clay belonging to phyllosilicate mineral group and its crystalline structure consists of multiple layers (each layer is made up of one octahedral alumina sheet sandwiched between two tetrahedral silica sheets). This structure permits to entrap cation and water. The crude mineral presents some native Lewis (Al^{3+} species) and Brönsted sites, but its acidic properties could be boosted by cation exchange processes (H^+, Fe^{3+}, Zn^{2+}, etc.)[119, 120]. In general, Montmorillonite could probably eliminate the trace of water, present in $Bi(OTf)_3$, the supposed responsible of the formation of the "unstable intermediate".

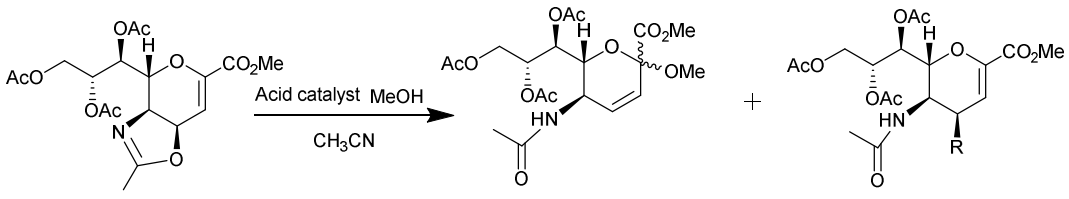

Oxazoline of Neu5Ac
14

Protected 3,4-unsaturated Ferrier derivatives
23a + 24a

By-products
25 R = OH
26 R = OMe

Entry	Acid catalyst	Temperature (°C)	Reaction time (h)	Yields (%)*	Obtained products*	Stereo-selectivity (α/β)
1	**$Bi(OTf)_3$ + Montmorillonite K-10**	RT	>30	70	α+β	13/87
2		50	1	68	α+β	22/78
3		80	0.5	73	α+β + 15% by-product (4-OMe)	45/55
4	**$Bi(OTf)_3$**	RT	3-5	40	α+β	15/85
5		30	1	50	α+β	28/72
6		50	1	60	α+β + 10-25% by-product (4-OMe)	43/57
7		80	0.5	40	α+β + 55% by-product (4-OMe)	40/60
8	**Montmorillonite K-10**	RT	>256	---	---	---
9		50	28	75	α+β	17/83
10		80	2-3	85	α+β	18/82

Table 3.6 *Investigation of reaction conditions using MeOH as nucleophile and CH_3CN as solvent. The effect of two acid catalysts at different temperatures on reaction time, yield and stereoselectivity has been tested. *after FLASH chromatography purification of the two chromatographically unseparable compounds.*

To confirm, this hypothesis, I dedicated part of my work to understand the structure of the unstable intermediate, responsible for the yield decrease of Ferrier reaction. Initially, I attempted to isolate this unstable compound using preparative TLC or flash chromatography, but all the tentative failed and the only compound isolable was the 4β-OH derivative of Neu5Ac **25**[37]. Thus, considering the hypothesis that this compound could form from the presence of water in an acidic medium, I simulate the moist acidic reaction conditions to obtain this by-product in high yield (Scheme 3.6). At this purpose, I dissolved oxazoline **14** in a mixture of CH_3CN/H_2O (1:1; v/v) and trifluoroacetic acid (TFA) and then, the reaction was stirred at 23°C. The oxazoline depletion was monitored by TLC and after 5-15 min, the time necessary to transform the starting material entirely in the intermediate **27**, the reaction was quenched by the addition of a weak basic resin (IRA-67), until neutral pH. Significantly, longer exposition times in these reaction conditions led to the formation of a mixture of both intermediate **27** and the final 4β-OH derivative **25**[37].

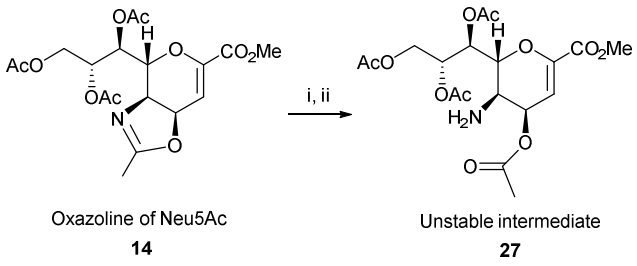

Scheme 3.6 *Intermediate formation and isolation. Reaction conditions: i) CH_3CN/dH_20, TFA; ii) After 5-15 min basic resin IRA-67.*

In this way, I accomplished to isolate a molecule with the same TLC Rf value of the intermediate **27**. In addition, the isolated compound was hydrolyzed in the same reaction conditions or in flash chromatography to the final 4β-OH NeuAc derivative **25**, as aspected. Overall, the collected data allow me to assert, with reasonable certainty, that I have isolated the intermediate **27,** which causes the decreasing in Ferrier's products yield. This molecule was immediately characterized by ^{1}H and ^{13}C NMR spectroscopy and mass spectrometry, to get all the information necessary to reconstruct the chemical structure of this newly and previously uncharacterized intermediate.

Then, a mechanism for the intermediate **27** formation, starting from oxazoline **14**, was proposed according to all the collected data. This interesting issue will be not discussed here, but the detailed description has been reported in Scheme 3.7.

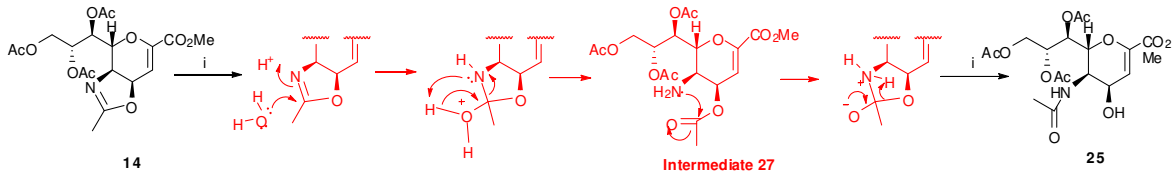

Scheme 3.7 *Hypothesized chemical mechanism for intermediate **27** formation and the subsequent transformation in the more stable 4-OH by-product. Water present in solution could perform a nucleophilic attack on the oxazoline **14** ring and, in the same time, the acidic environment permits the protonation of the nitrogen group, leading to oxazoline ring opening and the formation of a 4-OAc derivative with a free amino group at the C-5 (the unstable intermediate **27**). The presence of a free amine in β gives high instability to the molecule, in fact, it tends to react, immediately, with the acetyl moiety permitting the re-formation of a transient ring-close derivative. This molecule could, finally, evolve in the stable compound **25**.*

Finally, to support the hypothesized mechanism and the reactivity of the newly synthesized molecule, a chemical approach based on the direct acylation of intermediate **27** was performed (Scheme 3.8).

The protocol, depicted in Scheme 3.8, provided the formation of the intermediate **27** in the same conditions previously described, and the direct acylation of its amino group with propionyl chloride and weak basic resin (IRA-67), without any intermediate isolation. After the workup, compound **28** was isolated, having a propionyl amide at C5 and the acetyl residue at C-4, thus supporting expectations. At this point, I transformed the compound **28** into its oxazoline derivative **29**, using the classic reaction conditions described above: BF_3Et_2O, in CH_2Cl_2 at 80°C. Unreported oxazoline **29**, was achieved in good yield and high purity grade and completely chemical-physical characterized. Then, I decided to check whether the propionyl-oxazoline **29** had the same behavior (under moist acidic conditions) as the previously observed for acetyl-oxazoline **14**, generating an intermediate **30** derived from the exchange of the propionyl group from C5 to C4 position. Thus, propionyl-oxazoline **29** was treated with moist TFA to afford a new C4-propionyl intermediate **30**, derived from the expected scrambling. Finally, the treatment of compound **30** with acetyl chloride, in presence of basic resin, gave compound **31**.

In this way, I demonstrated that the acyl (both acetyl or propionyl) groups initially at position C5, after oxazoline formation and subsequent re-opening in acidic conditions, transpose at C4. This curious "scrambling" confirms the amine nature of the intermediates, able to react with different acylchlorides. Furthermore, this interestingly switch between position C5 and C4 could result useful for the future synthesis of new C4 and C5 substituted Neu5Ac derivatives.

Overall, these interesting investigations showed the important double role played by the use of Montmorillonite in Ferrier reaction: as a drying agent in the removing traces of water and as clean acid-catalyzer.

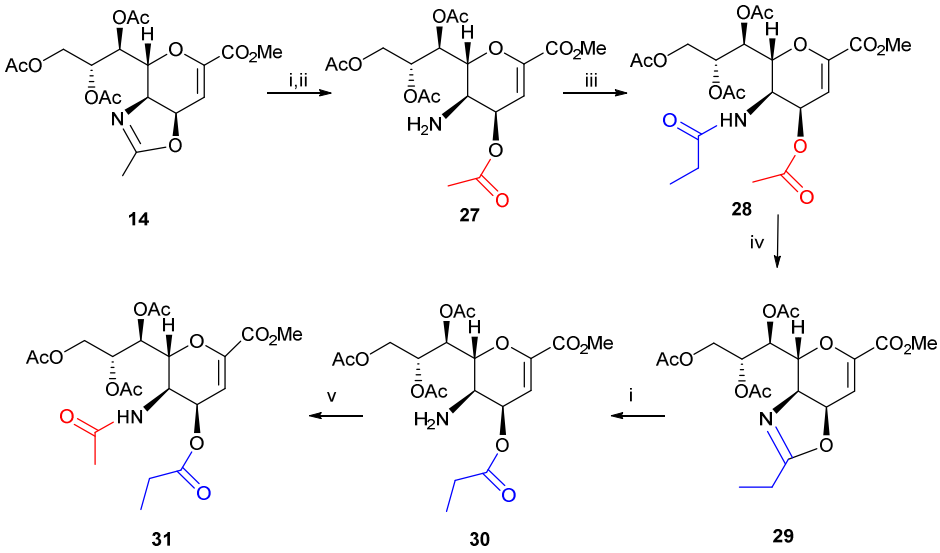

Scheme 3.8 *Demonstration and confirmation of the intermediate structure. Reaction conditions: i) CH_3CN/H_20, TFA; ii) After 6 min basic resin IRA-67 addition; iii) Propionyl chloride, basic resin IRA-67, CH_3CN; iv) BF_3Et_2O, CH_2Cl_2, 80°C; v) Acetyl chloride, basic resin IRA-67, CH_3CN.*

3.3.1.2 Setting up of optimal reaction conditions for other alcoholic and thiolic derivatives

I decided to test the selected Ferrier conditions (Montmorillonite K-10, 80°C in CH_3CN), using different alcoholic and thiolic nucleophiles (EtOH, iPrOH, nBuOH, EtSH and $CH_3(CH_2)_7SH$) obtaining the cromatographically unseparable mixtures of **23b+24b, 23c+24c, 23d+24d, 23e+24e** and **23f+24f**, respectively reported in Table 3.7 (using **23a+24a** as reference mixture). Surprisingly, the reaction works well with the selected conditions giving very good yields (68-80%), high stereoselectivity (mean ratio of 15/85), accompanied by low reaction times (4-5h), for all the nucleophiles tested. Thus, my synthetic conditions permit to achieve high yields also with bulkier nucleophiles, on the contrary of those of Ikeda and coworkers[6, 7] who found optimal conditions only for MeOH and EtOH.

Excited by the results, I attempted to use these conditions with other different nucleophiles than alcohols or thiols. Unfortunately, this reaction did not work using ammines, azido derivatives and silyl enol ethers.

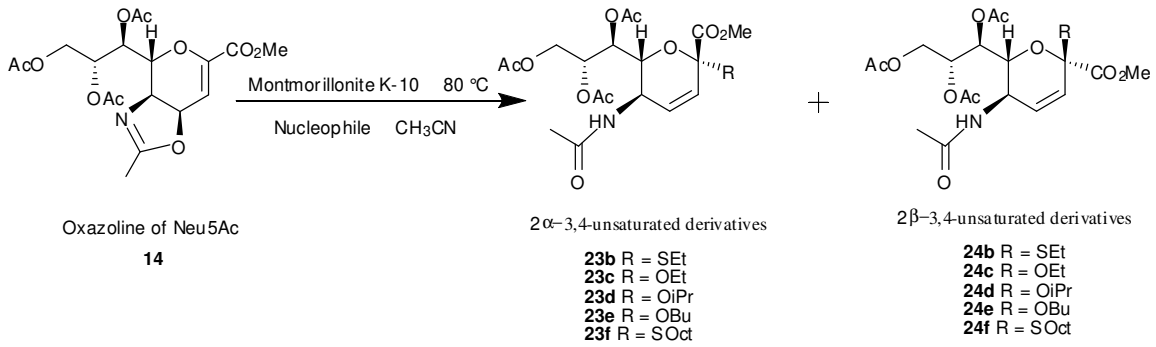

Oxazoline of Neu5Ac
14

2α–3,4-unsaturated derivatives
23b R = SEt
23c R = OEt
23d R = OiPr
23e R = OBu
23f R = SOct

2β–3,4-unsaturated derivatives
24b R = SEt
24c R = OEt
24d R = OiPr
24e R = OBu
24f R = SOct

Compound	Reaction Time (h)	Yields* (%)	Stereoselectivity (α/β)
23a + 24a	2-3	85	18/82
23b + 24b	4	68	14/86
23c + 24c	2-3	80	16/84
23d + 24d	5	70	15/85
23e + 24e	5	68	14/86
23f + 24f	5	70	15/85

Table 3.7 *Reaction time, yields and stereoselectivity of Ferrier reaction performed using the optimal conditions and different nucleophiles (SOct=SOctyl).*

**after FLASH chromatography purification of the two chromatographically unseparable compounds.*

3.3.1.3 Achievement of the deprotected 3,4-unsaturated Neu5Ac analogues and study of their stability

In order to achieve the free 3,4-unsaturated derivatives, initially, I set-up the hydrolytic conditions, using as model compounds the protected Ferrier product mixtures of **23a+24a** and **23b+24b** (Scheme 3.9). They were subjected to deacetylation with NaOMe in methanol, to obtain the corresponding methyl ester mixtures, that they were, successively, purified by flash chromatography to afford the α and β anomers **32a** and **33a**, **32b** and **33b**. After a full physico-chemical characterization, they were submitted to basic hydrolysis with KOH in water solution, using a different workup for **32a**, **33a** and for **32b**, **33b**. Alcoholic derivatives **32a** and **33a** were treated with a weak acidic resin until neutral pH, giving the corresponding derivatives, **21a** and **22a** as potassium salt**.** On the other hands, for thiolic derivatives **32b** and **33b** a strong acidic resin (Dowex 50WX8, H^+) was used to obtain the desired molecules **21b** and **22b** in the free acidic form.

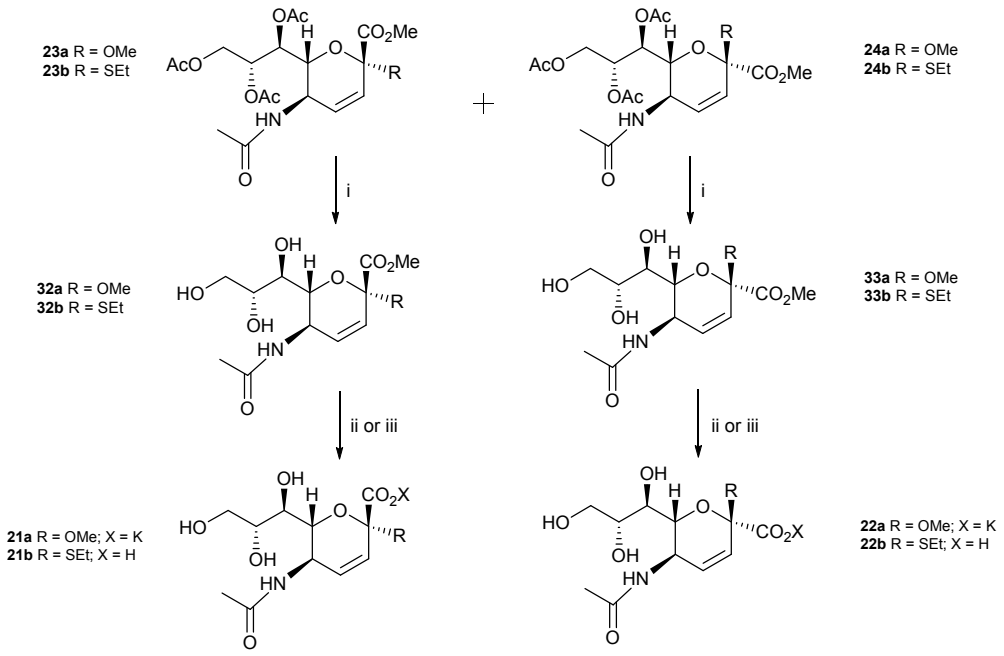

Scheme 3.9 *Synthesis of the free acid or potassium salt form of **21a,b** and **22a,b**. i) NaOMe, MeOH, 23°C, 1h, 80%; ii) KOH (aq) 0.5M, 23°C, 1h, then compounds **21a** and **22a** were obtained as Potassium salts after treatment with weak acidic resin (Amberlite CG50, H^+); iii) KOH (aq) 0.5M, 23°C, 1h, then compounds **21b** and **22b** were achieved in their free acidic stable form by treatment with strong acidic resin (Dowex 50WX8, H^+).*

This strategy was adopted on the basis of some preliminary results I performed on the stability of these compounds and by the support of the literature data[42]. Thiolic derivatives **21b** and **22b** remained stable in their free acidic form. On the other hand, I demonstrated that the acidic compounds **21a** and **22a** in free form, having an alcoholic function suffered a partial C2-epimerization both during the work-up with strong acidic resin (Dowex 50WX8, H^+) or if dissolved in methanol solution. A similar instability has been registered also using water. Interestingly, all these observations were not taken into account from Ikeda and coworkers[6, 7], who observed a dramatic change in α/β ratio and loss in yield, after deprotection. On the other hand, Maudrin *et al.*[42], in the in the final hydrolytic step of their laborious protocol observed an epimerization of the C-2 configuration in acidic environments, too.

Successively, all the other protected Ferrier product mixtures **23c+24c, 23d+24d, 23e+24e, 23f+24f** were subjected to deacetylation with NaOMe in methanol, to afford after flash chromatography the pure β anomers **33c-f** in good yields (66%) (Scheme 3.10). Then, I performed the two-step hydrolytic procedure giving **22c-e** as potassium salts or **22f** in free acid form (Scheme 3.10).

Before the biological activity evaluation, all the obtained final derivatives, and their precursors were submitted to an in depth characterization to assign all the NMR signals, performing ^1H,

^{13}C, COSY, HSQC and HMBC experiments. Then, the correct α or β anomeric configuration of the protected form, of their methyl esters and of the final deprotected ones, was determined using the method presented in the next paragraph (see paragraph 3.3.1.4). Finally, also mass spectrometry, elemental analysis and α_D determination, were performed (See material and method section).

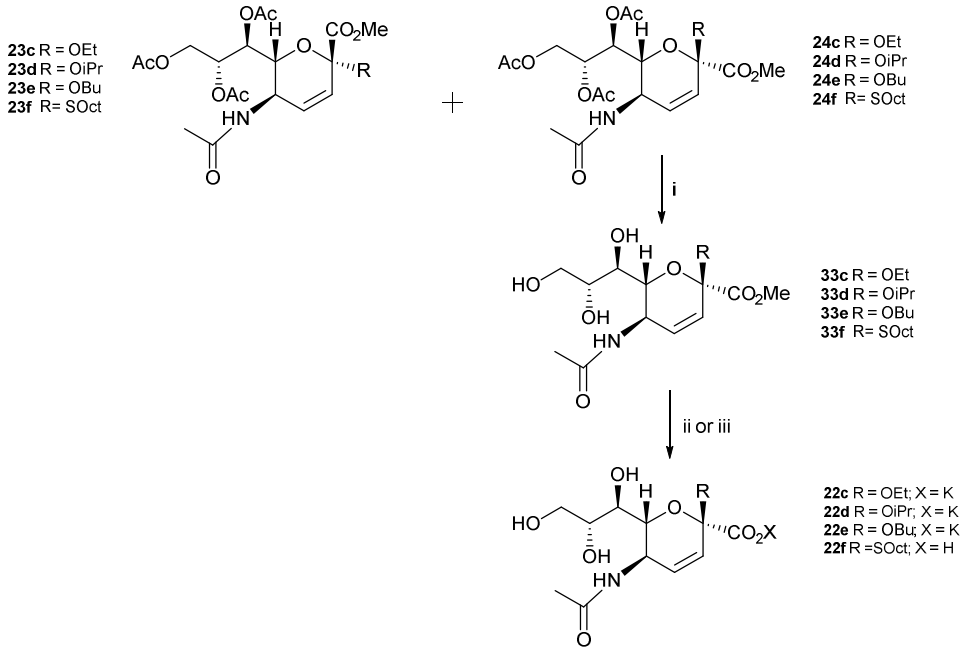

Scheme 3.10 *Synthesis of the free acid or potassium salt forms of compounds **22c-f**. i) NaOMe, MeOH, 23°C, 1h, 82%; ii) KOH (aq) 0.5M, 23°C, 1h, then compounds **22c-e** were obtained as potassium salts after treatment with weak acidic resin (Amberlite CG50, H$^+$); iii) KOH (aq) 0.5M, 23°C, 1h, then compound **22f** was achieved in its free acidic stable form by treatment with strong acidic resin (Dowex 50WX8, H$^+$).*

3.3.1.4 A simple method for the anomeric configuration attribution to the 3,4-unsaturated derivatives

The assignment of the anomeric configuration to these 3,4-unsaturated derivatives it is a very difficult challenge. About this, literature works reported a series of empirical rules to determine the correct anomeric stereochemistry for classical saturated protected and unprotected sialosides[121]:

1) A first one regards the chemical shift of the equatorial H3 proton (δ = 2.67-2.72 ppm for α-derivatives and δ = 2.25-2.40 ppm for β ones)[122];
2) A second one considers the chemical shift of H4 for protected[122] or methylester form of *O*-sialosides[123];

3) A third one interests the long-range coupling constants between C1 and the axial H3 proton[124, 125];
4) Another important rule regards the coupling constant between H7 and H8 (6.2-8.5 Hz for α anomers and 1.5-2.6 Hz for β anomers)[122, 126, 127];
5) A last one involves the chemical shift difference between H9a and H9b ($\Delta\delta$ < 0.5 ppm for α-derivatives and $\Delta\delta$ = 1 ppm for β ones)[126].

I decided to check these rules using as reference compounds the 2*O*-methyl derivatives **23a+24a**, **32a, 33a** and **21a, 22a** and the 2*S*-ethyl ones **23b+24b, 32b, 33b** and **21b, 22b**. After a deep and careful study, analyzing their NMR spectra, it could be observed that none of the literature proposed empirical rules could be used as predictive signals for the correct anomeric configuration attribution of the 3,4-unsaturated derivatives:

- The first three rules are not applicable to these derivatives due to the presence of an unsaturation between H3 and H4;
- The fourth one, valid only for protected derivatives, give no good matching in 2*O*-methyl and 2*S*-ethyl derivatives, in fact the coupling constant between H7 and H8 was of 6.3 Hz for α anomer **23a** and 5.4 Hz for β anomer **24a** and 6.1 Hz and 4.8 Hz, respectively, for **23b** and **24b**.
- The fifth rule, regarding the difference in chemical shift between H9a and H9b, is not respected in the protected compounds. In fact, I observed a $\Delta\delta$ = 0.42 ppm for **23a** and a $\Delta\delta$ = 0.26 ppm for **24a**, then a $\Delta\delta$ = 0.38 ppm for **23b** and a $\Delta\delta$ = 0.33 ppm for **24b**.

The C2 configuration attribution of these Ferrier products, achieved only by the assignment in analogy to 2*O*-methyl 3,4-unsaturated derivatives **21a** and **22a**, it is not a good method, in fact, some errors could occur. About this, I decided to consider the use of 1,7-lactonization reaction as a practical and fast method to overcome these difficulties[128, 129]. This reaction was already published by my laboratory, regarding some saturated sialic acid derivatives[106, 128], but, to date, no information about the use of this method to achieve the 3,4-unsaturated lactonic sialosides have been reported in literature. Thus, I successfully applied the classical lactonization protocol[128] to achieve these new and never characterized unsaturated 1,7-lactones (Scheme 3.11). I dissolved the potassium salts **21a** and **22a** and the free acids **21b** and **22b** in dimethylformamide (DMF) and tetrahydrofuran (THF) mixture. Then, triethylamine (Et_3N) and benzyl chloroformate (CbzCl), were rapidly and sequentially added, at 0°. For derivatives **22a,b** the reactions were maintained under stirring at 23°C and, after 30 minutes, all the starting material disappeared, giving a TLC spot compatible with lactonic

rings **34** and **35**, respectively. On the other hand, compounds **21a,b** gave only the starting material, even up 2 hours. The structure of the 3,4-unsaturated 1,7-lactones have been confirmed by ^{1}H and ^{13}C NMR analyses.

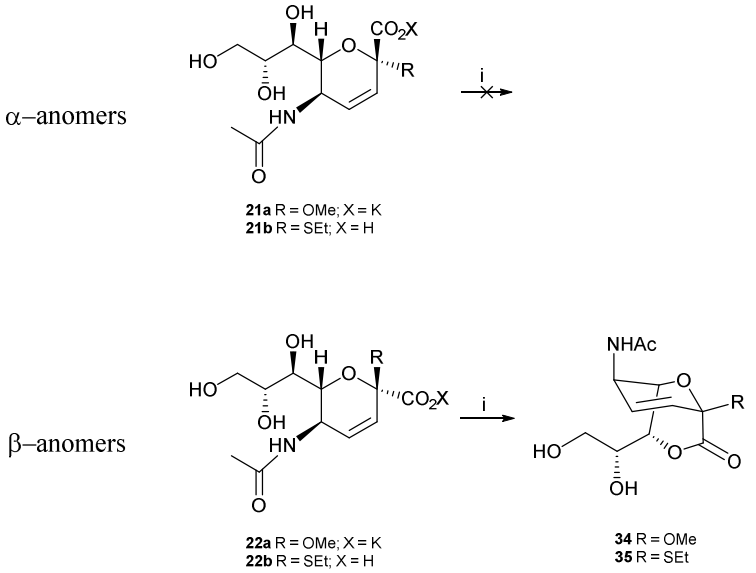

Scheme 3.11 *Lactonization reaction to obtain compound **34** and **35**. Reaction conditions: i) CbzCl, Et_3N, THF/DMF, 0°C to 23°C, 15-60 minutes, 36-40%.*

This experimental procedure permits to identify, without ambiguities, α of β anomers (Scheme 3.11). The first one could not lactonize under the described conditions, due to their spatial orientations. On the other hand, the β anomers afforded quite unstable but isolable and characterizable lactones. Finally, to further confirm these important results I saturated the obtained 3,4-unsaturated lactone **34** (Scheme 3.12), dissolving it in AcOEt in presence of Pd on carbon as catalyst, under H_2 atmosphere. I obtained the corresponding saturated compound **36**, presenting a classical $^{5}C_2$ chair conformation. The chemical properties of this molecule were perfectly superimposable to those of the lactone previously synthesized from the deprotected saturated β-derivative **37**[130] having a classical $^{5}C_2$ chair conformation. This result definitively confirmed the identity of the isolated 3,4-unsaturated lactones.

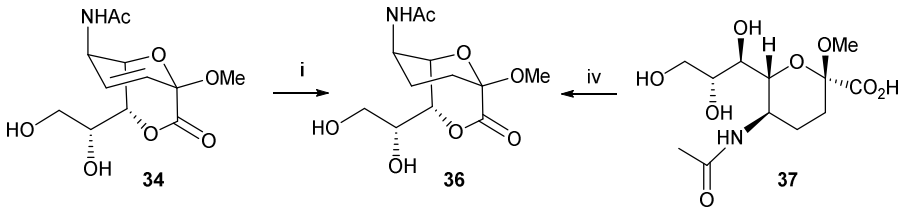

Scheme 3.12 *Demonstration and confirmation of the 3,4-unsaturated lactone identity. Reaction conditions: i) H_2, Pd on carbon, AcOEt, 23°C, 2h, 50%; ii) iv CbzCl, Et_3N, THF/DMF, 0°C to 23°C, 15-60 minutes, 75%.*

Finally, I dedicated part of my time to the identification of some potential diagnostic NMR signals, useful to determine some "new empirical rules" for the rapid and immediate assignment of the C2 configuration. At this purpose, focusing on 2*O*-methyl and 2*S*-ethyl derivatives (Table 3.8), I observed that α anomers present the C6 chemical shift values greater than 74.2 ppm ($\delta \geq 74.2$ ppm) while β ones present a value lower than 70.3 ppm ($\delta \leq 70.3$ ppm). This difference becomes very significant in methyl esters and acid or salt compounds reaching a $\Delta\delta$ (C6α-C6β) of 5.5 ppm (Table 3.8). Thus, C6 signal could be defined as a very important diagnostic one. It is obvious that, to definitively validate this new empirical rule, it is necessary to synthesized a higher number of molecules. I could anticipate that some preliminary studies on other alcoholic or thiolic derivatives confirmed this interesting new empirical rule.

Compound	δC-6 α anomer	δC-6 β anomer	Δδ (C6α-C6β)
23a+24a	74.4	70.4	4.0
23b+24b	74.2	70.6	3.6
32a and **33a**	77.2	71.7	5.5
32b and **33b**	77.3	71.8	5.5
21a and **22a**	75.8	70.3	5.5
21b and **22b**	77.4	71.8	5.6

Table 3.8 *C6 chemical shift for protected 2O-methyl and 2S-ethyl derivatives, their methyl esters and the corresponding free acid and salts.*

3.3.2 Neuraminidase inhibition assay (NI) on NDV-HN and hNEU3

After the synthesis and the full physico-chemical characterization of the obtained 3,4-unsaturated derivatives, I decided to screen, as suggested by preliminary docking simulations (indicating a possible accommodation of 2β substituents in C4 cavity, see paragraph 3.3.1), the synthesized β anomers (**22a-f**) as potential paramyxoviruses neuraminidase activity inhibitors, using NDV-HN as model. For this purpose, I evaluated their inhibitory potency towards NDV-HN by a fluorimetric assay (see Material and Methods) and the results were reported in Table 3.9.

As shown in the graph, increasing the steric hindrance of the 2β substituents a statistically significative increase in inhibitory activity towards NDV-HN was registered passing from the 2*O*-methyl sialoside **22a** (IC_{50} > 1000 μM) to the 2*O*-isopropyl compound **22d** (IC_{50} = 148

μM). The addition of longer alkyl chains in compounds **22e** and **22f**, 2*O*-butyl and 2*S*-octyl respectively, led to a subsequent decrease in inhibitory potency. These results permit to hypothesize that the isopropyl group (IC_{50}=148 μM) could be well accommodated inside the large C4 cavity but this is not sufficient to give new additional interactions.

All these compounds have been tested, also, against human NEU3 (hNEU3), according to general procedure described in Materials and Methods, to evaluate both their ability to inhibit this enzyme and their selectivity. A shown in Table 3.9 all these derivatives resulted inactive towards hNEU3, showing a selective inhibitory activity versus NDV-HN.

Successively, I decided to test also the inhibitory activity of 2α *O*-methyl **21a** and 2α *S*-ethyl **21b** compounds, observing that **21a** showed no activity towards NDV-HN and hNEU3 with an IC_{50} value above the selected threshold of 1mM. Interestingly, compound **21b** resulted the most potent inhibitor among all the 3,4-unsaturated synthesized derivatives (IC_{50} =100 μM against NDV-HN), but, unfortunately it lack of selectivity (showing an IC_{50} value of 130 μM versus hNEU3).

Taken together, these results permitted to speculate that, probably, the β anomers could be more selective for NDV-HN towards human NEU3, than α ones. This behavior could be associated to the different dimensions of the C4 cavity in paramyxovirues and mammalians.

Compound	IC_{50} (μM)[a] against NDV-HN	IC_{50} (μM)[a] against hNEU3
22a (2β-OMe)	>1000	>1000
22c (2β-OEt)	384 ± 55	>1000
22b (2β-SEt)	248 ± 18	>1000
22d (2β-iPr)	148 ± 12	>1000
22e (2β-OBu)	485 ± 118	>1000
22f (2β-SOct)	406 ± 100	>1000
21a (2α-OMe)	>1000	>1000
21b (2α-SEt)	100 ± 25	130 ± 25

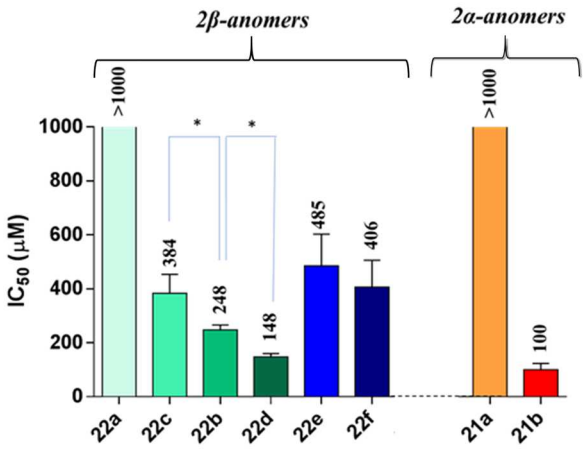

Table 3.9 *NI assay performed on all the 3,4-unsaturated synthesized derivatives against NDV-HN and hNEU3. In the table, all the IC50 values against NDV-HN and hNEU3 are reported. In the graph, the inhibitory activities against NDV-HN is depicted.*

*[a]Each concentration for all the inhibitors is tested in duplicate and the experiment repeated three times, * p<0.05 (t-test)*

4. CONCLUSIONS AND FUTURE PERSPECTIVES

My PhD thesis work was focused on the development of specific and selective inhibitors towards the hemagglutinin-neuraminidase of NDV, both as candidates for new drugs and as useful biochemical tools. In particular, I directed my attention to two classes of inhibitors derived from DANA through the use of a multidisciplinary approach.
The importance of the results obtained is summarized here, for convenience, divided into two sections: the C5 and C4/C5 modified 2,3-unsaturated Neu5Ac derivatives and the 3,4-unsaturated analogues.

- *C5 and C4/C5 modified 2,3-usaturated Neu5Ac derivatives (sections 3.1 and 3.2)*

In this part of my PhD work, I elucidated the role played by some C4 and C5 DANA substituents in enhancing the inhibitory activity against NDV-HN. Remarkably, the combined approach of molecular docking, biological assays and organic synthesis allowed me to discover several new inhibitors that are 5- to 15-fold more active than the, previously reported, most active compound, the *N*-trifluoroacetyl derivative of DANA (FANA). Furthermore, the synthesized inhibitors showed a significant selectivity for NDV-HN, when compared to NEU3; these results are consistent with the different ability of Paramyxoviridae HN and human sialidases to accommodate bulky C4 substituents. In addition, a careful evaluation of the obtained results permitted me also to formulate some interesting hypothesis about the involvement of Lys236 as key basic amino acid in inhibitor-active site interactions. In fact, Induced Fit docking results, performed on one of the nanomolar inhibitors synthesized, compound **12a**, having a *p*-toluensulfonamido substituent at C4, suggested that the sulfonyl group and the aromatic ring could give a hydrogen bonding and π-cation interactions, respectively, with Lys236. Thus, considering the key role of this aminoacid in NDV-HN catalytic site (Site I) activation (together with Arg174) and its implication in a series of conformational changes triggering the fusion promotion activity and the activation of the second sialic acid binding site (Site II) [76, 118], some speculation about the potential additional roles of the synthesized inhibitors in hemagglutinin and fusion promotion activity, could be done. In this regards, some preliminary assays on the hemagglutinin inhibitory activity of these new inhibitors excluded their ability to directly block the second sialic binding site (Site II) present on NDV-HN, maintaining unaltered the hemagglutinin activity. On the other hand, further biological investigations are necessary to clarify their role in fusion promotion activity, investigating the real potentiality of these compounds as drug candidates. In light of this, I planned, in collaboration with the Virology Unit of *Istituto Zooprofilattico Sperimentale delle*

Venezie, some in-depth biological evaluations about the capacity of these molecules to inhibit viral replication *in vitro* and *in vivo* (unreported results).

- *3,4-usaturated Neu5Ac derivatives (sections 3.3)*

In the second part of my PhD work, I clarified some important issues of the synthetic protocols to achieved the 3,4-unsaturated derivatives of Neu5Ac in high anomeric β stereoselectivity. In particular, I understood the effect of the use of some catalysts on the Ferrier's reaction (the key reaction to achieve 3,4-usaturated Neu5Ac), and, as a consequence of this, I set-up the optimal conditions to obtain some 3,4-unsaturated derivatives of Neu5Ac, presenting different substitutions at anomeric carbon (C2) in high yields and high β stereoselectivity. In addition, I developed a smart tool for the rapid and correct anomeric configuration attribution, based on 1,7-lactonization reaction. Furthermore, a deeply NMR spectra analysis allowed me to find a carbon signal that could be diagnostic for the discrimination between α and β anomers.
All these findings permitted me to enrich the knowledge about these molecules, in order to give all the necessary tools to design new inhibitors based on these backbone, or to use them as useful intermediate in the synthesis of 2,3-unsaturated derivatives through a new and rapid way.

Overall, these studies, focused on the development of specific and selective inhibitors towards the hemagglutinin-neuraminidase of NDV, contributed to enhance the knowledge about the highly flexible enzymatic active site of this protein and opened the way to the discovery of new potent paramyxoviruses HN inhibitors.

The results presented in sections 3.1 and 3.2 allowed the publication of two scientific articles:

- Rota, P., La Rocca, P., Piccoli, M., Montefiori, M., Cirillo, F., Olsen, L., Orioli, M., Allevi, P., and Anastasia, L. (2018) Potent Inhibitors against Newcastle Disease Virus Hemagglutinin-Neuraminidase, *ChemMedChem 13*, 236-240.
- Rota, P., Papini, N., La Rocca, P., Montefiori, M., Cirillo, F., Piccoli, M., Scurati, R., Olsen, L., Allevi, P., and Anastasia, L. (2017) Synthesis and chemical characterization of several perfluorinated sialic acid glycals and evaluation of their in vitro antiviral activity against Newcastle disease virus, *MedChemComm 8*, 1505-1513.

5. EXPERIMENTAL

5.1 Chemistry

General materials and methods. All chemicals and solvents used were of analytical grade and purchased from Sigma-Aldrich (St. Louis, MO, USA). Deionized water was prepared by filtering water on a Milli-Q Simplicity 185 filtration system from Millipore (Bedford, MA, USA). All solvents were dried using standard methods and distilled before use. The progress of all reactions was monitored by thin-layer chromatography (TLC) carried out on 0.25 mm Sigma-Aldrich silica gel plates (60 F254) using UV light, anisaldehyde/H_2SO_4/EtOH solution or 0.2% ninhydrin in ethanol and heat as the developing agent. Flash chromatography was performed with normal phase silica gel (Sigma-Aldrich 230–400 mesh silica gel), following the general protocol of Still[131].

Nuclear magnetic resonance spectra were recorded at 303K on a Bruker AM-500 spectrometer equipped with a 5 mm inverse-geometry broadband probe and operating at 500.13 MHz for ^1H and 125.76 MHz for ^{13}C. Chemical shifts are reported in parts per million and are referenced for ^1H spectra, to a solvent residue proton signal (δ = 7.26 and 3.31 ppm, respectively, for $CDCl_3$ and CD_3OD) and for ^{13}C spectra, to solvent carbon signal (central line at δ = 77.0 and 49.05 ppm, respectively, for $CDCl_3$ and CD_3OD). The chemical shifts obtained for D_2O solution are referenced to the internal $(CH_3)_3COH$ signal δ = 1.24 ppm for ^1H spectra and δ = 30.29 ppm for ^{13}C spectra. The ^1H and ^{13}C resonances were assigned by ^1H–^1H (COSY) and ^1H–^{13}C (HSQC and HMBC) correlation 2D experiments. The ^1H NMR data are tabulated in the following order: multiplicity (s = singlet, d = doublet, br s = broad singlet, t = triplet, m = multiplet), coupling constant(s) (*J*) are given in hertz ([Hz]), number of protons and assignment of proton(s). Optical rotations were taken on a Perkin-Elmer 241 polarimeter equipped with a 1 dm tube; $[\alpha]_D$ values are given in 10^{-1}deg cm^2g^{-1} and the concentrations are given in g per 100 mL. High-resolution mass spectrometry (HRMS) analyses were performed using a QTof 5600 ABSciexmass spectrometer equipped with an ESI ion source. The spectra were collected in continuous flow mode by connecting the integrated Harvard syringe pump directly to the ESI source. Compound solutions were infused at a flow rate of 0.01 mL $min^{-1}$and the spray voltage was set at 4.5 kV in the negative ion mode with a capillary temperature of 400°C. Full-scan mass spectra were recorded by scanning a *m/z* range of 50–700. Mass spectrometry was performed by using a ABSciex 4000Qtrap mass spectrometer equipped with an ESI ion source. The spectra were collected in a continuous flow mode by connecting the infusion pump directly to the ESI source. Solutions of the compounds were infused at a flow rate of 0.01 mL min^{-1}, the spray voltage was set at

4.5 kV in the negative ion mode with a capillary temperature of 550 °C. Full-scan mass spectra were recorded by scanning a *m/z* range of 100–2000.

The preparative HPLC purifications were performed on a Dionex Ultimate 3000 instrument equipped with a Dionex RS variable wavelength detector, using an Atlantis C-18-Preper T3 ODB (5 μm, 19 X 10 mm) column and starting from 100% aqueous 0.1% (v/v) formic acid to 100% CH_3CN as the eluent. The crude product was dissolved in water and the solution was filtered (polypropylene, 0.45 μm, 13 mm ø, PK/100) and in*J*ected into the HPLC, affording purified products.

5.1.1 The 2,3-unsaturated derivatives: C5 substitutions (Chapter 3.1)

5.1.1.1 Synthesis of precursor 7

Preparation of methyl 5-acetamido-4,7,8,9-tetra-O-acetyl-2,6-anhydro-3,5-dide-oxy-D-glycero-D-talo-non-2-enonate (**7**).

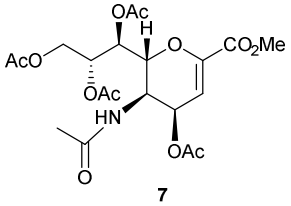

7

A solution of **5**[105] (615 mg, 1.3 mmol) in CH_2Cl_2 (7 mL) containing BF_3Et_2O (0.80 mL, 6.5 mmol) was heated at 80°C for 15 min. Then, after cooling at 23°C Ac_2O (2.8 mL, 30 mmol), Et_3N (2.2 mL, 16 mmol) and H_2O (2.3 mL, 130 mmol) were added and the solution was stirred for 10 min at 23°C. The crude was diluted with AcOEt and the organic layers were, at first, washed with saturated $NaHCO_3$ solution then with water and dried over anhydrous Na_2SO_4. Then, a rapid chromatography (eluting with AcOEt) afforded glycal **7** (566 mg, 92 %): ^{1}H NMR (500 MHz, $CDCl_3$): δ = 6.15 (d, $J_{3,4}$ = 5.4 Hz, 1H; H-3), 5.84 (d, $J_{NH,5}$ = 10.1 Hz, 1H; N*H*COCH$_3$), 5.45 (dd, $J_{7,6}$ = 2.1, $J_{7,8}$ = 3.8 Hz, 1H; H-7), 5.26 (ddd, $J_{8,9a}$ = 2.7, $J_{8,7}$= 3.8, $J_{8,9b}$ = 7.3 Hz, 1H; H-8), 5.11 (dd, $J_{4,5}$ = 4.6, $J_{4,3}$ = 5.4 Hz, 1H; H-4), 4.73 (dd, $J_{9a,8}$ = 2.7, $J_{9a,9b}$ = 12.4 Hz, 1H; H-9a), 4.53 (ddd, $J_{5,4}$ = 4.6, $J_{5,6}$ = $J_{5,NH}$ = 10.1 Hz, 1H; H-5), 4.24 (dd, $J_{6,7}$ = 2.1, $J_{6,5}$ = 10.1 Hz, 1H; H-6), 4.14 (dd, $J_{9b,8}$ = 7.3, $J_{9b,9a}$ = 12.4 Hz, 1H; H-9b), 3.75 (s, 3H; COOCH$_3$), 2.05 (overlapping, 6H; 2 X OCOCH$_3$), 2.03 (s, 3H; OCOCH$_3$), 2.01 (s, 3H; OCOCH$_3$), 1.88 ppm (s, 3H; NHCOC*H*$_3$). The other physico-chemical properties were in agreement with those previously reported[110].

5.1.1.2 N-transacylation procedure for the synthesis of 4-hydroxy N-perfluoro acylneuraminic acid glycals 6a-c and 8a-c.

General procedure.

<u>*For 4α derivatives*</u>: to a solution of compound **5**[105] (0.20 mmol) in CH_3CN (1 mL), Et_3N (1.8 mmol) and the appropriate perfluorinated anhydride (0.8 mmol) were added at 0 °C.

<u>*For 4β derivatives*</u>: to a solution of compound **7**[110] (0.42 mmol), in CH_3CN (2.1 mL), Et_3N (3.8 mmol) and the appropriate perfluorinated anhydride (1.9 mmol) were added at 0 °C.

The mixtures were warmed at 135 °C for 5-15 min in a sealed tube. Then, the reaction mixtures were cooled, quenched with methanol (10-20 µL) and evaporated under reduced pressure to afford crude residues. The crudes were diluted with AcOEt and the organic layers were, at first, washed with saturated NH_4Cl solution then with water and dried over anhydrous Na_2SO_4. The organic solvents were concentrated under vacuum and the residues purified by silica gel chromatography using a suitable solvent system.

Preparation of 4,7,8,9-tetra-O-acetyl-2,3-dehydro-2-deoxy-5-N-(2,2,2-trifluoroacetyl)-β-neuraminic acid methyl ester (**6a**).

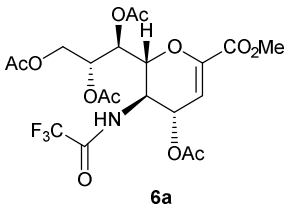

6a

The 4α-acetoxy glycal **5**[105] (95 mg, 0.20 mmol) was directly *N*-transacylated with trifluoroacetic anhydride (0.11 mL, 0.8 mmol) according to general procedure, to afford, after flash chromatography (eluting with hexane/AcOEt; 6:4, v/v), the fluorinated compound **6a** as a white solid (83 mg, 79%): ^{1}H NMR (500 MHz, $CDCl_3$) δ = 7.21 (d, $J_{NH,5}$ = 9.0 Hz, 1H; N*H*$COCH_3$), 5.97 (d, $J_{3,4}$ = 2.6 Hz, 1H; H-3), 5.65 (dd, $J_{4,3}$ = 2.6 Hz, $J_{4,5}$ = 8.0, 1H; H-4), 5.47 (dd, $J_{7,6}$ = 3.0 Hz, $J_{7,8}$ = 4.3, 1H; H-7), 5.29 (m, 1H; H-8), 4.71 (dd, $J_{9a,8}$ = 2.6 Hz, $J_{9a,9b}$ = 12.4, 1H; H-9a), 4.49 (dd, $J_{6,7}$ = 3.0 Hz, $J_{6,5}$ = 9.7, 1H; H-6), 4.34 (m, 1H; H-5), 4.18 (dd, $J_{9b,8}$ = 7.3 Hz, $J_{9b,9a}$ = 12.4, 1H; H-9b), 3.81 (s, 3H; $COOCH_3$); 2.11 (s, 3H; $OCOCH_3$ at C-7), 2.06 (overlapping, 6H; 2 X $OCOCH_3$), 2.04 ppm (s, 3H; $OCOCH_3$). The other physico-chemical properties were in agreement with those previously reported[102].

Preparation of 4,7,8,9-Tetra-O-acetyl-2,3-dehydro-2-deoxy-5-N-(2,2,3,3,3-pentafluoro propionyl)-β-neuraminic acid methyl ester (**6b**).

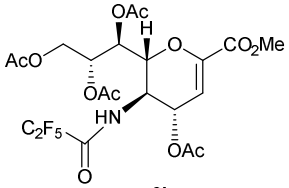

6b

The 4α-acetoxy glycal **5**[105] (95 mg; 0.20 mmol) was directly *N*-transacylated with pentafluoropropionic anhydride (0.16 mL, 0.8 mmol) according to general procedure to afford, after flash chromatography (eluting with hexane/AcOEt; 6:4, v/v), the fluorinated compound **6b** as a white solid (90 mg, 78%): ^{1}H NMR (500 MHz, $CDCl_3$) δ = 7.10 (d, $J_{NH,5}$ = 9.3 Hz, 1H; N*H*COCH$_3$), 5.98 (d, $J_{3,4}$ = 2.8 Hz, 1H; H-3), 5.70 (dd, $J_{4,5}$ = 8.0, $J_{4,3}$ = 2.8 Hz, 1H; H-4), 5.43 (dd, $J_{7,8}$ = 4.5, $J_{7,6}$ = 3.0 Hz, 1H; H-7), 5.31 (m, 1H; H-8), 4.67 (1H, dd, $J_{9a,9b}$ = 12.4, $J_{9a,8}$ = 2.9 Hz, H-9a), 4.51 (dd, $J_{6,5}$ = 9.7, $J_{6,7}$ = 3.0 Hz, 1H; H-6), 4.37 (m, 1H; H-5), 4.19 (dd, $J_{9b,9a}$ = 12.4, $J_{9b,8}$ = 6.8 Hz, 1H; H-9b), 3.84 (s, 3H; COOCH$_3$), 2.13 (s, 3H; OCOCH$_3$), 2.08 (s, 3H; OCOCH$_3$), 2.06 (s, 3H; OCOCH$_3$), 2.05 ppm (s, 3H; OCOCH$_3$). The other physico-chemical properties were in agreement with those previously reported[102].

Preparation of 4,7,8,9-tetra-O-acetyl-2,3-dehydro-2-deoxy-5-N-(2,2,3,3,4,4,4-heptafluoro butanoyl)-β-neuraminic acid methyl ester (**6c**)

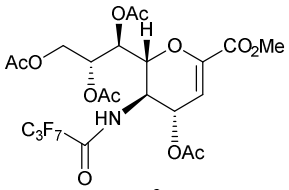

6c

The 4α-acetoxy glycal **5**[105] (95 mg; 0.20 mmol) was directly *N*-transacylated with heptafluorobutyric anhydride (0.19 mL, 0.8 mmol) according to general procedure to afford, after flash chromatography (eluting with hexane/AcOEt; 6:4, v/v), the fluorinated compound **6c**, as a white solid (102 mg, 81%): ^{1}H NMR (500 MHz, $CDCl_3$) δ = 7.21 (d, $J_{NH,2}$ = 9.0 Hz, 1H; N*H*COCH$_3$), 5.97 (d, $J_{3,4}$ = 2.6 Hz, 1H; H-3), 5.70 (dd, $J_{4,5}$ = 9.0, $J_{4,3}$ = 2.6 Hz, 1H; H-4), 5.43 (dd, $J_{7,8}$ = 4.4, $J_{7,6}$ = 2.8 Hz, 1H; H-7), 5.30 (m, 1H; H-8), 4.66 (dd, $J_{9a,9b}$ = 12.4, $J_{9a,8}$ = 2.6 Hz, 1H; H-9a), 4.53 (dd, $J_{6,5}$ = 9.8, $J_{6,7}$ = 2.8 Hz, 1H; H-6), 4.35 (q app., $J_{5,4}$ = $J_{5,6}$ = $J_{5,NH}$ = 9.0 Hz, 1H, H-5), 4.19 (dd, $J_{9b,9a}$ = 12.4, $J_{9b,8}$ = 6.8 Hz, 1H; H-9b), 3.81 (s, 3H; COOCH$_3$); 2.14 (s, 3H; OCOCH$_3$ at C-7), 2.07 (s, 3H; OCOCH$_3$), 2.06 (s, 3H; OCOCH$_3$), 2.00 (s, 3H;

$OCOCH_3$). The other physico-chemical properties were in agreement with those previously reported[102].

*Preparation of methyl 4,7,8,9-Tetra-O-acetyl-2,6-anhydro-3,5-dideoxy-5-(2,2,2-trifluoro acetamido)-D-glycero-D-talo-non-2-enonate (***8a***)*

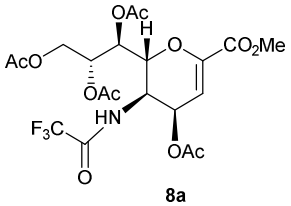

8a

The 4β-acetoxy glycal **7**[110] (200 mg, 0.42 mmol) was directly *N*-transacylated with trifluoroacetic anhydride (0.26 mL, 1.9 mmol) according general procedure, to afford, after flash chromatography (eluting with hexane/AcOEt; 6:4, v/v), the fluorinated compound **8a** as a white solid (186 mg, 84%): ^{1}H NMR (500 MHz, $CDCl_3$): δ = 6.76 (d, $J_{NH;5}$ = 10.1 Hz, 1H; N*H*$COCH_3$), 6.21 (d, $J_{3,4}$ = 5.5 Hz, 1H; H-3), 5.45 (dd, $J_{7,6}$ = 2.5, $J_{7,8}$ = 4.4 Hz, 1H; H-7), 5.30 (ddd, $J_{8,9a}$ = 2.9, $J_{8,7}$ = 4.4, $J_{8,9b}$ = 7.2 Hz, 1H; H-8), 5.26 (dd, $J_{4,5}$ = 4.2, $J_{4,3}$ = 5.5 Hz, 1H; H-4), 4.72 (dd, $J_{9a,8}$ = 2.9, $J_{9a,9b}$ = 12.4 Hz, 1 H; H-9a), 4.53 (ddd, $J_{5,4}$ = 4.2, $J_{5,6}$ = $J_{5,NH}$ = 10.1 Hz, 1H; H-5), 4.39 (dd, $J_{6,7}$ = 2.5, $J_{6,5}$ = 10.1 Hz, 1H; H-6), 4.17 (dd, $J_{9b,8}$ = 7.2, $J_{9b,9a}$ = 12.4 Hz, 1H; H-9b), 3.80 (s, 3H; $COOCH_3$), 2.10 (s, 3H; $OCOCH_3$), 2.09 (s, 3H; $OCOCH_3$), 2.07 (s, 3 H; $OCOCH_3$), 2.04 ppm (s, 3 H; $OCOCH_3$). The other physico-chemical properties were in agreement with those previously reported[110].

*Preparation of methyl 4,7,8,9-Tetra-O-acetyl-2,6-anhydro-5-(2,2,3,3,3-pentafluoropropion amido)-3,5-dideoxy-D-glycero-D-talo-non-2-enonate (***8b)**

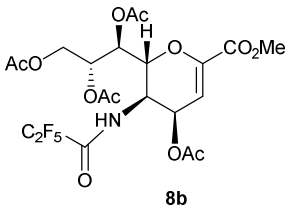

8b

The 4β-acetoxy glycal **7**[110] (200 mg, 0.42 mmol) was directly *N*-transacylated with pentafluoro propionic anhydride (0.38 mL, 1.9 mmol) according to general procedure, to afford, after flash chromatography (eluting with hexane/AcOEt; 6:4, v/v), the fluorinated compound **8b** as a white solid (198 mg, 82%): ^{1}H NMR (500 MHz, $CDCl_3$): δ = 6.85 (d, $J_{NH,5}$ = 9.7 Hz, 1H; N*H*$COCH_3$), 6.20 (d, $J_{3,4}$ = 5.4 Hz, 1H; H-3), 5.44 (dd, $J_{7,6}$ = 2.5, $J_{7,8}$ = 4.4 Hz, 1H; H-7), 5.32-5.27 (2H; overlapping, H-8 and H-4), 4.69 (dd, $J_{9a,8}$ = 2.8, $J_{9a,9b}$ = 12.5 Hz,

1H; H-9a), 4.55 (ddd, $J_{5,4}$ = 4.4, $J_{5,NH}$ = 9.7, $J_{5,6}$ = 10.3 Hz, 1H; H-5), 4.39 (dd, $J_{6,7}$ = 2.5, $J_{6,5}$ = 10.3 Hz, 1H; H-6), 4.16 (dd, $J_{9b,8}$ = 7.0, $J_{9b,9a}$ = 12.5 Hz, 1H; H-9b), 3.80 (s, 3 H; $OCOCH_3$), 2.09 (6 H; overlapping, 2 X $OCOCH_3$), 2.07 (s, 3 H; $OCOCH_3$), 2.04 ppm (s, 3 H; $OCOCH_3$). The other physico-chemical properties were in agreement with those previously reported[110].

Preparation of methyl 4,7,8,9-tetra-O-acetyl-2,6-anhydro-3,5-dideoxy-5-(2,2,3,3,4,4,4-heptafluorobutanamido)-D-glycero-D-talo-non-2-enonate (**8c**)

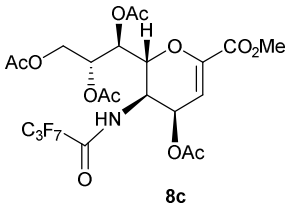

8c

The 4β-acetoxy glycal **7**[110] (200 mg, 0.42 mmol) was directly *N*-transacylated with heptafluorobutyric anhydride 0.45 mL, 1.9 mmol) according to general procedure, to afford, after flash chromatography (eluting with hexane/AcOEt; 6:4, v/v), the fluorinated compound **8c** as a white solid (210 mg, 80%): ^{1}H NMR (500 MHz, $CDCl_3$): δ = 6.62 (br s, 1H; NH), 6.22 (d, $J_{3,4}$ = 5.3 Hz, 1H; H-3), 5.46 (dd, $J_{7,6}$ = 2.6, $J_{7,8}$ = 4.5 Hz, 1H; H-7), 5.32 (ddd, $J_{8,9a}$ = 2.9, $J_{8,7}$ = 4.5, $J_{8,9b}$ = 6.8 Hz, 1H; H-8), 5.28 (dd, $J_{4,5}$ = 4.3, $J_{4,3}$ = 5.3 Hz, 1H; H-4), 4.70 (dd, $J_{9a,8}$ = 2.9, $J_{9a,9b}$ = 12.4 Hz, 1H; H-9a), 4.60 (ddd, $J_{5,4}$ = 4.3, $J_{5,6}$ = $J_{5,NH}$ = 10.2 Hz, 1H; H-5), 4.39 (dd, $J_{6,7}$ = 2.6, $J_{6,5}$ = 10.2 Hz, 1H; H-6), 4.18 (dd, $J_{9b,8}$ = 6.8, $J_{9b,9a}$ = 12.4 Hz, 1H; H-9b), 3.81 (s, 3H; $COOCH_3$), 2.11–2.08 (overlapping, 9H; 3 X $OCOCH_3$), 2.06 ppm (s, 3 H; $OCOCH_3$). The other physico-chemical properties were in agreement with those previously reported[110].

5.1.1.3 Acylation procedure for the synthesis of 4-hydroxy N-perfluoro acylneuraminic acid glycals 10a,b and N-unfluoroacylneuraminic acid glycals 11a,b.

To a solution of **9**[4] (250 mg, 0.56 mmol) in CH_2Cl_2 (8 mL), under argon, Et_3N (401 μL, 2.90 mmol) and the appropriate perfluoroacyl chloride or normal acyl chloride (0.87 mmol) were added at 0 °C. The mixture was stirred at 23°C for 3-5 h and then purified by silica gel chromatography (hexane/AcOEt, 7:3, v/v) to achieve the desired compound **10a,b** and **11a,b**.

Preparation of methyl 4,7,8,9-tetra-O-acetyl-2,6-anhydro-3,5-dideoxy-5-(perfluoropentan amido)-D-glycero-D-galacto-non-2-enonate (**10a**):

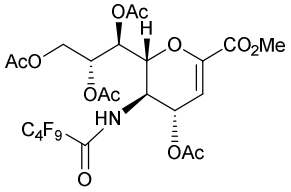

10a

Starting from intermediate **9**[4] (250 mg, 0.56 mmol), according to general procedure using perfluoropentanoyl chloride (147 µL, 0.87 mmol), compound **10a** was obtained (296 mg, 78%) as a white solid, showing: $[\alpha]_D^{23}$ = +58.6 (c=1.0 in chloroform); ^{1}H NMR (500 MHz, $CDCl_3$): δ = 7.37 (d, $J_{NH,5}$ = 9.3 Hz, 1H; N*H*COCH$_3$), 5.95 (d, $J_{3,4}$ = 2.6 Hz, 1H; H-3), 5.71 (dd, $J_{4,3}$ = 2.6, $J_{4,5}$ = 8.2 Hz, 1H; H-4), 5.43 (dd, $J_{7,6}$ = 2.4, $J_{7,8}$ = 4.2 Hz, 1H; H-7), 5.29-5.26 (m, 1H; H-8), 4.69 (dd, $J_{9a,8}$ = 2.7, $J_{9a,9b}$ = 12.4 Hz, 1H; H-9a), 4.50 (dd, $J_{6,7}$ = 2.4, $J_{6,5}$ = 9.9 Hz, 1H; H-6), 4.41-4.33 (m, 1H; H-5), 4.20 (dd, $J_{9b,8}$ = 7.0, $J_{9b,9a}$ = 12.4 Hz, 1H; H-9b), 3.81 (s, 3H; COOCH$_3$), 2.13 (s, 3H; OCOCH$_3$), 2.07 (s, 3H; OCOCH$_3$), 2.05 (s, 3H; OCOCH$_3$), 2.04 ppm (s, 3H; OCOCH$_3$); ^{13}C NMR (125 MHz, $CDCl_3$): δ = 170.8, 170.8, 170.7, 170.0 (4C; O*C*OCH$_3$), 161.2 (C-1), 157.8 (t, $J_{C,F}$ = 27.2 Hz, *C*OC$_4$F$_9$), 145.2 (C-2), 122.8-110.0 (4C; CO*C*$_4$F$_9$), 107.7 (C-3), 75.8 (C-6), 71.3 (C-8), 67.6 and 67.4 (C-4 and C-7), 61.9 (C-9), 52.6 (COO*C*H$_3$), 47.5 (C-5), 20.8, 20.6, 20.5, 20.5 ppm (4C; OCO*C*H$_3$); MS (ESI negative): *m/z* 676.2 [M-H]$^-$; elemental analysis calcd (%) for $C_{23}H_{24}F_9NO_{12}$: C 40.78, H 3.57, N 2.07; found: C 40.65, H 3.28, N 2.20.

Preparation of methyl 4,7,8,9-tetra-O-acetyl-2,6-anhydro-3,5-dideoxy-5 (perfluoro hexanamido)-D-glycero-D-galacto-non-2-enonate (**10b**):

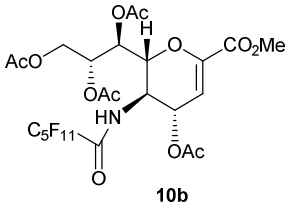

10b

Starting from intermediate **9**[4] (250 mg, 0.56 mmol), according to general procedure using perfluorohexanoyl chloride (174 µL, 0.87 mmol), compound **10b** was obtained (306 mg, 75%) as a white solid, showing: $[\alpha]_D^{23}$ = +53.0 (c=1.0 in chloroform); ^{1}H NMR (500 MHz, $CDCl_3$): δ = 7.40 (d, $J_{NH,5}$ = 9.3 Hz, 1H; N*H*COCH$_3$), 5.94 (d, $J_{3,4}$ = 2.7 Hz, 1H; H-3), 5.71 (dd, $J_{4,3}$ = 2.7, $J_{4,5}$ = 8.3 Hz, 1H; H-4), 5.44 (dd, $J_{7,6}$ = 2.6, $J_{7,8}$ = 4.4 Hz, 1H; H-7), 5.27 (ddd, $J_{8,9a}$ = 2.8, $J_{8,7}$ = 4.4, $J_{8,9b}$ = 7.1 Hz, 1H; H-8), 4.70 (dd, $J_{9a,8}$ = 2.8, $J_{9a,9b}$ = 12.4 Hz, 1H; H-9a), 4.50 (dd,

$J_{6,7}$ = 2.6, $J_{6,5}$ = 10.0 Hz, 1H; H-6), 4.43-4.31 (m, 1H; H-5), 4.20 (dd, $J_{9b,8}$ = 7.1, $J_{9b,9a}$ = 12.4 Hz, 1H; H-9b), 3.81 (s, 3H; $COOCH_3$), 2.12 (s, 3H; $OCOCH_3$), 2.06 (s, 3H; $OCOCH_3$), 2.05 (s, 3H; $OCOCH_3$), 2.04 ppm (s, 3H; $OCOCH_3$); ^{13}C NMR (125 MHz, $CDCl_3$): δ = 170.9, 170.8, 170.7, 170.0 (4C; O*C*OCH_3), 161.2 (C-1), 157.9 (t, $J_{C,F}$ = 27.0 Hz, *C*OC_5F_{11}), 145.2 (C-2), 122.8-110.0 (5C; CO*C*$_5F_{11}$), 107.8 (C-3), 75.9 (C-6), 71.3 (C-8), 67.7 and 67.4 (C-4 and C-7), 61.9 (C-9), 52.6 (COO*C*H_3), 47.6 (C-5), 20.8, 20.6, 20.5, 20.4 ppm (4C; OCO*C*H_3); MS (ESI negative): *m/z* 726.3 [M-H]- ; elemental analysis calcd (%) for $C_{24}H_{24}F_{11}NO_{12}$: C 39.63, H 3.33, N 1.93; found: C 39.75, H 3.18, N 2.11.

Acylation of compounds **11a** *and* **11b**: the data are not reported in this thesis but they were obtained according to general acylation procedure.

5.1.1.4 Deacetylation and selective removal of esteric function

General procedure. All the peracetylated glycals **5**[105], **6a-c**, **3a**, **8a-c**, **10a,b** and **11a,b** (0.14 or 0.20 mmol) were treated with a methanolic solution of NaOMe, freshly prepared by dissolving sodium metal (5 mg, 0.22 mmol,) in anhydrous MeOH (2 mL). Each reaction mixture was stirred at 23°C for 1 h, and then quenched with acidic resin (Dowex 50WX8, H^+). The resin was filtered off and washed with MeOH (2 mL X 3) and the combined filtrate and washes were evaporated under vacuum. Each crude compound was purified with flash chromatography and directly subjected to opportune selective hydrolysis (*Method A or B*):

Method A: Selective hydrolysis using moist K_2CO_3 methanol solution. The free glycals **1a-c**, **2b-e**, **3a**, **4b,c** were prepared by selective hydrolysis of appropriate methyl ester derivatives (0.10 mmol) performed in a methanol-water solution (0.54 mL, 10:1 v/v) containing K_2CO_3 (9 mg), kept at 23°C for 6-24 h. At this time, the reaction mixture was treated with acidic resin (Dowex 50WX8, H^+) until acidic pH, and then, the resin was filtered and washed with MeOH (2 mL X 3). Finally, the solvent was removed under reduced pressure and the residue was recovered with aqueous methanol and lyophilized to afford, after preparative HPLC, the desired free glycals.

Method B: Selective hydrolysis using moist Et_3N methanol solution. The free glycals **2a** and **3a** was prepared by selective hydrolysis of its methyl ester derivative (0.10 mmol) performed in a methanol-water solution (1.0 mL, 2:1 v/v) containing Et_3N (0.60 mL), kept at 23 °C for 12 h. Then the mixture was treated with acidic resin (Dowex 50WX8, H^+) until acidic pH and the resin was filtered and washed with MeOH (2 mL × 3). Finally, the solvent was removed

under reduced pressure and the residue was recovered with aqueous methanol and lyophilized, to afford, after preparative HPLC, the desired free glycals.

Preparation of 2,6-anhydro-5-(2,2,3,3,3-pentafluoropropionamido)-3,5-dideoxy-D-glycero-D-galacto-non-2-enoic acid (**2b**).

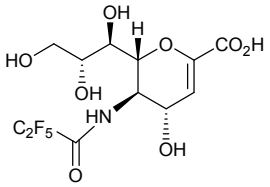

2b

Starting from protected glycal **6b** (80 mg, 0.14 mmol), according to the general two-step procedure Zemplén reaction followed by selective hydrolytic <u>*method A*</u>, glycal **2b** was obtained (48 mg, 86%), as a white solid, showing: $[\alpha]_D^{23}$= + 26.7 (c=1 in MeOH); ^{1}H NMR (500 MHz, CD_3OD): δ = 5.96 (d, $J_{3,4}$ = 2.2 Hz, 1H; H-3), 4.50 (dd, $J_{4,3}$ = 2.2, $J_{4,5}$ = 9.0 Hz, 1H; H-4), 4.41 (d app, $J_{6,5}$ = 11.0 Hz, 1H; H-6), 4.24 (dd, $J_{5,4}$ = 9.0, $J_{5,6}$ = 11.0 Hz, 1H; H-5), 3.86 (ddd, $J_{8,9a}$ = 2.9, $J_{8,9b}$ = 5.6, $J_{8,7}$ = 9.2 Hz, 1H; H-8), 3.80 (dd, $J_{9a,8}$ = 2.9, $J_{9a,9b}$ = 11.4 Hz, 1H; H-9a), 3.62 (dd, $J_{9b,8}$ = 5.6, $J_{9b,9a}$ 11.4 Hz, 1H; H-9b), 3.51 ppm (d app, $J_{7,8}$ = 9.2 Hz, 1H; H-7); ^{13}C NMR (125 MHz, CD_3OD): δ = 165.6 (C-1), 160.0 (t, $J_{C,F}$ = 26 Hz, *C*OC_2F_5), 145.3 (C-2), 125.0–110.0 (2C; CO*C*$_2F_5$), 113.6 (C-3), 77.2 (C-6), 71.5 (C-8), 70.1 (C-7), 68.0 (C-4), 65.0 (C-9), 52.2 ppm (C-5); HRMS (ESI-TOF, *m/z*): calcd for $C_{12}H_{13}F_5NO_8$ $[M-H]^-$ 394.0567, found 394.0559.

*Preparation of 2,6-anhydro-5-(2,2,3,3,4,4,4-heptafluorobutanamido)-3,5-dideoxy-D-glycero-D-galacto-non-2-enoic acid (***2c**).

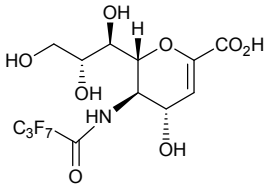

2c

Starting from protected glycal **6c** (88 mg, 0.14 mmol), according to the general two step procedure Zemplén reaction followed by selective hydrolytic <u>*method A*</u>, glycal **6c** was obtained (52 mg, 84%), as a white solid, showing: $[\alpha]_D^{23}$ = +19.9 (c=1 in MeOH); ^{1}H NMR (500 MHz, CD_3OD): δ = 5.96 (d, $J_{3,4}$ = 2.3 Hz, 1H; H-3), 4.50 (dd, $J_{4,3}$ = 2.3, $J_{4,5}$ = 8.9 Hz, 1H; 4-H), 4.41 (dd, $J_{6,7}$ < 1.0, $J_{6,5}$ = 11.0 Hz, 1H; H-6), 4.24 (dd, $J_{5,4}$ = 8.9, $J_{5,6}$ = 11.0 Hz, 1H; H-5), 3.89 (ddd, $J_{8,9a}$ = 2.8, $J_{8,9b}$ = 5.6, $J_{8,7}$ = 9.2 Hz, 1H; H-8), 3.82 (dd, $J_{9a,8}$ = 2.8, $J_{9a,9b}$ =

11.4 Hz, 1H; H-9a), 3.56 (dd, $J_{9b,8}$ = 5.6, $J_{9b,9a}$ = 11.4 Hz, 1H; H-9b), 3.52 ppm (dd, $J_{6,7}$ < 1.0, $J_{7,8}$ = 9.2 Hz, 1H; H-7); ^{13}C NMR (125 MHz, CD_3OD): δ = 165.6 (C-1), 159.8 (t, J_{C-F} = 26 Hz, *C*OC_3F_7), 145.3 (C-2), 122.0–110.0 (3C, CO*C*$_3F_7$), 113.6 (C-3), 77.2 (C-6), 71.5 (C-8), 70.2 (C-7), 67.9 (C-4), 65.0 (C-9), 52.3 ppm (C-5); HRMS (ESI-TOF, *m/z*): calcd for $C_{13}H_{13}F_7NO_8$ $[M-H]^-$ 444.0535, found 444.0551.

Preparation of 2,6-anhydro-3,5-dideoxy-5-(perfluoropentanamido)-D-glycero-D-galacto-non-2-enoic acid (**2d**)

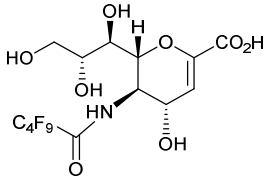

2d

Starting from protected glycal **10a** (135 mg, 0.20 mmol), according to the general two-step procedure Zemplén reaction followed by selective hydrolytic <u>*method A*</u>, glycal **2d** was obtained (74 mg, 75%) as a white solid, showing: $[\alpha]_D^{23}$= + 20.9 (c=1.0 in methanol); ^{1}H NMR (500 MHz, CD_3OD): δ = 5.95 (d, $J_{3,4}$ = 2.2 Hz, 1H; H-3), 4.51 (dd, $J_{4,3}$ = 2.2, $J_{4,5}$ = 8.8 Hz, 1H; H-4), 4.41 (dd, $J_{6,7}$ < 1.0, $J_{6,5}$ = 10.9 Hz, 1H; H-6), 4.24 (dd, $J_{5,4}$ = 8.8, $J_{5,6}$ = 10.9 Hz, 1H; H-5), 3.88 (ddd, $J_{8,9a}$ = 3.0, $J_{8,9b}$ = 5.7, $J_{8,7}$ = 9.1 Hz, 1H; H-8), 3.84 (dd, $J_{9a,8}$ = 3.0, $J_{9a,9b}$ = 11.4 Hz, 1H; H-9a), 3.62 (dd, $J_{9b,8}$ = 5.7, $J_{9b,9a}$ = 11.4 Hz, 1H; H-9b), 3.53 ppm (dd, $J_{7,6}$ < 1.0, $J_{7,8}$ = 9.1 Hz, 1H; H-7); ^{13}C NMR (125 MHz, CD_3OD): δ = 165.8 (C-1), 159.8 (t, $J_{C,F}$ = 26.1 Hz, 1C; *C*OC_4F_9), 145.4 (C-2), 122.8-110.0 (4C; CO*C*$_4F_9$), 113.5 (C-3), 77.2 (C-6), 71.6 (C-8), 70.2 (C-7), 67.9 (C-4), 65.0 (C-9), 52.4 ppm (C-5); MS (ESI negative): *m/z* 494.2 [M-H]-; elemental analysis calcd (%) for $C_{14}H_{14}F_9NO_8$: C 33.95, H 2.85, N 2.83; found: C 33.87, H 2.97, N 2.70.

Preparation of 2,6-anhydro-3,5-dideoxy-5-(perfluorohexanamido)-D-glycero-D-galacto non-2-enoic acid (**2e**).

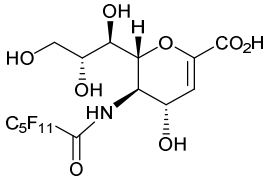

2e

Starting from protected glycal **10b** (145 mg, 0.20 mmol), according to the general two-step procedure Zemplén reaction followed by selective hydrolytic <u>*method A*</u>, glycal **2e** was

obtained (82 mg, 75%) as a white solid, showing: $[\alpha]^{D}_{23}$= +19.7 (c=1.0 in methanol); ^{1}H NMR (500 MHz, CD_3OD): δ = 5.97 (d, $J_{3,4}$ < 1.0 Hz, 1H; H-3), 4.50 (dd, $J_{4,3}$ < 1.0, $J_{4,5}$ = 8.8 Hz, 1H; H-4), 4.43 (dd, $J_{6,7}$ < 1.0, $J_{6,5}$ = 10.9 Hz, 1H; H-6), 4.27-4.21 (m, 1H; H-5), 3.91-3.86 (m, 1H; H-8), 3.83 (dd, $J_{9a,8}$ = 2.5, $J_{9a,9b}$ = 11.4 Hz, 1H; H-9a), 3.62 (dd, $J_{9b,8}$ = 5.7, $J_{9b,9a}$ = 11.4 Hz, 1H; H-9b), 3.54 ppm (dd, $J_{7,6}$ < 1.0, $J_{7,8}$ = 9.2 Hz, 1H; H-7); ^{13}C NMR (125 MHz, CD_3OD): δ = 165.7 (C-1), 159.8 (t, $J_{C,F}$ = 26.1 Hz, *C*OC_5F_{11}), 145.2 (C-2), 122.8-110.0 (5C; COC_5F_{11}), 113.7 (C-3), 77.1 (C-6), 71.5 (C-8), 70.2 (C-7), 67.9 (C-4), 65.0 (C-9), 52.3 ppm (C-5); MS (ESI negative): *m/z* 544.2 [M-H]-; elemental analysis calcd (%) for $C_{15}H_{14}F_{11}NO_8$: C 33.04, H 2.59, N 2.57; found: C 33.22, H 2.48, N 2.44.

*Preparation of 2,6-anhydro-5-acetamido-3,5-dideoxy-D-glycero-D-talo-non-2-enoic acid (***3a***).*

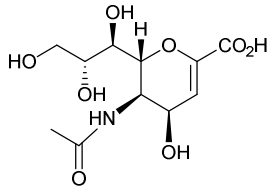

3a

Starting from protected glycal **7**[110] (66 mg, 0.14 mmol), according to the general two-step procedure Zemplén reaction followed by selective hydrolytic <u>*method A*</u>, glycal **3a** was obtained (31 mg, 75%), as a white solid, showing: $[\alpha]_D^{23}$ = -98.9 (c=1 in MeOH); ^{1}H NMR (500 MHz, CD_3OD): δ = 6.02 (d, $J_{3,4}$ = 5.0 Hz, 1H; H-3), 4.27-4.14 (overlapping, 3H; H-4, H-6 and H-5), 3.92 (ddd, $J_{8,9a}$ = 2.3, $J_{8,9b}$ = 5.3, $J_{8,7}$ = 9.2 Hz, 1H; H-8), 3.83 (dd, $J_{9a,8}$ = 2.3, $J_{9a,9b}$ = 11.4 Hz, 1H; H-9a), 3.67 (dd, $J_{9b,8}$ = 5.3, $J_{9b,9a}$ = 11.4 Hz, 1H; H-9b), 3.58 (d app, $J_{7,8}$ = 9.2 Hz, 1H; 7-H), 2.05 ppm (s, 3H; NHCOCH_3); ^{13}C NMR (125 MHz, CD_3OD): δ = 174.2 (C-1), 167.5 (NH*C*OCH_3), 148.2 (C-2), 108.6 (C-3), 73.3 (C-6), 71.5 (C-8), 70.1 (C-7), 65.0 (C-9), 62.1 (C-5), 49.4 (C-4), 22.8 ppm (NHCO*C*H_3); HRMS (ESI-TOF, *m/z*): calcd for $C_{11}H_{16}NO_8$ $[M-H]^-$ 290.0881, found 290.0855.

*Preparation of 2,6-anhydro-5-(2,2,2-trifluoroacetamido)-3,5-dideoxy-D-glycero-D-talo-non-2-enoic acid (***4a***).*

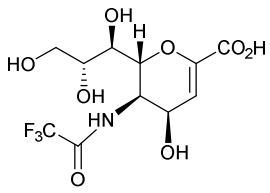

4a

Starting from protected glycal **8a** (74 mg, 0.14 mmol), according to the general two-step

procedure Zemplén reaction followed by selective hydrolytic <u>*method B*</u>, glycal **4a** was obtained (42 mg, 87%), as a white solid, showing: m.p. 112–114 °C (from MeOH-diisopropylether); $[\alpha]_D^{23}$ = -98.8 (c=1 in MeOH); ^{1}H NMR (500 MHz, CD_3OD): δ = 6.14 (d, $J_{3,4}$ = 5.6 Hz, 1H; H-3), 4.45 (d app, $J_{6,5}$ = 11.3 Hz, 1H; 6-H), 4.32 (dd, $J_{5,4}$ = 3.4, $J_{5,6}$ = 11.3 Hz, 1H; H-5), 4.28-4.23 (m, 1H; H-4), 4.00 (ddd, $J_{8,9a}$ = 2.1, $J_{8,9b}$ = 5.4, $J_{8,7}$ = 9.2 Hz, 1H; H-8), 3.84 (dd, $J_{9a,8}$ = 2.1, $J_{9a,9b}$ = 11.4 Hz, 1H; 9a-H), 3.67 (dd, $J_{9b,8}$ = 5.4, $J_{9b,9a}$ = 11.4 Hz, 1H; 9b-H), 3.67 ppm (d app, $J_{7,8}$ = 9.2 Hz, 1H; 7-H); ^{13}C NMR (125 MHz, CD_3OD): δ = 165.8 (C-1), 158.9 (q, $J_{C,F}$ = 37 Hz, 1C; *C*OCF_3), 146.4 (C-2), 121.0-114.0 (q, $J_{C,F}$ = 287 Hz, CO*C*F_3), 110.4 (C-3), 72.9 (C-6), 71.8 (C-8), 69.9 (C-7), 64.9 (C-9), 61.3 (C-5), 50.1 ppm (C-4); HRMS (ESI-TOF, *m/z*): calcd for $C_{11}H_{13}F_3NO_8$ $[M-H]^-$ 344.0599, found 344.0583.

Preparation of 2,6-anhydro-5-(2,2,3,3,3-pentafluoropropionamido)-3,5-dideoxy-D-glycero-D-talo-non-2-enoic acid (**4b**).

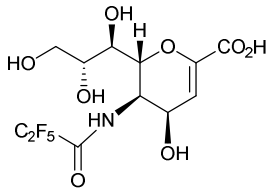

4b

Starting from protected glycal **8b** (81 mg, 0.14 mmol), according to the general two-step procedure Zemplén reaction followed by selective hydrolytic <u>*method A*</u>, glycal **4b** was obtained (40 mg, 72%), as a white solid, showing: m.p. 107-109 °C (from MeOH-diisopropylether); $[\alpha]_D^{23}$ = -119.2 (c=1 in methanol); ^{1}H NMR (500 MHz, CD_3OD): δ = 6.14 (d, $J_{3,4}$ = 5.7 Hz, 1H; H-3), 4.46 (d app, $J_{6,5}$ = 11.4 Hz, 1H; H-6), 4.36 (dd, $J_{5,4}$ = 3.6, $J_{5,6}$ = 11.4 Hz, 1H; H-5), 4.27–4.23 (m, 1H; H-4), 3.91 (ddd, $J_{8,9a}$ = 2.7, $J_{8,9b}$ = 5.6, $J_{8,7}$ = 9.2 Hz, 1H; H-8), 3.84 (dd, $J_{9a,8}$ = 2.7, $J_{9a,9b}$ = 11.4 Hz, 1H; H-9a), 3.65 (dd, $J_{9b,8}$ = 5.6, $J_{9b,9a}$ = 11.4 Hz, 1H; H-9b), 3.57 ppm (d app, $J_{7,8}$ = 9.2 Hz, 1H; H-7); ^{13}C NMR (125 MHz, CD_3OD): δ = 165.8 (C-1), 159.4 (t, $J_{C,F}$ = 26 Hz, *C*OC_5F_5), 146.4 (C-2), 123.0-106.0 (2C, *C*$_5F_5$), 110.5 (C-3), 72.9 (C-6), 71.8 (C-8), 70.0 (C-7), 65.0 (C-9), 61.3 (C-5), 50.1 ppm (C-4); HRMS (ESI-TOF, *m/z*): calcd for $C_{12}H_{13}F_5NO_8$ $[M-H]^-$ 394.0567, found 394.0560.

Preparation of 2,6-anhydro-5-(2,2,3,3,4,4,4-heptafluorobutanamido)-3,5-dideoxy-D-glycero -D-talo-non-2-enoic acid (**4c**).

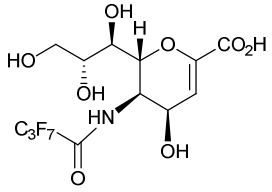

4c

Starting from protected glycal **8c** (88 mg, 0.14 mmol), according to the general two step procedure Zemplén reaction followed by selective hydrolytic <u>*method A*</u>, glycal **4c** was obtained (44 mg, 71%), as a white solid, showing: $[\alpha]_D^{23}$ = -103.6 (c=1 in methanol); ^{1}H NMR (500 MHz CD_3OD): δ = 6.13 (d, $J_{3,4}$ = 5.6 Hz, 1H; H-3), 4.47 (d app, $J_{6,5}$ = 11.3 Hz, 1H; H-6), 4.36 (dd, $J_{5,4}$ = 3.2, $J_{5,6}$ = 11.3 Hz, 1H; H-5), 4.24 (dd, $J_{4,5}$ = 3.2, $J_{4,3}$ = 5.6 Hz, 1H; H-4), 3.91 (ddd, $J_{8,9a}$ = 2.1, $J_{8,9b}$ = 5.6, $J_{8,7}$ = 9.1 Hz, 1H; H-8), 3.85 (dd, $J_{9a,8}$ = 2.1, $J_{9a,9b}$ = 11.4 Hz, 1H; H-9a), 3.65 (dd, $J_{9b,8}$ = 5.6, $J_{9b,9a}$ = 11.4 Hz, 1H; H-9b), 3.58 (d app, $J_{7,8}$ = 9.1 Hz, 1H; H-7); ^{13}C NMR (125 MHz, CD_3OD): δ = 166.0 (C-1), 159.2 (t, $J_{C,F}$ 26 Hz, 1C *C*OC_3F_7), 146.5 (C2), 121.0–106.0 (3C, CO*C*$_3F_7$), 110.3 (C-3), 72.9 (C-6), 71.9 (C8), 70.1 (C-7), 65.0 (C-9), 61.3 (C-5), 50.2 ppm (C-4); HRMS (ESI-TOF, *m/z*): calcd for $C_{13}H_{13}F_7NO_8$ [M-H]– 444.0535, found 444.0535.

Preparation of 2,6-anhydro-5-propionamido-3,5-dideoxy-D-glycero-D-galacto-non-2-enoic acid (**1b**).

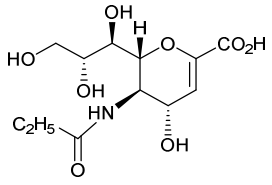

1b

Starting from protected glycal **11a** (68 mg, 0.14 mmol), according to the general two step procedure Zemplén reaction followed by selective hydrolytic <u>*method A*</u>, glycal **1b** was obtained (30 mg, 71%), as a white solid, showing: ^{1}H NMR (500 MHz, CD_3OD): δ = 5.87 (br s, 1H; H-3), 4.42 (d app, $J_{4,5}$ = 8.3 Hz, 1H; H-4), 4.15 (d app, $J_{6,5}$ = 10.7 Hz, 1H; H-6), 3.99 (dd, $J_{5,4}$ = 8.7, $J_{5,6}$ = 10.7 Hz, 1H; H-5), 3.93–3.86 (m, 1H; H-8), 3.82 (d app, $J_{9a,9b}$ = 11.3 Hz, 1H; H-9a), 3.65 (dd, $J_{9b,8}$ = 4.9, $J_{9b,9a}$ = 11.3 Hz, 1H; H-9b), 3.55 (d app, $J_{7,8}$ = 8.9 Hz, 1H; H-7), 2.32 (q, $J_{H,H}$ = 7.5 Hz, 2H; $COCH_2$), 1.16 ppm (t, $J_{H,H}$ = 7.5 Hz, 3H; $COCH_2CH_3$); ^{13}C NMR (125 MHz, CD_3OD): δ = 178.7 (C-1), 165.6 (NH*C*OCH_3), 145.5 (C-2), 111.8 (C-3),

77.9 (C-6), 71.3 (C-8), 70.3 (C-7), 68.2 (C-4), 65.0 (C-9), 51.9 (C5), 30.2 ($CO\mathit{C}H_2$), 10.3 ppm ($COCH_2\mathit{C}H_3$); MS (ESI negative, *m/z*): calcd for $C_{12}H_{19}NO_8$ $[M-H]^-$ 304.1, found 304.2.

Preparation of 2,6-anhydro-5-butyramido-3,5-dideoxy-D-glycero-D-galacto-non-2-enoic acid (**1c**).

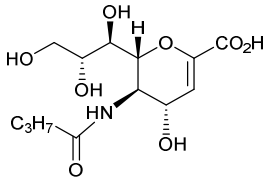

1c

Starting from protected glycal **11b** (70 mg, 0.14 mmol), according to the general two-step procedure Zemplén reaction followed by selective hydrolytic <u>*method A*</u>, glycal **1c** was obtained (32 mg, 71%), as a white solid, showing: ^{1}H NMR (500 MHz, CD_3OD): δ = 5.97 (d, $J_{3,4}$ = 2.1 Hz, 1H; H-3), 4.46 (dd, $J_{4,3}$ = 2.1, $J_{4,5}$ = 8.7 Hz, 1H; H-4), 4.19 (d app, $J_{6,5}$ = 10.8 Hz, 1H; H-6), 4.02 (dd, $J_{5,4}$ = 8.7, $J_{5,6}$ = 10.8 Hz, 1H; H-5), 3.92 (ddd, $J_{8,9a}$= 2.6, $J_{8,9b}$ = 5.4, $J_{8,7}$ = 9.1 Hz, 1H; H-8), 3.85 (dd, $J_{9a,8}$ = 2.6, $J_{9a,9b}$ = 11.4 Hz, 1H; H-9a), 3.66 (dd, $J_{9b,8}$ = 5.4, $J_{9b,9a}$ = 11.4 Hz, 1H; H-9b), 3.59 (d app, $J_{7,8}$ = 9.1 = Hz, 1H; H-7), 2.30 (t, $J_{H,H}$ = 7.2 Hz, 2H; $COC\mathit{H}_2CH_2CH_3$, 1.70 (m, 2H $COCH_2C\mathit{H}_2CH_3$), 1.00 ppm (t, $J_{H,H}$ = 7.2 Hz, 3H; $COCH_2CH_2C\mathit{H}_3$); ^{13}C NMR (125 MHz, CD_3OD): δ = 178.1 (C-1), 165.6 ($NH\mathit{C}OCH_3$), 145.5 (C-2), 113.5 (C-3), 78.2 (C-6), 71.1 (C-8), 70.4 (C-7), 68.0 (C-4), 65.1 (C-9), 51.9 (C-5), 39.0 ($CO\mathit{C}H_2CH_2CH_3$), 20.3 ($COCH_2\mathit{C}H_2CH_3$), 14.1 ppm ($COCH_2CH_2\mathit{C}H_3$); MS (ESI negative, *m/z*): calcd for $C_{13}H_{21}NO_8$ $[M-H]^-$ 318.1, found 318.1.

5.1.2 The 2,3-unsaturated derivatives: C4/C5 combined substitutions

5.1.2.1 N-transacylation procedure for the synthesis of 4-azido N-perfluoro acylneuraminic acid glycals (18b-d).

General procedure. To a solution of compound **15**[4] (1.32 mmol) in CH_3CN (6.6 mL) was added Et_3N (11.9 mmol) and the appropriate perfluorinated anhydride (5.94 mmol) at 0 °C. The mixture was warmed at 135 °C for 5-15 min in a sealed tube. Then, the reaction mixture was cooled, quenched with methanol (0.20 mL) and evaporated under reduced pressure to afford a crude residue. The crude was diluted with AcOEt and the organic layers were, at first, washed with saturated NH_4Cl solution then with water and dried over anhydrous Na_2SO_4. The organic solvent was concentrated under vacuum and the residue purified by silica gel chromatography using a suitable solvent system.

Preparation of methyl 7,8,9-tri-O-acetyl-2,6-anhydro-4-azido-3,4,5-trideoxy-5-(2,2,2-trifluoroacetamido)-D-glycero-D-galacto-non-2-enonate (**18b**):

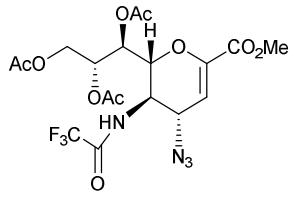

18b

Starting from protected glycal **15**[4] (600 mg, 1.32 mmol), according to the general procedure using trifluoroacetic anhydride (832 μL, 5.94 mmol) and after purification by silica gel chromatography (hexane/AcOEt, 65:35, v/v), glycal **18b** was obtained (538 mg, 80%) as a white solid, showing: $[\alpha]^{D}_{23}$ = +106.2 (c=1.0 in chloroform); ^{1}H NMR (500 MHz, $CDCl_3$): δ = 7.36 (d, $J_{NH,5}$ = 8.5 Hz, 1H; NH), 6.00 (d, $J_{3,4}$ = 2.6 Hz, 1H; H-3), 5.40 (dd, $J_{7,6}$ = 2.2, $J_{7,8}$ = 5.2 Hz, 1H; H-7), 5.30 (ddd, $J_{8,9a}$ = 2.8, $J_{8,7}$ = 5.2, $J_{8,9b}$ = 6.7 Hz, 1H; H-8), 4.69 (dd, $J_{9a,8}$ = 2.8, $J_{9a,9b}$ = 12.4 Hz, 1H; H-9a), 4.51 (dd, $J_{6,7}$ = 2.2, $J_{6,5}$ = 10.1 Hz, 1H; H-6), 4.46 (dd, $J_{4,3}$ = 2.6, $J_{4,5}$ = 9.0 Hz, 1H; H-4), 4.15 (dd, $J_{9b,8}$ = 6.7, $J_{9b,9a}$ = 12.4 Hz, 1H; H-9b), 3.99-3.92 (m, 1H; H-5), 3.81 (s, 3H; $COOCH_3$), 2.13 (s, 3H; $OCOCH_3$), 2.06 (s, 3H; $OCOCH_3$), 2.04 ppm (s, 3H; $OCOCH_3$); ^{13}C NMR (125 MHz, $CDCl_3$): δ = 171.0, 170.4, 170.3 (3C; O*C*OCH_3), 161.3 (C-1), 157.7 (q, $J_{C,F}$ = 38.1 Hz, 1C; *C*OCF_3), 145.2 (C-2), 115.4 (q, $J_{C,F}$ = 287.8 Hz, 1C; $COCF_3$), 107.1 (C-3), 75.0 (C-6), 70.5 (C8), 67.5 (C-7), 61.8 (C-9), 57.0 (C-4), 52.7 ($COOCH_3$), 49.1 (C-5), 20.8, 20.6, 20.6 ppm (3C; $OCOCH_3$); MS (ESI negative): *m/z* 509.3 $[M-H]^-$; elemental analysis calcd (%) for $C_{18}H_{21}F_3N_4O_{10}$: C 42.36, H 4.15, N 10.98; found: C 42.15, H 4.11, N 10.80.

*Preparation of methyl 7,8,9-tri-O-acetyl-2,6-anhydro-4-azido-3,4,5-trideoxy-5-(2,2,3,3,3-pentafluoropropionamido)-D-glycero-D-galacto-non-2-enonate (***18c***):*

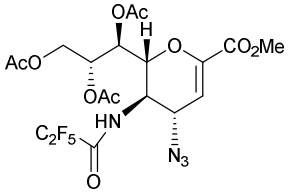

18c

Starting from protected glycal **15**[4] (600 mg, 1.32 mmol), according to the general procedure using pentafluoropropionic anhydride (1.15 mL, 5.94 mmol) and after purification by silica gel chromatography (hexane/AcOEt, 7:3, v/v), glycal **18c** was obtained (576 mg, 78%) as a white solid, showing: $[\alpha]_D^{23}$ = +71.3 (c=1.0 in chloroform); ^{1}H NMR (500 MHz, $CDCl_3$): δ = 7.57 (d, $J_{NH,5}$ = 8.3 Hz, 1H; N*H*COCH$_3$), 5.98 (d, $J_{3,4}$ = 2.6 Hz, 1H; H-3), 5.35 (dd, $J_{7,6}$ = 1.9, $J_{7,8}$ = 5.2 Hz, 1H; H-7), 5.26 (ddd, $J_{8,9a}$ = 2.7, $J_{8,7}$ = 5.2, $J_{8,9b}$ = 6.6 Hz, 1H; H-8), 4.67 (dd, $J_{9a,8}$ = 2.7, $J_{9a,9b}$ = 12.5 Hz, 1H; H-9a), 4.53 (dd, $J_{6,7}$ = 1.9, $J_{6,5}$ = 10.3 Hz, 1H; H-6), 4.48 (dd, $J_{4,3}$ = 2.6, $J_{4,5}$ = 9.1 Hz, 1H; H-4), 4.15 (dd, $J_{9b,8}$ = 6.6, $J_{9b,9a}$ = 12.5 Hz, 1H; H-9b), 3.96-3.89 (m, 1H; H-5), 3.80 (s, 3H; COOCH$_3$), 2.11 (s, 3H; OCOCH$_3$), 2.03 (s, 3H; OCOCH$_3$), 2.02 ppm (s, 3H; OCOCH$_3$); ^{13}C NMR (125 MHz, $CDCl_3$): δ = 171.0, 170.4, 170.3 (3C; O*C*OCH$_3$), 161.2 (C1), 158.3 (t, $J_{C,F}$ = 26.6 Hz, 1C; *C*OC$_2$F$_5$), 145.2 (C-2), 122.0-104.0 (2C; CO*C*$_2$F$_5$), 107.1 (C-3), 74.9 (C-6), 70.6 (C-8), 67.5 (C-7), 61.8 (C-9), 57.1 (C-4), 52.6 (COO*C*H$_3$), 49.3 (C-5), 20.6, 20.5, 20.4 ppm (3C; OCO*C*H$_3$); MS (ESI negative): *m/z* 559.3 $[M-H]^-$; elemental analysis calcd (%) for $C_{19}H_{21}F_5N_4O_{10}$: C 40.72, H 3.78, N 10.00; found: C 40.57, H 3.75, N 10.21.

Preparation of methyl 7,8,9-tri-O-acetyl-2,6-anhydro-4-azido-3,4,5-trideoxy-5-(2,2,3,3, 4,4,4- heptafluorobutyramido)-D-glycero-D-galacto-non-2-enonate (**18d**):

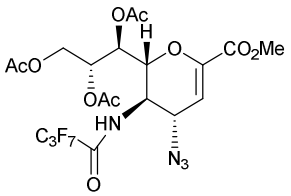

18d

Starting from protected glycal **15**[4] (600 mg, 1.32 mmol), according to the general procedure using heptafluorobutyric anhydride (1.43 mL, 5.94 mmol) and after purification by silica gel chromatography (hexane/AcOEt, 7:3, v/v), glycal **18d** was obtained (628 mg, 78%) as a white solid, showing: $[\alpha]_D^{23}$ = +67.3 (c=1.0 in chloroform); ^{1}H NMR (500 MHz, $CDCl_3$): δ =7.29

(d, $J_{NH,5}$ = 8.2 Hz, 1H; N*H*COCH$_3$), 6.04 (d, $J_{3,4}$ = 2.7 Hz, 1H; H-3), 5.38-5.31 (overlapping, 2H; H-7 and H-8), 4.72 (dd, $J_{4,3}$ = 2.7, $J_{4,5}$ = 8.9 Hz, 1H; H-4), 4.65-4.59 (overlapping, 2H; H-6 and H-9a), 4.23 (dd, $J_{9b,8}$ = 5.1, $J_{9b,9a}$ = 12.4 Hz, 1H; H-9b), 3.85 (s, 3H; COOCH$_3$), 3.76-3.68 (m, 1H; H-5), 2.17 (s, 3H; OCOCH$_3$), 2.08 (s, 3H; OCOCH$_3$), 2.05 ppm (s, 3H; OCOCH$_3$); ^{13}C NMR (125 MHz, CDCl$_3$): δ =170.8, 170.7, 170.1 (3C; O*C*OCH$_3$), 161.3 (C-1), 158.2 ($J_{C,F}$ = 38.1 Hz, 1C; *C*OC$_3$F$_7$), 145.1 (C-2), 122.0-108.0 (3C; CO*C*$_3$F$_7$), 106.9 (C-3), 73.9 (C-6), 69.8 (C-8), 67.5 (C-7), 61.6 (C-9), 56.1 (C-4), 52.7 (COOCH$_3$), 50.4 (C-5), 20.7, 20.6, 20.4 ppm (3C; OCOCH$_3$); MS (ESI negative): *m/z* 609.3 [M-H]$^-$; elemental analysis calcd (%) for C$_{20}$H$_{21}$F$_7$N$_4$O$_{10}$: C 39.35, H 3.47, N 9.18; found: C 39.56, H 3.38, N 9.21.

5.1.2.2 Hydrogenation procedure for the synthesis of 4-amino N-perfluoro acylneuraminic acid glycals (19b-d).

General procedure. To a solution of each azido derivative **18b-d** (0.80 mmol) in EtOH (10 mL) was added Lindlar catalyst (80 mg), and the mixture was stirred at 23°C o/n under H_2 atmosphere. Then, the catalyst was filtered off over Celite, and the "Celite bed" was washed with MeOH (10 mL X 3). The combined filtrates were evaporated under reduced pressure, and the residue was purified by silica gel chromatography using the appropriate solvent system to achieve the desired amino compounds **19b-d**.

Preparation of methyl 7,8,9-tri-O-acetyl-4-amino-2,6-anhydro-3,4,5-trideoxy-5-(2,2,2-trifluoroacetamido)-D-glycero-D-galacto-non-2-enonate (**19b**):

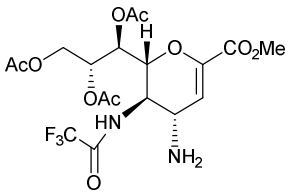

19b

Starting from protected compound **18b** (408 mg, 0.80 mmol), according to general hydrogenation procedure followed by silica gel purification chromatography (eluting with AcOEt/hexane, 9:1, v/v to AcOEt/MeOH, 95:5, v/v), the glycal **19b** was obtained (264 mg, 68%) as a white solid, showing: $[\alpha]_D^{23}$= + 66.3 (c=1.0 in chloroform); ^{1}H NMR (500 MHz, CDCl$_3$): δ = 7.46 (d, $J_{NH,5}$ = 9.2 Hz, 1H; N*H*COCH$_3$), 6.95 (d, $J_{3,4}$ = 2.4 Hz, 1H; H-3), 5.43 (dd, $J_{7,6}$ = 2.4, $J_{7,8}$ = 4.5 Hz, 1H; H-7), 5.27 (ddd, $J_{8,9a}$ = 2.8, $J_{8,7}$ = 4.5, $J_{8,9b}$ = 7.3 Hz, 1H; H-8), 4.72 (dd, $J_{9a,8}$ = 2.8, $J_{9a,9b}$ = 12.4 Hz, 1H; H-9a), 4.36 (dd, $J_{6,7}$ = 2.4, $J_{6,5}$ = 9.8 Hz, 1H; H-

6), 4.14 (dd, $J_{9b,8}$ = 7.3, $J_{9b,9a}$ = 12.4 Hz, 1H; H-9b), 3.88-3.81 (m, 1H; H-5), 3.77 (s, 3H; $COOCH_3$), 3.66 (dd, $J_{4,3}$ = 2.4, $J_{4,5}$ = 8.8 Hz, 1H; H-4), 2.09 (s, 3H; $OCOCH_3$), 2.02 (s, 6H; $OCOCH_3$), 1.75-1.70 ppm (br s, 2H; NH_2); ^{13}C NMR (125 MHz, $CDCl_3$): δ = 170.9, 170.4, 170.1 (3C; $OCOCH_3$), 161.9 (C-1), 157.9 (q, $J_{C,F}$ = 37.8 Hz, 1C; $COCF_3$), 143.2 (C-2), 115.6 (q, $J_{C,F}$ = 288.0 Hz, 1C; $COCF_3$), 114.0 (C-3), 75.8 (C-6), 71.2 (C-8), 67.9 (C-7), 62.0 (C-9), 52.4 ($COOCH_3$), 51.8 (C-5), 49.8 (C-4), 20.7, 20.6, 20.5 ppm (3C; $OCOCH_3$); MS (ESI negative): *m/z* 483.2 $[M-H]^-$; elemental analysis calcd (%) for $C_{18}H_{23}F_3N_2O_{10}$: C 44.63, H 4.79, N 5.78, O 33.03; found: C 44.89, H 4.92, N 5.60.

Preparation of methyl 7,8,9-tri-O-acetyl-4-amino-2,6-anhydro-3,4,5-trideoxy-5-(2,2,3,3,3-pentafluoropropionamido)-D-glycero-D-galacto-non-2-enonate (**19c**):

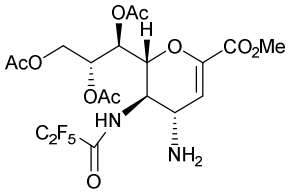

19c

Starting from protected compound **18c** (446 mg, 0.80 mmol), according to general hydrogenation procedure followed by silica gel purification chromatography (eluting with AcOEt/hexane, 85:15, v/v), the glycal **19c** was obtained (321 mg, 75%) as a white solid, showing: $[\alpha]_D^{23}$ = +67.8 (c=1.0 in chloroform); ^{1}H NMR (500 MHz, $CDCl_3$): δ = 7.05 (d, $J_{NH,5}$ = 7.9 Hz, 1H; N*H*$COCH_3$), 5.98 (d, $J_{3,4}$ = 2.3 Hz, 1H; H-3), 5.40 (dd, $J_{7,6}$ = 2.5, $J_{7,8}$ = 5.1 Hz, 1H; H-7), 5.33 (ddd, $J_{8,9a}$ = 2.8, $J_{8,7}$ = 5.1, $J_{8,9b}$ = 6.4 Hz, 1H; H-8), 4.64 (dd, $J_{9a,8}$ = 2.8, $J_{9a,9b}$ = 12.4 Hz, 1H; H-9a), 4.45 (dd, $J_{6,7}$ = 2.5, $J_{6,5}$ = 9.1 Hz, 1H; H-6), 4.18 (dd, $J_{9b,8}$ = 6.4, $J_{9b,9a}$ = 12.4 Hz, 1H; H-9b), 3.85-3.72 (overlapping, 5H; H-4, $COOCH_3$ and H-5), 2.12 (s, 3H; $OCOCH_3$), 2.06 (s, 3H; $OCOCH_3$), 2.04 (s, 3H; $OCOCH_3$), 1.70-1.57 ppm (br s, 2H; NH_2); ^{13}C NMR (125 MHz, $CDCl_3$): δ = 170.9, 170.6, 170.0 (3C; $OCOCH_3$), 162.0 (C-1), 158.5 (t, $J_{C,F}$ = 26.3 Hz, 1C; COC_2F_5), 143.1 (C-2), 122.0-103.0 (2C; COC_2F_5), 113.8 (C-3), 75.6 (C-6), 71.3 (C-8), 67.9 (C-7), 62.0 (C-9), 52.3 ($COOCH_3$), 52.0 (C-5), 49.6 (C-4), 20.6, 20.5, 20.4 ppm (3C; $OCOCH_3$); MS (ESI negative): *m/z* 533.2 $[M-H]^-$; elemental analysis calcd (%) for $C_{19}H_{23}F_5N_2O_{10}$: C 42.70, H 4.34, N 5.24; found: C 42.45, H 4.12, N 4.99.

Preparation of methyl 7,8,9-tri-O-acetyl-4-amino-2,6-anhydro-3,4,5-trideoxy-5-(2,2,3,3, 4,4,4-heptafluorobutyramido)-D-glycero-D-galacto-non-2-enonate (**19d**):

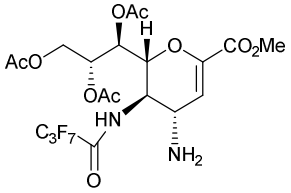

19d

Starting from protected compound **18d** (488 mg, 0.80 mmol), according to general hydrogenation procedure followed by silica gel purification chromatography (eluting with AcOEt/hexane, 9:1, v/v to AcOEt/MeOH, 95:5, v/v), the glycal **19d** was obtained (328 mg, 70%) as a white solid, showing: $[\alpha]_D^{23}$ = +62.5 (c=1.0 in chloroform); ^{1}H NMR (500MHz, $CDCl_3$): δ = 7.09 (d, $J_{NH,5}$ = 8.3 Hz, 1H; N*H*COCH$_3$), 5.99 (d, $J_{3,4}$ = 2.7 Hz, 1H; H-3), 5.40 (dd, $J_{7,6}$ = 2.4, $J_{7,8}$ = 5.7 Hz, 1H; H-7), 5.36 (ddd, $J_{8,9a}$ = 2.8, $J_{8,7}$ = 5.7, $J_{8,9b}$ = 5.9 Hz, 1H; H-8), 4.59 (dd, $J_{9a,8}$ = 2.8, $J_{9a,9b}$ = 12.5 Hz, 1H; H-9a), 4.50 (dd, $J_{6,7}$ = 2.4, $J_{6,5}$ = 9.7 Hz, 1H; H-6), 4.21 (dd, $J_{9b,8}$ = 5.9, $J_{9b,9a}$ = 12.5 Hz, 1H; H-9b), 3.93 (dd, $J_{4,3}$ = 2.7, $J_{4,5}$ = 8.5 Hz, 1H; H-4), 3.80 (s, 3H; COOCH$_3$), 3.74-3.66 (m, 1H; H-5), 2.72-2.59 (br s, 2H; NH$_2$), 2.13 (s, 3H; OCOCH$_3$), 2.06 (s, 3H; OCOCH$_3$), 2.04 ppm (s, 3H; OCOCH$_3$); ^{13}C NMR (125 MHz, $CDCl_3$): δ = 170.7, 170.3, 170.0 (3C; O*C*OCH$_3$), 162.0 (C-1), 158.2 (t, $J_{C,F}$ = 26.3 Hz, 1C; *C*OC$_3$F$_7$), 143.2 (C-2), 123.0-107.0 (3C; CO*C*$_3$F$_7$), 113.6 (C-3), 75.1 (C-6), 70.6 (C-8), 67.9 (C-7), 61.9 (C-9), 53.0 (COO*C*H$_3$), 52.4 (C-5), 48.9 (C-4), 20.7, 20.5, 20.5 ppm (3C; OCO*C*H$_3$); MS (ESI negative): *m/z* 583.3 [M-H]$^-$; elemental analysis calcd (%) for $C_{20}H_{23}F_7N_2O_{10}$: C 41.11, H 3.97, N 4.79; found: C 44.31, H 3.80, N 4.92.

5.1.2.3 Acylation procedure for the synthesis of 4-p-toluensolfonamido N-perfluoro acylneuraminic acid glycals (20b-d).

General procedure. To a solution of each C4 amino *N*-perfluoro glycal **19b-d** (0.50 mmol) in CH_2Cl_2 (6.7 mL) containing Et_3N (246 µL, 2.50 mmol), cooled at 0 °C, the *p*-toluenesulfonyl chloride (143 mg, 0.75 mmol) was added. The mixture was stirred at 23°C for 2-5 h and then purified by silica gel chromatography (hexane/AcOEt, 7:3, v/v) to achieve the desired compounds **20b-d**.

Preparation of methyl 7,8,9-tri-O-acetyl-2,6-anhydro-3,4,5-trideoxy-5-(2,2,2-trifluoro acetamido)-4-[(4- methylphenyl)sulfonamide]-D-glycero-D-galacto-non-2-enonate (**20b**)

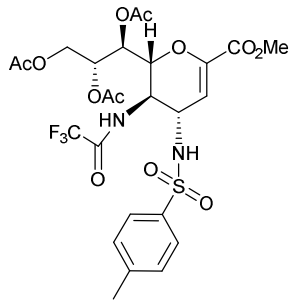

20b

Starting from protected glycal **19b** (255 mg, 0.50 mmol), according to the general acylation procedure glycal **20b** was obtained (273 mg, 81%) as a white solid, showing: $[\alpha]_D^{23}$ = +59.5 (c=1.0 in chloroform); ^{1}H NMR (500 MHz, $CDCl_3$): δ = 7.68 (overlapping, 2H; Ph), 7.55 (d, $J_{NH,5}$ = 9.1 Hz, 1H; N*H*COCH$_3$ at C-5), 7.27 (overlapping, 2H; Ph), 5.69 (d, $J_{3,4}$ = 2.3 Hz, 1H; H-3), 5.60 (d, $J_{NH,4}$ = 9.4 Hz, 1H; N*H*COCH$_3$ at C-4), 5.39 (dd, $J_{7,6}$ = 1.8, $J_{7,8}$ = 5.2 Hz, 1H; H-7), 5.28 (ddd, $J_{8,9a}$ = 2.6, $J_{8,7}$ = 5.2, $J_{8,9b}$ = 6.9 Hz, 1H; H-8), 4.62 (dd, $J_{9a,8}$ = 2.6, $J_{9a,9b}$ = 12.4 Hz, 1H; H-9a), 4.55 (dd, $J_{6,7}$ = 1.8, $J_{6,5}$ = 10.3 Hz, 1H; H-6), 4.36 (ddd, $J_{4,3}$ = 2.3, $J_{4,5}$ = $J_{4,NH}$ = 9.4 Hz, 1H; H-4), 4.15 (dd, $J_{9b,8}$ = 6.9, $J_{9b,9a}$ = 12.4 Hz, 1H; H-9b), 4.02-4.94 (m, 1H; H5), 3.74 (s, 3H; COOCH$_3$), 2.40 (s, 3H; PhCH$_3$), 2.05 (s, 3H; OCOCH$_3$), 2.03 (s, 3H; OCOCH$_3$), 2.01 ppm (s, 3H; OCOCH$_3$); ^{13}C NMR (125 MHz, $CDCl_3$): δ = 170.6, 170.4, 169.7 (3C; OCOCH$_3$), 161.3 (C-1), 158.1 (q, $J_{C,F}$ = 37.8 Hz, 1C; *C*OCF$_3$), 144.6 (1C; Ph), 144.0 (C-2), 137.1, 129.8, 126.7 (5C; Ph), 115. 3 (q, $J_{C,F}$ = 288.0 Hz, 1C; CO*C*F$_3$), 109.9 (C-3), 75.9 (C-6), 70.7 (C-8), 67.6 (C-7), 61.9 (C-9), 52.3 and 51.2 (COO*C*H$_3$ and C-4), 48.7 (C-5), 21.3 (1C; PhCH$_3$), 20.6, 20.5, 20.2 ppm (3C; OCO*C*H$_3$); MS (ESI negative): *m/z* 637.4 [M-H]$^-$; elemental analysis calcd (%) for $C_{25}H_{29}F_3N_2O_{12}S$: C 47.02, H 4.58, N 4.39; found: C 47.35, H 4.64, N 4.43.

Preparation of methyl 7,8,9-tri-O-acetyl-2,6-anhydro-3,4,5-trideoxy-5-(2,2,3,3,3-pentafluoro propionamido)-4-[(4-methylphenyl)sulfonamide]-D-glycero-D-galacto-non-2-enonate (**20c**):

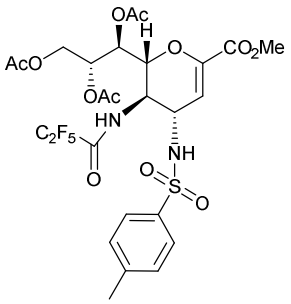

20c

Starting from protected glycal **19c** (260 mg, 0.50 mmol), according to the general acylation procedure glycal **20c** was obtained (250 mg, 75%) as a white solid, showing: $[\alpha]_D^{23}$ = +51.3 (c=1.0 in chloroform); ^{1}H NMR (500 MHz, $CDCl_3$): δ = 7.71 (overlapping, 2H; Ph), 7.63 (d, $J_{NH,5}$ = 8.9 Hz, 1H; N*H*COCH$_3$ at C-5), 7.29 (overlapping, 2H; Ph), 5.60 (d, $J_{3,4}$ = 2.4 Hz, 1H; H-3), 5.55 (d, $J_{NH,4}$ = 9.4 Hz, 1H; N*H*COCH$_3$ at C-4), 5.34 (dd, $J_{7,6}$ = 1.6, $J_{7,8}$ = 5.6 Hz, 1H; H7), 5.27 (ddd, $J_{8,9a}$ = 2.6, $J_{8,7}$ = 5.6, $J_{8,9b}$ = 6.3 Hz, 1H; H-8), 4.61-4.56 (overlapping, 2H; H-6 and H-9a), 4.45 (ddd, $J_{4,3}$ = 2.4, $J_{4,5}$ = $J_{4,NH}$ = 9.4 Hz, 1H; H-4), 4.16 (dd, $J_{9b,8}$ = 6.3, $J_{9b,9a}$ = 12.5 Hz, 1H; H-9b), 3.97-3.91 (m, 1H; H-5), 3.73 (s, 3H; COOCH$_3$), 2.41 (s, 3H; PhCH$_3$), 2.06 (s, 3H; OCOCH$_3$), 2.04 (s, 3H; OCOCH$_3$), 2.03 ppm (s, 3H; OCOCH$_3$); ^{13}C NMR (125 MHz, $CDCl_3$): δ = 170.7, 170.5, 169.8 (3C; O*C*OCH$_3$), 161.4 (C-1), 158.8 (t, $J_{C,F}$ = 26.5 Hz, 1C; *C*OC$_2$F$_5$), 144.6 (1C; Ph), 144.2 (C-2), 137.1, 129.9, 126.8 (5C; Ph), 124.0-104.0 (2C; CO*C*$_2$F$_5$), 109.5 (C-3), 75.4 (C-6), 70.6 (C-8), 67.5 (C-7), 61.8 (C-9), 52.4 and 50.7 (COOCH$_3$ and C-4), 49.1 (C-5), 21.4 (1C; PhCH$_3$), 20.6, 20.5, 20.3 ppm (3C; OCOCH$_3$); MS (ESI negative): *m/z* 687.3 $[M-H]^-$; elemental analysis calcd (%) for $C_{26}H_{29}F_5N_2O_{12}S$: C 45.35, H 4.25, N 4.07; found: C 45.18, H 4.38, N 4.20.

Preparation of methyl 7,8,9-tri-O-acetyl-2,6-anhydro-3,4,5-trideoxy-5-(2,2,3,3,4,4,4-hepta fluorobutyramido)-4-[(4-methylphenyl)sulfonamide]-D-glycero-D-galacto-non-2-enonate (**20d**):

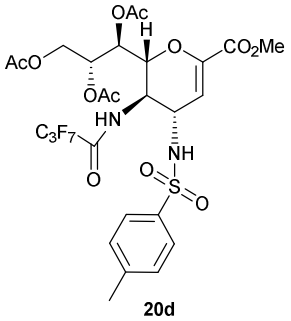

20d

Starting from protected glycal **19d** (291 mg, 0.50 mmol), according to the general acylation procedure glycal **20d** was obtained (295 mg, 80%) as a white solid, showing: $[\alpha]_D^{23}$ = +51.2 (c=1.0 in chloroform); ^{1}H NMR (500 MHz, $CDCl_3$): δ = 7.69 (overlapping, 2H; Ph), 7.55 (d, $J_{NH,5}$ = 8.6 Hz, 1H; N*H*COCH$_3$ at C-5), 7.28 (overlapping, 2H; Ph), 5.58 (d, $J_{3,4}$ = 2.5 Hz, 1H; H-3), 5.42 (d, $J_{NH,4}$ = 9.4 Hz, 1H; N*H*COCH$_3$ at C-4), 5.31 (dd, $J_{7,6}$ = 1.5, $J_{7,8}$ = 6.0 Hz, 1H; H7), 5.25 (ddd, $J_{8,9a}$ = 2.3, $J_{8,7}$ = 6.0, $J_{8,9b}$ = 5.9 Hz, 1H; H-8), 4.61 (dd, $J_{6,7}$ = 1.5, $J_{6,5}$ = 10.3 Hz, 1H; H-6), 4.54 (dd, $J_{9a,8}$ = 2.3, $J_{9a,9b}$ = 12.6 Hz, 1H; H-9a), 4.49 (ddd, $J_{4,3}$ = 2.5, $J_{4,5}$ = $J_{4,NH}$ = 9.4 Hz, 1H; H-4), 4.15 (dd, $J_{9b,8}$ = 5.9, $J_{9b,9a}$ = 12.6 Hz, 1H; H-9b), 3.88-3.80 (m, 1H; H-5), 3.72 (s, 3H; COOCH$_3$), 2.40 (s, 3H; PhCH$_3$), 2.05 (s, 3H; OCOCH$_3$), 2.03 (s, 3H; OCOCH$_3$), 2.01 ppm (s, 3H; OCOCH$_3$); ^{13}C NMR (125 MHz, $CDCl_3$): δ = 170.7, 170.5, 170.0 (3C; O*C*OCH$_3$), 161.4 (C-1), 158.6 (t, $J_{C,F}$ = 26.7 Hz, 1C; *C*OC$_3$F$_7$), 144.6 (1C; Ph), 144.2 (C-2), 137.0, 130.0, 126.9 (5C; Ph), 122.0-111.0 (3C; CO*C*$_3$F$_7$), 109.3 (C-3), 75.0 (C-6), 70.4 (C-8), 67.5 (C-7), 61.7 (C-9), 52.5 and 50.2 (COO*C*H$_3$ and C-4), 49.7 (C-5), 21.4 (1C; PhCH$_3$), 20.7, 20.4, 20.4 ppm (3C; OCO*C*H$_3$); MS (ESI negative): *m/z* 737.3 [M-H]$^-$; elemental analysis calcd (%) for $C_{27}H_{29}F_7N_2O_{12}S$: C 43.91, H 3.96, N 3.79; found: C 44.28, H 4.13, N 3.65.

5.1.2.4 Deacetylation and selective removal of esteric function

General procedure. All the peracetylated glycals **15**[4], **17**[117], **18b-d**, **20b,d** (0.20 mmol) were treated with a methanolic solution of NaOMe, freshly prepared by dissolving sodium metal (5 mg, 0.22 mmol) in anhydrous MeOH (2 mL). Each reaction mixture was stirred at 23°C for 1 h, and then quenched with acidic resin (Dowex 50WX8, H^+). The resin was filtered off and washed with MeOH (2 mL X 3) and the combined filtrate and washes were evaporated under vacuum. Each crude compound was purified with flash chromatography and directly subjected to opportune selective hydrolysis (*Method A or B*):

Method A: Selective hydrolysis using moist K_2CO_3 methanol solution. The free glycals **15**[4], **17**[117], **18c,d** and **19c,d** were prepared by selective hydrolysis of appropriate methyl ester derivatives performed in a methanol-water solution (0.75 mL, 10:1 v/v) containing K_2CO_3 (13 mg), kept at 23°C for 6-24 h. At this time, the reaction mixture was treated with acidic resin (Dowex 50WX8, H^+) until acidic pH, and then, the resin was filtered and washed with MeOH (2 mL X 3). Finally, the solvent was removed under reduced pressure and the residue was recovered with aqueous methanol and lyophilized to afford, after preparative HPLC, the desired free glycals.

Method B: Selective hydrolysis using moist Et_3N methanol solution. The free glycals **18b** and **20b** was prepared by selective hydrolysis of its methyl ester derivative performed in a methanol-water solution (1.5 mL, 2:1 v/v) containing Et_3N (0.90 mL), kept at 23 °C for 12 h. Then the mixture was treated with acidic resin (Dowex 50WX8, H^+) until acidic pH and the resin was filtered and washed with MeOH (2 mL × 3). Finally, the solvent was removed under reduced pressure and the residue was recovered with aqueous methanol and lyophilized, to afford, after preparative HPLC, the desired free glycals.

Preparation of 5-(acetamido)-2,6-anhydro-3,4,5-trideoxy-4-[(4-methylphenyl)sulfonamide]-D-glyceroD-galacto-non-2-enoic acid (**12a**):

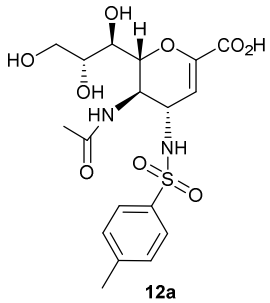

12a

Starting from protected glycal **17**[117] (117 mg, 0.20 mmol), according to the general two-step procedure Zemplén reaction followed by selective hydrolytic *method A*, glycal **12a** was obtained (68 mg, 77%) white solid, showing: $[\alpha]_D^{23}$ = +11.7 (c=1.0 in water); ^{1}H NMR (500 MHz, CD_3OD): δ = 7.79 (overlapping, 2H; Ph), 7.43 (overlapping, 2H; Ph), 5.54 (br s, 1H; H-3), 4.26 (br d, $J_{6,5}$ = 10.7 Hz, 1H; H-6), 4.21 (br d, $J_{4,5}$ = 9.4 Hz, 1H; H-4), 4.03-3.94 (m, 1H; H-5), 3.91-3.78 (overlapping, 2H; H-8 and H-9a), 3.65 (dd, $J_{9b,8}$ = 4.1, $J_{9b,9a}$ = 11.5 Hz, 1H; H-9b), 3.57 (br d, $J_{7,8}$ = 9.2 Hz, 1H; H-7), 2.46 (s, 3H; $PhCH_3$), 1.85 ppm (s, 3H; $NHCOCH_3$); ^{13}C NMR (125 MHz, CD_3OD:D_2O, 1:1 v/v): δ = 175.2 (C-1), 167.2 ($NHCOCH_3$), 146.8 (1C; Ph), 145.9 (C-2), 137.9, 131.2, 127.6 (5C; Ph), 110.0 (C-3), 77.2 (C-

6), 70.8 (C-8), 69.1 (C-7), 64.1 (C-9), 52.7 (C-4), 49.01 (C-5 under methanol signal), 23.0 (1C; NHCO*C*H_3), 21.6 ppm (1C; PhCH_3); MS (ESI negative): *m/z* 443.2 [M-H]-; elemental analysis calcd (%) for $C_{18}H_{24}N_2O_9S$: C 48.64, H 5.44, N 6.30; found: C 48.51, H 5.35, N 6.42.

Preparation of 2,6-anhydro-3,4,5-trideoxy-5-(2,2,2-trifluoroacetamido)-4-[(4- methylphenyl) sulfonamide]-D-glycero-D-galacto-non-2-enoic acid (**12b**):

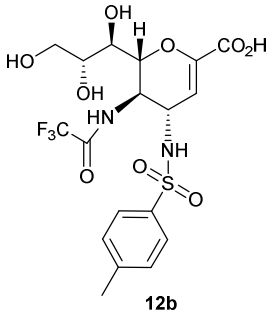

12b

Starting from protected glycal **20b** (128 mg, 0.20 mmol), according to the general two step procedure Zemplén reaction followed by selective hydrolytic <u>*method B*</u>, glycal **12b** was obtained (72 mg, 72%) as a white solid, showing: $[\alpha]_D^{23}$ = +13.5 (c=1.0 in methanol); ^{1}H NMR (500 MHz, CD_3OD): δ = 7.73 (overlapping, 2H; Ph), 7.41 (overlapping, 2H; Ph), 5.42 (br s, 1H; H-3), 4.44 (br d, $J_{6,5}$ = 10.7 Hz, 1H; H-6), 4.27 (br d, $J_{4,5}$ = 9.4 Hz, 1H; H-4), 4.20-4.11 (m, 1H; H-5), 3.89-3.79 (overlapping, 2H; H-8 and H-9a), 3.63 (dd, $J_{9b,8}$ = 5.5, $J_{9b,9a}$ = 11.5 Hz, 1H; H-9b), 3.54 (br d, $J_{7,8}$ = 9.2 Hz, 1H; H-7), 2.42 ppm (s, 3H; PhCH_3); ^{13}C NMR (125 MHz, CD_3OD): δ = 165.6 (C-1), 159.5 (q, $J_{C,F}$ = 37.8 Hz, 1C; *C*OCF_3), 146.1 (1C; Ph), 145.6 (C-2), 138.8, 131.1, 127.7 (5C; Ph), 116.0 (q, $J_{C,F}$ = 288.0 Hz, 1C; CO*C*F_3), 110.4 (C-3), 77.2 (C-6), 71.1 (C-8), 69.4 (C-7), 64.3 (C-9), 52.2 and 49.7 (C-4 and C-5), 21.5 ppm (1C; PhCH_3); MS (ESI negative): *m/z* 497.3 $[M-H]^-$; elemental analysis calcd (%) for $C_{18}H_{21}F_3N_2O_9S$: C 43.38, H 4.25, N 5.62; found: C 43.55, H 4.34, N 5.45.

Preparation of 2,6-anhydro-3,4,5-trideoxy-5-(2,2,3,3,3-pentafluoropropionamido)-4-[(4-methylphenyl)sulfonamide]-D-glycero-D-galacto-non-2-enoic acid (**12c**):

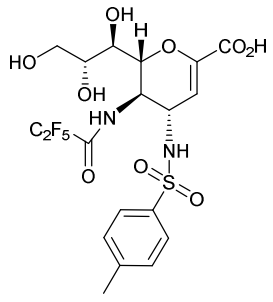

12c

Starting from protected glycal **20c** (133 mg, 0.20 mmol), according to the general two step procedure Zemplén reaction followed by selective hydrolytic *method A*, glycal **20c** was obtained (80 mg, 75%) as a white solid, showing: $[\alpha]_D^{20}$=+10.9 (c=1.0 in methanol); 1 H NMR (500 MHz, CD_3OD): δ = 7.77 (overlapping, 2H; Ph), 7.40 (overlapping, 2H; Ph), 5.37 (d, $J_{3,4}$ = 2.1 Hz, 1H; H-3), 4.43 (br d, $J_{6,5}$ = 10.6 Hz, 1H; H-6), 4.28 (dd, $J_{4,3}$ = 2.1, $J_{4,5}$ = 9.7 Hz, 1H; H6), 4.24-4.18 (m, 1H; H-5), 3.85-3.78 (overlapping, 2H; H-8 and H-9a), 3.61 (dd, $J_{9b,8}$ = 5.4, $J_{9b,9a}$ = 11.2 Hz, 1H; H-9b), 3.50 (br d, $J_{7,8}$ = 9.0 Hz, 1H; H-7), 2.44 ppm (s, 3H; $PhCH_3$); ^{13}C NMR (125 MHz, CD_3OD): δ = 165.2 (C-1), 159.9 (t, $J_{C,F}$ = 25.8 Hz, 1C; *C*OC_2F_5), 146.2 (1C; Ph), 145.0 (C-2), 140.2, 130.9, 127.9 (5C; Ph), 121.0- 107.0 (2C; CO*C*$_2F_5$), 110.5 (C-3), 77.7 (C-6), 71.4 (C-8), 70.1 (C-7), 64.9 (C-9), 52.5 and 49.9 (C-5 and C-4), 21.5 ppm (1C; $PhCH_3$); MS (ESI negative): *m/z* 547.3 [M-H]- ; elemental analysis calcd (%) for $C_{19}H_{21}F_5N_2O_9S$: C 41.61, H 3.86, N 5.11; found: C 41.46, H 3.67, N 5.23.

Preparation of 2,6-anhydro-3,4,5-trideoxy-5-(2,2,3,3,4,4,4-heptafluorobutyramido)-4-[(4-methylphenyl)sulfonamide]-D-glycero-D-galacto-non-2-enoic acid (**12d**):

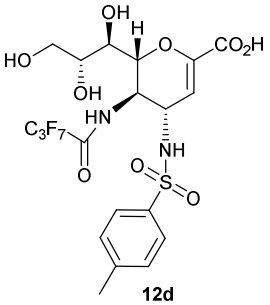

12d

Starting from protected glycal **20d** (147 mg, 0.20 mmol), according to the general two step procedure Zemplén reaction followed by selective hydrolytic *method A*, glycal **12d** was obtained (89 mg, 74%) as a white solid, showing: $[\alpha]_D^{23}$ = +9.1 (c=1.0 in methanol); ^{1}H NMR (500 MHz, CD_3OD): δ = 7.76 (overlapping, 2H; Ph), 7.39 (overlapping, 2H; Ph), 5.34 (br s, 1H; H-3), 4.40 (br d, $J_{6,5}$ = 10.4 Hz, 1H; H-6), 4.30-4.17 (overlapping, 2H; H-4 and H-5), 3.87- 3.76 (overlapping, 2H; H-8 and H-9a), 3.60 (dd, $J_{9b,8}$ = 4.9, $J_{9b,9a}$ = 10.7 Hz, 1H; H-9b), 3.49 (br d, $J_{7,8}$ = 9.0 Hz, 1H; H-7), 2.43 ppm (s, 3H; $PhCH_3$); ^{13}C NMR (125 MHz, CD_3OD): δ = 165.5 (C-1), 159.7 (t, $J_{C,F}$ = 25.6 Hz, 1C; *C*OC_3F_7), 146.5 (1C; Ph), 144.9 (C-2), 140.3, 131.0, 128.0 (5C; Ph), 122.0-111.0 (3C; CO*C*$_3F_7$), 110.0 (C-3), 77.6 (C-6), 71.4 (C-8), 70.1 (C-7), 64.9 (C-9), 52.6 and 50.0 (C-5 and C-4), 21.5 ppm (1C; $PhCH_3$); MS (ESI negative): *m/z* 597.2 $[M-H]^-$; elemental analysis calcd (%) for $C_{20}H_{21}F_7N_2O_9S$: C 40.14, H 3.54, N 4.68; found: C 40.06, H 3.67, N 4.71.

Preparation of 5-acetamido-2,6-anhydro-4-azido-3,4,5-trideoxy-D-glycero-D-galacto-non-2-enoic acid (**13a**):

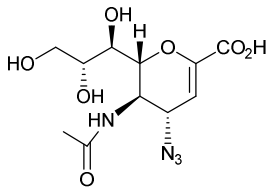

13a

Starting from protected glycal **15**[4, 37] (91 mg, 0.20 mmol), according to the general two step procedure Zemplén reaction followed by selective hydrolytic <u>*method A*</u>, the glycal **13a** was obtained (46 mg, 72%) as a white solid, showing: $[\alpha]_D^{23}$ = +39.8 (c=1.0 in methanol); ^{1}H NMR (500 MHz, D_20): δ= 5.97 (br s, 1H; H-3), 4.34 (br d, $J_{4,5}$ = 9.4 Hz, 1H; H-4), 4.30 (br d, $J_{6,5}$ = 10.8 Hz, 1H; H-6), 4.22-4.15 (m, 1H; H-5), 3.91-3.85 (m, 1H; H-8), 3.83 (dd, $J_{9a,8}$ = 1.8, $J_{9a,9b}$ = 12.0 Hz, 1H; H-9a), 3.63 (br d, $J_{7,8}$ = 9.7 Hz, 1H; H-7), 3.60 (dd, $J_{9b,8}$ = 6.1, $J_{9b,9a}$ = 12.0 Hz, 1H; H-9b), 2.02 ppm (s, 3H; NHCOCH_3). All other physico-chemical properties are superimposable to those previously reported[4, 37].

Preparation of 2,6-anhydro-4-azido-3,4,5-trideoxy-5-(2,2,2-trifluoroacetamido)-D-glycero-D-galactonon-2-enoic acid (**13b**):

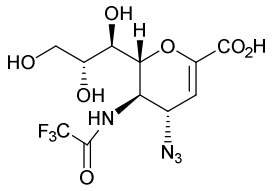

13b

Starting from protected glycal **18b** (102 mg, 0.20 mmol), according to the general two step procedure Zemplén reaction followed by selective hydrolytic <u>*method B*</u>, the glycal **13b** was obtained (50 mg, 68%) as a white solid, showing: $[\alpha]_D^{23}$ = + 28.1 (c=1.0 in methanol); ^{1}H NMR (500 MHz, CD_3OD): δ = 5.96 (d, $J_{3,4}$ = 2.1 Hz, 1H; H-3), 4.49 (dd, $J_{6,7}$ < 1.0, $J_{6,5}$ = 10.4 Hz, 1H; H-6), 4.36 (dd, $J_{4,3}$ = 2.1, $J_{4,5}$ = 9.4 Hz, 1H; H4), 4.32 (dd, $J_{5,4}$ = 9.4, $J_{5,6}$ = 10.4 Hz, 1H; H-5), 3.88 (ddd, $J_{8,9a}$ = 2.8, $J_{8,9b}$ = 5.4, $J_{8,7}$ = 9.4 Hz, 1H; H-8), 3.82 (dd, $J_{9a,8}$ = 2.8, $J_{9a,9b}$ = 11.5 Hz, 1H; H-9a), 3.66 (dd, $J_{9b,8}$ = 5.4, $J_{9b,9a}$ 11.5 = Hz, 1H; H-9b), 3.57 ppm (dd, $J_{7,6}$ < 1.0, $J_{7,8}$ = 9.4 Hz, 1H; H-7); ^{13}C NMR (125 MHz, CD_3OD): δ = 164.9 (C-1), 159.2 (q, $J_{C,F}$ = 37.0 Hz, 1C; *C*OCF_3), 147.4 (C-2), 120.8-114.0 (1C; CO*C*F_3), 107.8 (C-3), 77.3 (C-6), 71.4 (C-8), 69.8 (C-7), 64.8 (C-9), 59.8 (C-4), 49.9 ppm (C-5); HRMS (TOF-ESI, *m/z*): calcd for $C_{11}H_{12}F_3N_4O_7$ $[M-H]^-$ 369.0664, found 369.0659.

Preparation of 2,6-anhydro-4-azido-3,4,5-trideoxy-5-(2,2,3,3,3-pentafluoropropionamido)-D-glycero-Dgalacto-non-2-enoic acid (**13c**):

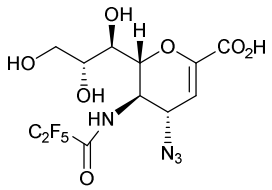

13c

Starting from protected glycal **18c** (112 mg, 0.20 mmol), according to the general two step procedure Zemplén reaction followed by selective hydrolytic *method A*, the glycal **13c** was obtained (55 mg, 65%) as a white solid, showing: $[\alpha]_D^{23}$ = +28.4 (c=1.0 in methanol); ^{1}H NMR (500 MHz, CD_3OD): δ = 5.96 (d, $J_{3,4}$ = 2.1 Hz, 1H; H-3), 4.52-4.45 (m, 1H; H-6), 4.37-4.28 (overlapping, 2H; H-4 and H5), 3.88 (ddd, $J_{8,9a}$ = 2.9, $J_{8,9b}$ = 5.5, $J_{8,7}$ = 9.0 Hz, 1H; H-8), 3.83 (dd, $J_{9a,8}$ = 2.9, $J_{9a,9b}$ = 11.4 Hz, 1H; H-9a), 3.64 (dd, $J_{9b,8}$ = 5.5, $J_{9b,9a}$ = 11.4 Hz, 1H; H-9b), 3.53 ppm (dd, $J_{6,7}$ < 1.0, $J_{7,8}$ = 9.0 Hz, 1H; H-7); ^{13}C NMR (125 MHz, CD_3OD): δ = 165.0 (C-1), 159.7 (t, $J_{C,F}$ = 27.0 Hz, 1C; *C*OC_2F_5), 147.5 (C-2), 120.2-110.1 (2C; CO*C*$_2F_5$), 107.8 (C-3), 77.2 (C-6), 71.4 (C-8), 69.8 (C-7), 64.8 (C-9), 60.0 (C-4), 49.8 ppm (C-5); MS (ESI negative): *m/z* 419.1 $[M-H]^-$; elemental analysis calcd (%) for $C_{12}H_{13}F_5N_4O_7$: C 34.30, H 3.12, N 13.33; found: C 34.56, H 3.22, N 13.13.

Preparation of 2,6-anhydro-4-azido--3,4,5-trideoxy-5-(2,2,3,3,4,4,4-heptafluorobutyramido) -D-glyceroD-galacto-non-2-enoic acid (**13d**):

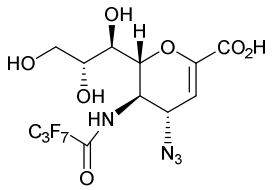

13d

Starting from protected glycal **18d** (122 mg, 0.20 mmol), according to the general two step procedure Zemplén reaction followed by selective hydrolytic *method A*, the glycal **13d** was obtained (64 mg, 68%) as a white solid, showing: $[\alpha]_D^{23}$ = +37.6 (c=1.0 in methanol); ^{1}H NMR (500 MHz, CD_3OD): δ = 5.98 (br s, 1H; H-3), 4.48 (dd, $J_{6,7}$ < 1.0, $J_{6,5}$ = 10.3 Hz, 1H; H-6), 4.37-4.29 (overlapping, 2H; H4 and H-5), 3.88 (ddd, $J_{8,9a}$ = 2.9, $J_{8,9b}$ = 5.6, $J_{8,7}$ = 9.8 Hz, 1H; H-8), 3.82 (dd, $J_{9a,8}$ = 2.9, $J_{9a,9b}$ = 11.4 Hz, 1H; H-9a), 3.64 (dd, $J_{9b,8}$ = 5.6, $J_{9b,9a}$ = 11.4 Hz, 1H; H-9b), 3.55 ppm (dd, $J_{6,7}$ < 1.0, $J_{7,8}$ = 9.8 Hz, 1H; H-7); ^{13}C NMR (125 MHz, CD_3OD):

δ = 165.0 (C-1), 159.6 (t, $J_{C,F}$ = 27.0 Hz, 1C; *C*OC_3F_7), 147.5 (C-2), 122.0-110.0 (3C; CO*C*$_3F_7$), 107.8 (C-3), 77.2 (C-6), 71.4 (C-8), 69.9 (C-7), 64.9 (C-9), 59.9 (C-4), 50.0 ppm (C-5); HRMS (TOF-ESI, *m/z*): calcd for $C_{13}H_{12}F_7N_4O_7$ $[M-H]^-$ 469.0600, found 469.0588.

5.1.3 The 3,4-unsaturated derivatives (Chapter 3.3)

5.1.3.1 Setting up of optimal Ferrier reaction conditions, using MeOH as a nucleophile

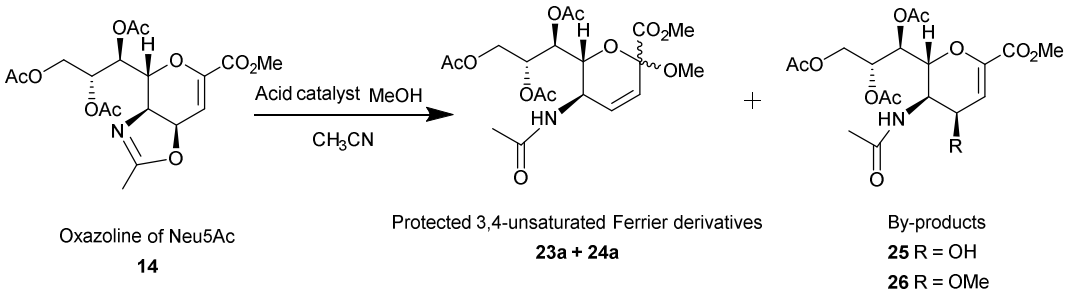

Oxazoline of Neu5Ac
14

Protected 3,4-unsaturated Ferrier derivatives
23a + 24a

By-products
25 R = OH
26 R = OMe

To a solution of oxazoline **14**[110] (300 mg, 0.73 mmol) in CH_3CN (7.2 mL) under argon MeOH (7.20 mmol) was added as nucleophile. Then, also the appropriate catalyst was introduced in the reaction and the mixture was stirred at the selected temperature until the disappearance of the starting material, according to the specific method (*Method 1-10*). Subsequently, the reaction was filtered over Celite and the solvent was then evaporated. Finally, the residue was purified by silica gel chromatography with the appropriate solvent system to achieve the desired mixture of the chromatographically inseparable compounds **23a** and **24a**.

- *Method 1:* $Bi(OTf)_3$-Montomorillonite K-10 (40% w/w; loading of 20% w/w $Bi(OTf)_3$) were selected as catalysts and the reaction was stirred at 23°C, 30h.
- *Method 2:* $Bi(OTf)_3$-Montomorillonite K-10 (40% w/w; loading of 20% w/w $Bi(OTf)_3$) were selected as catalysts and the reaction was stirred at 50°C, 1 h.
- *Method 3:* $Bi(OTf)_3$-Montomorillonite K-10 (40% w/w; loading of 20% w/w $Bi(OTf)_3$) were selected as catalysts and the reaction was stirred at 80°C, 30 min.
- *Method 4:* $Bi(OTf)_3$ (40% w/w) was selected as catalyst and the reaction was stirred at 23°C, 5h.
- *Method 5:* $Bi(OTf)_3$ (40% w/w) was selected as catalyst and the reaction was stirred at 30°C, 1h.
- *Method 6:* $Bi(OTf)_3$ (40% w/w) was selected as catalyst and the reaction was stirred at 50°C, 1h.
- *Method 7:* $Bi(OTf)_3$ (40% w/w) was selected as catalyst and the reaction was stirred at 80°C, 30 min.
- *Method 8:* Montmorillonite K-10 (40% w/w) was selected as catalyst and the reaction was stirred at 23°C, 256h.
- *Method 9:* Montmorillonite K-10 (40% w/w) was selected as catalyst and the reaction was stirred at 50°C, 28h.

- *Method 10:* Montmorillonite K-10 (40% w/w) was selected as catalyst and the reaction was stirred at 80°C, 2/3h.

For the obtained mixtures of **23a** and **24a** the ^{1}H and ^{13}C NMR assignments refer to:

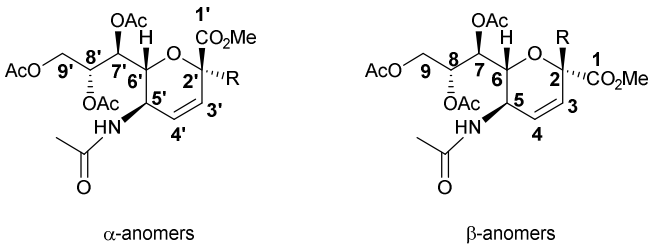

Preparation of the α/β-anomeric mixture of methyl (methyl-5-acetamido-7,8,9-tri-O-acetyl-3,4,5-trideoxy-D-manno-non-3-en-2-ulopyranosid)-onates (**23a**+**24a**)

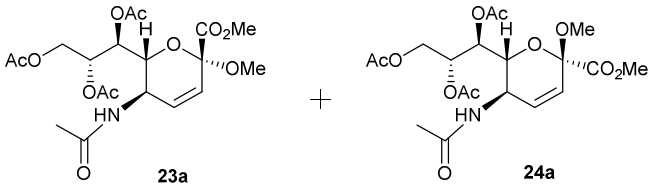

Starting from oxazoline **14**[110] (300 mg, 0.73 mmol) and using methanol as nucleophile (0.296 mL, 7.30 mmol), according to the general procedure, *Method 10*, mixture of **23a** and **24a** was obtained (276 mg, 85%; 2:8 α/β), after flash chromatographic separation using ethyl acetate/hexane (95:5, v/v), as a solvent system. The white solid mixture of **23a**+**24a** showed: ^{1}H NMR (500 MHz, $CDCl_3$): δ = 6.04 (d, $J_{3',5'}$ = 1.9, $J_{3',4'}$ = 10.1 Hz, 1H; H-3'), 5.91-5.84 (overlapping, 2H; H-3 and H-4), 5.75 (dd, $J_{4',5'}$ = 2.6, $J_{4',3'}$ = 10.1 Hz, 1H; H-4'), 5.66 (d, $J_{NH',5'}$ = 9.2 Hz, 1H; N*H*COCH$_3$'), 5.61 (d, $J_{NH,5}$ = 9.5 Hz, 1H; N*H*COCH$_3$), 5.41 (ddd, $J_{8',9a'}$ = 2.5, $J_{8',7'}$ = 6.3, $J_{8',9b'}$ = 8.9 Hz, 1H; H-8'), 5.39 (dd, $J_{7,6}$ = 2.4, $J_{7,8}$ = 5.4 Hz, 1H; H-7), 5.34-5.28 (overlapping, 2H; H-7' and H-8), 4.64-4.58 (overlapping, 2H; H-9a and H-5), 4.50 (dddd, $J_{5',3'}$ = 1.9, $J_{5',4'}$ = 2.6, $J_{5',6'}$ = $J_{5',NH'}$ = 9.2 Hz, 1H; H-5'), 4.46 (dd, $J_{9a',8'}$ = 2.5, $J_{9a',9b'}$ = 12.3 Hz, 1H; H-9a'), 4.24-4.18 (overlapping, 3H; H-6', H-9b and H-9b'), 4.06 (dd, $J_{6,7}$ = 2.4, $J_{6,5}$ = 10.3 Hz, 1H; 6-H), 3.78 (s, 3H; COOCH$_3$), 3.75 (s, 3H; COOCH$_3$'), 3.31 (s, 3H; OCH$_3$'), 3.27 (s, 3H; OCH$_3$), 2.13 (s, 3H; OCOCH$_3$), 2.11 (s, 3H; OCOCH$_3$'), 2.08 (s, 3H; OCOCH$_3$'), 2.06 (s, 3H; OCOCH$_3$), 2.05-2.02 (overlapping, 6H; OCOCH$_3$ and OCOCH$_3$'), 1.98-1.96 ppm (overlapping, 6H; NHCOC*H*$_3$ and NHCOC*H*$_3$); ^{13}C NMR (125 MHz, $CDCl_3$): δ = 170.6 (2C, O*C*OCH$_3$ and O*C*OCH$_3$'), 170.4 (O*C*OCH$_3$), 170.3 (O*C*OCH$_3$'), 170.2 (O*C*OCH$_3$'), 170.1 (O*C*OCH$_3$), 169.8 (2C, NHCOCH$_3$ and NHCOCH$_3$'), 166.5 (C-1'), 167.5 (C-1), 135.6 (C-3'), 133.7 (C-3), 125.8 (C-4), 125.6 (C'-4), 97.7 (C-2'), 96.5 (C-2), 74.4 (C-6'), 70.9 (C-8), 70.4

(C-6), 69.9 (C-8'), 68.1 (2C, C-7 and C-7'), 62.2 (2C, C-9 and C-9'), 52.8 (2C, $COOCH_3$ and $COOCH_3$'), 52.0 (OCH_3), 51.2 (OCH_3'), 43.1 (2C, C-5 and C-5'), 23.3 (2C, $NHCOCH_3$ and $NHCOCH_3$'), 21.1 ($OCOCH_3$'), 21.0 ($OCOCH_3$), 20.8 ($OCOCH_3$'), 20.7 ppm (3C, $OCOCH_3$, $OCOCH_3$, $OCOCH_3$'); MS (ESI positive): *m/z* 446.4 $[M+H]^+$, 468.4 $[M+Na]^+$.

5.1.3.2 Synthesis of the intermediate 27 and demonstration of its structure

Preparation of the intermediate ***27***

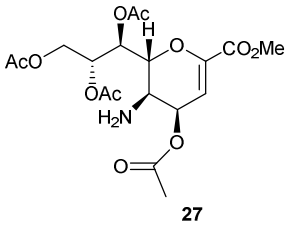

27

Oxazoline **14**[110] (100 mg, 0.24 mmol) was dissolved in 1.2 ml of a 0.1 M TFA solution in CH_3CN/H_20 (1:1, v/v) and the reaction was stirred at 23°C. The oxazoline depletion was monitored by TLC and after 5-15 min, the time necessary to transform the starting material entirely in the intermediate **27**, the reaction was quenched by the addition of a weak basic resin (IRA-67), until neutral pH. Successively, the obtained compound, was rapidly characterized: ^{1}H NMR (500 MHz, $CDCl_3$): δ = 6.17 (d, $J_{3,4}$ = 5.7 Hz, 1H; H-3), 5.65 (dd, $J_{7,6}$ = 1.4, $J_{7,8}$ = 6.0 Hz, 1H; H-7), 5.47 (ddd, $J_{8,9a}$ = 2.3, $J_{8,7}$ = $J_{8,9b}$ = 6.0 Hz, 1H; H-8), 5.30 (dd, $J_{4,5}$ = 4.2, $J_{4,3}$ 5.7 Hz, 1H; H-4), 4.70 (dd, $J_{9a,8}$ = 2.3, $J_{9a,9b}$ = 12.6 Hz, 1H; H-9a), 4.29 (dd, $J_{9b,8}$ = 6.0, $J_{9b,9a}$ = 12.6 Hz, 1H; H-9b), 4.04 (dd, $J_{6.7}$ = 1.4, $J_{6,5}$ = 10.8 Hz, 1H; H-6), 3.81 (s, 3H; $COOCH_3$), 2.95 (dd, $J_{5,4}$ = 4.2, $J_{5,6}$ = 10.8 Hz, 1H; H-5), 2.18 (s, 3H; $OCOCH_3$), 2.12 (overlapping, 6H; 2 X $OCOCH_3$), 2.08 (s, 3H; $OCOCH_3$), 1.67-1.49 ppm (overlapping, 2H; NH_2); ^{13}C NMR (125 MHz, $CDCl_3$): δ = 170.6 (2C; $OCOCH_3$ at C-7 and $OCOCH_3$ at C-9), 170.2 ($OCOCH_3$ at C-4), 169.9 (1C, $OCOCH_3$ at C-8), 162.1 (C-1), 146.2 (C-2), 105.9 (C-3), 75.5 (C-6), 70.8 (C-8), 68.6 (C-7), 65.7 (C-4), 62.0 (C-9), 52.5 ($COOCH_3$), 47.3 (C-5), 20.9 (2C; 2 X $OCOCH_3$), 20.7 ($OCOCH_3$), 20.6 ppm ($OCOCH_3$). MS (ESI positive): *m/z* 432.1 $[M+H]^+$, 454.1 $[M+Na]^+$.

Synthesis of compound **28**

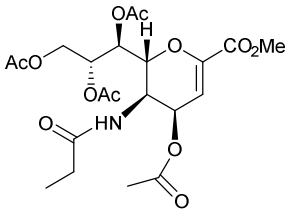

28

Starting from intermediate **27** (50 mg, 0.12 mmol) in 1.0 ml CH_2Cl_2 with weak basic resin (IRA-67) propionyl chloride (0.045mL, 0.54 mmol) was added. After purification and gel chromatography (eluting with AcOEt), compound **28** was obtained (44 mg, 75%) showing: $[\alpha]_D^{23}$ = -136.5 (c=1.0 in chloroform); ^{1}H NMR (500 MHz, $CDCl_3$): δ = 6.19 (d, $J_{3,4}$ = 5.6 Hz, 1H; H-3), 5.51 (d, $J_{NH,5}$ = 10.2 Hz, 1H; N*H*COCH$_3$), 5.47 (1H, dd, $J_{7,6}$ = 2.2, $J_{7,8}$ = 4.2 Hz, 1H; H-7), 5.30 (ddd, $J_{8,9a}$ = 2.6, $J_{8,7}$ = 4.2, $J_{8,9b}$ = 7.6 Hz, 1H; H-8), 5.14 (dd, $J_{4,5}$ = 4.1, $J_{4,3}$ = 5,6 Hz, 1H; H-4), 4.77 (dd, $J_{9a,8}$ = 2.6, $J_{9a,9b}$ = 12.5 Hz, 1H; H-9a), 4.60 (m, 1H; H-5), 4.28 (dd, $J_{6.7}$ = 2.2, $J_{6,5}$ = 11.0 Hz, 1H; H-6), 4.17 (dd, $J_{5,4}$ = 7.6, $J_{5,6}$ = $J_{5,NH}$ = 11.0 Hz, 1H; H-9a), 3.79 (s, 3H; COOCH$_3$), 2.18-2.11 (overlapping, 2H; NHCOC*H*$_2$CH$_3$), 2.10 (s, 3H; OCOC*H*$_3$), 2.09 (s, 3H; OCOC*H*$_3$), 2.07 (s, 3H; OCOC*H*$_3$), 2.05 (s, 3H; OCOC*H*$_3$), 1.05 ppm (m, 3H; NHCOCH$_2$C*H*$_3$); ^{13}C NMR (125 MHz, $CDCl_3$): δ = 173.2 (NH*C*OCH$_2$CH$_3$), 170.5 (2C, O*C*OCH$_3$ at C-8, O*C*OCH$_3$ at C-9), 170.0 (O*C*OCH$_3$ at C-7), 169.5 (O*C*OCH$_3$ at C-4), 161.7 (C-1), 146.3 (C-2), 105.9 (C-3), 74.0 (C-6), 71.9 (C-8), 67.7 (C-7), 64.9 (C-4), 62.1 (C-9), 52.5 (COOCH$_3$), 44.0 (C-5), 29.5 (NHCO*C*H$_2$CH$_3$), 20.9 (2C, 2 X OCO*C*H$_3$), 20.7 (2C, 2 X OCO*C*H$_3$), 9.2 ppm (NHCOCH$_2$*C*H$_3$); MS (ESI positive): *m/z* 488.2 $[M+H]^+$, 510.2 $[M+Na]^+$.

Synthesis of oxazoline derivative **29**

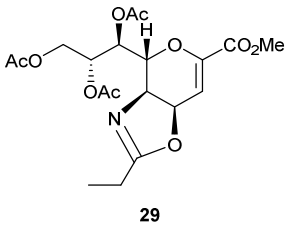

29

Starting from compound **28** (38 mg, 0.08 mmol) in CH_2Cl_2 (1 mL) containing BF_3Et_2O (0.05 mL, 0.4 mmol) was heated at 80°C for 15 min. The crude was diluted with AcOEt containing Et_3N and the organic layers were, at first, washed with saturated NH_4Cl solution then with water and dried over anhydrous Na_2SO_4. Then, a rapid chromatography (AcOEt/hexane 7:3, v/v, with 0.3% of Et_3N) afforded the desired compound (24 mg, 70%) showing: ^{1}H NMR (500

MHz, $CDCl_3$): δ = 6.33 (d, $J_{3,4}$ = 4.0 Hz, 1H; H-3), 5.57 (dd, $J_{7,6}$ = 3.0, $J_{7,8}$ = 5.7 Hz, 1H; H-7), 5.40 (ddd, $J_{8,9a}$ = 2.6, $J_{8,7}$ = 5.7, $J_{8,9b}$ = 6.6 Hz, 1H; H-8), 4.77 (dd, $J_{4,3}$ = 4.0, $J_{4,5}$ = 8.6 Hz, 1H; H-4), 4.51 (dd, $J_{9a,8}$ = 2.6, $J_{9a,9b}$ = 12.4 Hz, 1H; H-9a), 4.17 (dd, $J_{9b,8}$ = 6.6, $J_{9b,9a}$ = 12.4 Hz, 1H; H-9b), 3.92 (m, 1H, H-5), 3.76 (s, 3H; $COOCH_3$), 3.38 (1H, dd, $J_{6,7}$ = 3.0, $J_{6,5}$ = 9.9 Hz, H-6), 2.27 (overlapping, 2H; CCH_2CH_3), 2.10 (s, 3H; $OCOCH_3$), 2.20-1.98 (overlapping, 6H; 2 X $OCOCH_3$), 1.11 ppm (s, 3H; CCH_2CH_3); ^{13}C NMR (125 MHz, $CDCl_3$): δ = 171.0, 170.5, 169.7, 169.5 (4C, 3 X $OCOCH_3$ and $OCCH_2CH_3$), 161.8 (C-1), 146.9 (C-2), 107.5 (C-3), 76.7 (C-6), 71.9 (C-4), 70.3 (C-8), 69.2 (C-7), 61.9 (C-9), 61.8 (C-5), 52.3 ($COOCH_3$), 21.5 ($OCOCH_2CH_3$), 20.7 ($OCOCH_3$), 20.6 ($OCOCH_3$), 20.5 ($OCOCH_3$), 10.1 ppm ($OCOCH_2CH_3$).

Synthesis of compound **31**

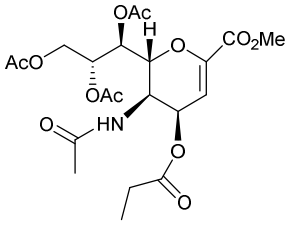

31

Oxazoline **29** (34 mg, 0.08 mmol) was dissolved in 0.8 ml of a 0.1 M TFA solution in CH_3CN/H_2O (1:1 v/v) and the reaction was stirred at 23°C. The oxazoline depletion was monitored by TLC and after 5-15 min, the reaction was quenched by the addition of a weak basic resin (IRA-67), until neutral pH. Then, acetyl chloride (29 mg, 0.4 mmol) was added. After purification and gel chromatography, compound **31** was obtained (31 mg, 80%) showing: $[\alpha]_D^{23}$ = -131.0 (c=1.0 in chloroform); ^{1}H NMR (500 MHz, $CDCl_3$): δ = 6.18 (d, $J_{3,4}$ = 5.6 Hz, 1H; H-3), 5.64 (d, $J_{NH,4}$ = 4.7, $J_{NH,5}$ = 10.9 Hz, 1H; $NHCOCH_3$), 5.47 (dd, $J_{7,6}$ = 2.2, $J_{7,8}$ = 4.1 Hz, 1H; H-7), 5.29 (ddd, $J_{8,9a}$ = 2.6, $J_{8,7}$ = 4.1 Hz, $J_{8,9b}$ = 7.3 Hz, 1H; H-8), 5.14 (dd, $J_{4,5}$ = 4.1, $J_{4,3}$ = 5,6 Hz, 1H; H-4), 4.74 (dd, $J_{9a,8}$ = 2.6, $J_{9a,9b}$ = 12.4 Hz, 1H; H-9a), 4.56 (dd, $J_{5,4}$ = 4.1, $J_{5,6}$ = $J_{5,NH}$ = 10.9 Hz, 1H; H-5), 4.26 (dd, $J_{6.7}$ = 2.2, $J_{6,5}$ = 10.9 Hz, 1H; H-6), 4.17 (dd, $J_{9b,8}$ = 7.3, $J_{9b,9a}$ = 12.4 Hz, 1H; H-9b), 3.77 (s, 3H; $COOCH_3$), 2.38-2.30 (overlapping, 2H; $OCOCH_2CH_3$), 2.08 (s, 3H; $OCOCH_3$), 2.05 (s, 3H; $OCOCH_3$), 2.03 (s, 3H; $OCOCH_3$), 1.91 (s, 3H; $NHCOCH_3$), 1.14 ppm (3H, t, $J_{5,4}$ = 4.1 Hz, $OCOCH_2CH_3$); ^{13}C NMR (125 MHz, $CDCl_3$): δ = 173.0 ($OCOCH_2CH_3$), 170.5 ($OCOCH_3$ at C-8 or C-9), 170.4 ($OCOCH_3$ at C-8 or C-9), 170.1 ($OCOCH_3$ at C-7), 169.6 ($NHCOCH_3$), 161.7 (C-1), 146.2 (C-2), 106.0 (C-3), 73.9 (C-6), 71.8 (C-8), 67.7 (C-7), 64.9 (C-4), 62.1 (C-9), 52.5 ($COOCH_3$), 44.3 (C-5), 27.4

(OCO*C*H$_2$CH$_3$), 23.1 (NHCO*C*H$_3$), 20.9 (OCO*C*H$_3$), 20.7 (OCO*C*H$_3$), 20.6 (OCO*C*H$_3$), 8.9 ppm (OCOCH$_2$*C*H$_3$). MS (ESI positive): *m/z* 488.2 $[M+H]^+$, 510.3 $[M+Na]^+$.

5.1.3.3 Synthesis of 3,4-unsaturated derivatives using other alcoholic or thiolic nucleophiles, via Ferrier reaction

General procedure. To a solution of oxazoline **14**[110] (300 mg, 0.73 mmol) in CH_3CN (7.2 mL) under argon the appropriate nucleophile (7.20 mmol) and Montmorillonite K-10 (40% w/w) were added and the reaction was stirred at 80 °C for 2-5 h. Subsequently the reaction was filtered over Celite and the solvent was then evaporated. Finally, the residue was purified by silica gel chromatography with the appropriate solvent system to achieve the desired mixture of compounds **23b+24b, 23c+24c, 23d+24d, 23e+24e** and **23f+24f**.

For the obtained chromatographically inseparable mixtures the ^{1}H and ^{13}C NMR assignments refer to:

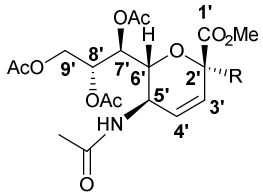

α-anomers

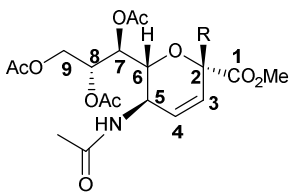

β-anomers

*Preparation of the α/β-anomeric mixture of methyl (2S-ethyl-5-acetamido-7,8,9-tri-O-acetyl-2,3,4,5-tetradeoxy-D-manno-non-3-en-2-ulopyranosid)-onates (***23b+24b***)*

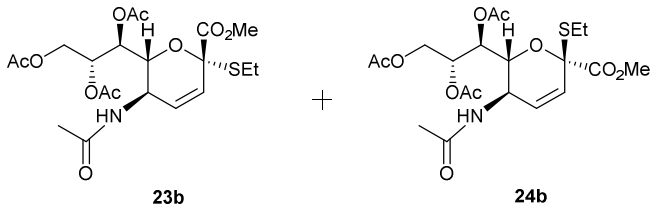

Starting from oxazoline **14**[110] (300 mg, 0.73 mmol) and using ethanethiol as nucleophile (0.527 mL, 7.30 mmol), according to general procedure, mixture of **23b+24b** was obtained (253 mg, 68%, 1:9 α/β), after flash chromatographic separation using ethyl acetate/hexane (eluting with AcOEt/hexane, 99:1 to 95:5, v/v), as a solvent system. The white solid mixture of **23b+24b** showed: ^{1}H NMR (500 MHz, $CDCl_3$): δ = 6.10 (dd, $J_{3,5}$ = 2.5, $J_{3,4}$ = 10.1 Hz, 1H; H-3), 5.91 (d, $J_{3',5'}$ = 2.5, $J_{3',4'}$ = 10.1 Hz, 1H; H-3'), 5.84 (dd, $J_{4',5'}$ = 1.7, $J_{4',5'}$ = 10.1 Hz, 1H; H-4'), 5.74 (dd, $J_{4,5}$ = 1.9, $J_{4,3}$ = 10.1 Hz, 1H; H-4), 5.57-5.52 (overlapping, 2H; N*H*COCH$_3$ and N*H*COCH$_3$'), 5.42 (ddd, $J_{8',9a'}$ = 2.5, $J_{8',7'}$ = 6.1, $J_{8',9b'}$ = 8.6 Hz, 1H; H-8'), 5.37 (dd, $J_{7,6}$

= 2.4, $J_{7,8}$ = 4.8 Hz, 1H; H-7), 5.33 (dd, $J_{7',6'}$ = 2.0, $J_{7',8'}$ = 6.1 Hz, 1H; H-7'), 5.22 (ddd, $J_{8,9a}$ = 2.4, $J_{8,7}$ = 4.8, $J_{8,7}$ = 6.8 Hz, 1H; H-8), 4.65-4.58 (overlapping, 2H; H-5 and H-9a), 4.53 (dd, $J_{9a',8'}$ = 2.5, $J_{9a',9b'}$ = 12.4 Hz, 1H; H-9a'), 4.45 (ddd, $J_{5',4'}$ = 2.5, $J_{5',6'}$ = $J_{5',NH'}$ = 9.8 Hz, 1H; H-5'), 4.33 (dd, $J_{6,7}$ = 2.4, $J_{6,5}$ = 10.0 Hz, 1H; 6-H), 4.28-4.20 (overlapping, 2H; H-9b and H-9b'), 3.92 (dd, $J_{6',7'}$ = 2.0, $J_{6',5'}$ = 9.8 Hz, 1H; H-6'), 3.80 (s, 3H; $COOCH_3$), 3.75 (s, 3H; $COOCH_3$'), 3.72-3.50 (overlapping, 4H; SCH_2CH_3 and SCH_2CH_3'), 2.13 (s, 3H; $OCOCH_3$), 2.12 (s, 3H; $OCOCH_3$'), 2.10 (s, 3H; $OCOCH_3$'), 2.08 (s, 3H; $OCOCH_3$), 2.03 (s, 3H; $OCOCH_3$'), 2.02 (s, 3H; $OCOCH_3$), 1.96 (s, 3H; $NHCOCH_3$), 1.95 (s, 3H; $NHCOCH_3$'), 1.24 (m, 3H; SCH_2CH_3'), 1.16 ppm (m, 3H; SCH_2CH_3); ^{13}C NMR (125 MHz, $CDCl_3$): δ=170.6 ($OCOCH_3$'), 170.5 (2C, $OCOCH_3$ and $OCOCH_3$'), 170.4 ($OCOCH_3$), 170.1 (2C, $OCOCH_3$ and $OCOCH_3$'), 169.8 ($NHCOCH_3$'), 169.7 ($NHCOCH_3$), 168.8 (C-1'), 167.3 (C-1), 131.4 (C-4'), 130.7 (C-4), 126.5 (C-3'), 126.3 (C-3), 85.7 (C-2), 84.6 (C-2'), 74.2 (C-6'), 71.4 (C-8), 70.6 (C-6), 70.4 (C-8'), 68.5 (C-7), 68.0 (C-7') 62.5 (C-9), 62.2 (C-9'), 52.9 ($COOCH_3$'), 52.8 ($COOCH_3$), 43.1 (C-5'), 43.0 (C-5), 24.4 (1C, SCH_2CH_3), 23.3 (3C, $NHCOCH_3$, $NHCOCH_3$' and SCH_2CH_3'), 21.1 (2C, $OCOCH_3$ and $OCOCH_3$'), 20.8 ($OCOCH_3$'), 20.7 (3C, 2 X $OCOCH_3$ and $OCOCH_3$'), 14.5 (SCH_2CH_3'), 14.0 ppm (SCH_2CH_3); MS (ESI positive): *m/z* 476.1 $[M+H]^+$, 498.5 $[M+Na]^+$.

*Preparation of the α/β-anomeric mixture of methyl (ethyl-5-acetamido-7,8,9-tri-O-acetyl-3,4,5-trideoxy-D-manno-non-3-en-2-ulopyranosid)-onates (***23c**+**24c***)*

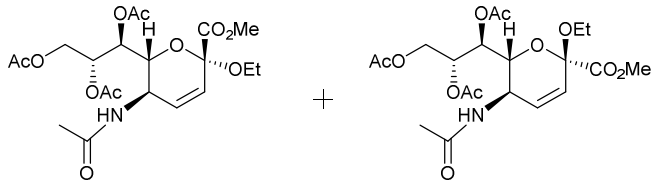

Starting from oxazoline **14**[110] (300 mg, 0.73 mmol) and using ethanol as nucleophile (0.426 mL, 7.30 mmol), according to general procedure, mixture of **23c**+**24c** was obtained (268 mg, 80%; 2:8 α/β), after flash chromatographic separation using AcOEt/hexane (eluting with AcOEt/hexane, 95:5, v/v) as a solvent system. The white solid mixture of **23c**+**24c** showed: ^{1}H NMR (500 MHz, $CDCl_3$): δ = 5.98 (d, $J_{3',5'}$ = 1.3, $J_{3',4'}$ = 10.1 Hz, 1H; H-3'), 5.90 (d, $J_{4,5}$ = 2.2, $J_{4,3}$ = 10.2 Hz, 1H; H-4), 5.85 (br d, $J_{3,4}$ = 10.2 Hz, 1H; H-3), 5.78 (dd, $J_{4',5'}$ = 2.5, $J_{4',3'}$ = 10.1 Hz, 1H; H-4'), 5.66 (d, $J_{NH',5'}$ = 9.3 Hz, 1H; $NHCOCH_3$'), 5.58 (d, $J_{NH,5}$ = 9.6 Hz, 1H; $NHCOCH_3$), 5.41 (ddd, $J_{8',9a'}$ = 2.2, $J_{8',7'}$ = 6.2, $J_{8',9b'}$ = 8.4 Hz, 1H; H-8'), 5.36 (dd, $J_{7,6}$ = 2.4, $J_{7,8}$ = 4.8 Hz, 1H; H-7), 5.31 (dd, $J_{7,6}$ = 1.7, $J_{7,8}$ = 6.2 Hz, 1H; H-7'), 5.26 (m, 1H; H-8), 4.68-

4.60 (overlapping, 2H; H-5 and H-9a), 4.51-4.43 (overlapping, 2H; H-5' and H-9a'), 4.24-4.17 (overlapping, 3H; H-6', H-9b and H-9b'), 4.04 (dd, $J_{6,7}$ = 2.1, $J_{6,5}$ = 10.2 Hz, 1H; H-6), 3.77 (s, 3H; *C*OOCH$_3$), 3.74 (s, 3H; COOCH$_3$'), 3.71-3.57 (overlapping, 2H; OC*H*$_2$CH$_3$ and OC*H*$_2$CH$_3$'), 3.50-3.34 (overlapping, 2H; OC*H*$_2$CH$_3$ and OC*H*$_2$CH$_3$'), 2.12 (s, 3H; OCOCH$_3$), 2.11 (s, 3H; OCOCH$_3$'), 2.09 (s, 3H; OCOCH$_3$'), 2.06 (s, 3H; OCOCH$_3$), 2.02-2.01 (overlapping, 6H; OCOCH$_3$ and OCOCH$_3$'), 1.98-1.95 (overlapping, 6H; NHCOC*H*$_3$ and NHCOC*H*$_3$'), 1.23-1.13 ppm (overlapping, 6H; OCH$_2$C*H*$_3$ and OCH$_2$C*H*$_3$'); ^{13}C NMR (125 MHz, CD$_3$OD): δ = 170.6 (O*C*OCH$_3$'), 170.5 (O*C*OCH$_3$), 170.4 (2C; O*C*OCH$_3$ and OCOCH$_3$'), 170.1 (OCOCH$_3$'), 170.0 (OCOCH$_3$), 169.8 (2C; NH*C*OCH$_3$ and NH*C*OCH$_3$'), 168.7 (C-1'), 167.7 (C-1), 134.9 (C-3'), 133.3 (C-3), 126.2 (C-4'), 126.1 (C-4), 97.6 (C-2'), 96.1 (C-2), 74.4 (C-6'), 71.3 (C-8), 70.6 (C-6), 70.1 (C-8'), 68.5 (C-7), 68.2 (C-7'), 62.3 (2C, C-9 and C-9'), 60.3 (O*C*H$_2$CH$_3$), 59.9 (O*C*H$_2$CH$_3$'), 52.7 (COO*C*H$_3$), 52.6 (COO*C*H$_3$'), 43.1 (C-5'), 43.0 (C-5), 23.2 (2C; NHCO*C*H$_3$ and NHCO*C*H$_3$'), 21.0 (OCOCH$_3$'), 20.9 (OCO*C*H$_3$), 20.7 (OCO*C*H$_3$'), 20.6 (3C; 2 X OCO*C*H$_3$ and OCO*C*H$_3$'), 15.3 ppm (2C; OCH$_2$*C*H$_3$ and OCH$_2$*C*H$_3$'). MS (ESI positive): *m/z* 460.2 [M+H]$^+$, 482.2 [M+Na]$^+$.

*Preparation of the α/β-anomeric mixture of methyl (isopropyl-5-acetamido-7,8,9-tri-O-acetyl-3,4,5-trideoxy-D-manno-non-3-en-2-ulopyranosid)-onates (***23d**+**24d***)*

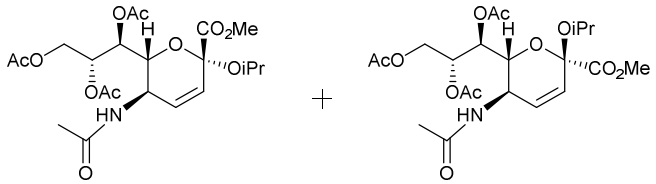

Starting from oxazoline **14**[110] (300 mg, 0.73 mmol) and using isopropanol as nucleophile (0.555 mL, 7.30 mmol), according to general procedure, mixture of **23d**+**24d** was obtained (242 mg, 70%; 2:8 α/β), after flash chromatographic separation using AcOEt/hexane (eluting with AcOEt/hexane, 95:5, v/v) as a solvent system. The white solid mixture of **23d**+**24d** showed: ^{1}H NMR (500 MHz, CDCl$_3$): δ = 6.02-5.95 (overlapping, 2H; H-4, H-3'), 5.83-5.77 (overlapping, 2H; 3-H, H-4'), 5.56 (d, $J_{NH',5'}$ = 9.1 Hz, 1H; N*H*COCH$_3$'), 5.52 (1H, d, $J_{NH,5}$ = 9.7 Hz, N*H*COCH$_3$), 5.41-5.36 (overlapping, 2H; H-8', H-7), 5.30 (dd, $J_{7',6'}$ = 1.9, $J_{7',8'}$ = 6.3 Hz, 1H; H-7'), 5.26 (ddd, $J_{8,9a}$ = 2.5, $J_{8,7}$ = 5.2, $J_{8,9b}$ = 7.7 Hz, 1H; H-8), 4.80 (dd, $J_{9a,8}$ = 2.5, $J_{9a,9b}$ = 12.4 Hz, 1H; H-9a), 4.68 (ddd, $J_{5,4}$ = 2.1, $J_{5,6}$ = $J_{5,NH}$ = 9.7 Hz, 1H; H-5), 4.51-4.43 (overlapping, 2H; H-9a' and H-5'), 4.28-4.21 (overlapping, $J_{9b,8}$ = 7.7, $J_{9b,9a}$ = 12.4, 2H; H-9b and H-9b'), 4.19 (dd, $J_{6',7'}$ = 1.9, $J_{6',5'}$ = 9.9 Hz, 1H; H'-6), 4.14-4.07 (overlapping, 2H; H-6

and OC*H*$(CH_3)_2$), 3.99- 3.91 (m, 1H; OC*H*$(CH_3)_2$'), 3.77 (s, 3H; $COOCH_3$), 3.74 (s, 3H; $COOCH_3$'), 2.12 (s, 3H; $OCOCH_3$), 2.11 (s, 3H; $OCOCH_3$'), 2.09 (s, 3H; $OCOCH_3$'), 2.06 (s, 3H; $OCOCH_3$), 2.03-2.00 (overlapping, 6H; $OCOCH_3$ and $OCOCH_3$'), 1.97 (s, 3H; NHCO*C*H_3'), 1.94 (s, 3H; NHCO*C*H_3), 1.22-1.18 (overlapping, 6H; OCH(C*H*$_3)_2$ and OCH(C*H*$_3)_2$'), 1.17 (m, 3H; OCH(C*H*$_3)_2$'), 1.07 ppm (m, 3H; OCH(C*H*$_3)_2$); ^{13}C NMR (125 MHz, $CDCl_3$): δ = 170.8 (2C; O*C*OCH$_3$' and O*C*OCH$_3$), 170.5 (O*C*OCH$_3$), 170.4 (O*C*OCH$_3$'), 170.1 (O*C*OCH$_3$'), 170.0 (O*C*OCH$_3$), 169.8 (NH*C*OCH$_3$'), 169.7 (NH*C*OCH$_3$), 168.9 (C-1'), 168.0 (C-1), 134.7, 132.3, 126.7, 126.6 (C-3', C-3, C-4', C-4), 98.0 (C-2'), 95.0 (C-2), 74.4 (C-6'), 72.4 (C-8), 71.2 (C-6), 70.3 (C-8'), 69.4 (C-7), 68.4 (C-7'), 68.2 (O*C*H$(CH_3)_2$'), 67.8 (O*C*H$(CH_3)_2$), 62.7 (C-9), 62.2 (C-9'), 52.6 (COO*C*H_3), 52.5 (COO*C*H_3'), 43.2 (C-5'), 43.0 (C-5), 24.5 (OCH(*C*$H_3)_2$), 24.2 (OCH(*C*$H_3)_2$'), 23.7 (OCH(*C*$H_3)_2$'), 23.2 (2C; NHCO*C*H_3, NHCO*C*H_3'), 22.7 (OCH(*C*$H_3)_2$), 21.1 (OCO*C*H_3'), 21.0 (OCO*C*H_3), 20.7 (3C; OCO*C*H_3', 2 X OCO*C*H_3), 20.6 ppm (OCO*C*H_3'). MS (ESI positive) *m/z* 474.5 $[M+H]^+$, 496.4 $[M+Na]^+$.

*Preparation of the α/β-anomeric mixture of methyl (buthyl-5-acetamido-7,8,9-tri-O-acetyl-3,4,5-trideoxy-D-manno-non-3-en-2-ulopyranosid)-onates (***23e+24e***)*

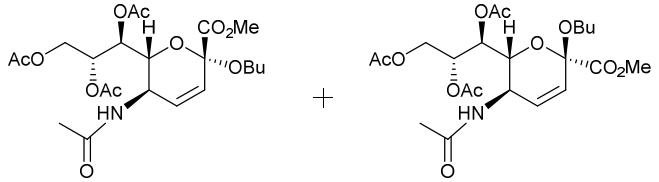

Starting from oxazoline **14**[110] (300 mg, 0.73 mmol) and using butanol as nucleophile (0.668 mL, 7.30 mmol), according to general procedure, mixture of **23e+24e** was obtained (242 mg, 68%; 1:9 α/β), after flash chromatographic separation using AcOEt/hexane (eluting with AcOEt/hexane, 85:15 to 10:0, v/v) as a solvent system. The white solid mixture of **23e+24e** showed:^{1}H NMR (500 MHz, $CDCl_3$): δ = 5.97 (dd, $J_{3',5'}$ = 1.9, $J_{3',4'}$ = 10.1 Hz, 1H; H-3'or H-4'), 5.91 (dd, $J_{4,5}$ = 2.5, $J_{4,3}$ = 10.1 Hz, 1H; H-4 or H-3), 5.84 (dd, $J_{3,5}$ = 1.7, $J_{3,4}$=10.1 Hz, 1H; H-3 or H-4), 5.78 (dd, $J_{4',5'}$ = 2.6, $J_{4',3'}$=10.1 Hz, 1H; H-4'or H-3'), 5.70 (1H; d, $J_{NH',5'}$ = 9.3 Hz, NHCOCH$_3$'), 5.61 (d, $J_{NH,5}$ = 9.4 Hz, 1H; N*H*COCH$_3$), 5.39 (1H; $J_{8',9a'}$ = 2.5, $J_{8',7'}$ = 6.1, $J_{8',9b'}$ = 8.7 Hz, H-8'), 5.37 (dd, $J_{7,6}$ = 2.5, $J_{7,8}$ = 4.2 Hz, 1H; H-7), 5.32 (dd, $J_{7',6'}$ = 2.1, $J_{7',8'}$ = 6.1 Hz, 1H; H-7'), 5.23 (ddd, $J_{8,9a}$ = 2.3, $J_{8,7}$ = 4.2, $J_{8,9b}$ = 6.8 Hz, 1H; H-8), 4.70-4.61 (overlapping, 2H; H-9a and H-5), 4.52-4.45 (overlapping, 2H; H-9a' and H-5'), 4.26-4.18 (overlapping, 3H; H-9b, H'-9b' and H-6'), 4.04 (dd, $J_{6,7}$ = 2.5, $J_{6,5}$ = 10.2 Hz, 1H; H-6), 3.77 (s, 3H; $COOCH_3$), 3.73 (s, 3H; $COOCH_3$'), 3.64-3.50 (overlapping, 2H; OC*H*$_2(CH_2)_2CH_3$ and OC*H*$_2(CH_2)_2CH_3$'), 3.39 (m, 1H; OC*H*$_2(CH_2)_2CH_3$'), 3.29 (m, 1H; OC*H*$_2(CH_2)_2CH_3$), 2.14 (s,

3H; $OCOCH_3$'), 2.09 (s, 3H; $OCOCH_3$'), 2.08 (s, 3H; $OCOCH_3$'), 2.05 (s, 3H; $OCOCH_3$), 2.01 (s, 3H; $OCOCH_3$), 1.96-1.94 (6H; overlapping, N*H*$COCH_3$ and N*H*$COCH_3$'), 1.59-1.45 (overlapping, 4H; $OCH_2(CH_2)_2CH_3$ and $OCH_2(CH_2)_2CH_3$'), 1.39-1.29 (overlapping, 4H; $OCH_2(CH_2)_2CH_3$ and $OCH_2(CH_2)_2CH_3$'), 0.92-0.86 ppm (overlapping, 6H; $OCH_2(CH_2)_2CH_3$ and $OCH_2(CH_2)_2CH_3$'); ^{13}C NMR (125 MHz, $CDCl_3$): δ = 170.6 ($OCOCH_3$'), 170.5 ($OCOCH_3$), 170.4 ($OCOCH_3$), 170.3 ($OCOCH_3$'), 170.1 ($OCOCH_3$'), 170.0 ($OCOCH_3$), 169.8 (2C, NH$COCH_3$ and NH$COCH_3$'), 168.7 (C-1'), 167.7 (C-1), 134.9 (C-3'or C-4'), 133.2 (C-3 or C-4), 126.2 (2C, C-4 or C-3 and C-4' or C-3'), 97.6 (C-2'), 96.0 (C-2), 74.4 (C-6'), 71.8 (C-8), 70.8 (C-6), 70.3 (C-8'), 68.7 (C-7), 68.2 (C-7'), 64.6 (C-9), 63.8 (C-9'), 62.5 ($OCH_2(CH_2)_2CH_3$), 62.3 ($OCH_2(CH_2)_2CH_3$'), 52.6 (2C; $COOCH_3$ and $COOCH_3$'), 43.1 (C-5'), 43.0 (C-5), 31.8 ($OCH_2CH_2CH_2CH_3$), 31.6 ($OCH_2CH_2CH_2CH_3$'), 23.2 (2C; $NHCOCH_3$ and $NHCOCH_3$'), 21.0 ($OCOCH_3$'), 20.9 ($OCOCH_3$), 20.7 ($OCOCH_3$'), 20.6 (3C; $OCOCH_3$, $OCOCH_3$ and $OCOCH_3$'), 19.1 ($OCH_2CH_2CH_2CH_3$), 19.0 ($OCH_2CH_2CH_2CH_3$'), 13.8 ($OCH_2CH_2CH_2CH_3$), 13.6 ppm ($OCH_2CH_2CH_2CH_3$'). MS (ESI positive) *m/z* 488.5 $[M+H]^+$, 510.5 $[M+Na]^+$.

Preparation of the α/β-anomeric mixture of methyl (2S-octyl-5-acetamido-7,8,9-tri-O-acetyl-2,3,4,5-tetradeoxy-D-manno-non-3-en-2-ulopyranosid)-onates (**23f+24f**)

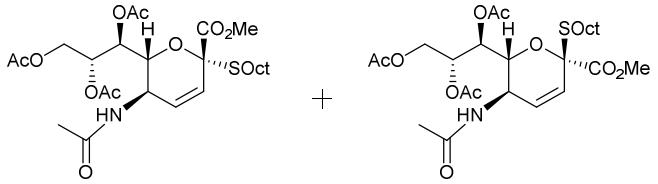

Starting from oxazoline **14**[110] (300 mg, 0.73 mmol) and using octanethiol as nucleophile (1.27 mL, 7.30 mmol), according to general procedure, mixture of **23f+24f** was obtained (286 mg, 70%; 2:8 α/β), after flash chromatographic separation using CH_2Cl_2/MeOH (eluting with CH_2Cl_2/MeOH, 10:0 to 96:4, v/v) as a solvent system. The white solid mixture of **23f+24f** showed: ^{1}H NMR (500 MHz, $CDCl_3$): 6.09 (dd, $J_{4,5}$ = 2.4, $J_{4,3}$ = 10.1 Hz, 1H; H-4 or H-3), 5.90 (dd, $J_{4',5'}$ = 2.5, $J_{4',3'}$ = 10.1 Hz, 1H; H-4' or H-3'), 5.83 (dd, $J_{3',5'}$ = 1.3, $J_{3',4'}$ = 10.1 Hz, 1H; H-3' or H-4'), 5.72 (dd, $J_{3,5}$ = 1.7, $J_{3,4}$ = 10.1 Hz, 1H; H-3 or H-4), 5.63 (d, $J_{NH,5}$ = 9.6 Hz, 1H; N*H*$COCH_3$), 5.54 (d, $J_{NH',5'}$ = 9.8 Hz, 1H; N*H*$COCH_3$'), 5.42-5.35 (overlapping, 2H; H-8' and H-7), 5.32 (dd, $J_{7',6'}$ = 1.8, $J_{7',8'}$ = 6.3 Hz, 1H; H-7'), 5.17 (ddd, $J_{8,9a}$ = 2.1, $J_{8,7}$ = 4.0, $J_{8,9b}$ = 7.2 Hz, H-8), 4.67-4.60 (overlapping, H-5 and H-9a), 4.51 (dd, $J_{9a',8'}$ = 2.4, $J_{9a',9b'}$ = 12.4 Hz, 1H; H-9a'), 4.43 (m; 1H; H-5'), 4.33 (dd, 1H; $J_{6,7}$ = 2.3, $J_{6,5}$ = 10.0 Hz, H-6), 4.28-4.21

(overlapping, 2H; H-9b and H-9b'), 3.90 (dd, $J_{6',7'}$ = 1.8, $J_{6',5'}$ = 9.9 Hz, 1H; H-6'), 3.78 (s, 3H; $COOCH_3$), 3.74 (s, 3H; $COOCH_3$'), 3.68-3.43 (overlapping, 4H; $SCH_2CH_2(CH_2)_5CH_3$, $SCH_2CH_2(CH_2)_5CH_3$'), 2.13-2.09 (overlapping, 6H; $OCOCH_3$ and $OCOCH_3$'), 2.09-2.04 (overlapping, 6H; $OCOCH_3$ and $OCOCH_3$'), 2.03-1.99 (overlapping, 6H; $OCOCH_3$ and $OCOCH_3$'), 1.96-1.91 (overlapping, 6H; $NHCOCH_3$ and $NHCOCH_3$'), 1.59-1.37 (overlapping, 4H; $SCH_2CH_2(CH_2)_5CH_3$ and $SCH_2CH_2(CH_2)_5CH_3$'), 1.35-1.15 (overlapping, 20H; $SCH_2CH_2(CH_2)_5CH_3$, $SCH_2CH_2(CH_2)_5CH_3$'), 0.88-0.80 ppm (overlapping, 6H; $SCH_2CH_2(CH_2)_5CH_3$, $SCH_2CH_2(CH_2)_5CH_3$');^{13}C NMR (125 MHz, $CDCl_3$) : δ = 170.4 (4C; $OCOCH_3$, $OCOCH_3$', $OCOCH_3$ and $OCOCH_3$'), 170.1 (2C, $OCOCH_3$ and $OCOCH_3$'), 169.8 (2C; $NHCOCH_3$ and $NHCOCH_3$'), 168.8 (C-1'), 167.3 (C-1), 131.4 (C-3' or C-4'), 130.6 (C-3 or C-4), 126.5 (C-4' or C-3'), 126.4 (C-4 or C-3), 85.4 (C-2), 84.5 (C-2'), 74.3 (C-6'), 71.6 (C-8), 70.8 (C-6), 70.6 (C-8'), 68.7 (C-7), 68.1 (C-7'), 62.5 (C-9), 62.2 (C-9'), 52.8 (2C; $COOCH_3$ and $COOCH_3$'), 43.1 (C-5'), 42.9 (C-5), 31.7, 30.1, 29.2, 29.1, 29.0 (12C, $SCH_2CH_2(CH_2)_5CH_3$ and $SCH_2CH_2(CH_2)_5CH_3$'), 23.2 (2C, $NHCOCH_3$ and $NHCOCH_3$'), 22.5 (2C, $SCH_2CH_2(CH_2)_5CH_3$ and $SCH_2CH_2(CH_2)_5CH_3$'), 21.1 ($OCOCH_3$'), 20.9 ($OCOCH_3$), 20.7 (2C, $OCOCH_3$ and $OCOCH_3$'), 20.6 (2C, $OCOCH_3$ and $OCOCH_3$'), 14.0 ppm ($SCH_2CH_2(CH_2)_5CH_3$ and $SCH_2CH_2(CH_2)_5CH_3$'). MS (ESI positive) *m/z* 560.7 $[M+H]^+$, 582.7 $[M+Na]^+$.

5.1.3.4 Deacetylation to achieve compounds 32a,b and 33a-f

General Zemplén reaction procedure. The peracetylated mixtures of **32a**,**b** or **33a-f** (200 mg, 0.45 mmol) was treated with a methanolic solution of NaOMe, freshly prepared by dissolving sodium metal (0.22 mmol, 5 mg) in anhydrous MeOH (2 mL). The reaction mixture was stirred at 23 °C for 1 h, and then quenched with acidic resin (Dowex 50WX8, H^+). The resin was filtered off and washed with MeOH (4 mL) and the combined filtrates were evaporated under vacuum. The crude compound was purified with flash chromatography to give compounds **32a** and **32b** or **33a**, **33b**, **33c**, **33d**, **33e** and **33f**.

Preparation of the methyl (methyl-5-acetamido-3,4,5-trideoxy-D-manno-non-3-en-2-ulopyranosid)-onates (**32a** and **33a**).

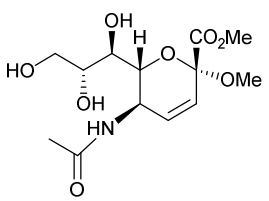

32a

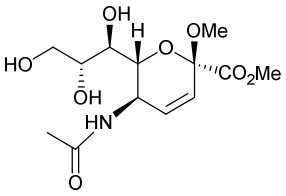

33a

Starting from mixture of **23a+24a** (200 mg, 0.45 mmol) and according to general Zemplén procedure, column chromatography (eluting with AcOEt/MeOH, 9:1 to 8:2, v/v) first afforded compound **32a** as a white solid (24 mg, 16%), showing: $[\alpha]_D^{23}$ = -64.7 (*c*=1 in methanol); ^{1}H NMR (500 MHz, CD_3OD): δ = 6.13 (d, $J_{3,4}$ = 10.1 Hz, 1H; H-3), 5.88 (dd, $J_{4,5}$ = 2.5, $J_{4,3}$ = 10.1 Hz, 1H; H-4), 4.72 (br d, $J_{5,6}$ = 9.7 Hz, 1H; H-5), 3.92-3.90 (m, 1H; H-8), 3.88 (d, $J_{6,5}$ = 9.7 Hz, 1H; H-6), 3.86 (dd, $J_{9a,8}$ = 2.1, $J_{9a,9b}$ = 11.4 Hz, 1H; H-9a), 3.81 (s, 3H; $COOCH_3$), 3.66 (dd, $J_{9b,8}$ = 5.8, $J_{9b,9a}$ = 11.4 Hz; 1H; H-9b), 3.56 (d, $J_{7,8}$ = 9.1 Hz, 1H; H-7), 3.33 (s, 3H; OCH_3), 1.97 ppm (s, 3H; NHCOC*H*$_3$); ^{13}C NMR (125 MHz, CD_3OD): δ = 174.0 (NH*C*OCH_3), 171.8 (C-1), 137.1 (C-3), 127.1 (C-4), 99.2 (C-2), 77.2 (C-6), 72.4 (C-8), 70.0 (C-7), 64.7 (C-9), 53.6 (COO*C*H$_3$), 51.3 (OCH_3), 44.5 (C-5), 22.6 ppm (NHCO*C*H$_3$). Other chemical-physical properties were superimposable with those previously reported in literature[42]. Further elution afforded compound **33a** (94 mg, 66 %): $[\alpha]_D^{23}$ = -183.1 (*c*=1 in methanol); ^{1}H NMR (500 MHz, CD_3OD): δ = 5.92 (d, $J_{3,4}$ = 10.1 Hz, 1H; H-3), 5.86 (dd, $J_{4,5}$ = 1.7, $J_{4,3}$ = 10.1 Hz, 1H; H-4), 4.72 (d, $J_{5,6}$ = 10.2 Hz, 1H; H-5), 4.03 (d, $J_{6,5}$ = 10.2 Hz, 1H; H-6), 3.82-3.76 (overlapping, 5H; H-8, H-9a and $COOCH_3$), 3.65 (dd, $J_{9b,8}$ = 5.4, $J_{9b,9a}$ = 11.4 Hz, 1H; H-9b), 3.47 (d, $J_{7,8}$ = 9.4 Hz, 1H; H-7), 3.28 (s, 3H; OCH_3), 1.93 ppm (s, 3H; $NHCOCH_3$); ^{13}C NMR (125 MHz, CD_3OD): δ = 173.7 (NH*C*OCH_3), 171.0 (C-1), 135.1 (C-3), 127.1 (C-4), 97.8 (C-2), 71.7 (C-6), 71.4 (C-8), 70.2 (C-7), 65.3 (C-9), 53.5 (COO*C*H$_3$), 52.3 (OCH_3), 44.5 (C-5), 22.7 ppm (NHCO*C*H$_3$). Other chemical-physical properties were superimposable with those previously reported in literature[42].

Preparation of the methyl (2S-ethyl-5-acetamido-2,3,4,5-tetradeoxy-D-manno-non-3-en-2-ulopyranosid)-onates (**32b** and **33b**).

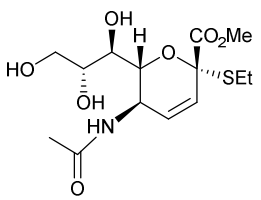

32b

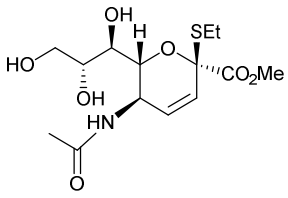

33b

Starting from compound **23b+24b** (214 mg, 0.45 mmol) and according to general procedure, column chromatography (eluting with AcOEt/MeOH, 9:1 to 85:15, v/v) first afforded compound **32b** as a white solid (13 mg, 9%), showing: $[\alpha]_D^{23}$ = -59.8 (*c*=1 in methanol); ^{1}H NMR (500 MHz, CD_3OD): δ = 6.02 (ddd, $J_{4,6}$ < 1.0, $J_{4,5}$ = 2.5, $J_{4,3}$ = 10.1 Hz, 1H; H-3), 5.94 (dd, $J_{3,5}$ = 1.4, $J_{3,4}$ = 10.1 Hz, 1H; H-4), 4.71 (br d, $J_{5,6}$ = 9.6 Hz, 1H; H-5), 3.93 (ddd, $J_{8,9a}$ = 2.4, $J_{8,9b}$ = 5.9, $J_{8,7}$ = 9.1 Hz, 1H; H-8), 3.86 (dd, $J_{9a,8}$ = 2.4, $J_{9a,9b}$ = 11.4 Hz, 1H; H-9a), 3.81 (s, 3H; $COOCH_3$), 3.65 (dd, $J_{9b,8}$ = 5.9, $J_{9b,9a}$ = 11.4 Hz, 1H; H-9b), 3.60 (dd, $J_{6,7}$ = 1.3, $J_{6,5}$ = 9.6 Hz, 1H; H-6), 3.54 (dd, $J_{7,6}$ = 1.3, $J_{7,8}$ = 9.1 Hz, 1H; H-7), 2.80-2.62 (overlapping, 2H; SCH_2CH_3), 1.97 (s, 3H; $NHCOCH_3$), 1.24 ppm (m, 3H; SCH_2CH_3); ^{13}C NMR (125 MHz, CD_3OD): δ = 174.1 ($NHCOCH_3$), 172.8 (C-1), 132.5 (C-4), 127.8 (C-3), 85.5 (C-2), 77.3 (C-6), 72.6 (C-8), 69.9 (C-7), 64.7 (C-9), 53.9 ($COOCH_3$), 44.3 (C-5), 24.2 (SCH_2CH_3), 22.6 ($NHCOCH_3$), 14.9 ppm (SCH_2CH_3). MS (ESI positive) *m/z* 350.1 $[M+H]^+$, 372.2 $[M+Na]^+$. Further elution afforded compound **33b** (115 mg, 73%) showing: $[\alpha]_D^{23}$ = -213.7 (*c*=1 in methanol); ^{1}H NMR (500 MHz, CD_3OD): δ = 6.13 (dd, $J_{4,5}$ = 2.3, $J_{4,3}$ = 10.1 Hz, 1H; H-3), 5.83 (dd, $J_{3,5}$ = 1.7, $J_{3,4}$ = 10.1 Hz, 1H; H-4), 4.79 (d, $J_{5,6}$ = 10.0 Hz, 1H; H-5), 4.36 (d, $J_{6,5}$ = 10.0 Hz, 1H; H-6), 3.86-3.75 (overlapping, 5H; H-8, H-9a and $COOCH_3$), 3.68 (dd, $J_{9b,8}$ = 5.3, $J_{9b,9a}$ = 11.3 Hz, 1H; H-9b), 3.53 (d, $J_{7,8}$ = 9.1 Hz, 1H; H-7), 2.78-2.69 (m, 1H; SCH_2CH_3), 2.64-2.54 (m, 1H; SCH_2CH_3), 1.97 (s, 3H; $NHCOCH_3$), 1.17 ppm (m, 3H; SCH_2CH_3); ^{13}C NMR (125 MHz, CD_3OD): δ = 173.6 ($NHCOCH_3$), 170.8 (C-1), 132.1 (C-3), 127.5 (C-4), 86.2 (C-2), 71.8 (C-6), 71.6 (C-8), 70.4 (C-7), 65.3 (C-9), 53.6 ($COOCH_3$), 44.5 (C-5), 25.0 (SCH_2CH_3), 22.7 ($NHCOCH_3$), 14.4 ppm (SCH_2CH_3). MS (ESI positive) *m/z* 350.1 $[M+H]^+$, 372.2 $[M+Na]^+$.

Preparation of the β-anomer of methyl (ethyl-5-acetamido-3,4,5-trideoxy-D-manno-non-3-en-2-ulopyranosid)-onates (**33c**).

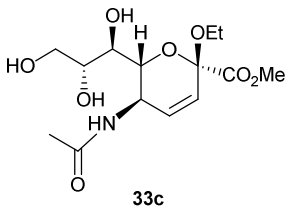

33c

Starting from mixture of **23c+24c** (207 mg, 0.45 mmol) and according to general Zemplén procedure, column chromatography (AcOEt/MeOH, 9:1 to 8:2, v/v) afforded compound **33c** (98 mg, 65%): ^{1}H NMR (500 MHz, CD_3OD): δ = 5.96 (dd, $J_{3,5}$ = 1.5, $J_{3,4}$ = 10.1 Hz, 1H; H-3), 5.93 (dd, $J_{4,5}$ = 2.1, $J_{4,3}$ = 10.1 Hz, 1H; H-4), 4.80 (br d, $J_{5,6}$ = 10.3 Hz, 1H; H-5), 4.13 (dd,

$J_{6,7}$<1.0, $J_{6,5}$ = 10.3 Hz, 1H; H-6), 3.89-3.78 (overlapping, 6H; H-8, H-9a, COOCH_3 and OCH_2CH$_3$), 3.67 (dd, $J_{9b,8}$ = 5.0, $J_{9b,9a}$ = 11.0 Hz, 1H; H-9b), 3.52 (br d, $J_{7,8}$ = 9.3 Hz, 1H; H-7), 3.31 (m, 1H; OCH_2CH$_3$), 1.99 (s, 3H; NHCOCH_3), 1.19 ppm (t, $J_{CH2,CH3}$ = 7.0 Hz, 3H; OCH$_2$CH_3); ^{13}C NMR (125 MHz, CD$_3$OD): δ = 173.7 (NH*C*OCH$_3$), 171.4 (C-1), 134.8 (C-3), 127.4 (C-4), 97.4 (C-2), 71.6 (C-6), 71.5 (C-8), 70.1 (C-7), 65.3 (C-9), 61.1 (O*C*H$_2$CH$_3$), 53.5 (COO*C*H$_3$), 44.5 (C-5), 22.7 (NH*C*OCH$_3$), 15.5 (OCH$_2$*C*H$_3$). MS (ESI positive): *m/z* 334.1 [M+H]$^+$, 356.2 [M+Na]$^+$.

*Preparation of the β-anomer of methyl (isopropyl-5-acetamido-3,4,5-trideoxy-D-manno-non-3-en-2-ulopyranosid)-onates (***33d***).*

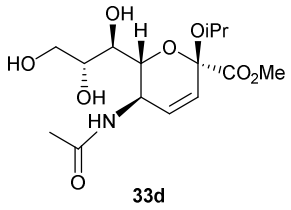

33d

Starting from mixture of **23d+24d** (213 mg, 0.45 mmol) and according to general procedure, column chromatography (AcOEt/MeOH, 9:1 to 8:2, v/v) afforded compound **33c** (102 mg, 65%): $[\alpha]_D^{23}$= -139.4 (*c*=1 in methanol); ^{1}H NMR (500 MHz, CD$_3$OD): δ = 5.97 (dd, $J_{4,5}$ = 2.4, $J_{4,3}$ = 10.2 Hz, 1H; H-3), 5.91 (dd, $J_{3,5}$ = 1.7, $J_{3,4}$ = 10.2 Hz, 1H; H-4), 4.75 (dd, $J_{5,6}$ = 10.2 Hz, 1H; H-5), 4.16 (m, 1H; OC*H*(CH$_3$)$_2$), 4.09 (d, $J_{6,5}$ = 10.2 Hz, 1H; H-6), 3.86-3.75 (overlapping, 5H; H-8, H-9a and COOCH$_3$), 3.68 (dd, $J_{9b,8}$ = 5.2, $J_{9b,9a}$ = 11.2 Hz, 1H; H-9b), 3.48 (d, $J_{7,8}$ = 9.5 Hz, 1H; H-7), 1.97 (s, 3H; NHCOCH_3), 1.22 (d, $J_{H,H}$ = 6.2 Hz, 3H; OCH(CH_3)$_2$), 1.05 ppm (d, $J_{H,H}$ = 6.2 Hz, 3H; OCH(CH_3)$_2$); ^{13}C NMR (125 MHz, CD$_3$OD): δ = 173.6 (NH*C*OCH$_3$), 171.8 (C-1), 134.1 (C-3 or C-4), 127.8 (C-3 or C-4), 96.2 (C-2), 71.8 (C-6), 71.4 (C-8), 70.6 (C-7), 68.9 (O*C*H(CH$_3$)$_2$), 65.3 (C-9), 53.4 (COO*C*H$_3$), 44.4 (C-5), 24.8 (OCH(*C*H$_3$)$_2$), 22.9 (OCH(*C*H$_3$)$_2$), 22.7 ppm (NHCO*C*H$_3$); MS (ESI positive): *m/z* 348.4 [M+H]$^+$, 370.3 [M+Na]$^+$.

Preparation of the β-anomer of methyl (buthyl-5-acetamido-3,4,5-trideoxy-D-manno-non-3-en-2-ulopyranosid)-onates (**33e**).

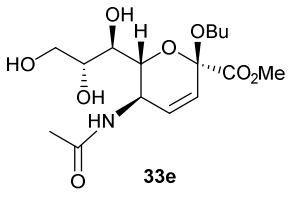

33e

Starting from mixture of **23e+24e** (219 mg, 0.45 mmol) and according to general Zemplén procedure, column chromatography (AcOEt/MeOH, 9:1 to 8:2, v/v) afforded compound **33e** as a white solid (120 mg, 74%): $[\alpha]_D^{23}$ = -145.3 (c=1 in MeOH); ^{1}H NMR (500 MHz, CD_3OD): δ = 5.94 (d, $J_{3,4}$ = 10.1 Hz, 1H; H-3 or H-4), 5.93 (dd, $J_{4,5}$ = 1.9, $J_{4,3}$ = 10.1 Hz, 1H; H-4 or H-3), 4.78 (d, $J_{5,6}$ = 10.3 Hz, 1H; H-5), 4.09 (d, $J_{6,5}$ = 10.3 Hz, 1H; H-6), 3.85-3.77 (overlapping, 6H; H-8, H-9a, $COOCH_3$ and $OCH_2(CH_2)_2CH_3$), 3.69 (dd, $J_{9b,8}$ = 5.0, $J_{9b,9a}$ = 11.1 Hz, 1H; H-9b), 3.52 (d, $J_{7,8}$ = 9.1 Hz, 1H; H-7), 3.23 (m, 1H; $OCH_2(CH_2)_2CH_3$), 1.97 (s, 3H; $NHCOCH_3$), 1.54 (m, 2H; $OCH_2CH_2CH_2CH_3$), 1.39 (m, 2H; $OCH_2CH_2CH_2CH_3$), 0.91 ppm (m, 3H; $OCH_2CH_2CH_2CH_3$); ^{13}C NMR (125 MHz, CD_3OD): δ = 173.6 ($NHCOCH_3$), 171.4 (C-1), 134.7 (C-3 or C-4), 127.4 (C-4 or C-3), 97.4 (C-2), 71.7 (C-6), 71.5 (C-8), 70.2 (C-7), 65.3 (2C; overlapping C-9 and $OCH_2(CH_2)_2CH_3$), 53.5 ($COOCH_3$), 44.4 (C-5), 32.9 ($OCH_2CH_2CH_2CH_3$), 22.7 ($NHCOCH_3$), 20.2 ($OCH_2CH_2CH_2CH_3$), 14.3 ppm ($OCH_2(CH_2)_2CH_3$). MS (ESI positive): *m/z* 362.2 $[M+H]^+$, 384.1 $[M+Na]^+$.

Preparation of the β-anomer of methyl (S-octhyl-5-acetamido-2,3,4,5-tetradeoxy-D-manno-non-3-en-2-ulopyranosid)-onates (**33f**).

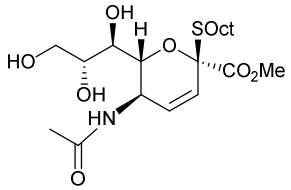

Starting from mixture of **23f+24f** (252 mg, 0.45 mmol) and according to general procedure, column chromatography (AcOEt/MeOH, 9:1 to 8:2, v/v) first afforded compound **33f** a as a white solid (128 mg, 66 %), showing: $[\alpha]_D^{23}$ = -178.2 (c=1 in methanol); ^{1}H NMR (500 MHz, CD_3OD): δ = 6.12 (d, $J_{4,3}$ = 10.1 Hz, 1H; H-4 or H-3), 5.82 (d, $J_{3,4}$ = 10.1 Hz, 1H; H-3 or H-4), 4.80 (d, $J_{5,6}$ = 10.0 Hz, 1H; H-5), 4.35 (d, $J_{6,5}$ = 10.0 Hz, 1H; H-6), 3.85-3.75 (overlapping, 5H; H-8, H-9a and $COOCH_3$), 3.68 (dd, $J_{9b,8}$ = 5.2, $J_{9b,9a}$ = 11.1 Hz, 1H; H-9b), 3.51 (d, $J_{7,8}$ = 9.1 Hz, 1H; H-7), 2.73 (m, 1H; $SCH_2CH_2(CH_2)_5CH_3$), 2.59 (m, 1H; $SCH_2CH_2(CH_2)_5CH_3$), 1.97 (s, 3H; $NHCOCH_3$), 1.60-1.42 (overlapping, 2H; $SCH_2CH_2(CH_2)_5CH_3$), 1.42-1.20 (overlapping, 10H; $SCH_2CH_2(CH_2)_5CH_3$), 0.90 ppm (m, 3H; $SCH_2CH_2(CH_2)_5CH_3$); ^{13}C NMR (125 MHz, D_2O): δ = 173.6 ($NHCOCH_3$), 170.9 (C-1), 132.1 (C-4 or C-3), 127.5 (C-3 or C-4), 86.1 (C-2), 71.8 (C-6), 71.7 (C-8), 70.5 (C-7), 66.2 (C-9), 53.6 ($COOCH_3$), 44.5 (C-5), 33.0, 30.8, 30.3, 30.1, 23.7 (7C, $SCH_2CH_2(CH_2)_5CH_3$), 22.7 ($NHCOCH_3$), 14.4 ($SCH_2CH_2(CH_2)_5CH_3$). (ESI positive): *m/z* 434.4 $[M+H]^+$, 456.4 $[M+Na]^+$.

5.1.3.5 Removal of esteric function to obtain the final compounds 21a,b and 22a-f

General procedure. The final 3,4-unsaturated compounds **21a,b and 22a-f** were prepared by hydrolysis of appropriate methyl ester derivatives **32a,b** and **33a-f** (0.10 mmol) performed in aqueous solution of KOH 0.5 M (0.8 mL) kept at 23°C for 1 h. Then, the reaction mixture was treated using *Method A or B*:

Method A: Weak acidic resin (Amberlite CG50, H^+) until neutral pH, and then, the resin was filtered and washed with H_2O (2 mL X 3).

Method B: Strong acidic resin (Dowex 50WX8, H^+) treatment until acidic pH, and then, the resin was filtered and washed with MeOH-H_2O (1:1, v/v; 2 mL X 3);

Finally, the solvent was removed under reduced pressure to give the desired deprotected 3,4-unsaturated compounds.

Preparation of the potassium salt of 2αO-methyl (5-acetamido-3,4,5-trideoxy-D-manno-non-3-en-2-ulopyranosid) acid (**21a**)

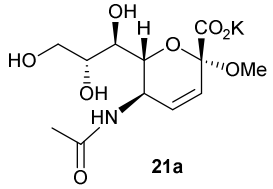

21a

Starting from compound **32a** (32 mg, 0.10 mmol), according to general procedure using *Method A*, the desired compound **21a** was obtained as white solid potassium salt (30 mg, 87%), showing: $[\alpha]_D^{23}$ = - 22.1 (*c*=1.0 in water); ^{1}H NMR (500 MHz, D_2O): δ = 6.03 (br d, $J_{4,3}$ = 10.1 Hz, 1H; H-3), 5.98 (br d, $J_{3,4}$ = 10.1 Hz, 1H; H-4), 4.69 (br d, $J_{5,6}$ = 10.3 Hz, 1H; H-5), 3.98-3.85 (overlapping, 3H; H-6, H-8 and H-9a), 3.65 (dd, $J_{9b,8}$ = 6.4, $J_{9b,9a}$ = 11.9 Hz, 1H; H-9b), 3.60 (dd, $J_{7,6}$ < 1.0, $J_{7,8}$ = 9.5 Hz, 1H; H-7), 3.32 (s, 3H; OCH_3), 2.06 (s, 3H; $NHCOCH_3$); ^{13}C NMR (125 MHz, D_2O): δ = 175.1 (C-1), 175.0 ($NHCOCH_3$), 133.7 (C-3), 128.7 (C-4), 100.2 (C-2), 75.8 (C-6), 71.8 (C-8), 68.7 (C-7), 63.4 (C-9), 51.5 (OCH_3), 43.7 (C-5), 22.5 ppm ($NHCOCH_3$) ppm; MS (ESI negative): *m/z* 304.1 $[M-H]^-$; elemental analysis calcd (%) for $C_{12}H_{18}KNO_8$: C 41.98, H 5.28, N 4.08; found: C 42.09, H 5.34, N 4.15.

Preparation of the potassium salt of 2βO-methyl (5-acetamido-3,4,5-trideoxy-D-manno-non-3-en-2-ulopyranosid) acid (**22a**).

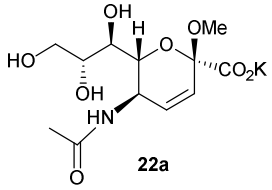

22a

Starting from compound **33a** (32 mg, 0.10 mmol), according to general procedure using <u>*method A*</u>, the desired compound **22a** was obtained as white solid potassium salt (29 mg, 85%), showing: $[\alpha]_D^{24}$ = -184.7 (*c*=1.0 in water); ^{1}H NMR (500 MHz, D_2O): δ = 5.96-5.91 (overlapping, 2H; H-3 and H-4), 4.72 (d app, $J_{5,6}$ = 10.3 Hz, 1H; H-5), 3.95 (dd, $J_{6,7}$ < 1.0, $J_{6,5}$ = 10.3 Hz, 1H; H-6), 3.91 (ddd, $J_{8,9a}$ = 2.5, $J_{8,9b}$ = 5.6, $J_{8,7}$=9.5 Hz, 1H; H-8), 3.87 (dd, $J_{9a,8}$ = 2.5, $J_{9a,9b}$ = 12.0 Hz, 1H; H-9a), 3.69 (dd, $J_{9b,8}$ = 5.6, $J_{9b,9a}$=12.0 Hz, 1H; H-9b), 3.57 (dd, $J_{7,6}$ < 1.0, $J_{7,8}$ = 9.5 Hz, 1H; H-7), 3.27 (s, 3H; OCH_3), 2.01 ppm (s, 3H; NH*C*OCH_3); ^{13}C NMR (125 MHz, D_2O): δ = 175.0 (C-1), 174.9 (NH*C*OCH_3), 133.2 (C-3), 128.2 (C-4), 98.4 (C-2), 70.5 (C-8), 70.3 (C-6), 69.0 (C-7), 64.1 (C-9), 51.7 (OCH_3), 43.9 (C-5), 22.7 ppm (NHCO*C*H_3); MS (ESI negative): *m/z* 304.1 $[M-H]^-$; elemental analysis calcd (%) for $C_{12}H_{18}KNO_8$: C 41.98, H 5.28, N 4.08; found: C 42.00, H 5.26, N 4.01.

Preparation of the 2αS-ethyl (5-acetamido-2,3,4,5-tetradeoxy-D-manno-non-3-en-2-ulopyranosid) acid (**21b**)

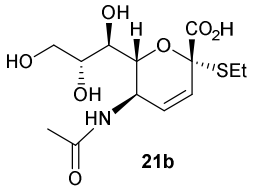

21b

Starting from compound **32b** (35 mg, 0.10 mmol), according to general procedure using <u>*method B*</u>, the desired compound **21b** was obtained as white solid in acidic form (29 mg, 87%), showing: $[\alpha]_D^{24}$ = -69.4 (*c*=1.0 in methanol); ^{1}H NMR (500 MHz, CD_3OD): δ = 6.06 (dd, $J_{4,5}$ = 2.5, $J_{4,3}$ = 10.1 Hz, 1H; H-3), 5.92 (dd, $J_{3,5}$ = 1.7, $J_{3,4}$ = 10.1 Hz, 1H; H-4), 4.69 (ddd, $J_{5,3}$ = 1.7, $J_{5,4}$ = 2.5, $J_{5,6}$ = 9.5 Hz, 1H; H-5), 3.92 (ddd, $J_{8,9a}$ = 2.6, $J_{8,9b}$ = 5.8, $J_{8,7}$ = 9.2 Hz, 1H; H-8), 3.85 (dd, $J_{9a,8}$ = 2.6, $J_{9a,9b}$ = 11.4 Hz, 1H; H-9a), 3.65 (dd, $J_{9b,8}$ = 5.8, $J_{9b,9a}$ = 11.4 Hz, 1H; H-9b), 3.61 (dd, $J_{6,7}$ = 2.0, $J_{6,5}$ = 9.5 Hz, 1H; H-6), 3.56 (dd, $J_{7,6}$ = 2.0, $J_{7,8}$ = 9.2 Hz, 1H; H-7), 2.80-2.65 (overlapping, 2H; SC$H_2$$CH_3$), 1.97 (s, 3H; NHCO$CH_3$), 1.25 ppm (t, $J_{CH2,CH3}$ = 7.5

Hz, 3H; SCH_2CH_3); ^{13}C NMR (125 MHz, CD_3OD): δ = 174.2 (C-1), 173.5 ($NHCOCH_3$), 132.0 (C-4), 128.5 (C-3), 85.6 (C-2), 77.4 (C-6), 72.7 (C-8), 69.8 (C-7), 64.7 (C-9), 44.4 (C-5), 24.3 (SCH_2CH_3), 22.6 ($NHCOCH_3$), 14.9 ppm (SCH_2CH_3); MS (ESI negative): *m/z* 334.1 $[M-H]^-$; elemental analysis calcd (%) for $C_{13}H_{21}NO_7S$: C 46.56, H 6.31, N 4.18; found: C 46.40, H 6.42, N 4.12.

Preparation of the 2βS-ethyl (5-acetamido-2,3,4,5-tetradeoxy-D-manno-non-3-en-2-ulopyranosid) acid (**22b**)

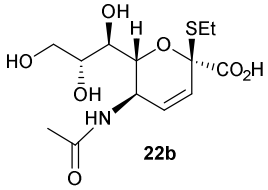

22b

Starting from compound **33b** (35 mg, 0.10 mmol), according to general procedure using <u>*method B*</u>, the desired compound **22b** was obtained as white solid in acidic form (30 mg, 89%), showing $[\alpha]_D^{23}$ = -217.2 (*c*=1 in methanol); ^1H NMR (500 MHz, CD_3OD): δ = 6.12 (dd, $J_{4,5}$ = 2.4, $J_{4,3}$ = 10.1 Hz, 1H; H-3), 5.81 (dd, $J_{3,5}$ = 1.9, $J_{3,4}$ = 10.1 Hz, 1H; H-4), 4.80 (ddd, $J_{5,3}$ = 1.9, $J_{5,4}$ = 2.4, $J_{5,6}$ = 10.1 Hz, 1H; H-5), 4.38 (dd, $J_{6,7}$ < 1.0, $J_{6,5}$=10.1 Hz, 1H; H-6), 3.83 (dd, $J_{9a,8}$ = 2.9, $J_{9a,9b}$ = 11.3 Hz, 1H; H-9a), 3.77 (ddd, $J_{8,9a}$ = 2.9, $J_{8,9b}$ = 5.4, $J_{8,7}$ = 9.2 Hz, 1H; H-8), 3.68 (dd, $J_{9b,8}$ = 5.4, $J_{9b,9a}$ = 11.3 Hz, 1H; H-9b), 3.52 (dd, $J_{7,6}$ < 1.0, $J_{7,8}$ = 9.2 Hz, 1H; H-7), 2.79-2.67 (m, 1H; CH_2CH_3), 2.66-2.55 (m, 1H; SCH_2CH_3), 1.97 (s, 3H; $NHCOCH_3$), 1.21 ppm (t, $J_{CH2,CH3}$ = 7.5 Hz, 3H; SCH_2CH_3); ^{13}C NMR (125 MHz, CD_3OD, 23 °C): δ = 173.6 (C-1), 172.2 ($NHCOCH_3$), 131.9 (C-4), 128.0 (C-3), 86.5 (C-2), 71.8 (C-6), 71.6 (C-8), 70.4 (C-7), 65.2 (C-9), 44.5 (C-5), 25.1 (SCH_2CH_3), 22.7 ($NHCOCH_3$), 14.3 ppm (SCH_2CH_3); MS (ESI negative): *m/z* 334.2 $[M-H]^-$; elemental analysis calcd (%) for $C_{13}H_{21}NO_7S$: C 46.56, H 6.31, N 4.18; found: C 46.64, H 6.41, N 4.23.

Preparation of the potassium salt of 2βO-ethyl (5-acetamido-3,4,5-trideoxy-D-manno-non-3-en-2-ulopyranosid) acid (**22c**).

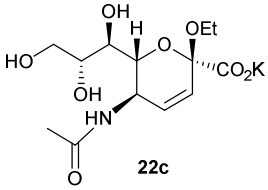

22c

Starting from compound **33c** (33 mg, 0.10 mmol), according to general procedure using <u>*method A*</u>, the desired compound **22c** was obtained as white solid potassium salt (29 mg, 80%),

showing: $[\alpha]_D^{23}$= -142.5 (*c*=1.0 in water); ^{1}H NMR (500 MHz, D_2O): δ = 5.97-5.91 (overlapping, 2H; H-3 and H-4), 4.73 (d app, $J_{5,6}$ = 10.3 Hz, 1H; H-5), 3.99 (d, $J_{6,5}$ = 10.3 Hz, 1H; H-6), 3.88 (ddd, $J_{8,9a}$ = 2.6, $J_{8,9b}$ = 5.4, $J_{8,7}$ = 9.4 Hz, 1H; H-8), 3.84 (dd, $J_{9a,8}$ = 2.6, $J_{9a,9b}$ = 12.0 Hz, 1H; H-9a), 3.74-3.68 (overlapping, 2H; H-9b and OC*H*$_2$CH$_3$), 3.56 (d app, $J_{7,8}$ = 9.4 Hz, 1H; 7-H), 3.41 (1H; m, OC*H*$_2$CH$_3$), 2.03 (s, 3H; NHCOCH$_3$), 1.18 ppm (t, $J_{CH2,CH3}$ = 7.0 Hz, 3H; OCH$_2$C*H*$_3$); ^{13}C NMR (125 MHz, D_2O): δ = 175.2 (NH*C*OCH$_3$ or C-1), 175.0 (NH*C*OCH$_3$ or C-1), 133.0 (C-3), 128.5 (C-4), 98.1 (C-2), 70.6 (C-8), 70.3 (C-6), 69.0 (C-7), 64.1 (C-9), 60.7 (O*C*H$_2$*C*H$_3$), 44.0 (C-5), 22.7 (NHCO*C*H$_3$), 15.1 ppm (OCH$_2$*C*H$_3$). MS (ESI negative): *m/z* 318.1 [M-H]$^-$; elemental analysis calcd (%) for $C_{13}H_{20}KNO_8$: C 43.69, H 5.64, N 3.92; found: C 43.78, H 5.60, N 3.82.

Preparation of the potassium salt of 2βO-isopropyl (5-acetamido-3,4,5-trideoxy-D-manno-non-3-en-2-ulopyranosid) acid (**22d**).

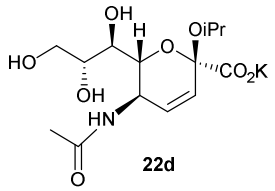

22d

Starting from compound **33d** (35 mg, 0.10 mmol), according to general procedure using <u>*method A*</u>, the desired compound **22d** was obtained as white solid potassium salt (30 mg, 81%), showing: $[\alpha]_D^{23}$= -117.2 (*c*=1 in water); ^{1}H NMR (500 MHz, D_2O) : δ = 6.03 (dd, $J_{4,5}$ = 2.4, $J_{4,3}$ = 10.1 Hz, 1H; H-3 or H-4), 5.88 (dd, $J_{3,5}$ = 1.8, $J_{3,4}$ = 10.1 Hz, 1H; H-3 or H-4), 4.70 (ddd, $J_{3,5}$ = 1.8, $J_{4,5}$ = 2.4, $J_{5,6}$ = 10.2 Hz, 1H; H-5), 4.15-4.05 (m, 1H; OC*H*(CH$_3$)$_2$), 3.98-3.89 (overlapping, 2H; H-6 and H-8), 3.85 (dd, $J_{9a,8}$ = 2.7, $J_{9a,9b}$ = 12.1 Hz, 1H; H-9a), 3.72 ($J_{9b,8}$ = 5.4, $J_{9a,9b}$ = 12.1 Hz, 1H; H-9b), 3.53 (d app, $J_{7,8}$ = 9.5 Hz, 1H; H-7), 2.02 (s, 3H; NHCO*C*H$_3$), 1.21 (m, 3H; OCH(C*H*$_3$)$_2$), 1.14 ppm (m, 3H; OCH(C*H*$_3$)$_2$); ^{13}C NMR (125 MHz, D_2O): δ = 175.5 (C-1), 174.9 (NH*C*OCH$_3$), 131.8 (C-3 or C-4), 129.3 (C-3 or C-4), 97.1 (C-2), 70.4, 70.3 (C-6 and C-8), 69.5 (C-7), 69.2 (O*C*H(CH$_3$)$_2$), 64.1 (C-9), 43.9 (C-5), 24.4 (OCH(*C*H$_3$)$_2$), 22.7, 22.6 and (*C*H$_3$CONH and OCH(*C*H$_3$)$_2$); MS (ESI negative): *m/z* 332.1 [M-H]$^-$; elemental analysis calcd (%) for $C_{14}H_{22}KNO_8$: C 45.27, H 5.97, N 3.77; found: C 45.31, H 5.90, N 3.81.

*Preparation of the potassium salt of 2βO-buthyl (5-acetamido-3,4,5-trideoxy-D-manno-non-3-en-2-ulopyranosid) acid (***22e***).*

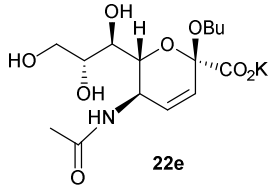

22e

Starting from protected compound **33e** (36 mg, 0.10 mmol), according to general procedure using <u>*method A*</u> the desired compound **22e** was obtained as white solid potassium salt (31 mg, 80%), showing: $[\alpha]_D^{23}$ = -122.2 (*c*=1 in water); ^{1}H NMR (500 MHz, D_2O): δ = 5.99-5.90 (overlapping, 2H; H-3 and H-4), 4.71 (d app, $J_{5,6}$ = 10.2 Hz, 1H; H-5), 3.98 (d app, $J_{6,5}$ = 10.2 Hz, 1H; H-6), 3.93-3.84 (m, $J_{9a,9b}$ = 12.1 Hz, 2H; H-8 and H-9a), 3.76-3.73 (overlapping, 2H; H-9b and $OCH_2CH_2CH_2CH_3$), 3.56 (d app, 1H; $J_{7,8}$ = 9.3 Hz H-7), 3.35 (1H; m, $OCH_2CH_2CH_2CH_3$), 2.03 (s, 3H; $NHCOCH_3$), 1.55 (m, 2H; $OCH_2CH_2CH_2CH_3$), 1.34 (m, 2H; $OCH_2CH_2CH_2CH_3$), 0.89 (m, 3H; $OCH_2CH_2CH_2CH_3$); ^{13}C NMR (125 MHz, D_2O): δ = 175.2 ($NHCOCH_3$ or C-1), 174.9 ($NHCOCH_3$ or C-1), 132.8 (C-3 or C-4), 128.5 (C-4 or C-3), 98.0 (C-2), 70.6 (C-8), 70.3 (C-6), 69.1 (C-7), 65.0 ($OCH_2CH_2CH_2CH_3$), 64.1 (C-9), 43.9 (C-5), 31.7 ($OCH_2CH_2CH_2CH_3$), 22.7 ($NHCOCH_3$), 19.4 ($OCH_2CH_2CH_2CH_3$), 13.9 ($OCH_2CH_2CH_2CH_3$). MS (ESI negative): *m/z* 346.2 $[M-H]^-$; elemental analysis calcd (%) for $C_{15}H_{24}KNO_8$: C 46.74, H 6.28, N 3.63; found: C 46.81, H 6.32, N 3.65.

*Preparation of the of 2βS-octyl (5-acetamido-2,3,4,5-tetradeoxy-D-manno-non-3-en-2-ulopyranosid) acid (***22f***).*

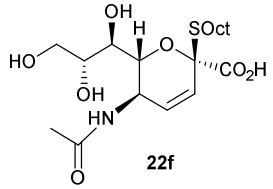

22f

Starting from protected compound **33f** (43 mg, 0.10 mmol), according to general procedure using <u>*method B*</u>, the desired compound **22f** was obtained as white solid potassium salt (34 mg, 80%), showing: $[\alpha]_D^{23}$ = -182.6 (*c*=1 in methanol); ^{1}H NMR (500 MHz, CD_3OD): δ = 6.13 (dd, $J_{4,5}$ = 2.4, $J_{4,3}$ = 10.1 Hz, 1H; H-4), 5.81 (dd, $J_{3,5}$ = 1.9, $J_{3,4}$ = 10.1 Hz, 1H; H-3), 4.81 (dd, $J_{5,3}$ = 1.9, $J_{5,4}$ = 2.4, $J_{5,6}$ = 10.1 Hz, 1H; H-5), 4.37 (dd, $J_{6,7}$ = 0.9, $J_{6,5}$ = 10.1 Hz, 1H; H-6), 3.84 (dd, $J_{9a,8}$ = 2.9, $J_{9a,9b}$ = 11.2 Hz, 1H; H-9a), 3.76 ($J_{8,9a}$ = 2.9, $J_{8,9b}$ = 5.4, $J_{8,7}$ = 9.2 Hz, 1H; H-8), 3.68 (dd, $J_{9b,8}$ = 5.4, $J_{9b,9a}$ = 11.2, 1H; H-9b), 3.53 (dd, $J_{7,6}$ = 0.9, $J_{7,8}$ = 9.2 Hz, 1H; H-7), 2.77-2.51 (m, 2H; $SCH_2(CH_2)_6CH_3$), 1.97 (s, 3H; $NHCOCH_3$), 1.66-1.45 (m, 2H; $SCH_2CH_2(CH_2)_5CH_3$), 1.44-1.17 (m, 10H; $SCH_2CH_2(CH_2)_5CH_3$), 0.9 ppm (m, 3H;

$SCH_2(CH_2)_6CH_3$); ^{13}C NMR (125 MHz, CD_3OD): δ = ^{13}C NMR (125 MHz, CD_3OD): δ = 173.6 (C-1), 172.3 ($NHCOCH_3$), 131.9 (C-3), 128.0 (C-4), 86.4 (C-2), 71.8 (C-8), 71.7 (C-6), 70.5 (C-7), 65.1 (C-9), 44.5 (C-5), 33.0, 31.0, 30.4 , 30.3, 30.3, 30.2 23.7 (7C, $SCH_2(CH_2)_6CH_3$), 22.7 ($NHCOCH_3$), 14.5 ppm ($SCH_2(CH_2)_6CH_3$); MS (ESI negative): *m/z* 418.2 $[M-H]^-$; elemental analysis calcd (%) for $C_{19}H_{33}NO_7S$: C 54.40, H 7.93, N 3.34; found: C 54.51, H 7.90, N 3.39.

5.1.3.6 Synthesis of unsaturated 1,7-lactones 34 and 35 and saturated lactone 36.

General procedure. The appropriate starting material **21a** and **22a**, or **21b** and **22b** (0.10 mmol), dissolved in DMF (1.0 mL) under stirring, was cooled to 0 °C and diluted with THF (1.5 mL). Then CbzCl (0.03 mL; 0.25 mmol, 2.5 equiv) in THF (0.4 mL) was added in a single portion, followed by Et_3N (0.04 mL; 0.3 mmol) in a single addition. The mixture was then stirred for 15-60 min at 23 °C. At this time, water (0.3 mL) was added and the stirring was continued for 15 min. Evaporation of the solvent under reduced pressure afforded a crude residue. The ^1H-NMR were performed on crude products.

- Compounds **21a** and **21b** did not give any 1,7-lactones and the only molecules present in the crude were the starting materials (Data not shown).
- Compounds **22a** and **22b** give, after purification by flash chromatography, the appropriate pure lactones **34** or **35**.

Preparation of the 2O-methyl (5-acetamido-3,4,5-trideoxy-D-manno-non-3-en-2-ulopyranosid) acid 1,7-lactone (**34**)

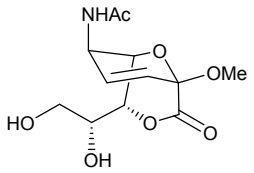

34

Starting from compound **22a** (34 mg, 0.10 mmol), according to general procedure, compound **34** was obtained (11 mg, 36%), after purification by flash chromatography (eluting with CH_3CN/MeOH, 10:0 to 9:1, v/v) as a white solid, showing: ^1H NMR (500 MHz, D_2O) : δ = 6.43 (ddd, $J_{4,6}$ = 1.0, $J_{4,5}$ = 5.0, $J_{4,3}$ = 10.0 Hz, 1H; H-4), 6.13 (dd, $J_{3,5}$ = 1.1, $J_{3,4}$ = 10.0 Hz, 1H; H-3), 4.67 (dd, $J_{6,4}$ = 1.0, $J_{6,7}$ = 2.9 Hz, 1H; H-6), 4.56 (dd, $J_{7,6}$ = 2.9, $J_{7,8}$=5.3 Hz, 1H; H-7), 4.27 (d, $J_{5,4}$ = 5.0 Hz, 1H; H-5), 4.05 (m, 1H; H-8), 3.79 (dd, $J_{9a,8}$ = 4.4, $J_{9a,9b}$ = 12.0 Hz, 1 H; H-9a), 3.75 (dd, $J_{9b,8}$ = 6.1, $J_{9b,9a}$ = 12.0 Hz, 1H; H-9b), 3.50 (s, 3H; OCH_3), 2.06 ppm (3H; s,

NHCOC*H*$_3$); ^{13}C NMR (125 MHz, CD_3OD): δ = 172.6 (NH*C*OCH$_3$), 166.9 (C-1), 130.4 (C-4), 126.7 (C-3), 92.2 (C-2), 78.4 (C-7), 71.0 (C-6), 70.5 (C-8), 59.9 (C-9), 50.7 (OCH_3), 44.8 (C-5), 20.5 ppm (NHCO*C*H$_3$).

Preparation of the 2S-ethyl (5-acetamido-2,3,4,5-tetradeoxy-D-manno-non-3-en-2-ulopyranosid) acid 1,7-lactone (**35**)

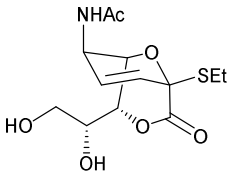

35

Starting from compound **22b** (34 mg, 0.10 mmol), according to general procedure, compound **35** was obtained (13 mg, 40%), after purification by flash chromatography (eluting with acetonitrile/methanol, 10:0 to 9:1, v/v) as a white solid, showing: ^{1}H NMR (500 MHz, D_2O): δ = 6.29 (ddd, $J_{4,6}$ = 1.0, $J_{4,5}$ = 5.4, $J_{4,3}$ = 9.9 Hz, 1H; H-4), 6.12 (dd, $J_{3,5}$ = 1.1, $J_{3,4}$ = 9.9 Hz, 1H; H-3), 4.53 (br d, $J_{6,7}$ = 3.6 Hz, 1H; H-6), 4.45 (dd, $J_{7,6}$ = 3.6, $J_{7,8}$ = 4.8 Hz, 1H; H-7), 4.11 (d, $J_{5,4}$ = 5.4 Hz, 1H; H-5), 4.01 (m, 1H; H-8), 3.74 (dd, $J_{9a,8}$ = 4.6, $J_{9a,9b}$ = 12.0 Hz, 1H; H-9a), 3.68 (dd, $J_{9b,8}$ = 6.3, $J_{9b,9a}$ = 12.0 Hz, 1H; H-9b), 2.80-2.63 (overlapping, 2H; SC*H*$_2$CH$_3$), 2.00 (3H; s, NHCOC*H*$_3$), 1.22 ppm (m, 3H; SCH$_2$C*H*$_3$); ^{13}C NMR (125 MHz, CD_3OD): δ = 174.5 (NH*C*OCH$_3$), 169.2 (C-1), 129.2 and 129.1 (C-3 and C-4), 83.5 (C-2), 80.2 (C-7), 72.4 (C-8), 72.0 (C-6), 61.6 (C-9), 46.3 (C-5), 23.5 (S*C*H$_2$CH$_3$), 22.4 (NHCO*C*H$_3$), 14.4 ppm (SCH$_2$*C*H$_3$).

Preparation of 5-acetamido-2,6-anhydro-2-methyl-3,4,5-trideoxy-D-glycero-D-galacto-non-3-enoic acid 1,7-lactone (**36**)

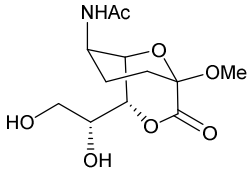

37

The saturated lactone **36** was obtained following two different synthetic pathways:

<u>*Path 1*</u>: the unsaturated 1,7-lactone **34** (10 mg, 0.035 mmol) was diluted with AcOEt (4 mL), the catalyst Pd/C (10% w/w) was added and, then, the mixture was stirred at 23°C for 2.5 h under H_2 atmosphere. The catalyst was filtered off and washed with AcOEt-THF (10 mL) and the combined filtrates were evaporated under vacuum, giving the compound **36** (5mg, 50%) after purification by flash chromatography (eluting with ethyl acetate/methanol, 95:5 to,

85:15, v/v) as a white solid, showing: ^{1}H NMR (500 MHz, CD_3OD): 4.59 (s, 1 H; H-6), 4.36 (d, $J_{7,8}$ = 8.1 Hz, 1 H; H-7), 3.99 (br s, 1H; H-5), 3.81-3.74 (overlapping, 2H; H-8 and H-9a), 3.70 (dd, $J_{9b,8}$ = 5.8, $J_{9b,9a}$ = 12.4 Hz, 1 H; H-9b), 3.37 (s, 3H; OCH_3), 2.09-1.72 ppm (overlapping, 7H; NHCOC*H*$_3$, H-3a, H-3b¸ H-4a, H-4b); ^{13}C NMR (125 MHz, CD_3OD): δ = 173.0 (C-1), 168.8 (NH*C*OCH_3), 99.0 (C-2), 80.9 (C-7), 73.3 (C-8), 72.9 (C-6), 63.5 (C-9), 52.4 (C-5), 47.7 (OCH_3), 30.0, 24.4 (C-3 and C-4), 22.5 ppm (NHCO*C*H_3). MS (ESI negative): *m/z* 300.1 $[M-H]^-$; elemental analysis calcd (%) for $C_{13}H_{19}NO_7$: C 51.82, H 6.36, N 4.65; found: C 51.67, H 6.42, N 4.61.

Path 2: compound **37** (30 mg, 0.10 mmol), dissolved in DMF (1.0 mL) under stirring, was cooled to 0 °C and diluted with THF (1.5 mL). Then CbzCl (0.03 mL; 0.25 mmol, 2.5 equiv) in THF (0.4 mL) was added in a single portion, followed by Et_3N (0.04 mL; 0.3 mmol) in a single addition. The mixture was then stirred for 30 min at 23 °C. At this time, methanol (0.3 mL) was added and the stirring was continued for 15 min. Evaporation of the solvent under reduced pressure afforded a crude residue. Compound **36** was obtained (22 mg, 75%), after purification by flash chromatography (eluting with ethyl acetate/methanol, 95:5 to, 85:15, v/v) as a white solid, showing the same chemical-physical characteristic above reported[130].

5.2 Biological materials and methods

The above listed *biological materials and methods* were used for all the classes of compounds present in this thesis and described in *Chapters 3.1*, *3.2* and *3.3*.

5.2.1 Viruses and cell lines

- NDV "Clone 30" (LaSota), used in neuraminidase inhibition assays (NI) and hemagglutinin inhibition assay (HI), was grown and purified as described previously in the literature[75]. Stock viruses were harvested, titrated, and stored at −80 °C until use.
- COS7 cells were obtained from the American Type Culture Collection and maintained at 37 °C (in an atmosphere of 5% CO_2) in Dulbecco's Modified Eagle's Medium (DMEM) supplemented with L-glutamine (4 mM), penicillin–streptomycin (100 $U*ml^{-1}$ –100 $\mu g*ml^{-1}$), and heat inactivated fetal bovine serum (FBS) at 10% v/v (all reagents were from Sigma).
- Stable NEU3 overexpressing Hek293a cells were obtained as previously described[132] and maintained at 37°C in 5% CO_2 and 95% air-humidified atmosphere in Dulbecco's modified Eagle's medium (DMEM) with high glucose, 4.5 g/L (Sigma-Aldrich) with 10% (v/v) fetal bovine serum (FBS, Sigma-Aldrich), 2 mM glutamine (Sigma-Aldrich), penicillin/streptomycin 1X (Euroclone).
- cRBC used in HI assay were provided from "Istituto Zooprofilattico Sperimentale delle Venezie". The freshly cRBC were washed 3 times in PBS and the obtained solution (0.5 or 1% of cRBC) was conserved for one week at 4°C.

5.2.2 Neuraminidase inhibition assay (NI) on NDV-HN

Neuraminidase activity inhibition assay was performed, according to Venerando *et al.*[112], using 4-MU-Neu5Ac as the artificial substrate. Briefly, the incubation mixture (final volume of 100 µL) contained 0.2 µg of NDV "Clone 30", different amounts of the inhibitors (0-2.0 mM), 0.12 mM 4-MU-Neu5Ac, 600 µg of bovine serum albumin (BSA) and 200 mM sodium citrate/phosphate buffer pH 6.8. After incubation at 37 °C for 15 min, the reactions were stopped by the addition of 1.5 mL of 0.2 M glycine buffered with NaOH at pH 10.8, and the neuraminidase activity was determined by spectrofluorometric measurement (Varioskan LUX Multimode Microplate reader, Thermo Fisher Scientific) of the 4-methylumbelliferone released (λ excitation 365 nm, λ emission 448 nm). One mU of neuraminidase activity is defined as the amount of enzyme releasing 1 nmol product *N*-acetylneuraminic acid per

minute at 37 °C. Six/seven concentrations of each inhibitor were used to determine the IC_{50} for all compounds maintaining a fixed concentration (0.12 mM) of 4-MUNeu5Ac.

5.2.2 Hemagglutinin inhibition assay (NI) on NDV-HN

This assay was performed according to the literature[4]. Briefly, the synthesized inhibitors DANA **1a**, FANA **2a** and compounds **12a,b** and **13b,d** were assessed in duplicate in V-bottom 96 well plates. Compounds were diluted in PBS as a 4X solution for each concentration tested (25 µL/well, 1X final). Each dilution was mixed with 4 hemagglutination units (HAU) of NDV (25 µL/well, 1 HAU final) and incubated for 30min at room temperature. The plate was, then, transferred on ice, and an equivalent volume of ice-cold 0.5% cRBC (50 µL/well) was added to each well. Plate was incubated for 1.5h at 23°C before reading hemagglutination results. The IC_{50} value for HI assays was defined as the compound concentration that gives similar agglutination to that observed in a well containing only 0.5 HAU of NDV and cRBC.

5.2.3 Protein extraction from stable NEU3 overexpressing Hek293a cells and quantification.

Stable Neu3 overexpressing Hek293a cells, maintained in Dulbecco's modified Eagle's medium (DMEM) were harvested by centrifugation and resuspended in PBS, containing protease and phosphatase inhibitor cocktail (Sigma-Aldrich). Total cells suspensions were lysed by sonication and then centrifuged at 800g for 10 min at 4°C to eliminate unbroken cells and nuclear components. The obtained supernatants were subsequently centrifuged at 115,000 X g at 4°C for 90 min on an Avanti *J*-30I Ultracentrifuge (Beckman Coulter) to obtain cytosolic and particulate (or membrane) fractions. Total protein content was determined with the BCA Protein Assay Kit (Pierce) following, in detail, the manufacturer's instructions.

5.2.4 Neuraminidase inhibition assay (NI) on hNEU3

The sialidase activity present in the particulate fraction from HEK293A cells was assayed according to the above protocol. Briefly, 40 µg of proteins from the particulate fraction were incubated with different amounts of the inhibitors (0-1.0 mM), 0.12 mM 4-MU-Neu5Ac, 600 µg of bovine serum albumin (BSA) and 12.5 mM sodium citrate/phosphate buffer pH 3.8. After incubation at 37 °C for 1 hour, the reactions were stopped by the addition of 1.5 mL of 0.2 M glycine buffered with NaOH at pH 10.8, and the neuraminidase activity was determined by spectrofluorometric measurement (Varioskan LUX Multimode Microplate reader, Thermo

Fisher Scientific). One mU of sialidase activity is defined as the amount of enzyme liberating 1 nmol product *N*-acetylneuraminic acid per minute at 37 °C. Six concentrations of each inhibitor were used to determine the IC_{50} for all compounds maintaining a fixed concentration (0.12 mM) of 4-MUNeu5Ac.

5.2.5 MTT assay (Citotoxicity assay)

The cytotoxicity of the compounds was analyzed by MTT assay following the manufacturer's protocol (Sigma Aldrich). Briefly, COS7 cells were seeded in 6-well plates at an initial density of 1 X 10^5 cells per well. The cells were incubated with different concentrations of the compounds at 37 °C in 5% CO_2 in an incubator for 24 h. MTT solution (5 mg mL^{-1}) was added to the cells, which were further incubated for 30 min. Then, the medium was discarded and 1 ml of MTT solubilization solution (10% Triton X-100 plus 0.1 N HCl in anhydrous isopropanol) was added for 10 min to dissolve the resulting formazan product. The absorbance of each well was measured at 570 nm using a spectrophotometer (*J*asco V-530 Spectrophotometer). Each experiment was performed in triplicate, and experiments were repeated at least three times. The cytotoxicity was expressed as the CC_{50}, which was the concentration of the test substances that inhibited the growth of COS7 cells by 50% compared with the growth of the untreated cells.

5.3.6 Statistical analysis

The IC_{50} values were determined by nonlinear regression analysis using GraphPad Prism 7 (GraphPad Software Inc., La *J*olla, CA). by nonlinear regression (curve fit), dose–response inhibition and three parameters logistic. Typical concentration–response plots were obtained from the average values of triplicate assay results. The results were presented as the mean of three independent experiments carried out in triplicate. IC_{50} values were compared with *t*-test using Prism 7. Values of $p < 0.05$ were considered statistically significant.

5.3 Computational methods

5.3.1 Rigid Docking simulations for compounds 1a and 2a-c (Chapter 3.1)

The protein structure of NDV (PDB 1e8v) was downloaded from PDB[53]. Then, it was prepared for docking using Schrödinger Protein Preparation Wizard (Schrödinger release 2016-3)[133] with standard settings, except that all water molecules were retained. DANA **1a** and the perfluorinated derivatives **2a-c** were prepared using Schrödinger LigPrep and the protonation state assessed with Epik[133]. The most stable ligand conformations were identified using Monte Carlo Multiple Minimum (MCMM) in Macromodel[134, 135]. OPLS3 force field (OPLS3, Schrödinger, Inc., New York, NY, 2013) was used[136]. Docking of the substrates was performed with Glide[137, 138] using the extra precision (XP) mode[139]. Unless otherwise stated, default settings were applied. The best pose was selected using the glide E-model score (kcal mol^{-1}), and the Glide XP score (kcal mol^{-1}) was used to compare the docking poses of the different substrates.

The small difference of the IC_{50} values measured for compounds **1a** and **2a-c** is reflected in the small variation of the Glide XP GScore. Poses with a difference in energy within 2 kcal mol^{-1} are often difficult to distinguish because of the limitations of the scoring function[137, 138] so the values of the GScore cannot be used to rank the quality of the interaction. In this case, only a qualitative analysis of the best scored poses, highlighting they key interactions, was done (see Results and Discussion 3.1.3).

5.3.2 Rigid Docking simulations for compounds 1a, 12a (Chapter 3.2) and 22b (Chapter 3.3)

The protein structure (PDB 1e8v1) of NDV-NH was downloaded from PDB[53]. In this analysis Chain B was chosen (instead of A) so to keep the important water molecules (2108, 1209 and 2110) that act as a bridge between the protein and the ligand[53]. The protein was prepared using Schrödinger Protein Preparation Wizard (Schrödinger release 2017- 3)[133] using the standard settings. All water molecules more than 5Å away from the ligand (or making less than 2 non-water contacts) were removed. The ligands **1a** (DANA), *p*-toluensolfonamido derivative **12a** and the 3,4-unsaturated Neu5Ac derivative **22b** where prepared using Schrödinger LigPrep and the protonation state assessed with Epik[133]. After LigPrep, Macromodel[134, 135] with Monte Carlo Multiple Minimum (MCMM) was used to select the most stable ligand conformation. For all simulations, the selected force field was OPLS3 (OPLS3, Schrödinger, Inc., New York, NY, 2013)[136].

The rigid docking studies of compounds **1a** (DANA), **12a** and **22b** were run with Glide[137-139] using the extra precision (XP) mode[137]. Unless otherwise stated, default settings were applied. Then, the best pose was selected using the glide E-model score (kcal mol^{-1}) and the Glide XP GScore (kcal mol^{-1}) was then used to compare the stability of the different ligands. The results were presented in Results and Discussion, paragraph 3.2.1 (for DANA **1a** and compound **12a**) and paragraph 3.3.1 (for compound **22b**).

5.3.3 Induced Fit Docking (IFD) simulations for compounds 1a and 12a (Chapter 3.2)

The additional IFD studies, performed on DANA **1a** and compound **12a**, after the same preparation described in paragraph 5.3.2, were accomplished with Induced Fit (Schrödinger Suite 2017- 3 Induced Fit Docking protocol; Glide, Schrödinger, LLC, New York, NY, 2016; Prime, Schrödinger, LLC, New York, NY, 2017)[140-142] using Glide extra precision (XP) mode[137] for redocking.

The best pose was selected using the glide E-model score (kcal mol^{-1}) and the Glide XP (kcal mol^{-1}) GScore was, then, used to compare the stability of the different ligands. The results were presented in Results and Discussion, paragraph 3.2.1

6. BIBLIOGRAPHY

[1] Islam, T., and von Itzstein, M. (2007) Anti-influenza drug discovery: are we ready for the next pandemic?, *Advances in carbohydrate chemistry and biochemistry 61*, 293-352.

[2] Alymova, I. V., Taylor, G., Takimoto, T., Lin, T. H., Chand, P., Babu, Y. S., Li, C., Xiong, X., and Portner, A. (2004) Efficacy of novel hemagglutinin-neuraminidase inhibitors BCX 2798 and BCX 2855 against human parainfluenza viruses in vitro and in vivo, *Antimicrobial agents and chemotherapy 48*, 1495-1502.

[3] Dirr, L., El-Deeb, I. M., Chavas, L. M. G., Guillon, P., and Itzstein, M. V. (2017) The impact of the butterfly effect on human parainfluenza virus haemagglutinin-neuraminidase inhibitor design, *Scientific reports 7*, 4507.

[4] El-Deeb, I. M., Guillon, P., Winger, M., Eveno, T., Haselhorst, T., Dyason, J. C., and von Itzstein, M. (2014) Exploring human parainfluenza virus type-1 hemagglutinin-neuraminidase as a target for inhibitor discovery, *Journal of medicinal chemistry 57*, 7613-7623.

[5] Guillon, P., Dirr, L., El-Deeb, I. M., Winger, M., Bailly, B., Haselhorst, T., Dyason, J. C., and von Itzstein, M. (2014) Structure-guided discovery of potent and dual-acting human parainfluenza virus haemagglutinin-neuraminidase inhibitors, *Nature communications 5*, 5268.

[6] Ikeda, K., Ueno, Y., Kitani, S., Nishino, R., and Sato, M. (2008) Ferrier glycosylation reaction catalyzed by Bi(OTf)(3)-montmorillonite K-10: Efficient synthesis of 3,4-unsaturated sialic acid derivatives, *Synlett*, 1027-1030.

[7] Oba, M., Ueno, Y., Kitani, S., Hayakawa, T., Takahashi, T., Suzuki, T., Sato, M., and Ikeda, K. (2014) FERRIER GLYCOSYLATION REACTION CATALYZED BY Bi(OTf)(3)-MONTMORILLONITE K-10: EFFICIENT SYNTHESIS OF 3,4-UNSATURATED SIALIC ACID DERIVATIVES: SYNTHESIS AND BIOLOGICAL EVALUATION AS INHIBITORS OF HUMAN PARAINFLUENZA VIRUS TYPE 1, *Heterocycles 89*, 69-81.

[8] Varki, A., Schnaar, R. L., and Schauer, R. (2015) Sialic Acids and Other Nonulosonic Acids, In *Essentials of Glycobiology* (rd, Varki, A., Cummings, R. D., Esko, J. D., Stanley, P., Hart, G. W., Aebi, M., Darvill, A. G., Kinoshita, T., Packer, N. H., Prestegard, J. H., Schnaar, R. L., and Seeberger, P. H., Eds.), pp 179-195, Cold Spring Harbor (NY).

[9] Varki, A., and Schauer, R. (2009) Sialic Acids, In *Essentials of Glycobiology* (nd, Varki, A., Cummings, R. D., Esko, J. D., Freeze, H. H., Stanley, P., Bertozzi, C. R., Hart, G. W., and Etzler, M. E., Eds.), Cold Spring Harbor (NY).

[10] Tanner, M. E. (2005) The enzymes of sialic acid biosynthesis, *Bioorganic chemistry 33*, 216-228.

[11] Monti, E., Bonten, E., D'Azzo, A., Bresciani, R., Venerando, B., Borsani, G., Schauer, R., and Tettamanti, G. (2010) SIALIDASES IN VERTEBRATES: A FAMILY OF ENZYMES TAILORED FOR SEVERAL CELL FUNCTIONS, In *Advances in Carbohydrate Chemistry and Biochemistry, Vol 64* (Horton, D., Ed.), pp 403-479, Elsevier Academic Press Inc, San Diego.

[12] Vimr, E. R., Kalivoda, K. A., Deszo, E. L., and Steenbergen, S. M. (2004) Diversity of microbial sialic acid metabolism, *Microbiology and molecular biology reviews : MMBR 68*, 132-153.

[13] Severi, E., Hood, D. W., and Thomas, G. H. (2007) Sialic acid utilization by bacterial pathogens, *Microbiology 153*, 2817-2822.

[14] Juge, N., Tailford, L., and Owen, C. D. (2016) Sialidases from gut bacteria: a mini-review, *Biochemical Society transactions 44*, 166-175.

[15] Giacopuzzi, E., Bresciani, R., Schauer, R., Monti, E., and Borsani, G. (2012) New insights on the sialidase protein family revealed by a phylogenetic analysis in metazoa, *PloS one 7*, e44193.

[16] Taylor, G. (1996) Sialidases: structures, biological significance and therapeutic potential, *Current opinion in structural biology 6*, 830-837.

[17] Colman, P. M., Hoyne, P. A., and Lawrence, M. C. (1993) Sequence and structure alignment of paramyxovirus hemagglutinin-neuraminidase with influenza virus neuraminidase, *Journal of virology 67*, 2972-2980.

[18] Chavas, L. M., Tringali, C., Fusi, P., Venerando, B., Tettamanti, G., Kato, R., Monti, E., and Wakatsuki, S. (2005) Crystal structure of the human cytosolic sialidase Neu2. Evidence for the dynamic nature of substrate recognition, *The Journal of biological chemistry 280*, 469-475.

[19] Heightman, T. D., and Vasella, A. T. (1999) Recent Insights into Inhibition, Structure, and Mechanism of Configuration-Retaining Glycosidases, *Angewandte Chemie 38*, 750-770.

[20] Zechel, D. L., and Withers, S. G. (2000) Glycosidase mechanisms: anatomy of a finely tuned catalyst, *Accounts of chemical research 33*, 11-18.

[21] KOSHLAND, D. E. (1953) STEREOCHEMISTRY AND THE MECHANISM OF ENZYMATIC REACTIONS, *Biological Reviews 28*, 416-436.

[22] Phillips, D. C. (1967) THE HEN EGG-WHITE LYSOZYME MOLECULE, *Proceedings of the National Academy of Sciences of the United States of America 57*, 483-495.

[23] Chong, A. K. J., Pegg, M. S., Taylor, N. R., and Vonitzstein, M. (1992) EVIDENCE FOR A SIALOSYL CATION TRANSITION-STATE COMPLEX IN THE REACTION OF SIALIDASE FROM INFLUENZA-VIRUS, *Eur. J. Biochem. 207*, 335-343.

[24] Taylor, N. R., and von Itzstein, M. (1994) Molecular modeling studies on ligand binding to sialidase from influenza virus and the mechanism of catalysis, *Journal of medicinal chemistry 37*, 616-624.

[25] Chan, J., and Bennet, A. J. (2012) Enzymology of Influenza Virus Sialidase, In *Influenza Virus Sialidase - A Drug Discovery Target* (von Itzstein, M., Ed.), pp 47-66, Springer Basel, Basel.

[26] Thomas, A., Jourand, D., Bret, C., Amara, P., and Field, M. J. (1999) Is there a covalent intermediate in the viral neuraminidase reaction? A hybrid potential free-energy study, *Journal of the American Chemical Society 121*, 9693-9702.

[27] Watts, A. G., Damager, I., Amaya, M. L., Buschiazzo, A., Alzari, P., Frasch, A. C., and Withers, S. G. (2003) Trypanosoma cruzi trans-sialidase operates through a covalent sialyl-enzyme intermediate: tyrosine is the catalytic nucleophile, *Journal of the American Chemical Society 125*, 7532-7533.

[28] Watts, A. G., Oppezzo, P., Withers, S. G., Alzari, P. M., and Buschiazzo, A. (2006) Structural and kinetic analysis of two covalent sialosyl-enzyme intermediates on Trypanosoma rangeli sialidase, *The Journal of biological chemistry 281*, 4149-4155.

[29] Dirr, L., El-Deeb, I. M., Guillon, P., Carroux, C. J., Chavas, L. M., and von Itzstein, M. (2015) The catalytic mechanism of human parainfluenza virus type 3 haemagglutinin-neuraminidase revealed, *Angewandte Chemie 54*, 2936-2940.

[30] Meindl, P., Bodo, G., Palese, P., Schulman, J., and Tuppy, H. (1974) Inhibition of neuraminidase activity by derivatives of 2-deoxy-2,3-dehydro-N-acetylneuraminic acid, *Virology 58*, 457-463.

[31] Meindl, P., and Tuppy, H. (1969) Über 2-Deoxy-2,3-dehydro-sialinsäuren, 1. Mitt.: Synthese und Eigenschaften von 2-Deoxy-2,3-dehydro-N-acylneuraminsäuren und deren Methylestern, *Monatshefte für Chemie / Chemical Monthly 100*, 1295-1306.

[32] Portner, A. (1981) The HN glycoprotein of Sendai virus: analysis of site(s) involved in hemagglutinating and neuraminidase activities, *Virology 115*, 375-384.

[33] Holzer, C. T., von Itzstein, M., Jin, B., Pegg, M. S., Stewart, W. P., and Wu, W. Y. (1993) Inhibition of sialidases from viral, bacterial and mammalian sources by analogues of 2-deoxy-2,3-didehydro-N-acetylneuraminic acid modified at the C-4 position, *Glycoconjugate journal 10*, 40-44.

[34] Guo, T. L., Datwyler, P., Demina, E., Richards, M. R., Ge, P., Zou, C. X., Zheng, R. X., Fougerat, A., Pshezhetsky, A. V., Ernst, B., and Cairo, C. W. (2018) Selective Inhibitors of Human Neuraminidase 3, *Journal of medicinal chemistry 61*, 1990-2008.

[35] Quosdorf, S., Schuetz, A., and Kolodziej, H. (2017) Different Inhibitory Potencies of Oseltamivir Carboxylate, Zanamivir, and Several Tannins on Bacterial and Viral Neuraminidases as Assessed in a Cell-Free Fluorescence-Based Enzyme Inhibition Assay, *Molecules 22*.

[36] Rudrawar, S., Dyason, J. C., Rameix-Welti, M. A., Rose, F. J., Kerry, P. S., Russell, R. J., van der Werf, S., Thomson, R. J., Naffakh, N., and von Itzstein, M. (2010) Novel sialic acid derivatives lock open the 150-loop of an influenza A virus group-1 sialidase, *Nature communications 1*, 113.

[37] Schreiner, E., Zbiral, E., Kleineidam, R. G., and Schauer, R. (1991) STRUCTURAL VARIATIONS ON N-ACETYLNEURAMINIC ACID .20. SYNTHESIS OF SOME 2,3-DIDEHYDRO-2-DEOXYSIALIC ACIDS STRUCTURALLY VARIED AT C-4 AND THEIR BEHAVIOR TOWARDS SIALIDASE FROM VIBRIO-CHOLERAE, *Liebigs Annalen Der Chemie*, 129-134.

[38] Hinou, H., Miyoshi, R., Takasu, Y., Kai, H., Kurogochi, M., Arioka, S., Gao, X. D., Miura, N., Fujitani, N., Omoto, S., Yoshinaga, T., Fujiwara, T., Noshi, T., Togame, H., Takemoto, H., and Nishimura, S. (2011) A strategy for neuraminidase inhibitors using mechanism-based labeling information, *Chemistry, an Asian journal 6*, 1048-1056.

[39] Li, J., and McClane, B. A. (2014) The Sialidases of Clostridium perfringens type D strain CN3718 differ in their properties and sensitivities to inhibitors, *Applied and environmental microbiology 80*, 1701-1709.

[40] Zhang, Y., Albohy, A., Zou, Y., Smutova, V., Pshezhetsky, A. V., and Cairo, C. W. (2013) Identification of selective inhibitors for human neuraminidase isoenzymes using C4,C7-modified 2-deoxy-2,3-didehydro-N-acetylneuraminic acid (DANA) analogues, *Journal of medicinal chemistry 56*, 2948-2958.

[41] Cairo, C. W. (2014) Inhibitors of the human neuraminidase enzymes, *MedChemComm 5*, 1067-1074.

[42] Maudrin, J., Barrere, B., Chantegrel, B., Deshayes, C., Quash, G., and Doutheau, A. (1994) SYNTHESIS OF 5-ACETAMIDO-3,4,5-TRIDEOXY-D-MANNO-NON-3-EN-2-ULOSONIC ACID ALPHA AND BETA-METHYL KETOSIDE AND THEIR BEHAVIOR TOWARDS THE SIALIDASE FROM INFLUENZA-VIRUS, *Bull. Soc. Chim. Fr. 131*, 400-406.

[43] Ferraris, O., Kessler, N., and Lina, B. (2005) Sensitivity performed of influenza viruses to zanamivir and oseltamivir: A study on viruses circulating in France prior to the introduction of neuraminidase inhibitors in clinical practice, *Antiviral research 68*, 43-48.

[44] Brouillette, W. J., Atigadda, V. R., Luo, M., Air, G. M., Babu, Y. S., and Bantia, S. (1999) Design of benzoic acid inhibitors of influenza neuraminidase containing a cyclic substitution for the N-acetyl grouping, *Bioorg Med Chem Lett 9*, 1901-1906.

[45] Howes, P. D., Cleasby, A., Evans, D. N., Feilden, H., Smith, P. W., Sollis, S. L., Taylor, N., and Wonacott, A. J. (1999) 4-Acetylamino-3-(imidazol-1-yl)-benzoic acids as novel inhibitors of influenza sialidase, *Eur. J. Med. Chem. 34*, 225-234.

[46] de Mello, C. P. P., Drusano, G. L., Adams, J. R., Shudt, M., Kulawy, R., and Brown, A. N. (2018) Oseltamivir-zanamivir combination therapy suppresses drug-resistant H1N1 influenza A viruses in the hollow fiber infection model (HFIM) system, *Eur. J. Pharm. Sci. 111*, 443-449.

[47] Hader, S. (2011) Synthesis and evaluation of fluorinated sialic acid derivatives as novel 'mechanism-based' neuraminidase inhibitors, University of Bath.

[48] Tai, S. H., Agafitei, O., Gao, Z., Liggins, R., Petric, M., Withers, S. G., and Niikura, M. (2015) Difluorosialic acids, potent novel influenza virus neuraminidase inhibitors, induce fewer drug resistance-associated neuraminidase mutations than does oseltamivir, *Virus research 210*, 126-132.

[49] Kai, H., Hinou, H., Naruchi, K., Matsushita, T., and Nishimura, S. (2013) Macrocyclic mechanism-based inhibitor for neuraminidases, *Chemistry 19*, 1364-1372.

[50] Shen, Z., Lou, K., and Wang, W. (2015) New small-molecule drug design strategies for fighting resistant influenza A, *Acta pharmaceutica Sinica. B 5*, 419-430.

[51] Rajasekaran, D., Palombo, E. A., Chia Yeo, T., Lim Siok Ley, D., Lee Tu, C., Malherbe, F., and Grollo, L. (2013) Identification of traditional medicinal plant extracts with novel anti-influenza activity, *PloS one 8*, e79293.

[52] Drzeniek, R. (1972) Viral and bacterial neuraminidases, *Current topics in microbiology and immunology 59*, 35-74.

[53] Crennell, S., Takimoto, T., Portner, A., and Taylor, G. (2000) Crystal structure of the multifunctional paramyxovirus hemagglutinin-neuraminidase, *Nature structural biology 7*, 1068-1074.

[54] Gamblin, S. J., and Skehel, J. J. (2010) Influenza Hemagglutinin and Neuraminidase Membrane Glycoproteins, *J. Biol. Chem. 285*, 28403-28409.

[55] Shtyrya, Y. A., Mochalova, L. V., and Bovin, N. V. (2009) Influenza virus neuraminidase: structure and function, *Acta naturae 1*, 26-32.

[56] Yang, H., Carney, P. J., Mishin, V. P., Guo, Z., Chang, J. C., Wentworth, D. E., Gubareva, L. V., and Stevens, J. (2016) Molecular Characterizations of Surface Proteins Hemagglutinin and Neuraminidase from Recent H5Nx Avian Influenza Viruses, *Journal of virology 90*, 5770-5784.

[57] von Itzstein, M. (2007) The war against influenza: discovery and development of sialidase inhibitors, *Nature reviews. Drug discovery 6*, 967-974.

[58] Influenza A virus, In *Animal Influenza*.

[59] Vonitzstein, M., Wu, W. Y., Kok, G. B., Pegg, M. S., Dyason, J. C., Jin, B., Phan, T. V., Smythe, M. L., White, H. F., Oliver, S. W., Colman, P. M., Varghese, J. N., Ryan, D. M., Woods, J. M., Bethell, R. C., Hotham, V. J., Cameron, J. M., and Penn, C. R. (1993) RATIONAL DESIGN OF POTENT SIALIDASE-BASED INHIBITORS OF INFLUENZA-VIRUS REPLICATION, *Nature 363*, 418-423.

[60] vonItzstein, M., Dyason, J. C., Oliver, S. W., White, H. F., Wu, W. Y., Kok, G. B., and Pegg, M. S. (1996) A study of the active site of influenza virus sialidase: An approach to the rational design of novel anti-influenza drugs, *Journal of medicinal chemistry 39*, 388-391.

[61] Wu, Y., Qin, G., Gao, F., Liu, Y., Vavricka, C. J., Qi, J., Jiang, H., Yu, K., and Gao, G. F. (2013) Induced opening of influenza virus neuraminidase N2 150-loop suggests an important role in inhibitor binding, *Scientific reports 3*, 1551.

[62] Kerry, P. S., Mohan, S., Russell, R. J., Bance, N., Niikura, M., and Pinto, B. M. (2013) Structural basis for a class of nanomolar influenza A neuraminidase inhibitors, *Scientific reports 3*, 2871.

[63] Varghese, J. N., Colman, P. M., van Donkelaar, A., Blick, T. J., Sahasrabudhe, A., and McKimm-Breschkin, J. L. (1997) Structural evidence for a second sialic acid binding

site in avian influenza virus neuraminidases, *Proceedings of the National Academy of Sciences of the United States of America 94*, 11808-11812.

[64] Dai, M., McBride, R., Dortmans, J. C., Peng, W., Bakkers, M. J., de Groot, R. J., van Kuppeveld, F. J., Paulson, J. C., de Vries, E., and de Haan, C. A. (2017) Mutation of the Second Sialic Acid-Binding Site, Resulting in Reduced Neuraminidase Activity, Preceded the Emergence of H7N9 Influenza A Virus, *Journal of virology 91*.

[65] Brown, V. R., and Bevins, S. N. (2017) A review of virulent Newcastle disease viruses in the United States and the role of wild birds in viral persistence and spread, *Veterinary research 48*, 68.

[66] Gogoi, P., Ganar, K., and Kumar, S. (2017) Avian Paramyxovirus: A Brief Review, *Transbound. Emerg. Dis. 64*, 53-67.

[67] Ganar, K., Das, M., Sinha, S., and Kumar, S. (2014) Newcastle disease virus: Current status and our understanding, *Virus research 184*, 71-81.

[68] Alexander, D. J., Aldous, E. W., and Fuller, C. M. (2012) The long view: a selective review of 40 years of Newcastle disease research, *Avian pathology : journal of the W.V.P.A 41*, 329-335.

[69] Moscona, A. (2005) Entry of parainfluenza virus into cells as a target for interrupting childhood respiratory disease, *The Journal of clinical investigation 115*, 1688-1698.

[70] Sheehan, J. P., Iorio, R. M., Syddall, R. J., Glickman, R. L., and Bratt, M. A. (1987) Reducing agent-sensitive dimerization of the hemagglutinin-neuraminidase glycoprotein of Newcastle disease virus correlates with the presence of cysteine at residue 123, *Virology 161*, 603-606.

[71] Morrison, T. G. (1988) STRUCTURE, FUNCTION, AND INTRACELLULAR PROCESSING OF PARAMYXOVIRUS MEMBRANE-PROTEINS, *Virus research 10*, 113-135.

[72] McGinnes, L. W., and Morrison, T. G. (1994) THE ROLE OF THE INDIVIDUAL CYSTEINE RESIDUES IN THE FORMATION OF THE MATURE, ANTIGENIC HN PROTEIN OF NEWCASTLE-DISEASE VIRUS, *Virology 200*, 470-483.

[73] Markwell, M. A., and Fox, C. F. (1980) Protein-protein interactions within paramyxoviruses identified by native disulfide bonding or reversible chemical cross-linking, *Journal of virology 33*, 152-166.

[74] Ryan, C., Zaitsev, V., Tindal, D. J., Dyason, J. C., Thomson, R. J., Alymova, I., Portner, A., von Itzstein, M., and Taylor, G. (2006) Structural analysis of a designed inhibitor

complexed with the hemagglutinin-neuraminidase of Newcastle disease virus, *Glycoconjugate journal 23*, 135-141.

[75] Garcia Sastre, A., Cobaleda, C., Cabezas, J. A., and Villar, E. (1991) On the inhibition mechanism of the sialidase activity from Newcastle disease virus, *Biological chemistry Hoppe-Seyler 372*, 923-927.

[76] Zaitsev, V., von Itzstein, M., Groves, D., Kiefel, M., Takimoto, T., Portner, A., and Taylor, G. (2004) Second sialic acid binding site in Newcastle disease virus hemagglutinin-neuraminidase: implications for fusion, *Journal of virology 78*, 3733-3741.

[77] Porotto, M., Salah, Z., DeVito, I., Talekar, A., Palmer, S. G., Xu, R., Wilson, I. A., and Moscona, A. (2012) The second receptor binding site of the globular head of the Newcastle disease virus hemagglutinin-neuraminidase activates the stalk of multiple paramyxovirus receptor binding proteins to trigger fusion, *Journal of virology 86*, 5730-5741.

[78] Porotto, M., Murrell, M., Greengard, O., Lawrence, M. C., McKimm-Breschkin, J. L., and Moscona, A. (2004) Inhibition of parainfluenza virus type 3 and Newcastle disease virus hemagglutinin-neuraminidase receptor binding: effect of receptor avidity and steric hindrance at the inhibitor binding sites, *Journal of virology 78*, 13911-13919.

[79] Porotto, M., Fornabaio, M., Greengard, O., Murrell, M. T., Kellogg, G. E., and Moscona, A. (2006) Paramyxovirus receptor-binding molecules: engagement of one site on the hemagglutinin-neuraminidase protein modulates activity at the second site, *Journal of virology 80*, 1204-1213.

[80] Bousse, T. L., Taylor, G., Krishnamurthy, S., Portner, A., Samal, S. K., and Takimoto, T. (2004) Biological significance of the second receptor binding site of Newcastle disease virus hemagglutinin-neuraminidase protein, *Journal of virology 78*, 13351-13355.

[81] Henrickson, K. J. (2003) Parainfluenza viruses, *Clinical microbiology reviews 16*, 242-264.

[82] Lawrence, M. C., Borg, N. A., Streltsov, V. A., Pilling, P. A., Epa, V. C., Varghese, J. N., McKimm-Breschkin, J. L., and Colman, P. M. (2004) Structure of the haemagglutinin-neuraminidase from human parainfluenza virus type III, *Journal of molecular biology 335*, 1343-1357.

[83] Winger, M., and von Itzstein, M. (2012) Exposing the flexibility of human parainfluenza virus hemagglutinin-neuraminidase, *Journal of the American Chemical Society 134*, 18447-18452.

[84] Porotto, M., Fornabaio, M., Kellogg, G. E., and Moscona, A. (2007) A second receptor binding site on human parainfluenza virus type 3 hemagglutinin-neuraminidase contributes to activation of the fusion mechanism, *Journal of virology 81*, 3216-3228.

[85] Palermo, L. M., Porotto, M., Greengard, O., and Moscona, A. (2007) Fusion promotion by a paramyxovirus hemagglutinin-neuraminidase protein: pH modulation of receptor avidity of binding sites I and II, *Journal of virology 81*, 9152-9161.

[86] Streltsov, V. A., Pilling, P., Barrett, S., and McKimm-Breschkin, J. L. (2015) Catalytic mechanism and novel receptor binding sites of human parainfluenza virus type 3 hemagglutinin-neuraminidase (hPIV3 HN), *Antiviral research 123*, 216-223.

[87] Alymova, I. V., Taylor, G., Mishin, V. P., Watanabe, M., Murti, K. G., Boyd, K., Chand, P., Babu, Y. S., and Portner, A. (2008) Loss of the N-linked glycan at residue 173 of human parainfluenza virus type 1 hemagglutinin-neuraminidase exposes a second receptor-binding site, *Journal of virology 82*, 8400-8410.

[88] Mishin, V. P., Watanabe, M., Taylor, G., Devincenzo, J., Bose, M., Portner, A., and Alymova, I. V. (2010) N-linked glycan at residue 523 of human parainfluenza virus type 3 hemagglutinin-neuraminidase masks a second receptor-binding site, *Journal of virology 84*, 3094-3100.

[89] Bousse, T., and Takimoto, T. (2006) Mutation at residue 523 creates a second receptor binding site on human parainfluenza virus type 1 hemagglutinin-neuraminidase protein, *Journal of virology 80*, 9009-9016.

[90] Alymova, I. V., Portner, A., Mishin, V. P., McCullers, J. A., Freiden, P., and Taylor, G. L. (2012) Receptor-binding specificity of the human parainfluenza virus type 1 hemagglutinin-neuraminidase glycoprotein, *Glycobiology 22*, 174-180.

[91] Watanabe, M., Mishin, V. P., Brown, S. A., Russell, C. J., Boyd, K., Babu, Y. S., Taylor, G., Xiong, X., Yan, X., Portner, A., and Alymova, I. V. (2009) Effect of hemagglutinin-neuraminidase inhibitors BCX 2798 and BCX 2855 on growth and pathogenicity of Sendai/human parainfluenza type 3 chimera virus in mice, *Antimicrobial agents and chemotherapy 53*, 3942-3951.

[92] Alymova, I. V., Watanabe, M., Boyd, K. L., Chand, P., Babu, Y. S., and Portner, A. (2009) Efficacy of the novel parainfluenza virus haemagglutinin-neuraminidase inhibitor BCX 2798 in mice - further evaluation, *Antiviral therapy 14*, 891-898.

[93] Alymova, I. V., Portner, A., Takimoto, T., Boyd, K. L., Babu, Y. S., and McCullers, J. A. (2005) The novel parainfluenza virus hemagglutinin-neuraminidase inhibitor BCX 2798 prevents lethal synergism between a paramyxovirus and Streptococcus pneumoniae, *Antimicrobial agents and chemotherapy 49*, 398-405.

[94] Pascolutti, M., Dirr, L., Guillon, P., Van Den Bergh, A., Ve, T., Thomson, R. J., and von Itzstein, M. (2018) Structural Insights into Human Parainfluenza Virus 3 Hemagglutinin-Neuraminidase Using Unsaturated 3- N-Substituted Sialic Acids as Probes, *ACS chemical biology 13*, 1544-1550.

[95] Schwerdtfeger, S. M., and Melzig, M. F. (2010) Sialidases in biological systems, *Die Pharmazie 65*, 551-561.

[96] Magesh, S., Suzuki, T., Miyagi, T., Ishida, H., and Kiso, M. (2006) Homology modeling of human sialidase enzymes NEU1, NEU3 and NEU4 based on the crystal structure of NEU2: Hints for the design of selective NEU3 inhibitors, *J. Mol. Graph. 25*, 196-207.

[97] Zou, Y., Albohy, A., Sandbhor, M., and Cairo, C. W. (2010) Inhibition of human neuraminidase 3 (NEU3) by C9-triazole derivatives of 2,3-didehydro-N-acetyl-neuraminic acid, *Bioorg. Med. Chem. Lett. 20*, 7529-7533.

[98] Zhang, Y., Albohy, A., Zou, Y., Smutova, V., Pshezhetsky, A. V., and Cairo, C. W. (2013) Identification of Selective Inhibitors for Human Neuraminidase Isoenzymes Using C4,C7-Modified 2-Deoxy-2,3-didehydro-N-acetylneuraminic Acid (DANA) Analogues, *Journal of medicinal chemistry 56*, 2948-2958.

[99] Purser, S., Moore, P. R., Swallow, S., and Gouverneur, V. (2008) Fluorine in medicinal chemistry, *Chemical Society reviews 37*, 320-330.

[100] Ojima, I. (2004) Use of fluorine in the medicinal chemistry and chemical biology of bioactive compounds--a case study on fluorinated taxane anticancer agents, *Chembiochem : a European journal of chemical biology 5*, 628-635.

[101] Gillis, E. P., Eastman, K. J., Hill, M. D., Donnelly, D. J., and Meanwell, N. A. (2015) Applications of Fluorine in Medicinal Chemistry, *Journal of medicinal chemistry 58*, 8315-8359.

[102] Rota, P., Allevi, P., Mattina, R., and Anastasia, M. (2010) Reaction of N-acetylneuraminic acid derivatives with perfluorinated anhydrides: a short access to N-perfluoracylated glycals with antiviral properties, *Organic & biomolecular chemistry 8*, 3771-3776.

[103] Rota, P., Allevi, P., Costa, M. L., and Anastasia, M. (2010) High yielding N-transacylation of secondary amides in acids labile molecules by the action of perfluorinated anhydrides in the presence of a mild base, *Tetrahedron-Asymmetry 21*, 2681-2686.

[104] Rota, P., Allevi, P., Colombo, R., Costa, M. L., and Anastasia, M. (2010) General and chemoselective N-transacylation of secondary amides by means of perfluorinated anhydrides, *Angewandte Chemie 49*, 1850-1853.

[105] Kulikova, N. Y., Shpirt, A. M., and Kononov, L. O. (2006) A facile synthesis of N-acetylneuraminic acid glycal, *Synthesis*, 4113-4114.

[106] Rota, P., Cirillo, F., Piccoli, M., Gregorio, A., Tettamanti, G., Allevi, P., and Anastasia, L. (2015) Synthesis and biological evaluation of several dephosphonated analogues of CMP-Neu5Ac as inhibitors of GM3-synthase, *Chemistry 21*, 14614-14629.

[107] Rota, P., Allevi, P., Agnolin, I. S., Mattina, R., Papini, N., and Anastasia, M. (2012) A simple synthesis of N-perfluoroacylated and N-acylated glycals of neuraminic acid with a cyclic aminic substituent at the 4alpha position as possible inhibitors of sialidases, *Organic & biomolecular chemistry 10*, 2885-2894.

[108] Anastasia, L., Holguera, J., Bianchi, A., D'Avila, F., Papini, N., Tringali, C., Monti, E., Villar, E., Venerando, B., Munoz-Barroso, I., and Tettamanti, G. (2008) Over-expression of mammalian sialidase NEU3 reduces Newcastle disease virus entry and propagation in COS7 cells, *Biochimica et biophysica acta 1780*, 504-512.

[109] Allevi, P., Rota, P., Agnolin, I. S., Gregorio, A., and Anastasia, M. (2013) A Simple Synthetic Access to Differently 4-Substituted Neu5Ac2en Glycals Combining Elements of Molecules with Anti-Neuraminidase Activity, *Eur. J. Org. Chem.*, 4065-4077.

[110] Agnolin, I. S., Rota, P., Allevi, P., Gregorio, A., and Anastasia, M. (2012) Simple and Rapid Procedures for the Synthesis of 5-Acylated 4 beta-Acylamido- and 4 beta-Acetoxyneuraminic Acid Glycals, *Eur. J. Org. Chem.*, 6537-6547.

[111] Rota, P., Agnolin, I. S., Allevi, P., and Anastasia, M. (2012) Facile Diastereoselective Entry to 4 beta-Acylamidation of Neu5Ac2en Glycals Using Their N-Perfluoroacylated Congeners as Key Tools, *Eur. J. Org. Chem.*, 2508-2510.

[112] Venerando, B., Cestaro, B., Fiorilli, A., Ghidoni, R., Preti, A., and Tettamanti, G. (1982) Kinetics of Vibrio cholerae sialidase action on gangliosidic substrates at different supramolecular-organizational levels, *The Biochemical journal 203*, 735-742.

[113] Meng, X. Y., Zhang, H. X., Mezei, M., and Cui, M. (2011) Molecular docking: a powerful approach for structure-based drug discovery, *Current computer-aided drug design 7*, 146-157.

[114] Chand, P., Babu, Y. S., Rowland, S. R., and Lin, T. H. (2002) COMPOUNDS USEFUL FOR INHIBITING PARAMYXOVIRUS NEURAMINIDASE.

[115] Vonitzstein, M., El-Deeb, I. M., dirr, L., Guillon, P., and Winger, M. (2016) Antiviral agents and uses thereof.

[116] Pagadala, N. S., Syed, K., and Tuszynski, J. (2017) Software for molecular docking: a review, *Biophysical reviews 9*, 91-102.

[117] El-Deeb, I. M., Guillon, P., Dirr, L., and von Itzstein, M. (2017) Exploring inhibitor structural features required to engage the 216-loop of human parainfluenza virus type-3 hemagglutinin-neuraminidase, *MedChemComm 8*, 130-134.

[118] Takimoto, T., Taylor, G. L., Connaris, H. C., Crennell, S. J., and Portner, A. (2002) Role of the hemagglutinin-neuraminidase protein in the mechanism of paramyxovirus-cell membrane fusion, *Journal of virology 76*, 13028-13033.

[119] Das, R., and Mukhopadhyay, B. (2016) Chemical O-Glycosylations: An Overview, *ChemistryOpen 5*, 401-433.

[120] Cecilia, J. A., Garcia-Sancho, C., Vilarrasa-Garcia, E., Jimenez-Jimenez, J., and Rodriguez-Castellon, E. (2018) Synthesis, Characterization, Uses and Applications of Porous Clays Heterostructures: A Review, *Chem. Rec. 18*, 1085-1104.

[121] Boons, G. J., and Demchenko, A. V. (2000) Recent advances in o-sialylation, *Chemical reviews 100*, 4539-4566.

[122] Paulsen, H., and Tietz, H. (1982) Synthesis of Trisaccharide Moieties from N-Acetylneuraminic Acid and N-Acetyllactosamine, *Angewandte Chemie International Edition in English 21*, 927-928.

[123] van der Vleugel, D. J. M., van Heeswijk, W. A. R., and Vliegenthart, J. F. G. (1982) A facile preparation of alkyl α-glycosides of the methyl ester of N-acetyl-d-neuraminic acid, *Carbohydrate research 102*, 121-130.

[124] Hori, H., Nakajima, T., Nishida, Y., Ohrui, H., and Meguro, H. (1988) A simple method to determine the anomeric configuration of sialic acid and its derivatives by 13C-NMR, *Tetrahedron Letters 29*, 6317-6320.

[125] HAVERKAMP, J., HALBEEK, H., DORLAND, L., VLIEGENTHART, J. F. G., PFEIL, R., and SCHAUER, R. (1982) High-Resolution 1H-NMR Spectroscopy of

Free and Glycosidically Linked O- Acetylated Sialic Acids, *Eur. J. Biochem. 122*, 305-311.

[126] Okamoto, K., Kondo, T., and Goto, T. (1987) Glycosylation of 4,7,8,9-tetra-O-acetyl-2-deoxy-2.BETA.,3.BETA.-epoxy-N-acetylneuraminic acid methyl ester, *Bull. Chem. Soc. Jpn. 60*, 637-643.

[127] Christian, R., Schulz, G., Brandstetter, H. H., and Zbiral, E. (1987) On the side-chain conformation of N-acetylneuraminic acid and its epimers at C-7, C-8, and C-7,8, *Carbohydrate research 162*, 1-11.

[128] Colombo, R., Anastasia, M., Rota, P., and Allevi, P. (2008) The first synthesis of N-acetylneuraminic acid 1,7-lactone, *Chemical communications*, 5517-5519.

[129] Yu, R. K., and Ledeen, R. (1969) Configuration of the ketosidic bond of sialic acid, *The Journal of biological chemistry 244*, 1306-1313.

[130] Ooi, H. C., Marcuccio, S. M., and Jackson, W. R. (1999) An alternative synthesis of N-acetyl-4-deoxyneuraminic acid, *Aust. J. Chem. 52*, 937-940.

[131] Still, W. C., Kahn, M., and Mitra, A. (1978) Rapid chromatographic technique for preparative separations with moderate resolution, *The Journal of Organic Chemistry 43*, 2923-2925.

[132] Cirillo, F., Ghiroldi, A., Fania, C., Piccoli, M., Torretta, E., Tettamanti, G., Gelfi, C., and Anastasia, L. (2016) NEU3 Sialidase Protein Interactors in the Plasma Membrane and in the Endosomes, *The Journal of biological chemistry 291*, 10615-10624.

[133] Sastry, G. M., Adzhigirey, M., Day, T., Annabhimoju, R., and Sherman, W. (2013) Protein and ligand preparation: parameters, protocols, and influence on virtual screening enrichments, *Journal of computer-aided molecular design 27*, 221-234.

[134] Saunders, M., Houk, K. N., Wu, Y. D., Still, W. C., Lipton, M., Chang, G., and Guida, W. C. (1990) Conformations of cycloheptadecane. A comparison of methods for conformational searching, *Journal of the American Chemical Society 112*, 1419-1427.

[135] Chang, G., Guida, W. C., and Still, W. C. (1989) An internal-coordinate Monte Carlo method for searching conformational space, *Journal of the American Chemical Society 111*, 4379-4386.

[136] Shivakumar, D., Harder, E., Damm, W., Friesner, R. A., and Sherman, W. (2012) Improving the Prediction of Absolute Solvation Free Energies Using the Next

Generation OPLS Force Field, *Journal of chemical theory and computation 8*, 2553-2558.

[137] Friesner, R. A., Murphy, R. B., Repasky, M. P., Frye, L. L., Greenwood, J. R., Halgren, T. A., Sanschagrin, P. C., and Mainz, D. T. (2006) Extra precision glide: docking and scoring incorporating a model of hydrophobic enclosure for protein-ligand complexes, *Journal of medicinal chemistry 49*, 6177-6196.

[138] Friesner, R. A., Banks, J. L., Murphy, R. B., Halgren, T. A., Klicic, J. J., Mainz, D. T., Repasky, M. P., Knoll, E. H., Shelley, M., Perry, J. K., Shaw, D. E., Francis, P., and Shenkin, P. S. (2004) Glide: a new approach for rapid, accurate docking and scoring. 1. Method and assessment of docking accuracy, *Journal of medicinal chemistry 47*, 1739-1749.

[139] Halgren, T. A., Murphy, R. B., Friesner, R. A., Beard, H. S., Frye, L. L., Pollard, W. T., and Banks, J. L. (2004) Glide: a new approach for rapid, accurate docking and scoring. 2. Enrichment factors in database screening, *Journal of medicinal chemistry 47*, 1750-1759.

[140] Sherman, W., Day, T., Jacobson, M. P., Friesner, R. A., and Farid, R. (2006) Novel procedure for modeling ligand/receptor induced fit effects, *Journal of medicinal chemistry 49*, 534-553.

[141] Sherman, W., Beard, H. S., and Farid, R. (2006) Use of an induced fit receptor structure in virtual screening, *Chemical biology & drug design 67*, 83-84.

[142] Farid, R., Day, T., Friesner, R. A., and Pearlstein, R. A. (2006) New insights about HERG blockade obtained from protein modeling, potential energy mapping, and docking studies, *Bioorganic & medicinal chemistry 14*, 3160-3173.

I would like to express my special appreciation and thanks to the PhD course coordinator Sandro Sonnino and my supervisor Professor Pietro Allevi, who gave me the opportunity to enrich my scientific knowledge through this wonderful experience.

I am extremely grateful to my research guide, Dr. Paola Rota, for encouraging my scientific activities every day, permitting me to become a mature research scientist. She taught me everything since the beginning of my PhD course and she encouraged and helped me at every stage of my personal and academic life.

I would also like to express my gratitude to Prof Luigi Anastasia and all the members of the Laboratory of Stem Cells for Tissue Engineering (PSD). I considered them not only coworkers but also precious fellow travelers.

I gratefully acknowledge Prof. Mario Anastasia for the valuable suggestions and his unrelenting encouragement and Ms. Irene Delcarro who has been a great and kind support, always ready to help with her skilled technical assistance. Furthermore, special thanks go to ALL the chemists of "Via Saldini laboratories", in particular, Prof. Patrizia Ferraboschi and all the members of her research group.

I also greatly appreciate the support received through the collaborative work with Prof. Lars Olsen and Dr. Marco Montefiori of the University of Copenhagen as well as Dr. Calogero Terregino and Dr. Francesco Bonfante from the "Istituto Zooprofilattico Sperimentale delle Venezie". They permitted me to enrich my knowledge in both computational simulation studies and viral biological assays (fundamental for the implementation of the multidisciplinary approach I used in my PhD project).

I also feel grateful towards my PhD colleagues and all the scientist and wonderful peoples I met during these three years, remembering "all the precious moments" passed together.

Finally, infinite thanks go to my family: my mum, my dad and my brother and all the other people who have been close to me. Words cannot express how grateful I am to my mother and father for the numerous sacrifices that they have made on my behalf. I would also like to thank all my friends who supported me while I was writing my thesis and encouraged me to strive towards my goal. Thank you.

"E so che ogni cosa la devo alle palle quadre di mio padre al suo sudore
Al sorriso di mia madre Al viso di ogni nonno che proietta amore
A mio fratello piccolo ora più alto di me e nonna mi protegge sulla stella più bella che c'è
Eee… ai miei amici esauriti Alle notti felici di vizi proibiti realizzi che lo stile è quando siamo uniti
Solo quando stiamo assieme La sturia è vivibile Passa parola a ogni persona visibile Tutto possibile
Per chi non si arrende e difende il sogno che ha Mentre il sole che scende saluterà Noi gente che spera.."

(Gente che spera – Articolo 31)